387

INFLUENCE OF THE HYPERSTATIC MODELING ON THE BEHAVIOR OF TRANSMISSION LINE LATTICE STRUCTURES

Working Group
B2.08

August 2009

Working Group B2.08

Influence of the hyperstatic modelling on the behaviour of transmission line lattice structures

Members

Convenor: J.B.G.F. da Silva (BR), **Secretary:** D. Hughes (GB), L. Binette (CA), J. Fernadez (ES), A. Fuchs (DE), R. Jansson (SE), L. Kempner (US), D.I. Lee (KR), N. Masaoka (JP), G. Nesgard (NO), V. Numminen (FI), L. Pellet (FR), J. Peralta (PO), R.C. Ramos de Menezes (BR), J. Rogier (BE), J.D. Serrano (ZA), E. Thorsteins (IS), S. Villa (IT)

Corresponding Members

C.G. Alamo (VE), G. Brown (AU), G. Gheorghita (RO), R. Guimarães (BR), H. Hawes (AU), C. Laub (CZ), F. Legeron (CA), T. Leskinen (FI), M. Ishac (CA), J.M. Menéndez (CU), F. Meza Rosso (BO), K. Nieminen (FI), R. C. Peixoto (BR), J. Prieto (ES), C. Thorn (GB), J. Toth (CA), K. Van Dam (BE), M. Vanner (GB)

Contributors: J. Kaminski Jr. (BR), L. Fadel Miguel (BR).

ISBN: 978-2-85873-063-6

TABLE OF CONTENTS

TABLE OF FIGURES

LIST OF TABLES

1. ABSTRACT

The article published by the Cigré, in 1991, “An Experiment to Measure the Variation in Lattice Tower Strength Due to Local Design Practices” [1], has confirmed what the designers of latticed supports for transmission lines had already anticipated: when the same structure is analyzed by different designers, discrepancies may appear among the predictions themselves and, especially, between the predictions and the results achieved by prototype tests in real scale. Also, in accordance with the above-mentioned document, although the discrepancies between the values calculated and measured for the main bars are not very big, they become substantial for the diagonals, particularly, for the lightly ones. One of the conclusions of the above research was, therefore, that for the specific case of the diagonals, new studies should be carried out in order to allow a complete understanding of the discrepancies and the related causes. Actually, the designers of structures for transmission lines have always known that the proposed modelling may greatly influence the degree of convergence between the theoretical predictions and the real results achieved in the tests. For the purpose of investigating this subject, the Working Group WG08 – Supports for Transmission Lines, of the Study Committee B2 – Overhead Lines, has developed a new study, under which three new and almost identical prototype structures with different hyperstatic degrees in their modelling were developed. These prototypes were analyzed by designers from several countries and subsequently built and tested. The results from the tests, in many aspects, very much confirmed the conclusions obtained in [1]. Additional and inedited informations, however, were obtained especially regarding those so called lightly loaded diagonals. This brochure shows the various details of this study.

Keywords: Lattice towers, modelling influence, isostatic and hyperstatic structures, prototype testing.

2. INTRODUCTION

The study of discrepancies of transmission tower strengths began at the Cigré in the middle of the 80's. At that time, a special motivation was behind such studies as there was a demand from the scientific community for the proper definitions of the strength factors Φ_R of the components, which are required for the application of the probabilistic method to transmission line designs [2]. As defined in reference [2], the suspension structures must be considered as the "weakest link" in the system and its reliability should be defined within the logic of a preferential sequence of failure. The main concern of the Cigré Working Group at the time [3] was to understand and quantify the degree of discrepancies of the supports strengths (here named strength factor Φ_R).

The variations of the towers strength were defined as being the result of the discrepancies of the following factors:

- Variation of strengths due to local design practices, knowledge, modelling, software, design standards, etc;
- Variation due to discrepancies in the properties of the materials (quality);
- Discrepancies due to the tolerances of manufacturing processes;
- Variations due to the erection practices.

Part of such studies (the two initial bullets) has already been completed by the WG08 Working Group, published and made available [1], [4], [5]. The other remaining two bullets are still in the study phase.

As quoted in [1], one of the questions still outstanding, which required additional studies, has to do with the influence of structure modelling. The main concern of the design engineers have always been that, a hyperstatic model can provide decisive contribution for the increase of discrepancies. Structures with a higher degree of hyperstaticity present more options of force balance and its final balance can be influenced by unexpected factors, such as distortion in the properties of the materials, eccentricity in connections, partial fixing moments, manufacturing and erection tolerances and others. During the investigations performed by the Cigré at that time, one remarkable fact was noticed: a large dispersion between the values expected and the values measured on members forces, mainly on lightly loaded diagonals.

Normally, it consisted of diagonals on orthogonal faces (or almost orthogonal) to the direction of the load and, considering the overall structural spatiality, they would receive forces not predicted from the overall redistribution of the loads.

In order to better investigate the matter, the WG08 Working Group decided to create a special "Task Force", here named TF4, for the development of the relevant theoretical studies. For doing so, three prototype structures were developed, analyzed and bar forces calculated by the Cigré group, with the subsequent construction for real scale prototype testing. During those tests, the most important bars were monitored in real time by sophisticated strain-gage system. This new study has had an ample international participation, where the most advanced softwares currently available in the world were employed by different engineers from different countries to carry out the analyses.

The results of the calculations of the participants were compared to highlight the predictions and their discrepancies. Although they used different softwares, with distinct considerations (mainly in definitions of beam or truss elements and consequently fictitious bars, besides the linear or geometrical non-linear analysis), the obtained internal members forces showed quite similar magnitudes. Within such context, in the work done afterwards by Kaminski Jr. [7], which is presented in this brochure, different mechanical models for the Cigré structures using advanced features, were modeled and analyzed.

The observed dispersion between the numeric results among the different models and the prototype tests data was used to compare the results. It may be observed that the more refined models with advanced features, such as, slippage connections, present a closer behaviour to those measured of the prototype tests.

3. THE IMPACT OF MODELLING

The former Cigré experiment [1] showed the important role played by the "modelling" in the structural behaviour of the towers, promoting convergences or dispersions.

During the first Cigré experiment, it could be observed great discrepancies between the participants predictions and the measured values mainly for bar forces in lightly loaded diagonals. Great anxiety was established among the WG08 members trying to understand from where those discrepancies and differences were coming. If from calculation mistakes from some participants, accuracy on the data acquisition system, imperfection on the strain gages arrangements or test station normal tolerances. Other opinions were that, perhaps, the measured forces in the members were correct and the discrepancies observed could be distortions between the theoretical behaviour and the real structural balance which could be affected, for example, by influence of the modelling adopted for the prototypes.

To investigate the cause of the discrepancies, J. da Silva proposed a theoretical simulation, where fictitious nodes were created on some particular points of prototype 2 (see Figure 1) improving its isostaticity condition.

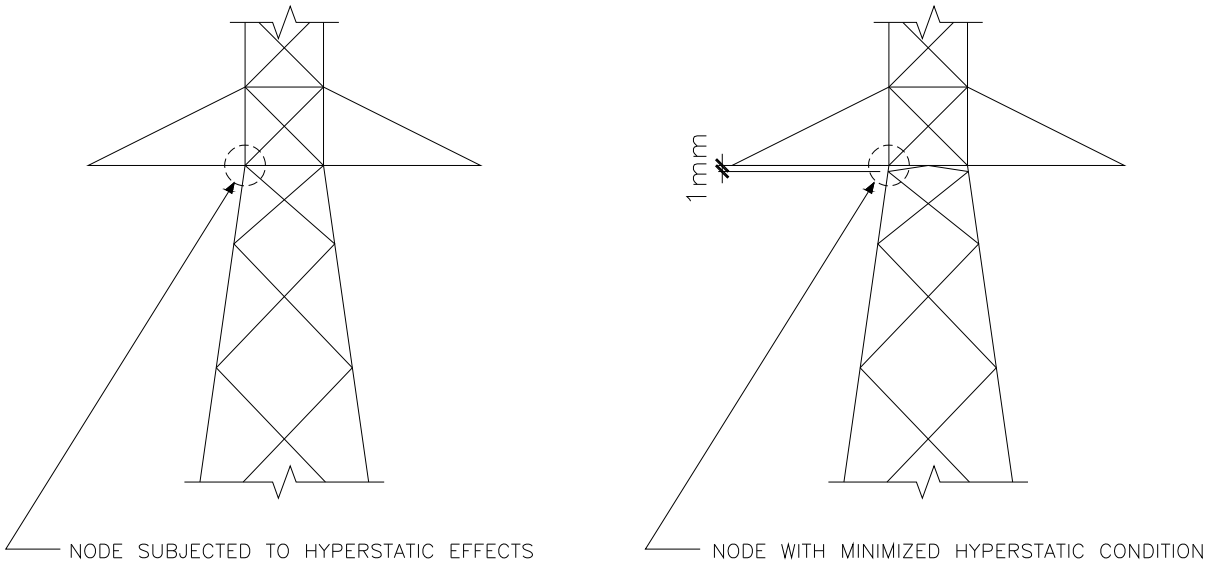

Figure 1: Isostaticity Condition

The calculations assuming this new structural model on prototype 2 showed that, all the calculated bar force values approached those previously measured during the tests. According to J. da Silva, one conclusion could be that the real "structural balance", perhaps, would be in "an intermediate stage" in-between the hyperstatic (statically indeterminate) model as the prototype was constructed and a "fictitious isostatic" (statically determinate) condition

reached by the structure through, for example the “clearances on the holes” and/or “bolts slippage”. In addition, J. da Silva had already observed similar behaviour in other tests, but as those tests had not been real time strain gage monitored, it could not be confirmed. J. da Silva stressed that these effects could impact directly those so called “lightly loaded” diagonals which are very sensitive to the structural elastic deformation and the degree of hyperstaticity. As an example, on models shown in figure 2, longitudinal diagonals (green) are supposed to be loaded on model number 2 for transverse loading while those diagonals are expected to be unloaded on the structure model number 1.

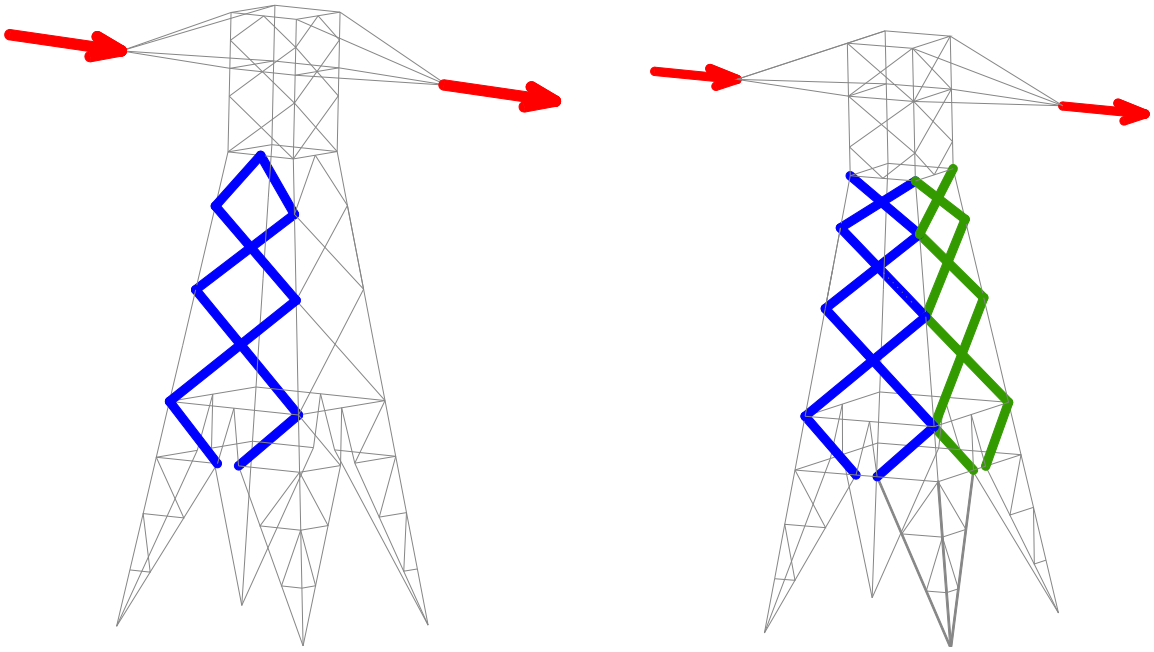

Model 1 Model 2

Figure 2: Impact of Modelling

The longitudinal diagonals of the structural model number 2 (Figure 2) are loaded by such transverse loading condition due to its three dimensional geometry and basically due to its degree of hyperstaticity (or more rigidity). As the structural elastic deformation occurs, facilitated by the “bolt slippage” on joints and/or the “clearances on holes”, the structural balance can change and as a consequence, those longitudinal diagonals can have “relieves” on their loads. These considerations could help to understand the discrepancies observed in measured forces on some bars (especially the so called lightly loaded ones) as compared with those calculated values.

As said before, the first Cigré experiment [1] to determine the variation in design was successful in illustrating the potential areas and sources of variation in transmission line tower design.

As per those conclusions, *"Typical sources that had been identified include"*:

- ***Modelling Accuracy*** *– Analytical models that are available to engineers contain many variations and options for application of the model, such as linear, non-linear, elastic, inelastic, large displacements, etc. These options are provided because there is no singular method to characterize the complexity of the behaviour of a lattice transmission tower to various loading conditions. As evidenced by the test data, lightly loaded members are particularly difficult to model and analyze. This is insignificant to the overall structure analysis capability, since the variation on main members or heavily loaded members is significantly lower, COV of 3,6%.*
- ***Modelling error*** *– In applying the analysis options available, the engineer makes assumptions about the selection and applications of member type, analysis solution techniques and other parameters available to him. This is not quite a trial and error exercise, but is generally founded on sound engineering judgment and experience gathered by tests or years of field experience. There is however, the variation in assumptions made by individual engineers that are reflected in the variation in the results reviewed.*

The following main conclusions could be drawn from the first experiment:

- Predicting the reactions of main members under load is generally good, typical COV of 3,6%.
- Predicting the reactions of lightly loaded members has much larger dispersion. For heavily loaded members the dispersions between estimated and real values are not expected to be significant.
- The experiment indicated that the assumptions and application of analysis tools and techniques by engineers has a significant impact on the modelling accuracy.
- Additional tests and modelling capabilities are needed for bracing members, in particular to improve the overall accuracy of available modelling techniques.

The main objective of this study is to investigate the impact of tower modelling on bracing members, especially those which are lightly loaded.

4. THE NEW WG08 TF4 RESEARCH

4.1 Objectives of the New Proposed Experience

As seen in the previous section, the lattice structural system proposed (hereinafter named just model) may influence, to a substantial degree, the level of discrepancies or to cause distortions between the mathematical model idealized during the design phase and the actual physical model achieved at the end of the construction process.

The question being dealt with in this work is not the difficulty of modelling and/or of predicting the behaviour of the structures. Nowadays, this can be done by means of sophisticated structural analysis softwares, several of them, equipped with advanced modelling techniques. The discussion here goes a step further. It has to do with the verification or monitoring of the evolution of the accuracy (or verification of the error) of the initial predictions, after the subsequent stages of the process, such as the detailing design that can introduce imperfections such as partial fixing and/or eccentricities, variations in the mechanical properties of the materials, the fabrication and erection with their practices and tolerances. At the end of the whole process, could anyone say that the structural behaviour continues as anticipated in the initial calculations? The experience has shown that for some structures and some members the answer is yes; for others, not quite so. Some structures are more sensitive to distortions. This will depend to a great extent on the modelling adopted by the designer.

As mentioned before, the proposal of this study by the WG08 Working Group has the main objective of evaluating the influence of modelling as a contributing factor for a bigger or smaller degree of dispersion of theoretical predictions when compared to the results of actual towers under loading.

4.2 Description of the Prototypes 1, 2 and 2A

For this purpose, three prototype structures 1, 2 and 2A, were created; they are almost identical containing slight modifications in their structural configurations. The proposed differences are typical variations in the latticework that can take place in the usual

development of the supports for transmission lines. However, they are capable of causing the structure type 1, for example, to become more isostatic than structures 2 and 2A, or otherwise, 2 and 2A more hyperstatic than 1. This is sufficient to produce big changes in the force balance process of the three structures, changing even the loads to be transmitted to the foundations. Differences are also expected in the degrees of discrepancies between mathematical and physical models for the three structures proposed.

It is important to note that the towers used in this investigation had similar structural systems to those of overhead line lattice structures. The prototypes were developed to fulfill the Cigré experiment group needs. The prototypes 1, 2 and 2A silhouettes as well as sections to identify horizontal diaphragms are shown on Figures 3, 4 and 5. It can be observed that the three towers have the same overall external dimensions like the total high of 11m, the upper depth of 1.4m and the base width of 4m. The real differences are basically on the arrangements of some bracing/diagonals:

- The existence of members B14T and B14L on structures 2 and 2A (not existing in structure 1) giving them more stiffness in those regions.
- The arrangements of the diagonals on the transitions region between the upper and lower parts of the structures provoking differences on the forces distributions on the main members as shown on figures 3, 4 and 5.

For a better understanding it is important to observe that the members were named using the following criteria:

- The letter “F” was used to identify the main members;
- “T” and “L” were used to name the diagonals of the transverse and longitudinal faces respectively;
- The letter “P” identifies the leg diagonals;
- The dashed lines indicated redundant members.

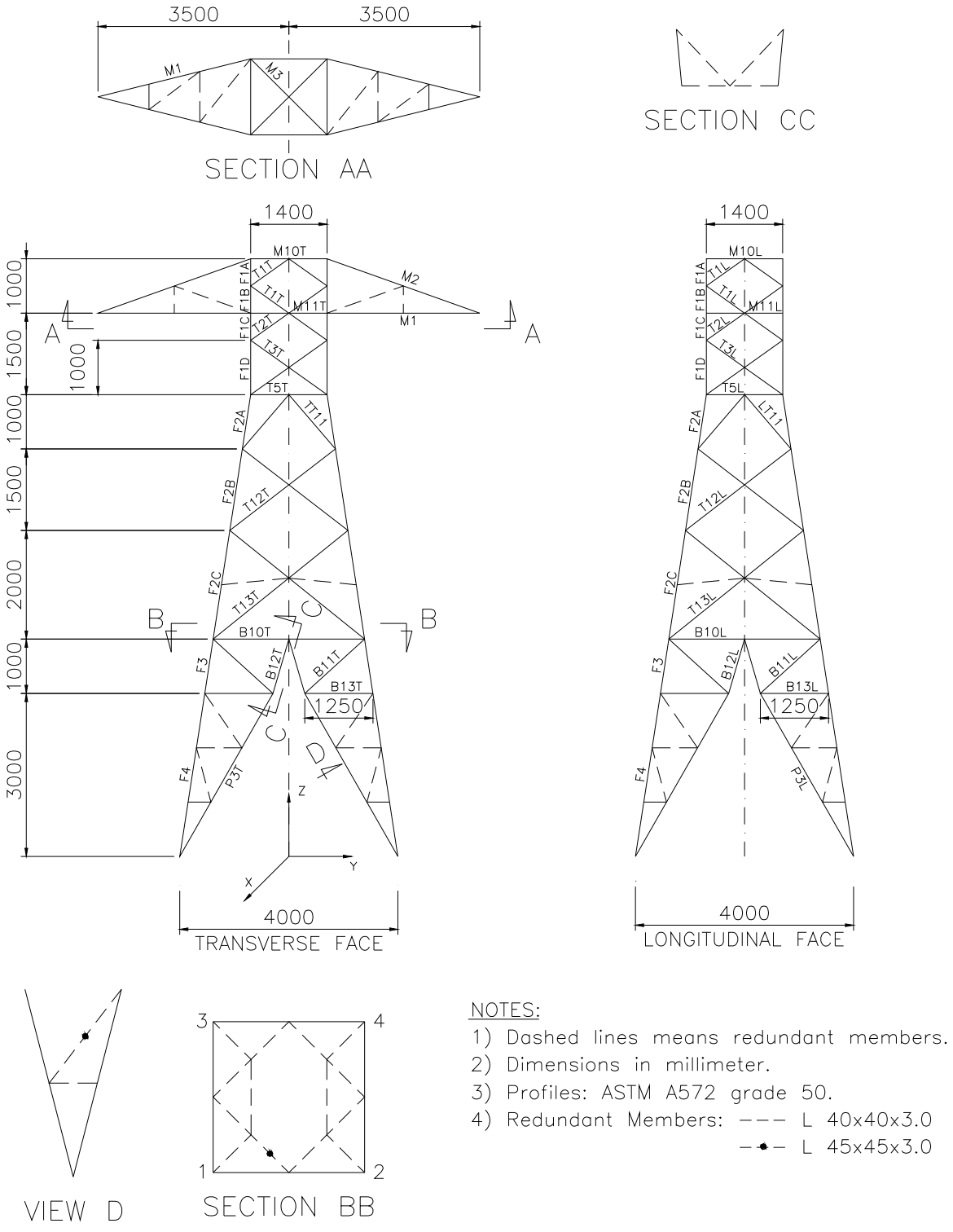

Figure 3: Prototype 1 – Transverse Face, Longitudinal Face and Sections

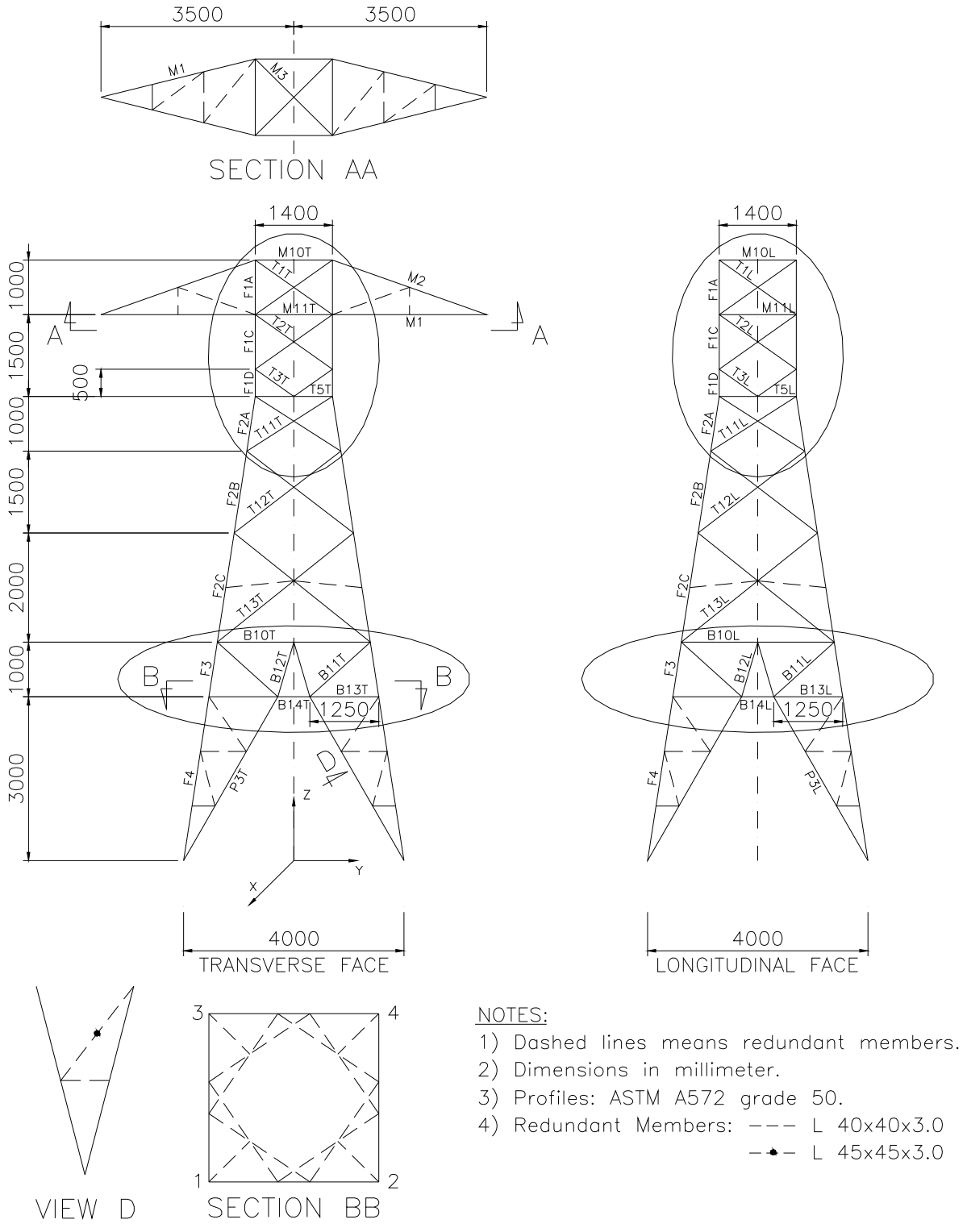

Figure 4: Prototype 2 – Transverse Face, Longitudinal Face and Sections

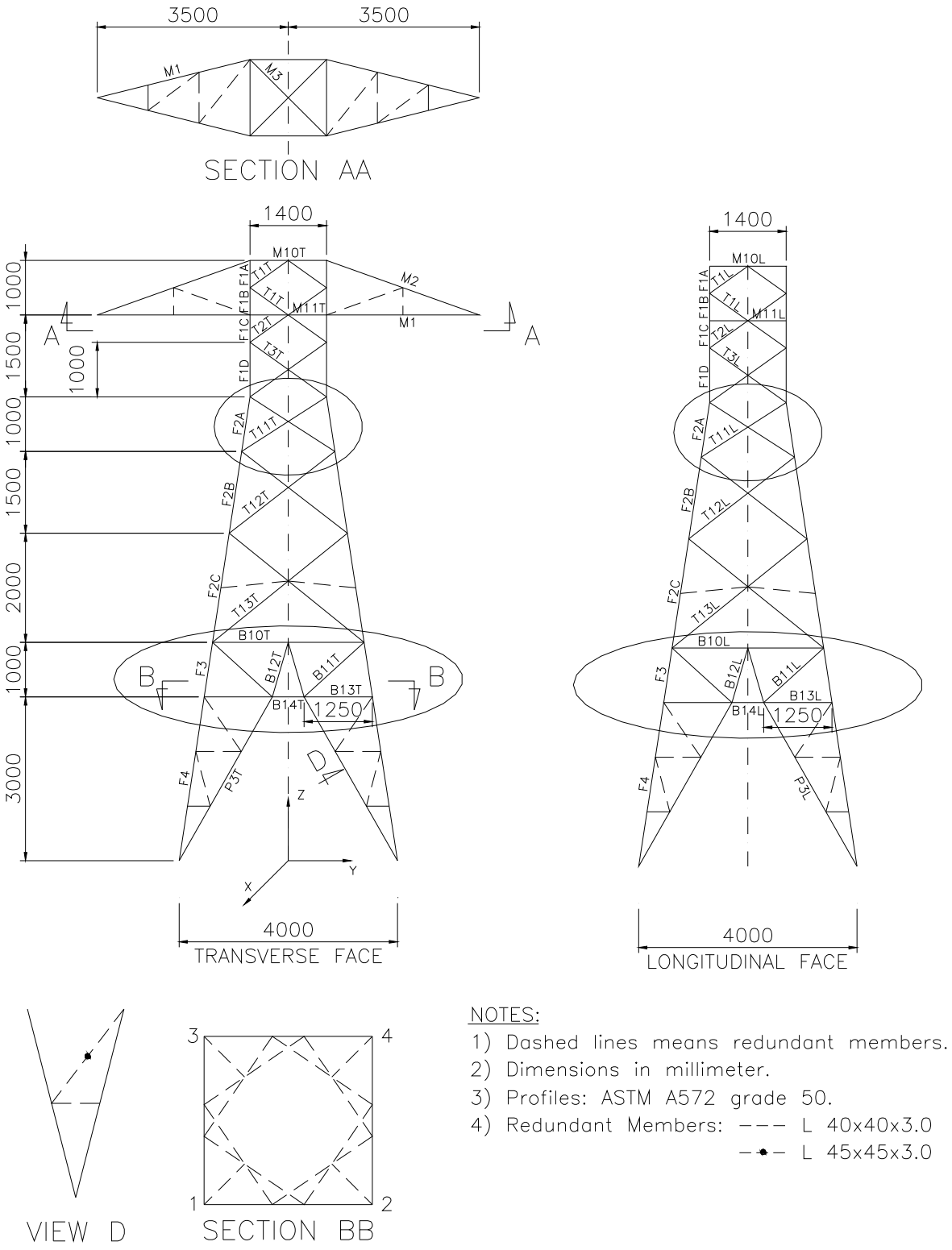

Figure 5: Prototype 2A – Transverse Face, Longitudinal Face and Sections

4.3 Load Cases

The same load cases were proposed for the three prototypes. In order to check the isolated influence of each loading on the behaviour of the prototypes, individual load components (transverse, longitudinal and vertical) acting separately were proposed: vertical (cases 1, 1D), transverse (cases 2, 2D), longitudinal load (cases 3, 3D). An additional load case was also used, with all loads acting together (cases 4, 4D). In addition, the loads were applied in a symmetrical configuration (both sides, cases 1D, 2D, 3D, 4D), or in an asymmetrical configuration (only one side loaded, cases 1, 2, 3, 4). Thus, it was possible to check the influence of the structural modelling on the behaviour of the prototypes for each type of loading. All load cases are shown in Figures 6 to 9.

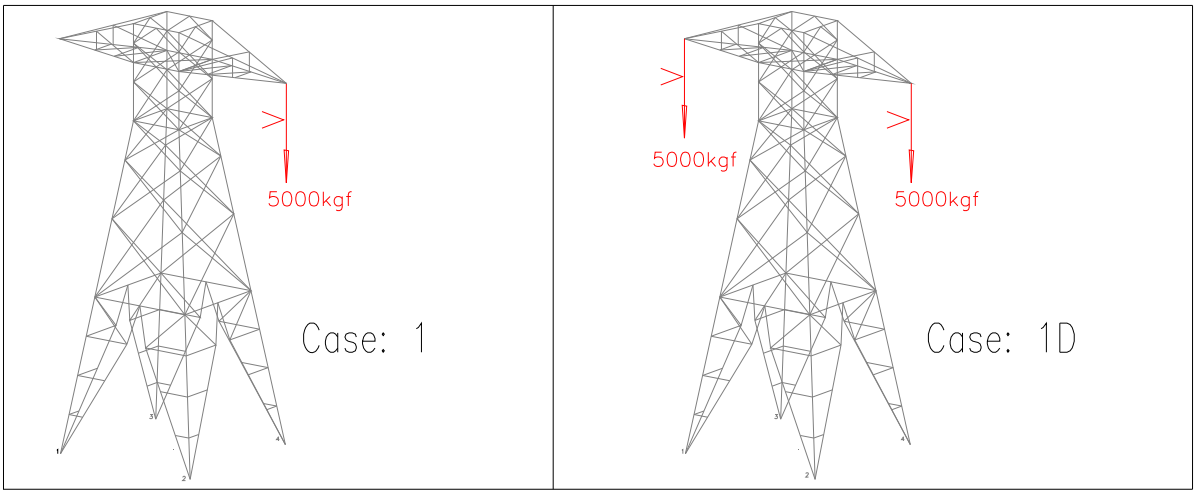

Figure 6: Load Cases 1 and 1D

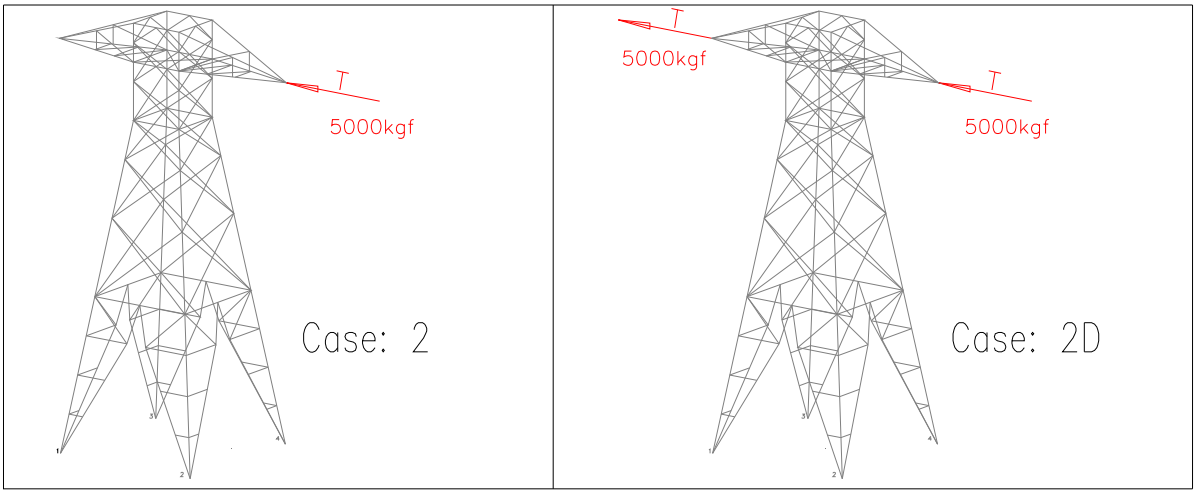

Figure 7: Load Cases 2 and 2D

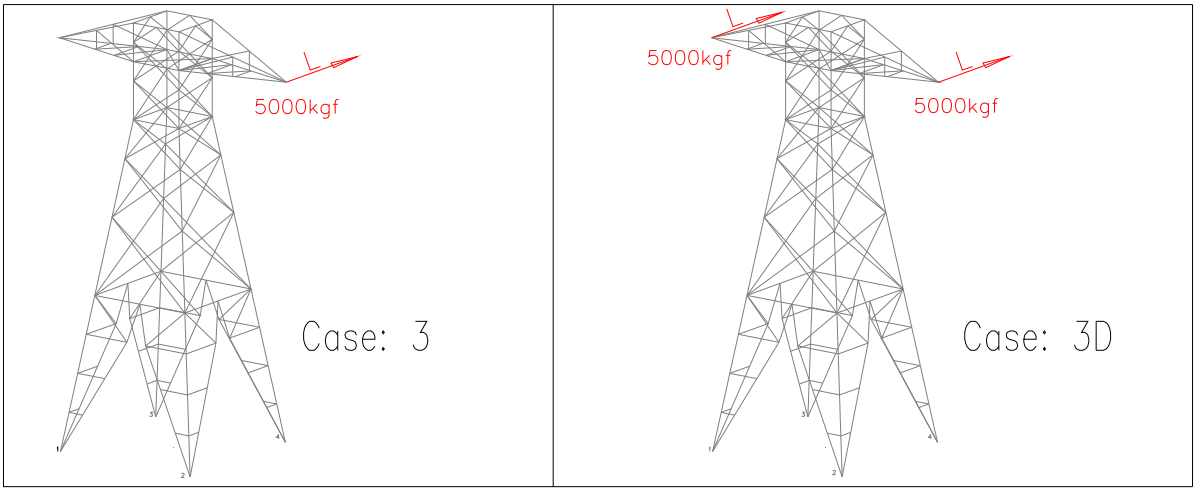

Figure 8: Load Cases 3 and 3D

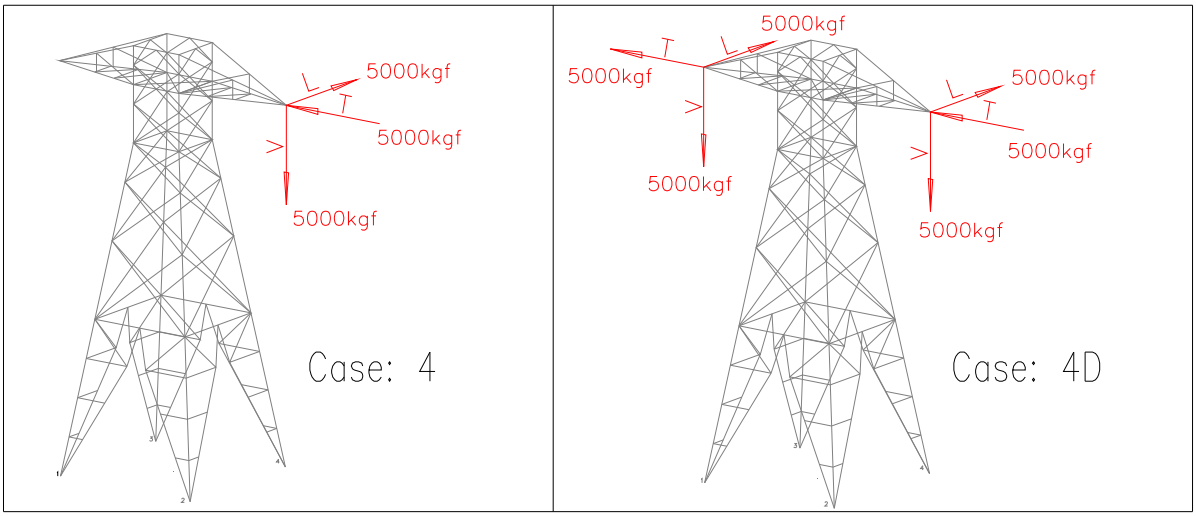

Figure 9: Load Cases 4 and 4D

4.4 Prototypes Detailing

In this study, with the aim of isolating the "variability of structural modelling," an attempt was made to eliminate or attenuate the influence from other sources of discrepancies, which may occur in the structural behaviour, such as: types of loads, quality of the materials, detailing practices, design and manufacturing standards, detailing of the connections, etc. To do this, the three prototypes were developed by the same designer, using the same design standards and practices, types of materials, connections details, etc. The detailed drawings for each prototype are shown on Figures 10 to 18.

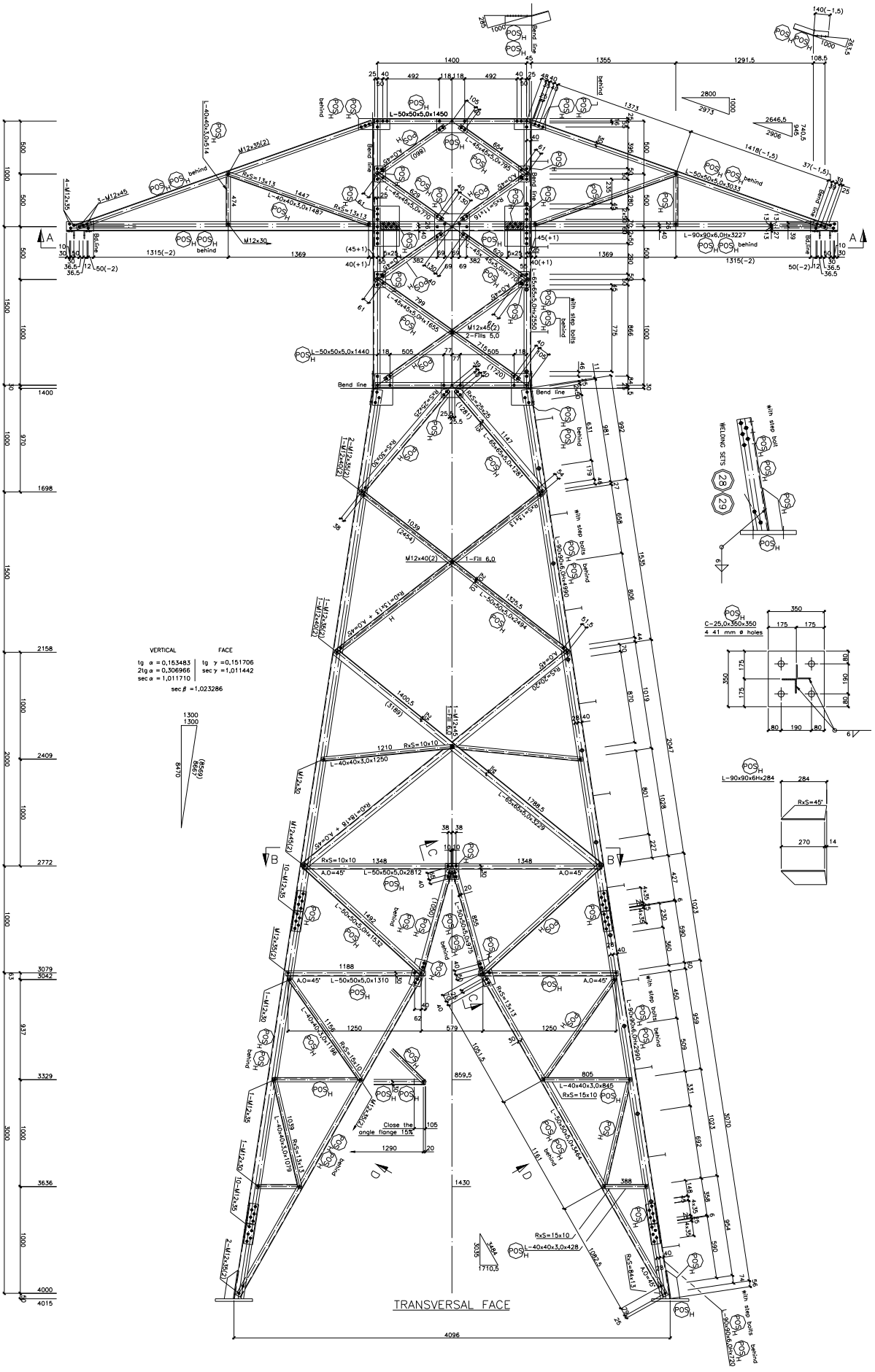

Figure 10: Structure 1 – Transverse Face

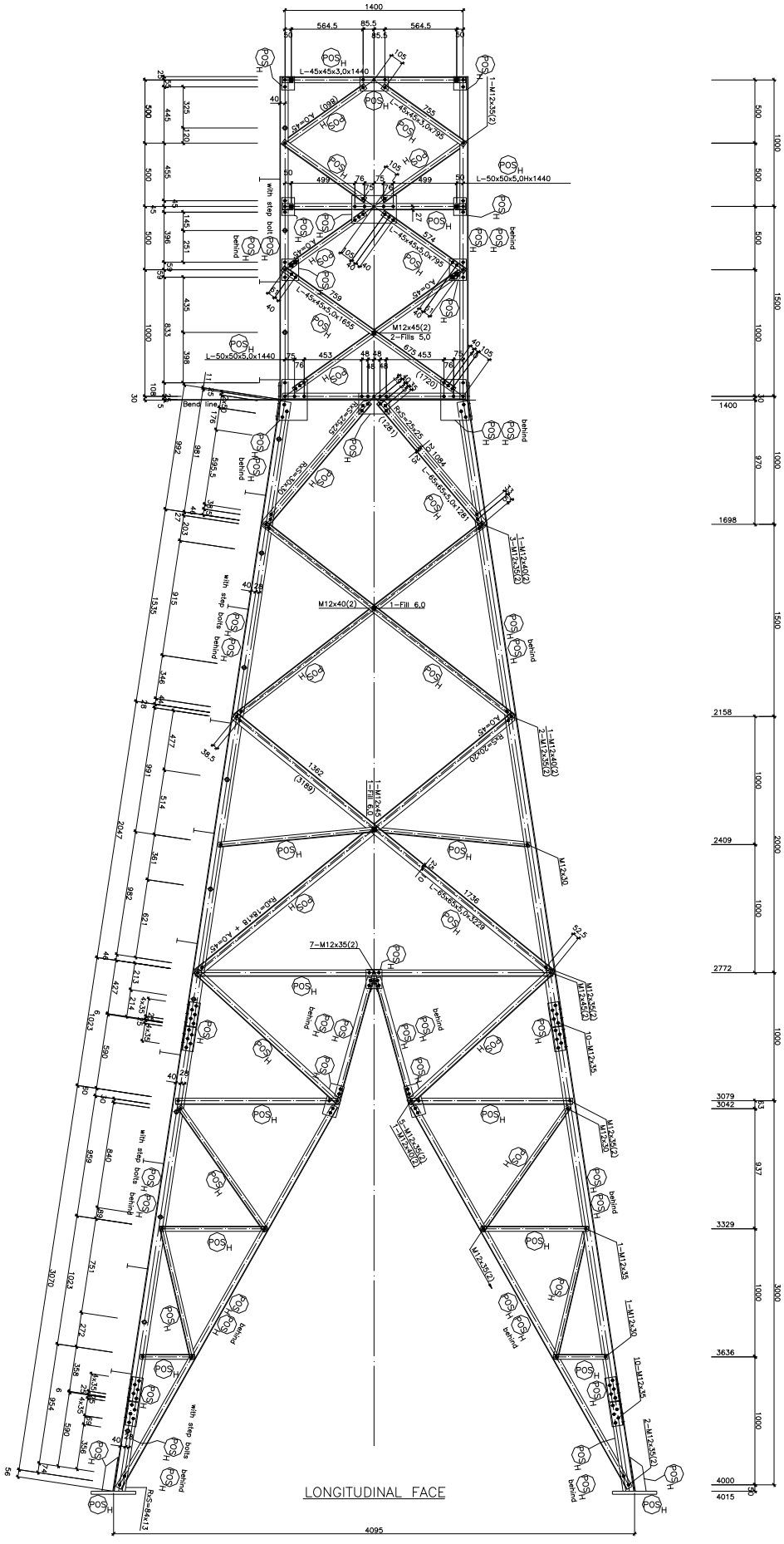

Figure 11: Structure 1 – Longitudinal Face

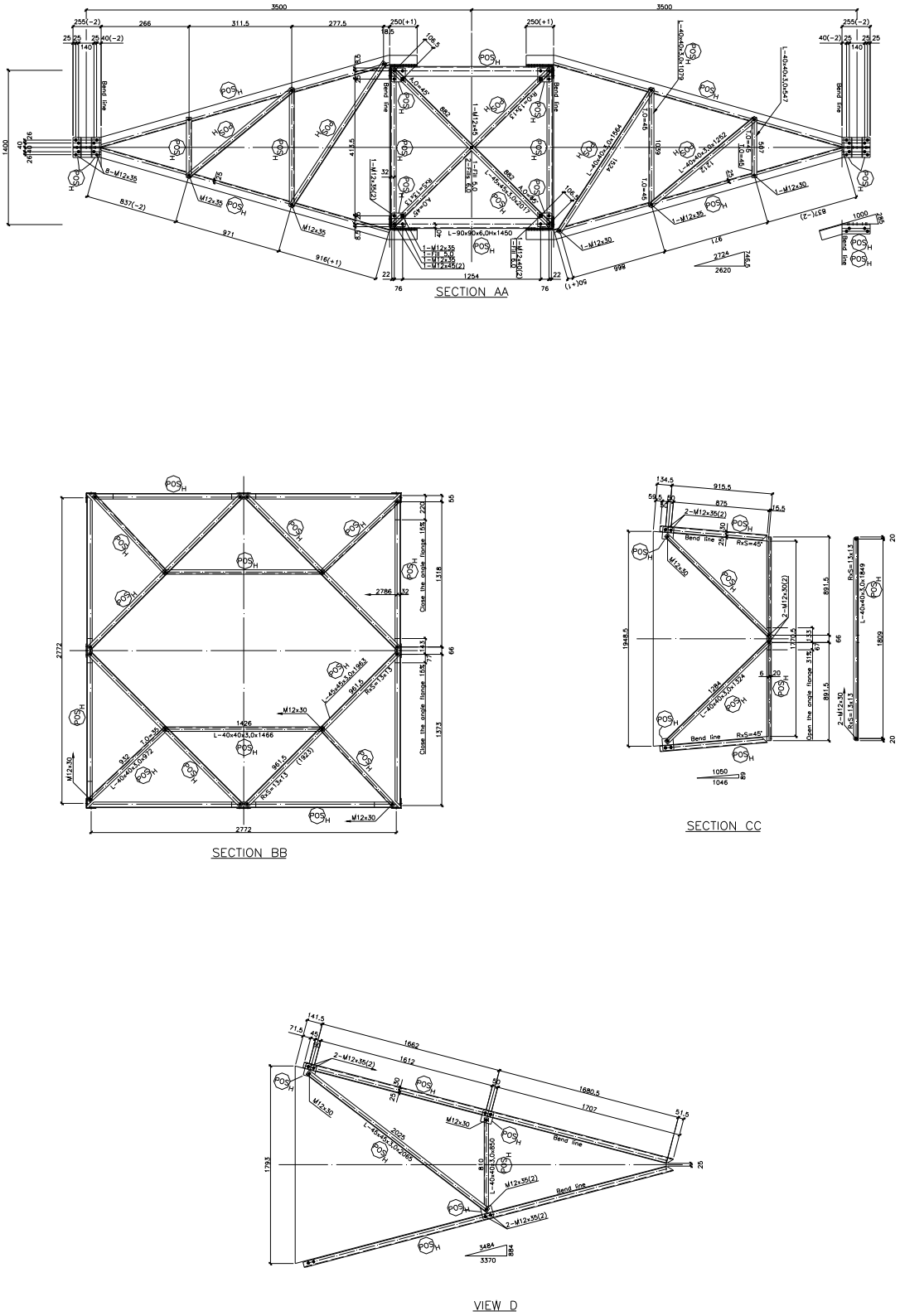

Figure 12: Structure 1 – Sections AA, BB, CC and View D

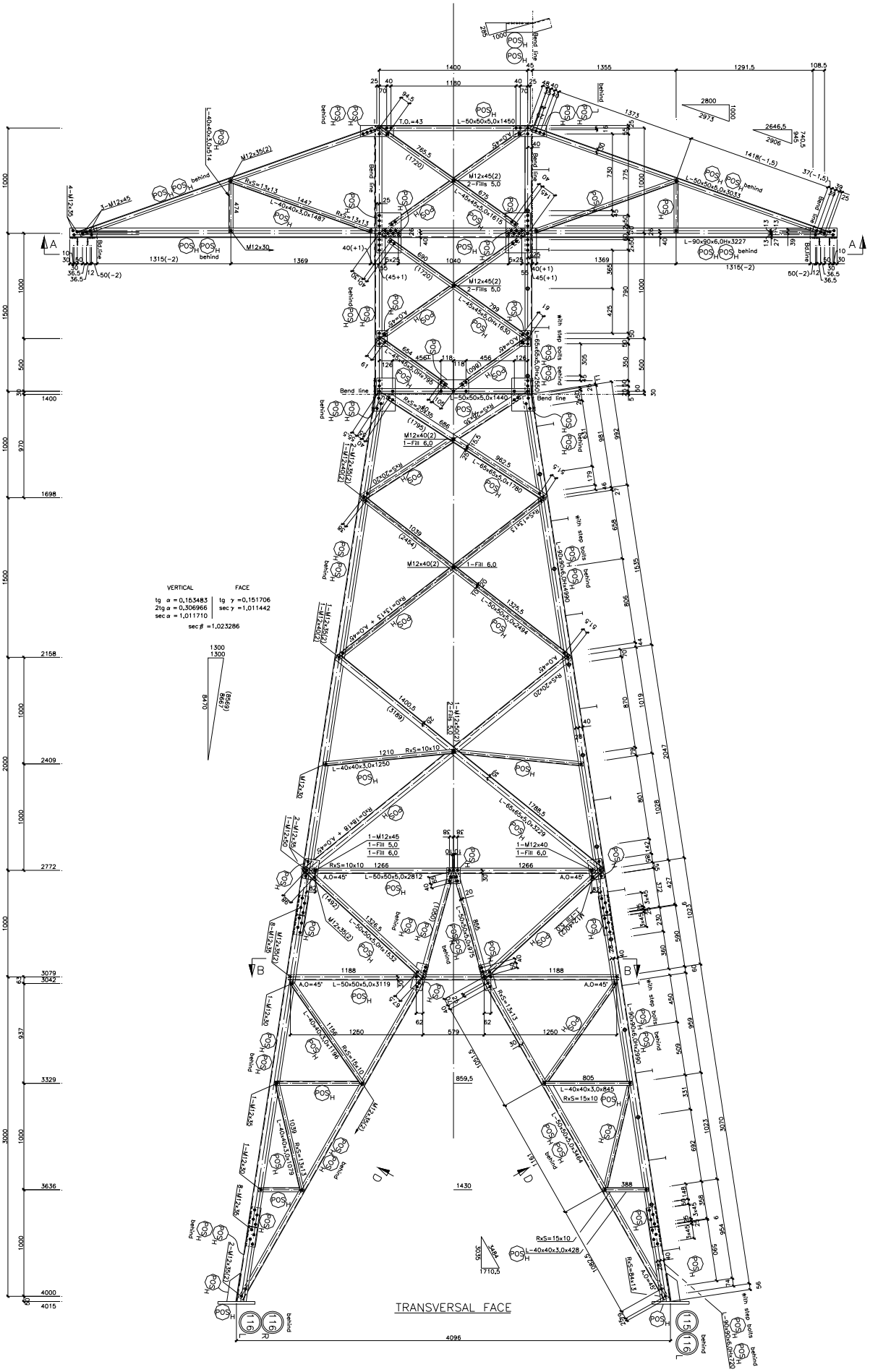

Figure 13: Structure 2 – Transverse Face

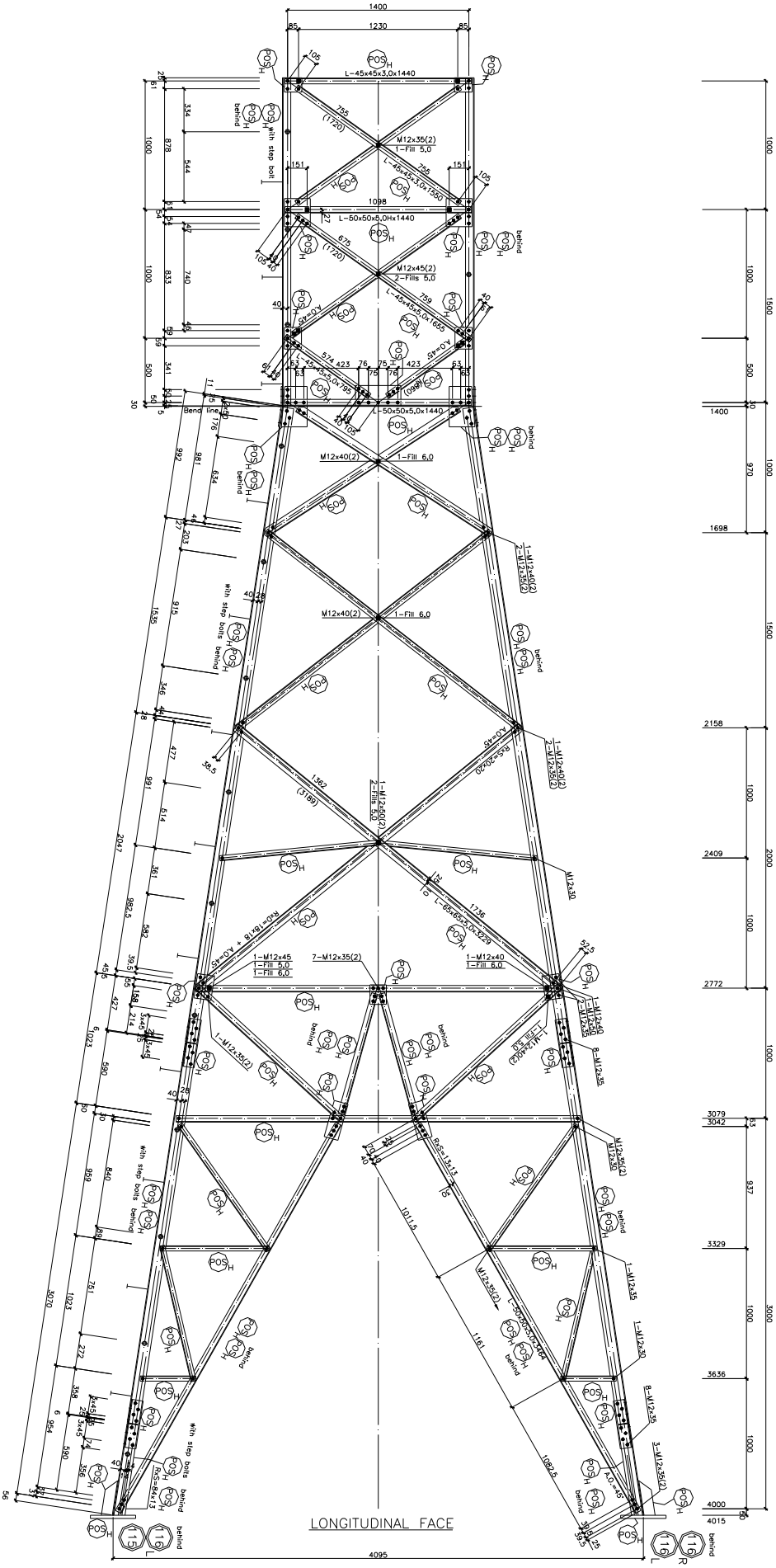

Figure 14: Structure 2 – Longitudinal Face

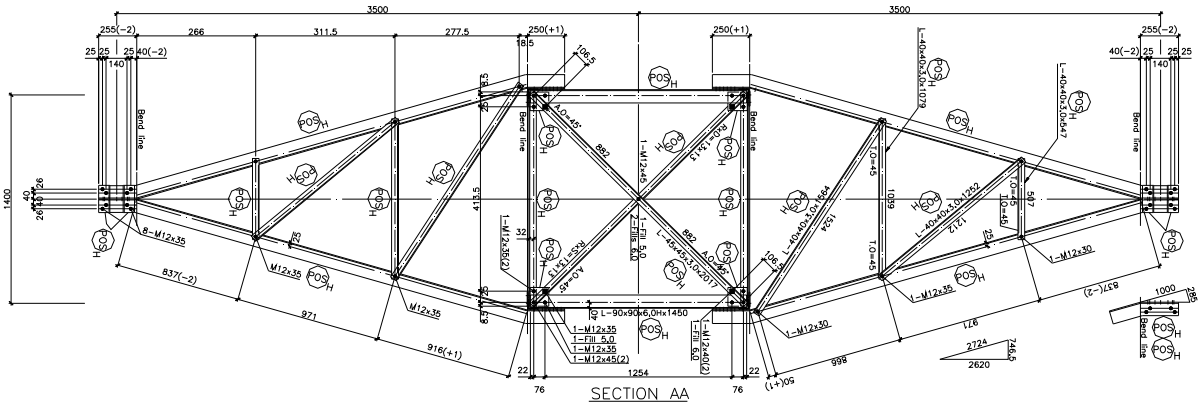

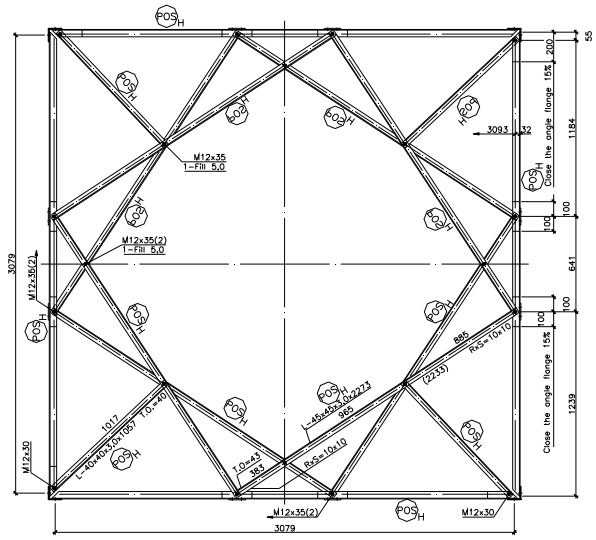

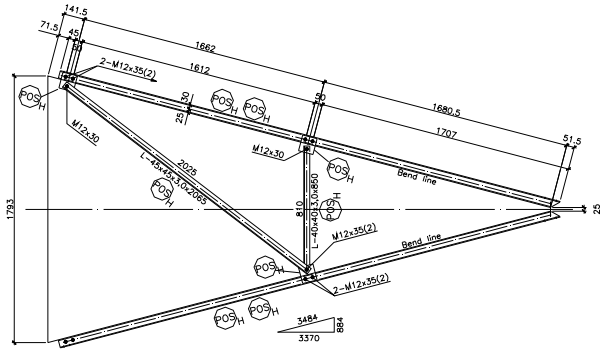

Figure 15: Structure 2 –Section AA, Section BB and View D

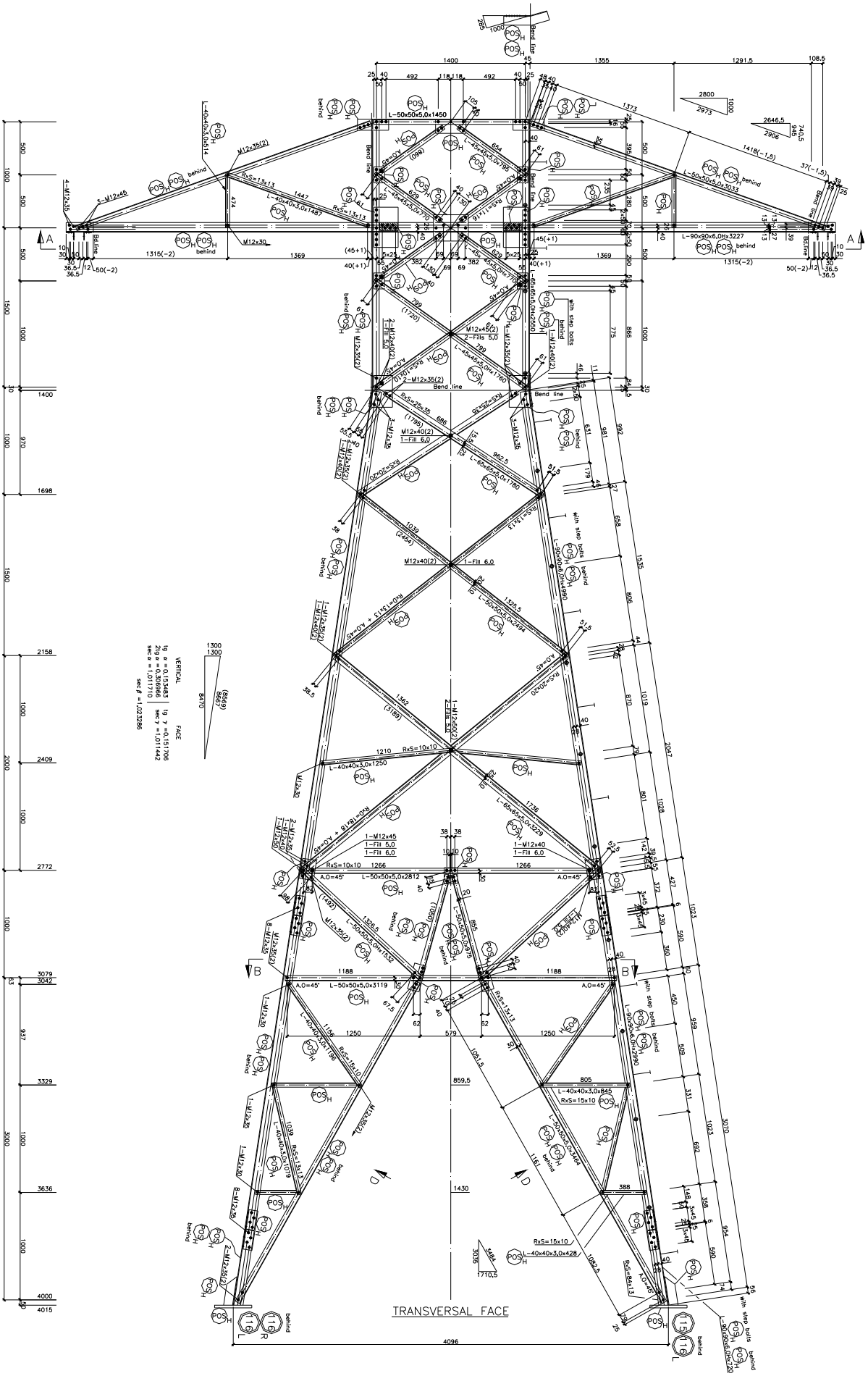

Figure 16: Structure 2A – Transverse Face

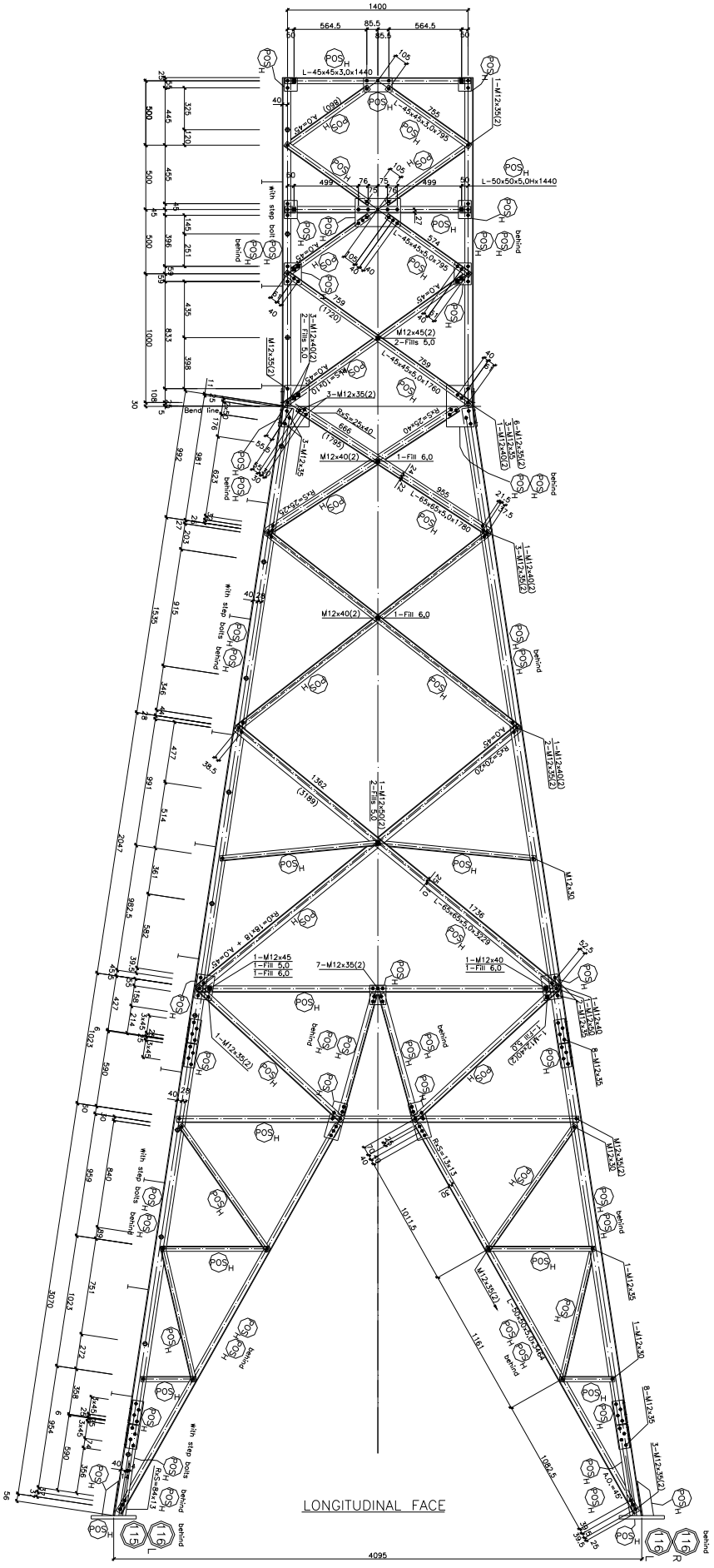

Figure 17: Structure 2A – Longitudinal Face

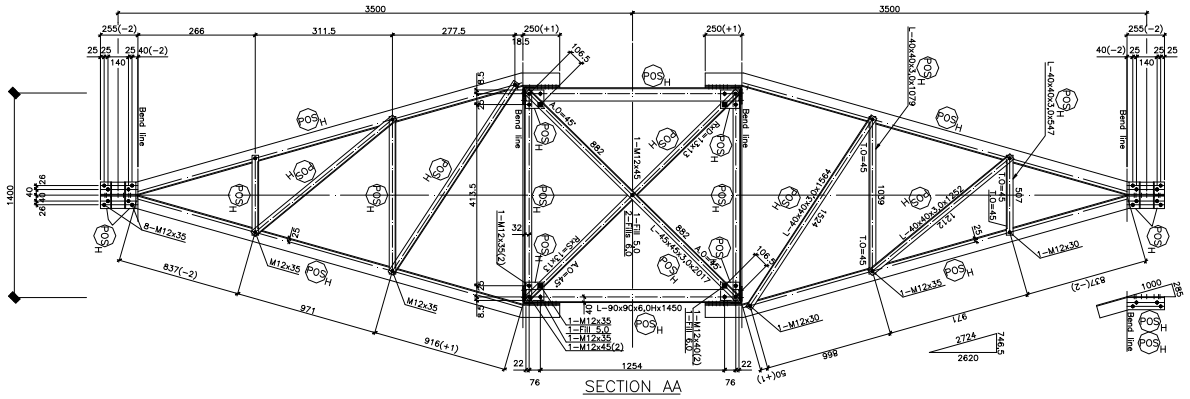

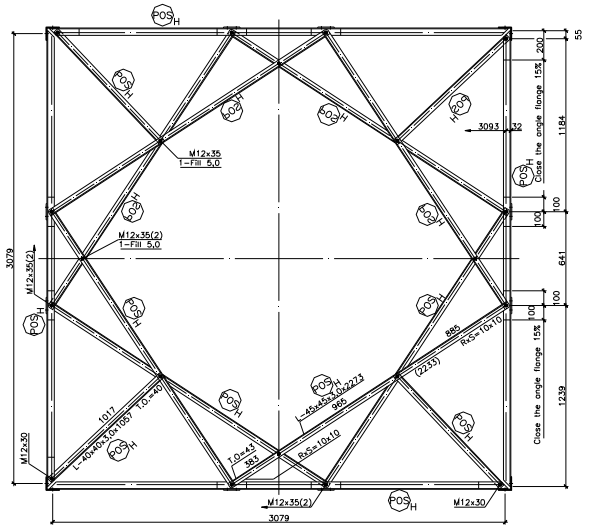

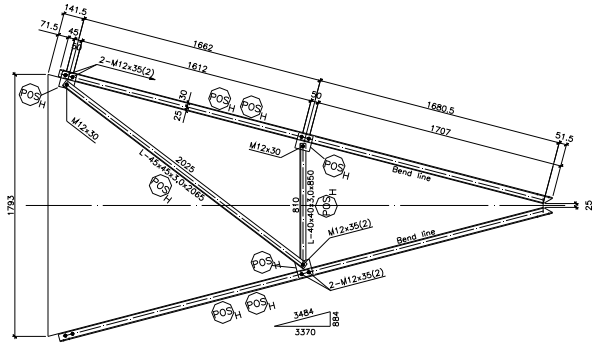

Figure 18: Structure 2A –Section AA, Section BB and View D

5. STRUCTURAL ANALYSIS OF THE PROTOTYPES

5.1 Relevant Information for the Structural Exercise

In order to know the state-of-the-art in terms of structural analysis softwares and, at the same time, achieve representativeness at worldwide level, all the members of the WG08 Working Group were asked to calculate member forces for the three prototypes. All participants started working on the structures whose detail drawings had already been prepared, therefore making them subject to the same degree of accuracy and/or inaccuracy. To be able to make their predictions, all the participants used, however, their own knowledges and structural analysis softwares. To allow everyone to analyze the structures using the same assumptions, a document was produced (which is attached on Annex A), containing the basic information required for the structural analysis, such as: silhouette drawings (Figures 3, 4 and 5), load cases (Figures 6 to 9), angles used for the bars (see Table 1 and Figure 19), types and quantities of bolts in connections (Table 2), detailing drawings (Figures 10 to 18), etc.

Table 1: Angles - Properties for designing

Size and Thickness (mm)	Weight kg/m	Área cm^2	Axis X-X / Y-Y				Axis Z-Z	B/T
			I cm^4	S cm^3	r cm	e_x cm		
L 40 X 40 X 3.0	1.84	2.35	3.45	1.18	1.21	1.07	0.78	10.33
L 40 X 40 X 5.0	2.97	3.79	5.43	1.91	1.2	1.16	0.77	5.8
L 45 X 45 X 3.0	2.09	2.66	4.93	1.49	1.36	1.18	0.88	11.67
L 45 X 45 X 5.0	3.38	4.3	7.84	2.43	1.35	1.28	0.87	6.6
L 50 X 50 X 5.0	3.77	4.8	11	3.05	1.51	1.4	0.97	7.6
L 50 X 50 X 6.0	4.47	5.69	12.8	3.61	1.5	1.45	0.97	6.17
L 65 X 65 X 5.0	4.95	6.31	24.7	5.21	1.98	1.76	1.28	10.2
L 65 X 65 X 6.0	5.91	7.53	29.2	6.21	1.97	1.8	1.27	8.33
L 75 X 75 X 5.0	5.78	7.36	38.6	7.01	2.29	1.99	1.48	12
L 75 X 75 X 6.0	6.87	8.75	45.6	8.35	2.28	2.04	1.47	9.83
L 75 X 75 X 8.0	9.03	11.5	58.9	11	2.26	2.13	1.45	7.12
L 90 X 90 X 6.0	8.3	10.6	80.3	12.2	2.76	2.41	1.78	12.17
L 90 X 90 X 7.0	9.58	12.2	92.4	14.1	2.75	2.46	1.77	10.28

Table 2 shows the angles used in the structures 1, 2 and 2A, indicating for each bar the respective quantity of bolts.

Table 2: Members, angles and bolts in structures 1, 2 and 2A

MEMBERS	ANGLE SIZE	NUMBER OF BOLTS		
		STRUCTURE 1	STRUCTURE 2	STRUCTURE 2A
B10L	L 50 x 50 x 5,0 H	1	2	2
B10T	L 50 x 50 x 5,0 H	1	2	2
B11L	L 50 x 50 x 5,0 H	1	2	2
B11T	L 50 x 50 x 5,0 H	1	2	2
B12L	2L 50 x 50 x 5,0 H	2	2	2
B12T	2L 50 x 50 x 5,0 H	2	2	2
B13L	L 50 x 50 x 5,0 H	1	1	1
B13T	L 50 x 50 x 5,0 H	1	1	1
B14L	L 50 x 50 x 5,0 H	Not Applicable	1	1
B14T	L 50 x 50 x 5,0 H	Not Applicable	1	1
F1A	L 65 x 65 x 5,0 H	4	4	4
F1B	L 65 x 65 x 5,0 H	-	-	-
F1C	L 65 x 65 x 5,0 H	-	-	-
F1D	L 65 x 65 x 5,0 H	4	6	4
F2A	L 90 x 90 x 6,0 H	6	6	6
F2B	L 90 x 90 x 6,0 H	-	-	-
F2C	L 90 x 90 x 6,0 H	-	-	-
F3	L 90 x 90 x 6,0 H	10	8	8
F4	L 90 x 90 x 6,0 H	10	8	8
M1	L 90 x 90 x 6,0 H	7	7	7
M2	L 50 x 50 x 5,0 H	3	3	3
M3	L 45 x 45 x 3,0 H	2	2	2
M10L	L 45 x 45 x 3,0 H	2	2	2
M10T	L 50 x 50 x 5,0 H	3	3	3
M11L	L 50 x 50 x 5,0 H	2	2	2
M11T	L 90 x 90 x 6,0 H	7	7	7
P3L	L 50 x 50 x 5,0 H	2	3	3
P3T	L 50 x 50 x 5,0 H	2	2	2
T1L	L 45 x 45 x 3,0 H	1	1	1
T1T	L 45 x 45 x 5,0 H	2	2	2
T2L	L 45 x 45 x 5,0 H	3	3	3
T2T	L 45 x 45 x 5,0 H	2	2	2
T3L	L 45 x 45 x 5,0 H	3	3	3
T3T	L 45 x 45 x 5,0 H	2	2	2
T5L	L 50 x 50 x 5,0 H	3	3	Not Applicable
T5T	L 50 x 50 x 5,0 H	2	2	Not Applicable
LT11	L 65 x 65 x 5,0 H	3	Not Applicable	Not Applicable
T11L	L 65 x 65 x 5,0 H	Not Applicable	2	3
TT11	L 65 x 65 x 5,0 H	2	Not Applicable	Not Applicable
T11T	L 65 x 65 x 5,0 H	Not Applicable	2	2
T12L	L 50 x 50 x 5,0 H	2	2	2
T12T	L 50 x 50 x 5,0 H	2	2	2
T13L	L 65 x 65 x 5,0 H	2	2	2
T13T	L 65 x 65 x 5,0 H	1	1	2

Notes:

a) Steel for plates: ASTM A36 (σ_y=2530 kgf/cm^2).

b) Steel for profiles: ASTM A572 GRADE 50 (σ_y=3515 kgf/cm^2).

c) Bolt diameter is 12mm (M12).

d) Shear on bolts should be taken through their bodies.

The Figure 19 represents the specified axes which were used in order to indicate the angles on Table 1.

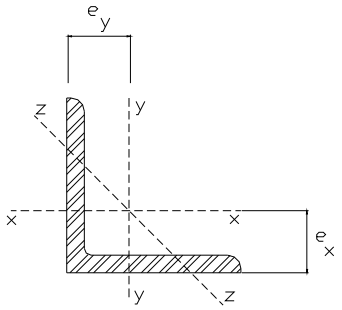

Figure 19: Angle sections used in the prototypes

In order to assess these predictions, the results of the participants are compared. Although they used different softwares, with distinct considerations (mainly in definitions of beam or truss elements and consequently fictitious bars, besides the linear or geometrical non-linear analysis), the obtained member internal forces compared quite similar. The countries and participants involved are cited in Section 5.2.

5.2 Countries and Participants Involved

A significant participation of members of the WG08 at the international level was obtained. Around 24 contributions coming from 13 different countries in all continents were received. Table 3 shows the participants involved and their respective nationalities.

The results of the predictions of each participant were submitted to the members of the WG08 Task Force 4 for evaluation and comparisons. An incredible amount of data was accumulated.

Table 3: Participants involved

Name	Company	Country
Adrian Copoiu	Romelectro Engineering	Romania
Aureo P. Ruffier	Cepel	Brazil
Egill Thorsteins	Linuhonnum Consulting Engineers	Iceland
Ezio Del Bello	Dessau Consultants	Canada
Fábio Andrade / Rosemary Veloso	CHESF	Brazil
Franz Ritky	ABB	Australia
Frédéric Légeron	University of Sherbrooke	Canada
Geir Nesgard	Norconsult A/S	Norway
Henry Hawes	Powerlink Queensland	Australia
Jan Rogier / André Herman	Bel Engineering	Belgium
José Fernandez	FUNTAM	Spain
Jose Peralta	REN–Rede Elétrica Nacional SA	Portugal
José Serrano	ESKOM	South Africa
Kai Nieminen	Ivo Power Engineering Ltda	Finland
Leon Kempner	BPA – Boneville Power	USA
Luc Binette	Hydro Quebec	Canada
Paulo Liberato	Engetower	Brazil
João BGF Silva / Rania Peixoto	ABB / DAMP Electric	Brazil
Roger Jansson	Vattenfall Transmission AB	Sweden
Rogério Guimarães	ABB / SAE Towers	Brazil
Ruy Menezes	UFRGS	Brazil
S.Kitipornchai / FGA Albermani	University of Queensland	Australia
Tapio Leskinen	Fortum	Finland

5.3 Structural Modelling Used

As mentioned earlier, each participant used his own knowledge and analysis software. In this aspect, some particular modelling characteristics were used by each engineer (geometric linear or non-linear analysis, definition of truss or beam bars and positioning of fictitious bars, for example).

For simplification reasons, here in this item and in the following items 6 and 7, only the results of some representative members of the prototypes will be shown: main member (F4), longitudinal diagonal (T13L) and transverse diagonal (B11T).

As was mentioned earlier, the obtained internal forces provided by the different engineers showed quite similar comparison. Figures 20 to 28 show a unique line because individual results are almost coincident.

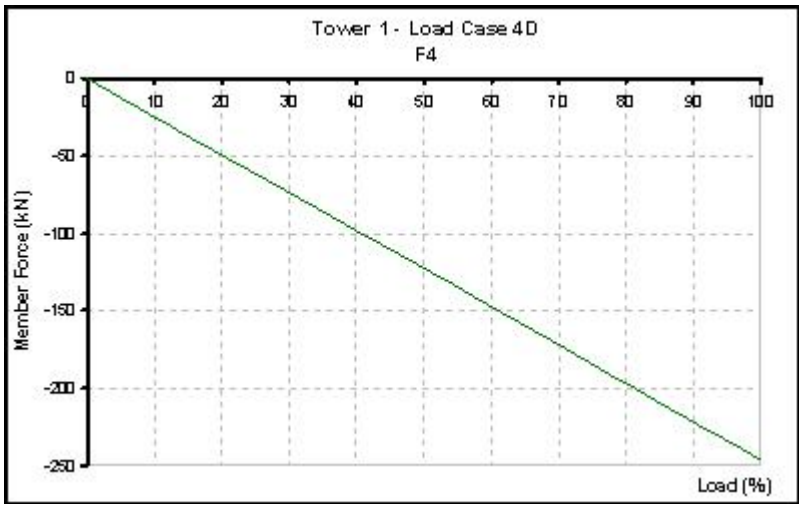

Figure 20: Results of calculation of member F4, for prototype 1, and LC 4D

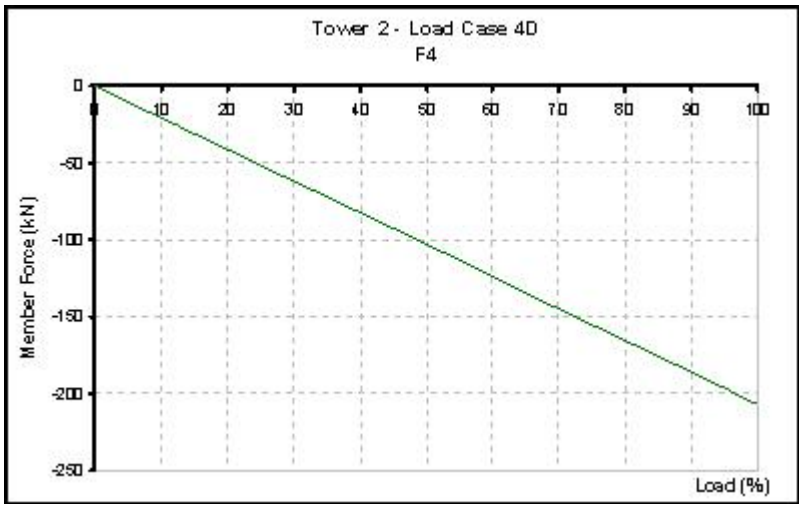

Figure 21: Results of calculation of member F4, for prototype 2, and LC 4D

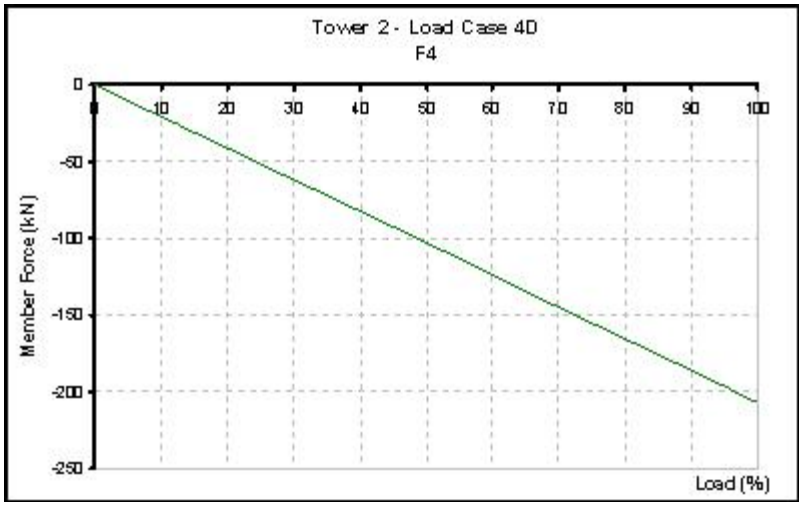

Figure 22: Results of calculation of member F4, for prototype 2, and LC 4D

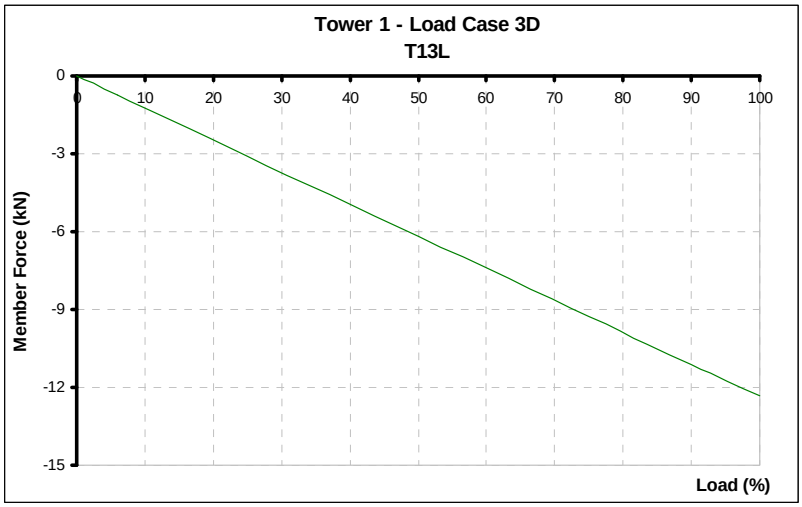

Figure 23: Results of calculation of member T13L, for prototype 1, and LC 3D

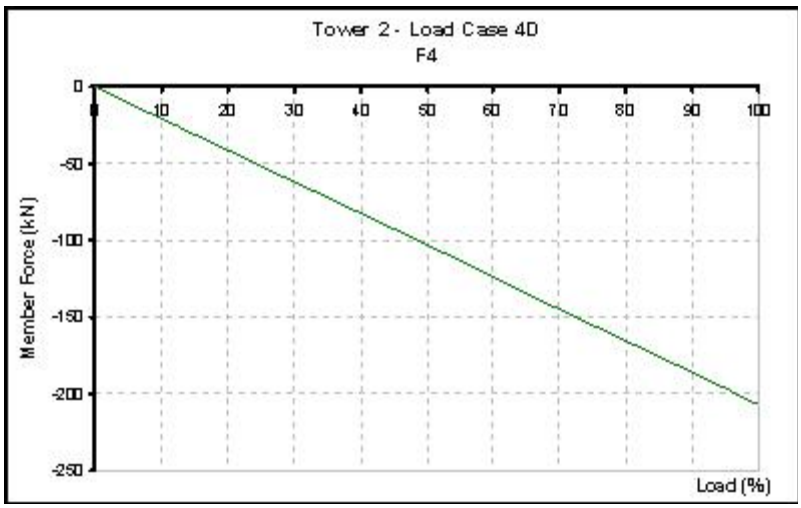

Figure 24: Results of calculation of member T13L, for prototype 2, and LC 3D

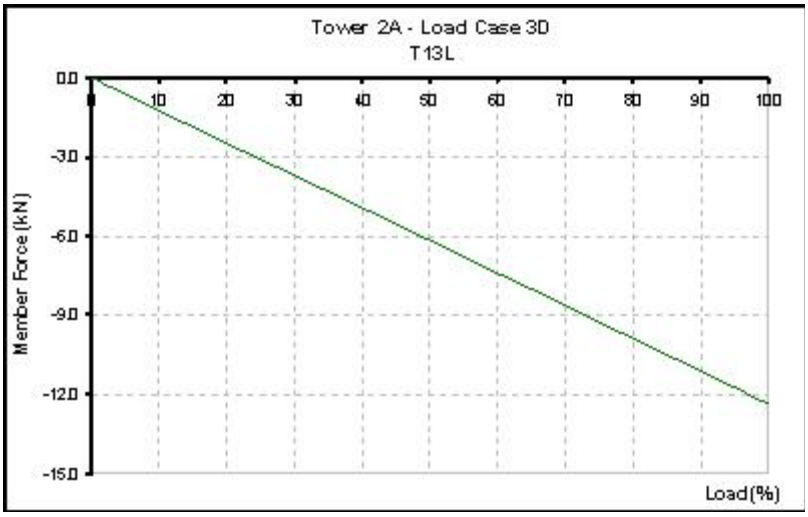

Figure 25: Results of calculation of member T13L, for prototype 2A, and LC 3D

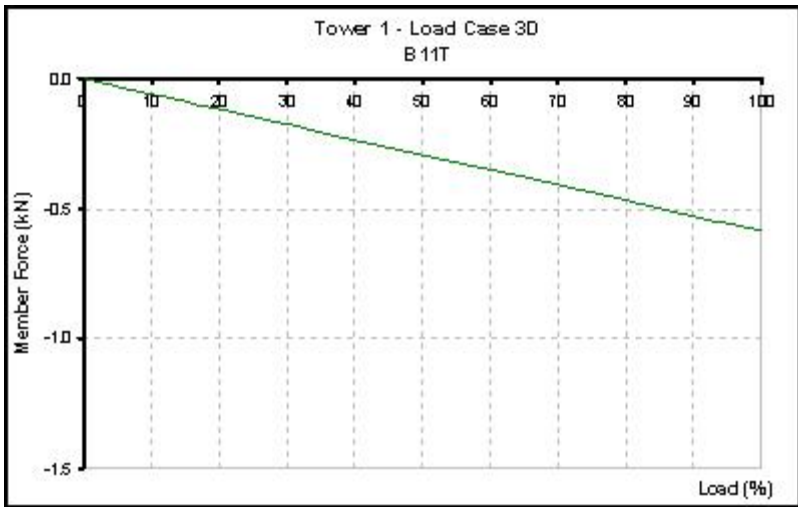

Figure 26: Results of calculation of member B11T, for prototype 1, and LC 3D

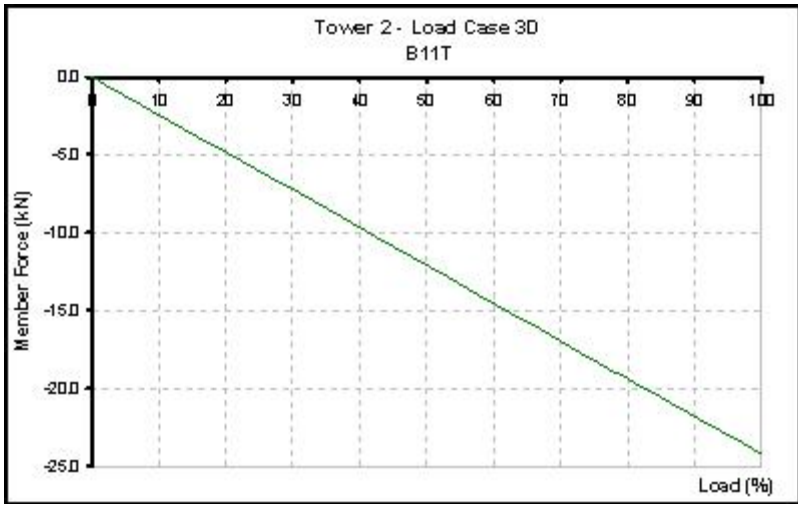

Figure 27: Results of calculation of member B11T, for prototype 2, and LC 3D

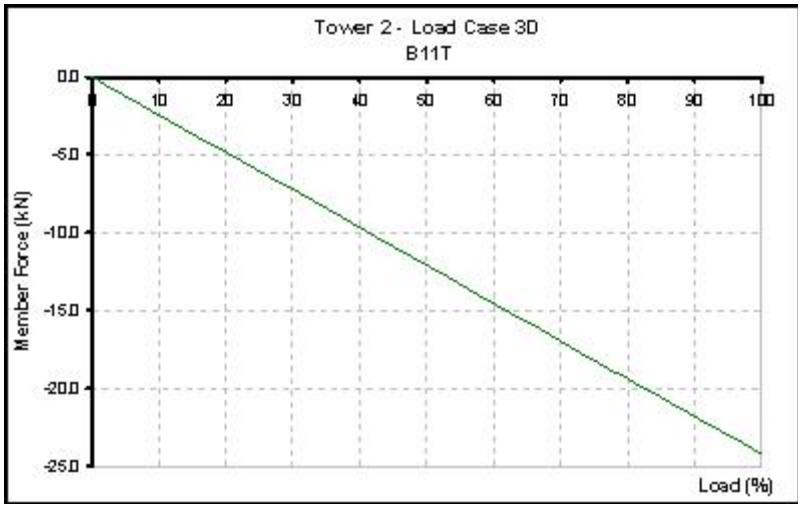

Figure 28: Results of calculation of member B11T, for prototype 2A, and LC 3D

6. PROTOTYPE FABRICATION

6.1 Steel, Angles and Bolts Used

The standards used for the structural calculations were also specified by agreement, as ASCE 10/97 for Design/Calculation, ASTM A572 GR50 for angles steel, ASTM A36 for plates and ISO 898-1 for Bolts. The list of the geometrical properties of the angles used is shown at Table 1, in accordance with the axes specified in Figure 19.

6.2 Prototype Fabrication

The structures were fabricated by the company ABB in Brazil and donated to the Cigré for the purpose of conducting this research. A special attention was used during fabrication in order that all parts and pieces presented a finishing free of edges, burrs, imperfections, rugged or dilacerated edges. The fabrication operations (cutting, punching, bending, abrading, welding, marking, etc.) were completely executed prior to hot dip galvanizing.

After the galvanization, the diameters of the holes were, at most, 1.6mm (1/16") larger than the nominal diameter of the bolts. All holes were spaced with accuracy and correctly marked over the punching axis on the pieces, obeying the dimensions of the drawings. The maximum allowed variation for the dimensions, as regards to the values indicated in the drawings, for all holes of the bolts, was 0.8mm (1/32"), for the spacing between holes and 1.6mm (1/16"), for the diameter of the holes. Markings were made in the external part of the bars in order to avoid that similar pieces destined to different supports were mixed. Besides that, all pieces of the structures were hot dip galvanized, in accordance to ASTM A123, A153 and A143 standard, after the operations of cutting, punching, bending, abrading, marking and cleaning.

Prototypes 1, 2 and 2A are shown in Figures 29, 30 and 31.

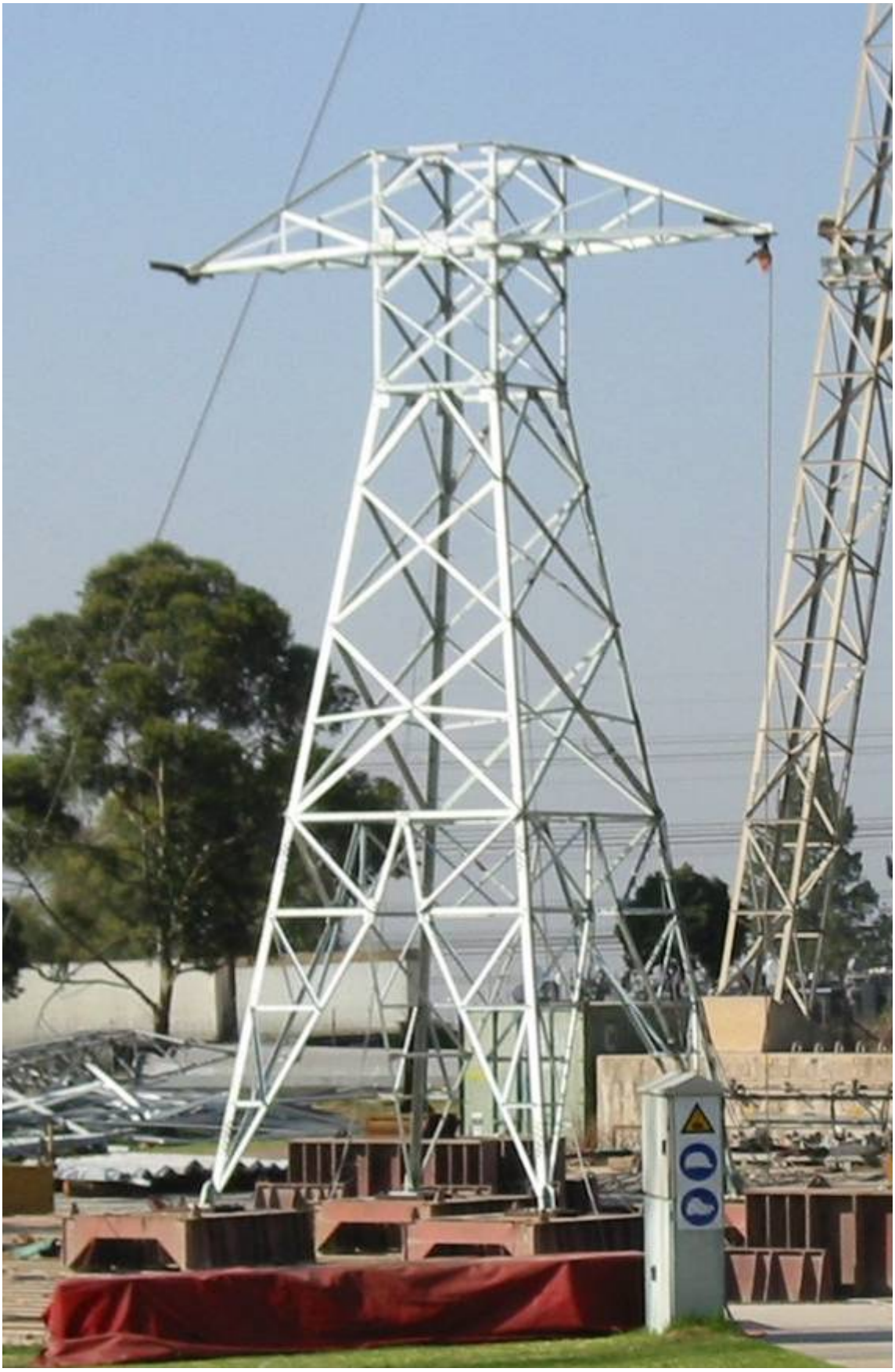

Figure 29: Prototype 1

Figure 30: Prototype 2

Figure 31: Prototype 2A

Figure 32 shows a comparison between the mathematical model, the detailing and the real structure for the node that connects bars F2C, F3, B11T, B11L, T13T, T13L. As can be observed, attention was used in order to minimize the eccentricities of the real structure.

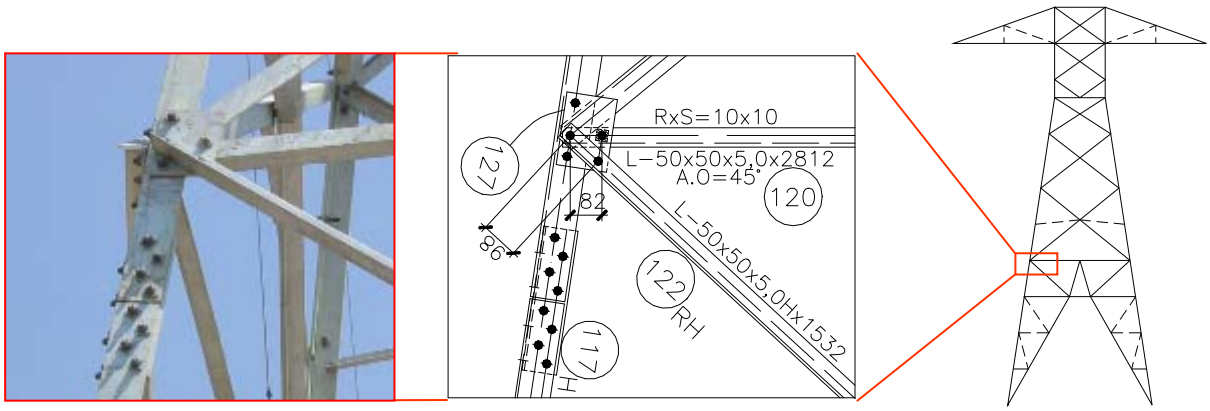

Figure 32: Typical connection detailing.

6.3 Quality of the Material, Statistical Treatment

In order to evaluate the quality (yield and tensile strengths) of the material used on the prototypes, five samples of each angle size were submitted to tension tests. The certificate with the obtained results is shown in Figure 33.

After the samples were tested, a statistical study was carried out. The yield strength was adjusted with a Rayleigh shifted distribution while for tensile strength the best adjusted occurred with a Gumbel distribution.

These curves were used to apply the softwares MORENA and PBA/CVA, which use probabilistic concepts. In this way, as the statistical distributions of the members are known, the distribution of member parameters in the structural analysis is considered.

Figures 34 and 35 show the statistical distributions for yield and tensile strength.

ABB LTDA

Cliente/ Client : CIGRÉ
Certificado/Certificate Nº 10834
Boletim/Our Order : 6175
Assunto/Object : Comprovação de qualidade
Data/Date: 31/08/2001

TESTE DE TRAÇÃO
TENSION TEST

CONFORME NORMA ASTM A370
AS PER SPEC

CORPO DE PROVA Nº SAMPLE	Nº POSIÇÃO PIECE MARK CORRIDA HEAT	SEÇÃO SECTION SIZE (mm)	QUALIDADE DO AÇO STEEL QUALITY	** L. E. Y. S. (MPA)	** L. R. T. S. (MPA)	** A. L. % E L % (EM 200 mm) (*EM 50mm)
CR 687Z	41189261	L 40 X 40 X 3,0	ASTM A572 GR50	412	539	*34,0
CR 687Z	41189261	L 40 X 40 X 3,0	ASTM A572 GR50	393	528	*31,2
CR 687Z	41189261	L 40 X 40 X 3,0	ASTM A572 GR50	385	524	*30,8
CR 687Z	41189261	L 40 X 40 X 3,0	ASTM A572 GR50	433	602	*29,4
CR 687Z	41189261	L 40 X 40 X 3,0	ASTM A572 GR50	429	563	*27,6
CR 181Z	41188282	L 45 X 45 X 3,0	ASTM A572 GR50	405	540	*30,0
CR 181Z	41188282	L 45 X 45 X 3,0	ASTM A572 GR50	427	562	*32,0
CR 181Z	41188282	L 45 X 45 X 3,0	ASTM A572 GR50	393	528	*32,0
CR 181Z	41188282	L 45 X 45 X 3,0	ASTM A572 GR50	422	597	*30,0
CR 181Z	41188282	L 45 X 45 X 3,0	ASTM A572 GR50	385	519	*30,4
CR 440Z	41227298	L 45 X 45 X 5,0	ASTM A572 GR50	381	522	*32,0
CR 440Z	41227298	L 45 X 45 X 5,0	ASTM A572 GR50	385	520	*34,6
CR 440Z	41227298	L 45 X 45 X 5,0	ASTM A572 GR50	395	531	*27,6
CR 440Z	41227298	L 45 X 45 X 5,0	ASTM A572 GR50	406	538	*26,0
CR 440Z	41227298	L 45 X 45 X 5,0	ASTM A572 GR50	413	546	*33,8
CR 501Z	41228055	L 50 X 50 X 5,0	ASTM A572 GR50	422	535	*27,2
CR 501Z	41228055	L 50 X 50 X 5,0	ASTM A572 GR50	413	538	*31,6
CR 501Z	41228055	L 50 X 50 X 5,0	ASTM A572 GR50	398	532	*31,0
CR 501Z	41228055	L 50 X 50 X 5,0	ASTM A572 GR50	392	521	*30,4
CR 501Z	41228055	L 50 X 50 X 5,0	ASTM A572 GR50	395	529	*28,8
CR 381Z	130450	L 65 X 65 X 5,0	ASTM A572 GR50	421	543	27,0
CR 381Z	130450	L 65 X 65 X 5,0	ASTM A572 GR50	418	526	23,0
CR 381Z	130450	L 65 X 65 X 5,0	ASTM A572 GR50	396	501	24,5
CR 381Z	130450	L 65 X 65 X 5,0	ASTM A572 GR50	425	535	26,0
CR 381Z	130450	L 65 X 65 X 5,0	ASTM A572 GR50	408	521	31,5
CR 633Z	41156663	L 75 X 75 X 6,0	ASTM A572 GR50	406	549	27,0
CR 633Z	41156663	L 75 X 75 X 6,0	ASTM A572 GR50	395	528	27,0
CR 633Z	41156663	L 75 X 75 X 6,0	ASTM A572 GR50	393	523	27,0
CR 633Z	41156663	L 75 X 75 X 6,0	ASTM A572 GR50	385	492	27,5
CR 633Z	41156663	L 75 X 75 X 6,0	ASTM A572 GR50	387	521	26,0
CR 331Z	41162209	L 90 X 90 X 6,0	ASTM A572 GR50	391	523	26,5
CR 331Z	41162209	L 90 X 90 X 6,0	ASTM A572 GR50	372	493	25,0
CR 331Z	41162209	L 90 X 90 X 6,0	ASTM A572 GR50	374	503	26,5
CR 331Z	41162209	L 90 X 90 X 6,0	ASTM A572 GR50	396	531	25,0
CR 331Z	41162209	L 90 X 90 X 6,0 *********	ASTM A572 GR50	375	508	23,0

Notas / Notes:
1) MATERIAL UTILIZADO NA FABRICAÇÃO DAS TORRES DO PROJETO CIGRÉ.
2) ESTRUTURAS TIPOS: STRUCTURE 1 (ST1), STRUCTURE 2 (ST2) e STRUCTURE 2A (T2A).
3) CERTIFICADOS DE ORIGEM EM ANEXO.

ABB LTDA
Hideraldo de Souza Andrade
PTHV/LQ - LABORATÓRIO

ABB LTDA
Geraldo Donizete Pinto
PTHV/LQ - QUALIDADE

CLIENTE / CLIENT

**L E => Limite de escoamento. **L R => Limite de ruptura. **A L => Alongamento.
**Y S => Yield strength. **T S => Tensile strength. **E L => Elongation.

C:\EXCEL\CERTIFIC\TRA_LAM.XLS

Figure 33: Sample tension test results

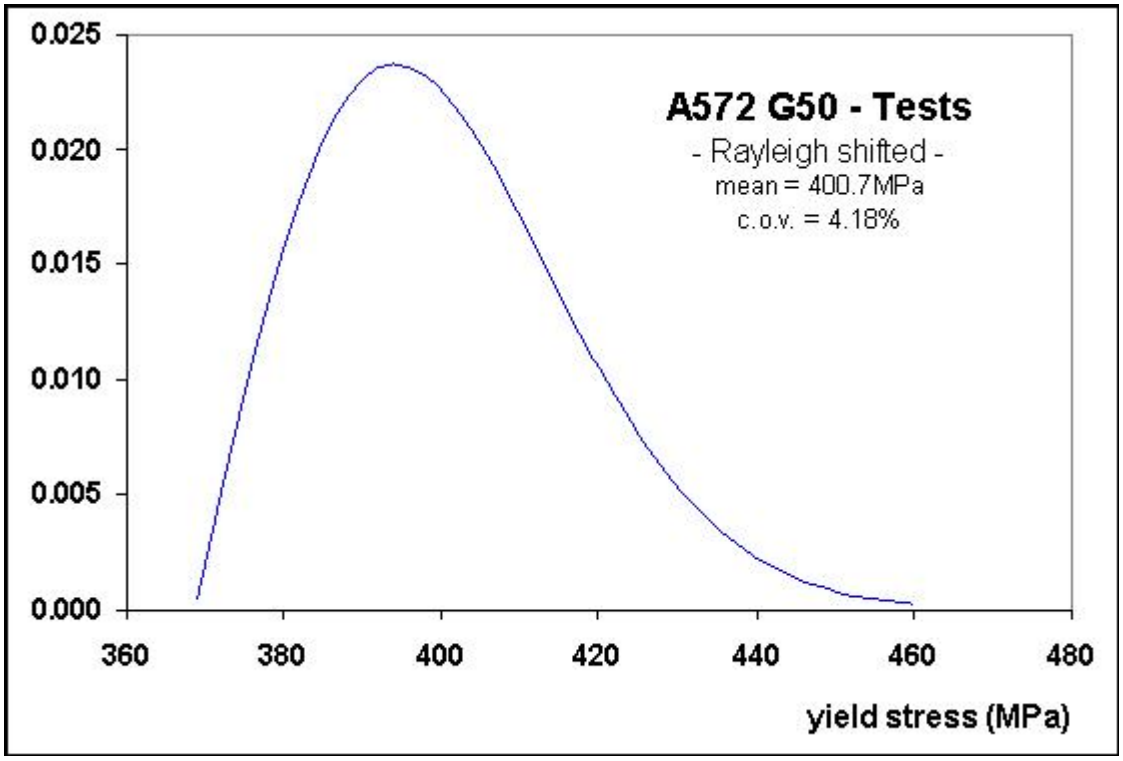

Figure 34: Yield stress statistical distribution.

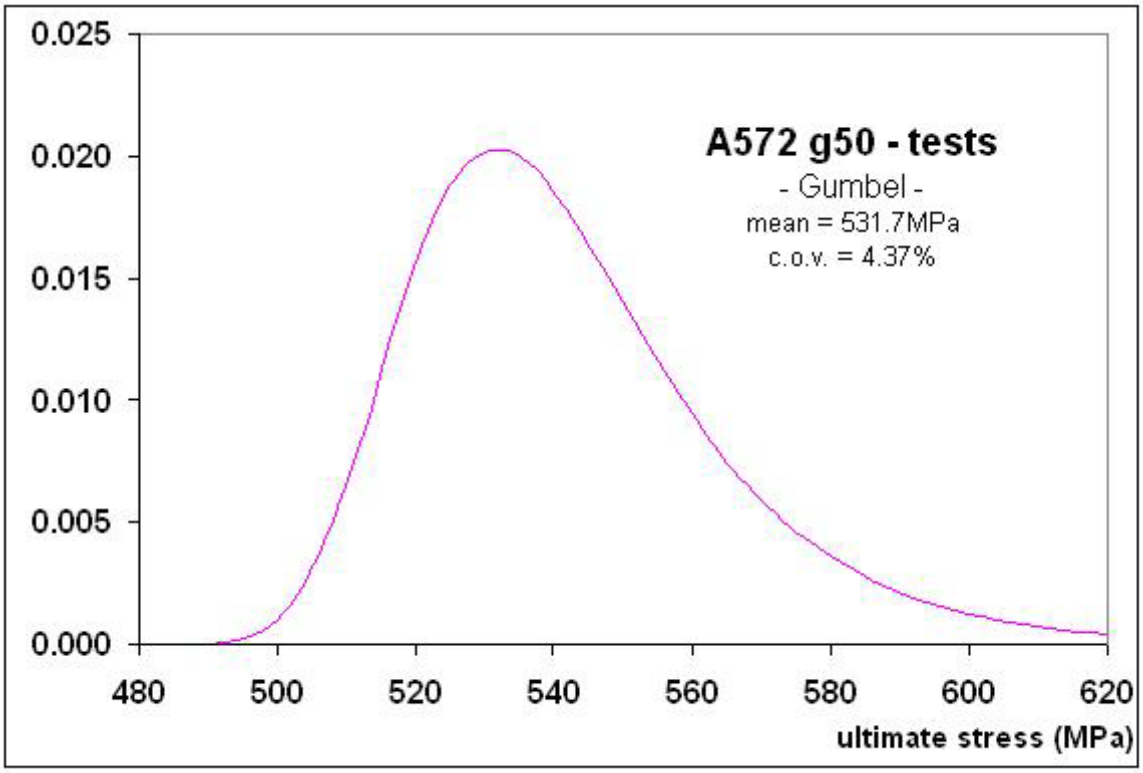

Figure 35: Ultimate stress statistical distribution.

7. PROTOTYPE TESTS

7.1 Relevant Tests Data

The tests on the prototypes were performed (also as a donation) at the Eskom Transmission Group test station, located in South Africa, in October/November, 2001 (Fig. 36), which has the following equipment:

- crane for erection of up to 70m high structures, with lifting capacity of up to 80kN (≅8tf);
- three metallic frames for application of loads on the structure;
- "universal" foundations, that is, a block with large dimensions, with rails to allow anchoring the tower feet up to 24m wide. The maximum allowable reactions, for each leg of the structure, are: 7310kN in compression and 6170kN in tension, simultaneously with 1560kN of horizontal reaction.
- system of load application with 36 hydraulic jacks and remote control from the control house.
- electronic remote system of data acquisition for applied loads and deformation in the bars.

Figure 36: *ESKOM* Test station facilities.

The three towers were tested with all the eight load cases mentioned in chapter 4 and shown in Figures 6 to 9, which are the design loads. The loads were applied in a simultaneous and gradual way, with load application velocities in the order of 1500N/min. In these tests the stresses on the selected bars were determined and also the displacements at points A, B, C and D, identified in Figures 39 to 40, for the following levels of load: 25%, 50%, 75%, 90% and 100% of the design loads. At last, tests to evaluate the capacity of each tower for load case 4D were performed. Figure 37 shows prototype 1 as erected at the test station for load application testing.

Figure 37: Prototype 1 under tests.

7.2 Monitored Members

As mentioned before, during the tests on the prototypes, a real-time monitoring was performed on some of the bars with the purpose of obtaining the actual stresses acting on them. Such monitoring was made through the installation of sophisticated strain-gages (Fig. 38) systems, installed on selected structural members.

These bars were identified as following:

• Prototype 1:

Main bars: F2B and F4;

Diagonals: T11T, L11T, T12T, T12L, T13L, B11T, B11L;

Leg Diagonal: P3L.

• Prototype 2:

Main bars: F2B and F4;

Diagonals: T11T, T11L, T12T, T12L, T13L, B11T, B11L;

Leg Diagonal: P3L.

• Prototype 2A:

Main bars: F2B and F4;

Diagonals: T11T, T11L, T12T, T12L, T13L, B11T, B11L;

Horizontal bars: B14T and B14L;

Leg Diagonal: P3L.

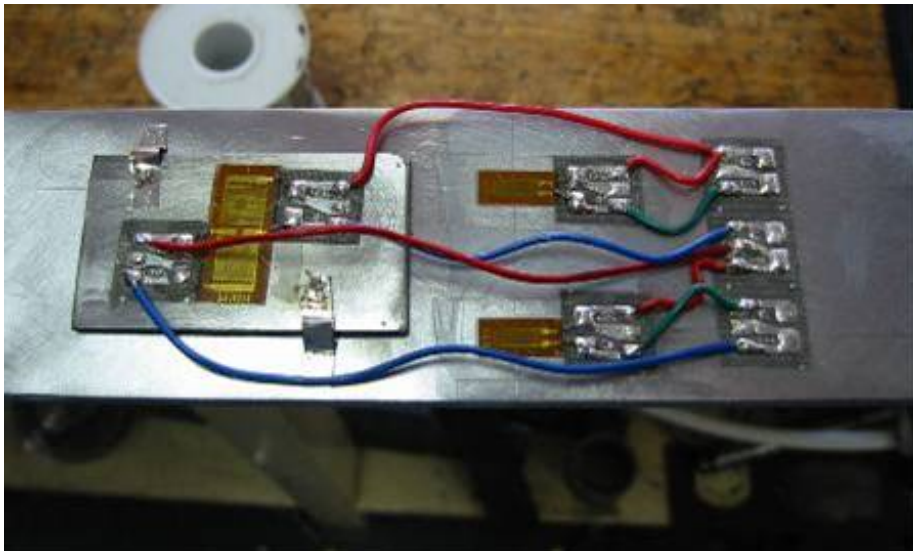

Figure 38: Strain gage assembly.

The selection of the bars whose stresses should be monitored during the prototypes tests (Figs. 39 to 41) was previously made by the WG08 Task Force 4 members. For that selection, an attempt was made to obtain a sample of bars that could represent the structures as a whole. For this purpose, main members, leg diagonals, extension and base bars and diagonals of the transverse and longitudinal faces of the shaft or body of the structures were selected. Another assumption adopted for the choice was the selection of bars where the discrepancies being investigated are currently more frequent and representative.

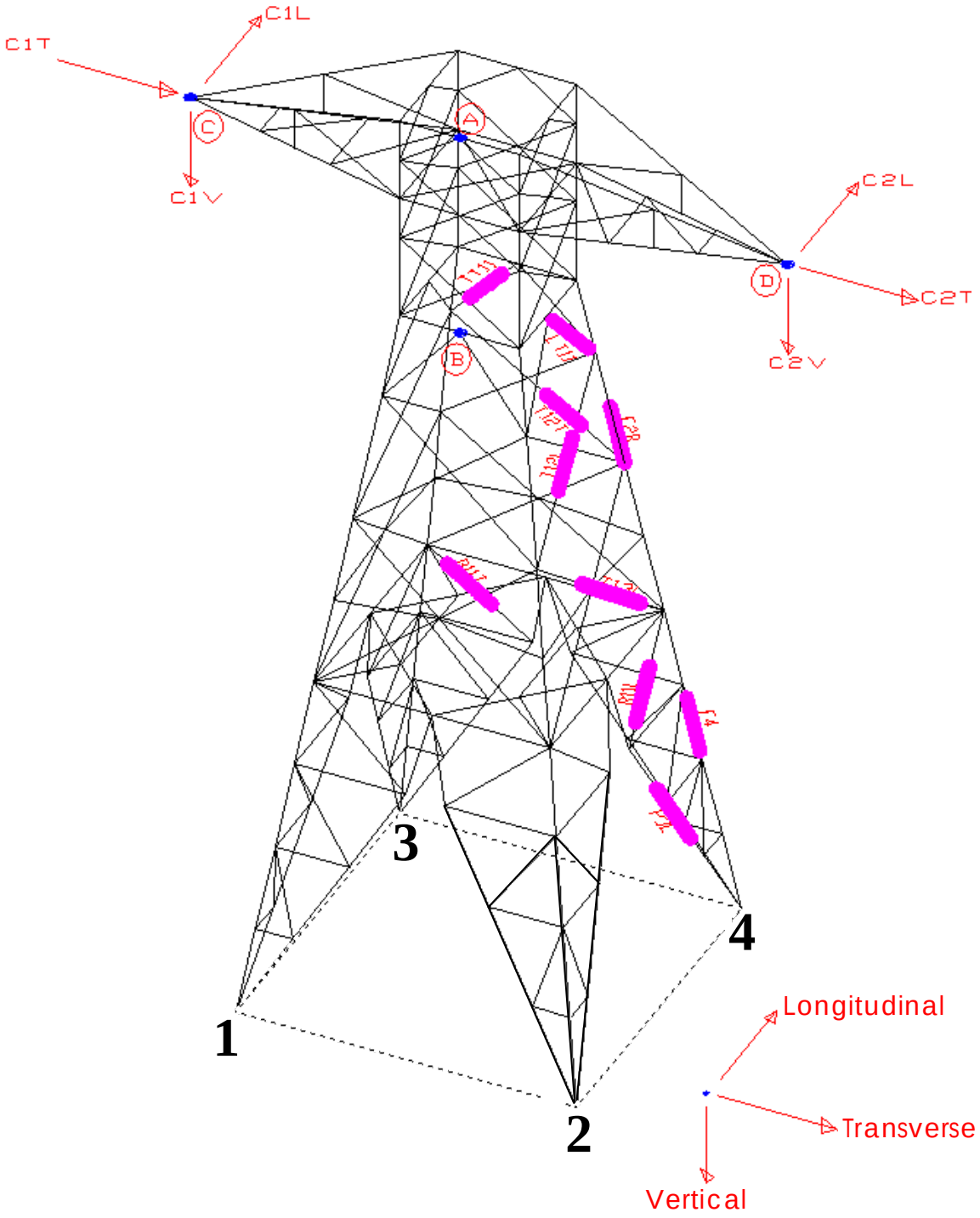

Figure 39: Monitored members and displacement measurement points A, B, C and D on prototype 1.

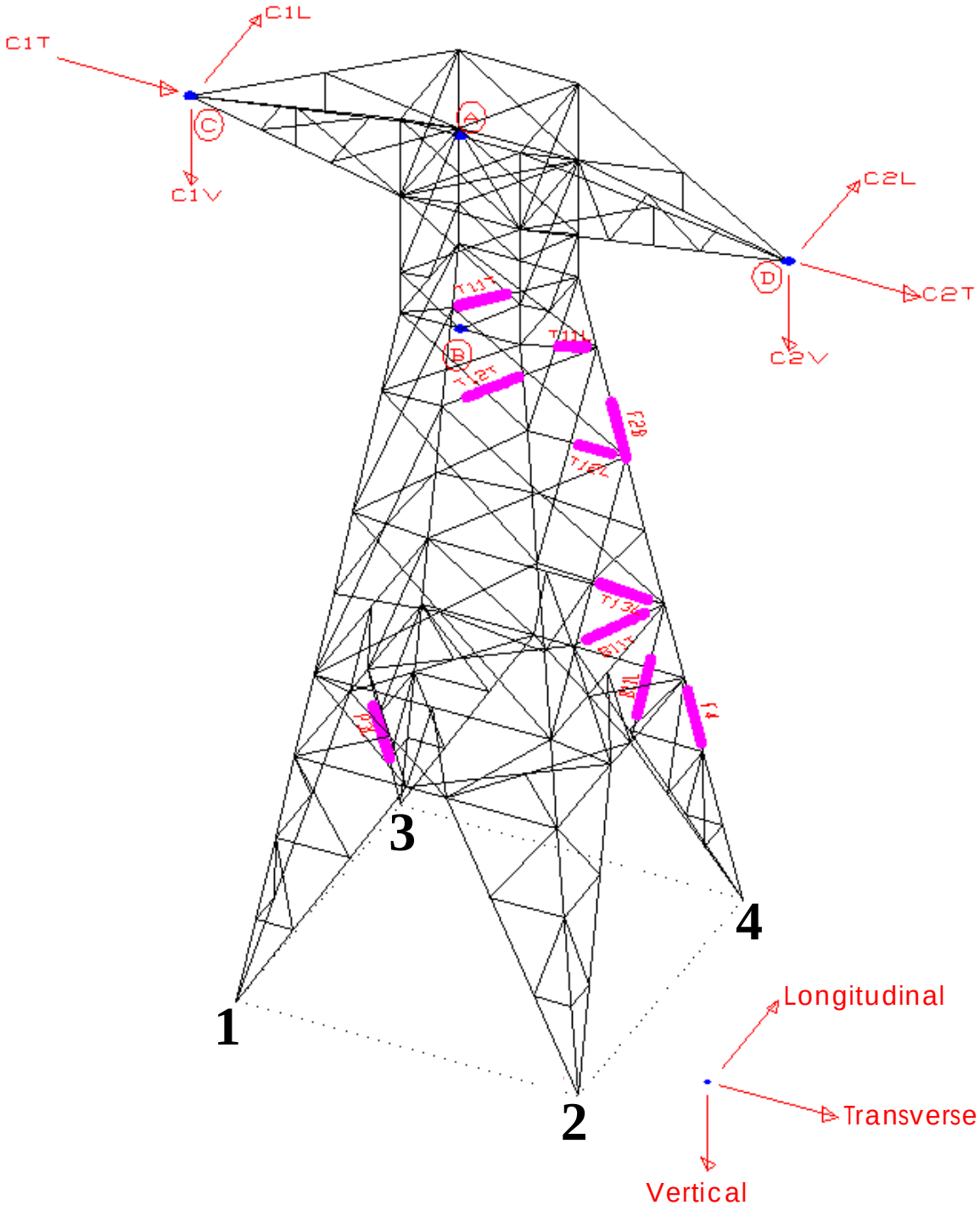

Figure 40: Monitored members and displacement measurement points A, B, C and D on prototype 2.

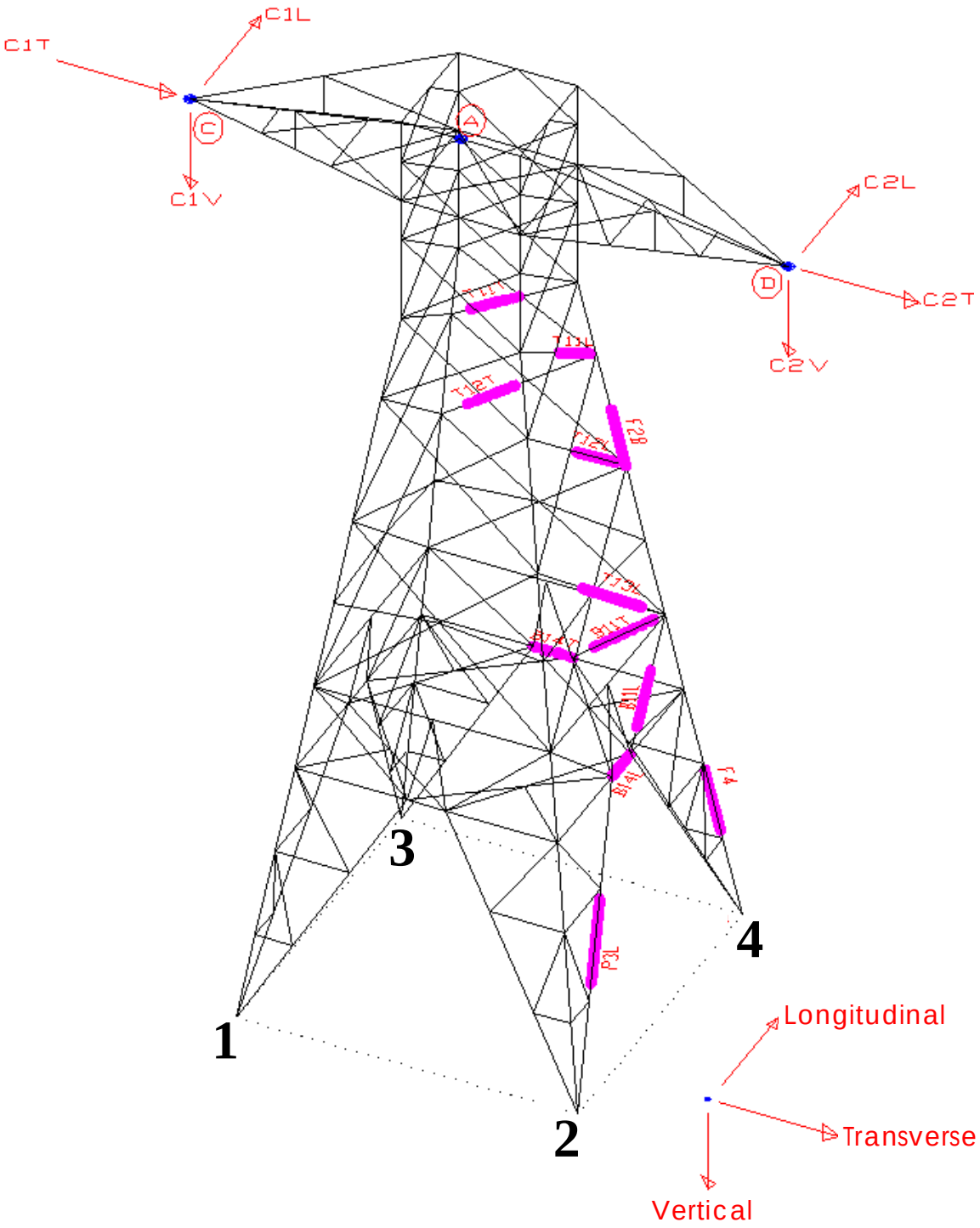

Figure 41: Monitored members and displacement measurement points A, B, C and D on prototype 2A.

7.3 Strain-gage Results

The displacements at points A, B, C and D in the three prototypes, (Figs. 36 to 38) were obtained for the eight load cases from optical instruments readings, assembled on fixed surfaces and with accuracy of 10mm. Each one of the angles selected in the three prototypes (Figures 39 to 41) were instrumented with three strain gages, disposed as shown in Figure 42.

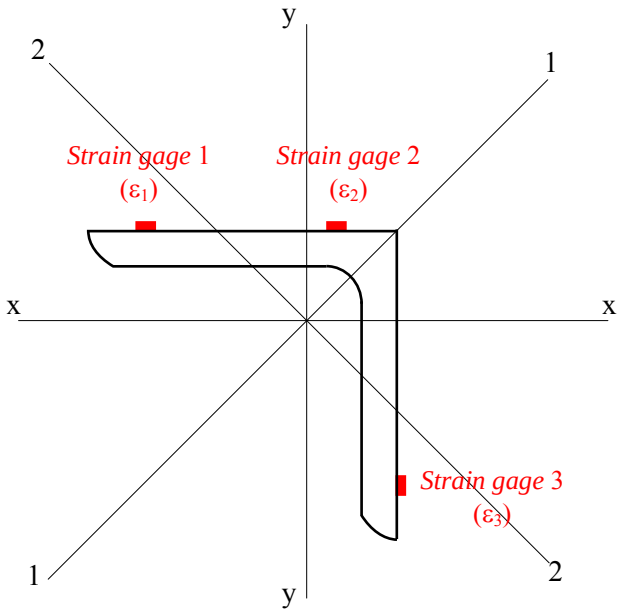

Figure 42: Strain gage positions on angle member.

The deformations obtained in the strain gages (ε_1, ε_2 and ε_3) for each bar can be related with the equation of Strength of Materials for the calculations of normal stress for combined bending and axial load (Beer and Johnston, 1995):

$$\varepsilon_1 = \frac{1}{E}\left(\frac{P}{A} + \frac{M_{11}\,\ell_{11}}{I_{11}} + \frac{M_{22}\,\ell_{21}}{I_{22}}\right) \quad (1)$$

$$\varepsilon_2 = \frac{1}{E}\left(\frac{P}{A} + \frac{M_{11}\,\ell_{12}}{I_{11}} + \frac{M_{22}\,\ell_{22}}{I_{22}}\right) \quad (2)$$

$$\varepsilon_3 = \frac{1}{E}\left(\frac{P}{A} + \frac{M_{11}\,\ell_{13}}{I_{11}} + \frac{M_{22}\,\ell_{23}}{I_{22}}\right) \quad (3)$$

Where:

E is the Young's modulus (modulus of elasticity) of the steel;

A is the area of the transversal section of the angle bars;

I_{11} and I_{22} are the moment of inertia in relation to the principal axis of inertia 1-1 and 2-2, respectively;

ℓ_{ij} is the distance from axis "i" to strain gage "j"

P is the axial stress on the bar

M11 and M22 are the bending moments on the bars, around axis 1-1 and 2-2, respectively.

Thus, knowing the values of ε_1, ε_2 and ε_3, and solving the equation system formed by expressions 1, 2 and 3, the axial stress (P) and the bending moments (M_{11} e M_{22}) of each bar are determined. In this research only the axial stresses are evaluated, since the bending moments which are developed in the prototypes bars are very small.

The strain gage system was previously calibrated, with the application of known stresses, in a way that, besides the strains, the actual stresses on the bars could be furnished in real time. This system was designed and supervised by the *Laboratory of Stress Analysis and Mechanical Technologies* – TSI of ESKOM. In Figure 43 the three strain gages are shown glued on each bar to measure the deformations ε_1, ε_2 and ε_3. Additional strain gages shown in the figure have the function to eliminate the influence of temperature variations from the results.

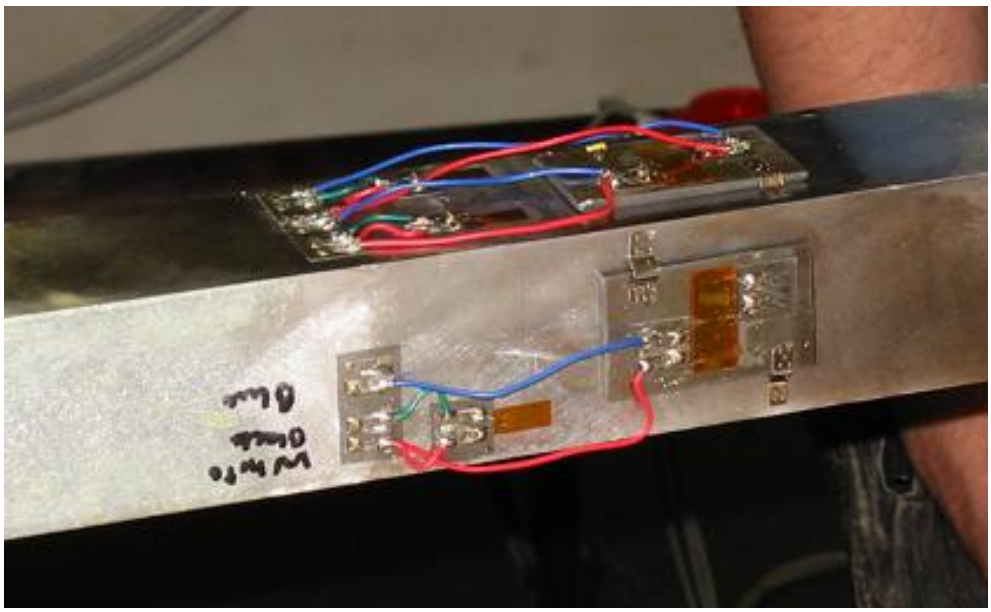

Figure 43: Strain gage arrangements.

Figure 44 presents the experimental results of the displacements at points A, B, C and D of the prototypes for load case 4D.

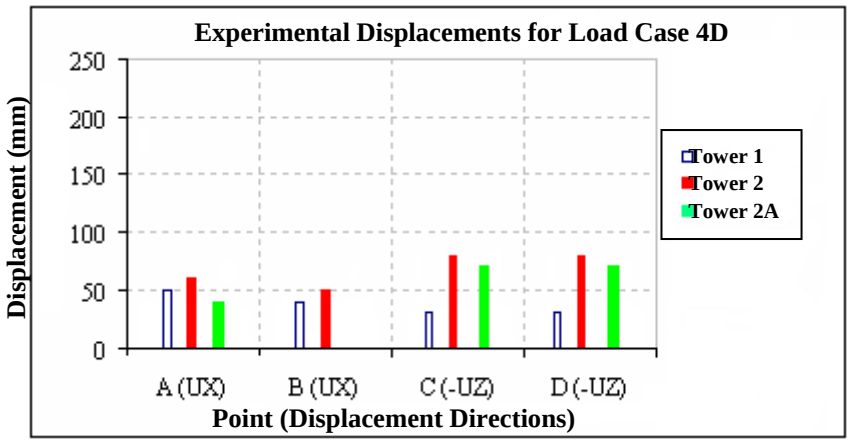

Figure 44: Experimental displacements A, B, C and D for load case 4D

At points A and B the displacements are transversal, that is, measured in the "x" axis direction, while at points C and D the displacements are longitudinal, that is, measured in the "z" direction. The values of the axial stresses on the selected bars of the three prototypes, obtained during the load tests, are presented in Figures 45 to 53. Annexes B and C present the test results for all monitored bars of the three prototypes.

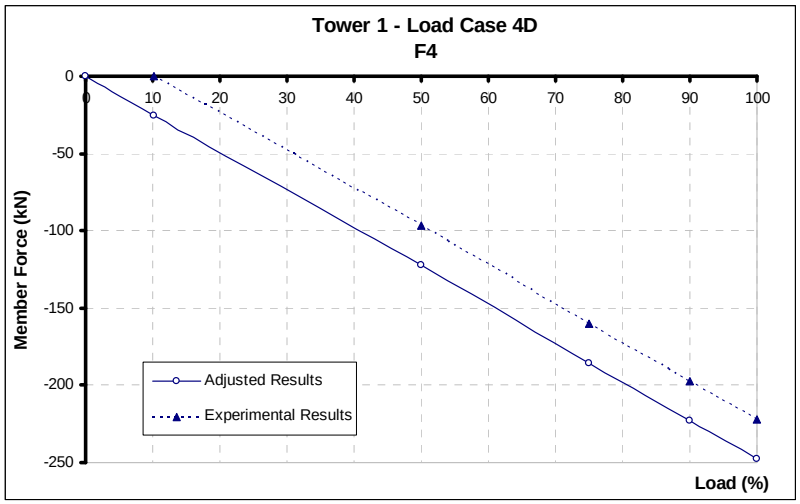

Figure 45: Force (kN) on bar F4 - Prototype 1 for load case 4D

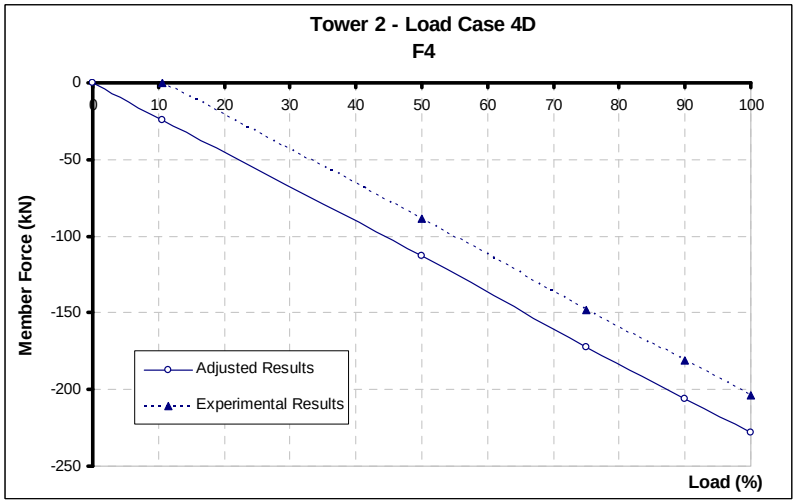

Figure 46: Force (kN) on bar F4 - Prototype 2 for load case 4D

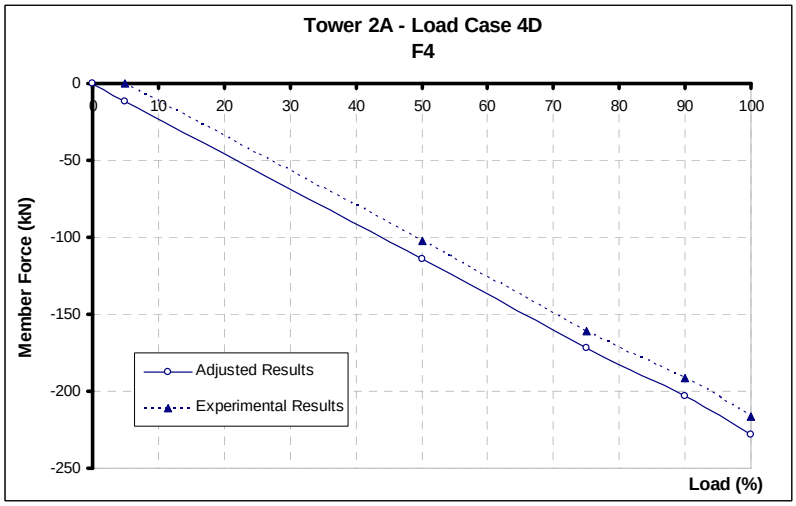

Figure 47: Force (kN) on bar F4 - Prototype 2A for load case 4D

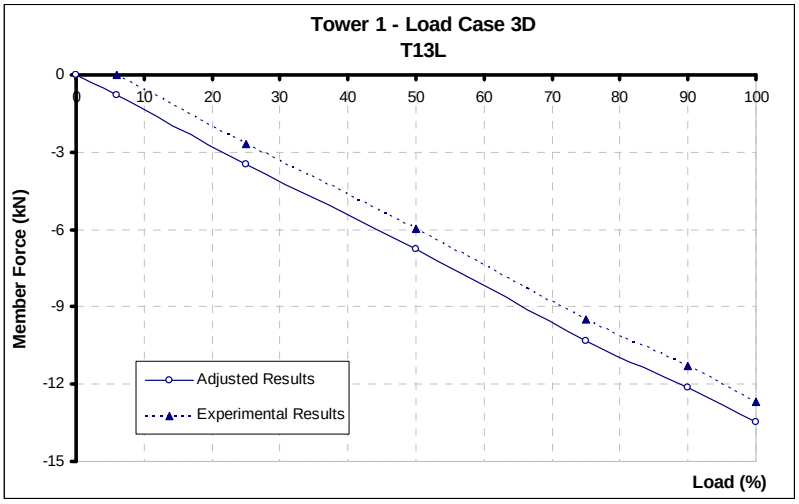

Figure 48: Force (kN) on bar T13L - Prototype 1 for load case 3D

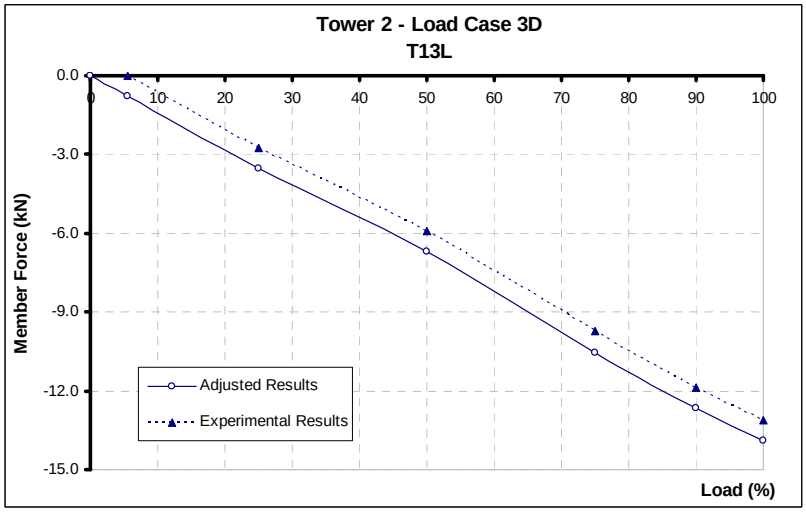

Figure 49: Force (kN) on bar T13L - Prototype 2 for load case 3D

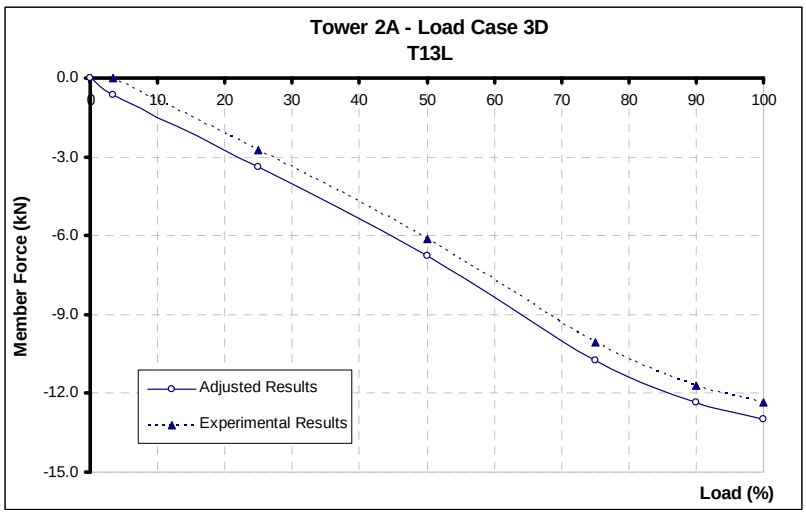

Figure 50: Force (kN) on bar T13L - Prototype 2A for load case 3D

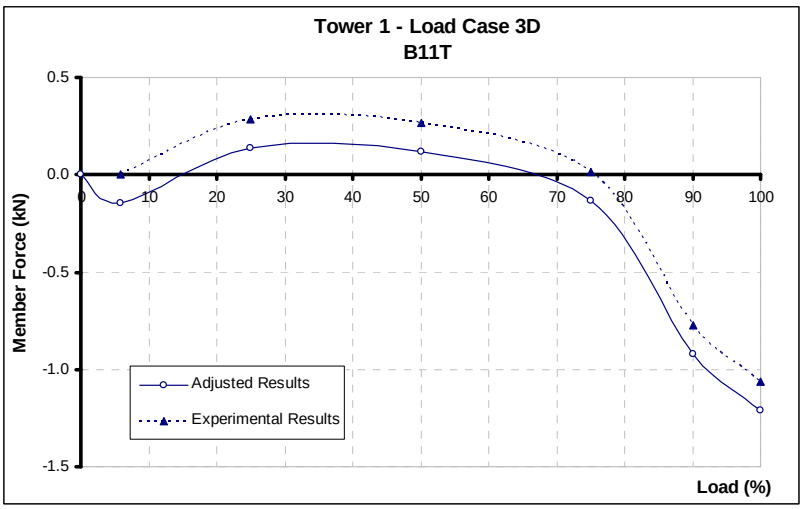

Figure 51: Force (kN) on bar B11T - Prototype 1 for load case 3D

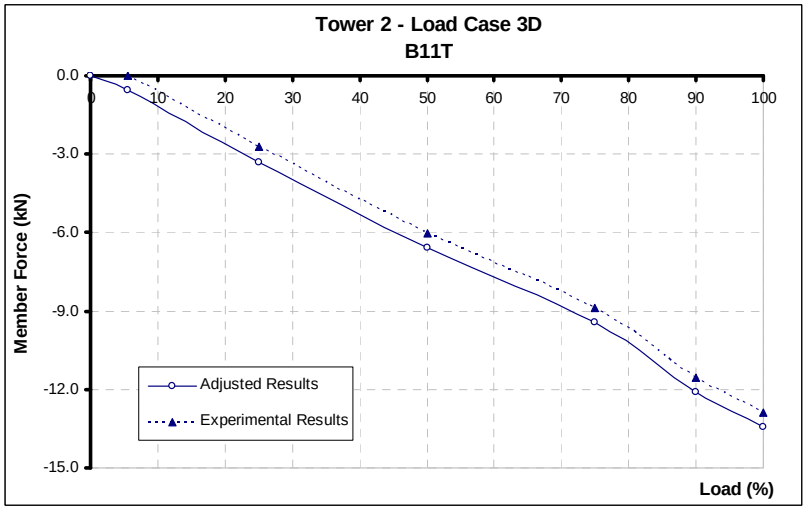

Figure 52: Force (kN) on bar B11T - Prototype 2 for load case 3D

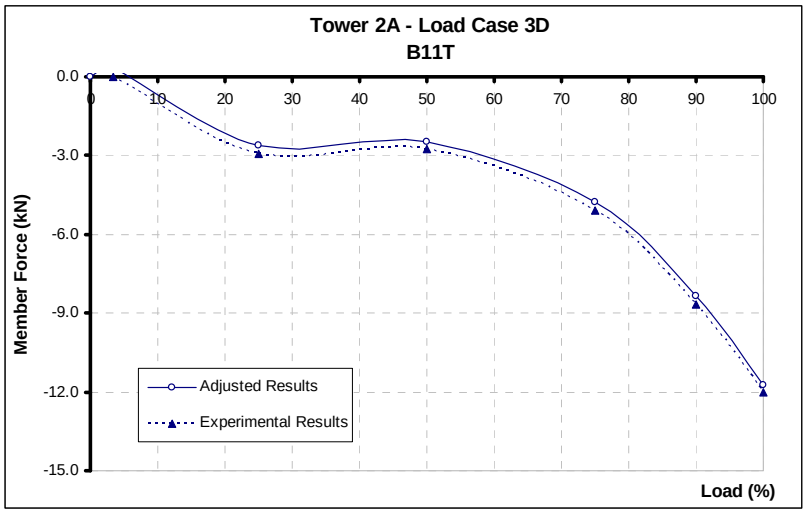

Figure 53: Force (kN) on bar B11T - Prototype 2A for load case 3D

In the graphs of figures 45 to 53 it can be observed that the stresses obtained experimentally were "corrected", once the strains, and consequently the stresses, begin to be recorded from a initial (testing adjustments) load level (above 10% of the design load). This correction is made for all load cases in the three prototypes, with the following procedure:

a) a line is adjusted to the four first points of the graph "load x member force" obtained experimentally, where the 4th point corresponds to 75% of the design load. Up to this level of load the behaviour of the structure can be accepted as linear, even though it is known that the sliding of the connections occurs with a very small load level.

b) once the linear coefficient of this line is known (where the line cuts the ordinates axis), this value (in module) is added to the normal force values obtained during testing (also in module), thus providing the "corrected results."

7.4 Discrepancies Readings

In this item, it is graphically shown a comparison between experimental and theoretical expected results. Figures 54 to 63 are presented below in order to illustrate these observations.

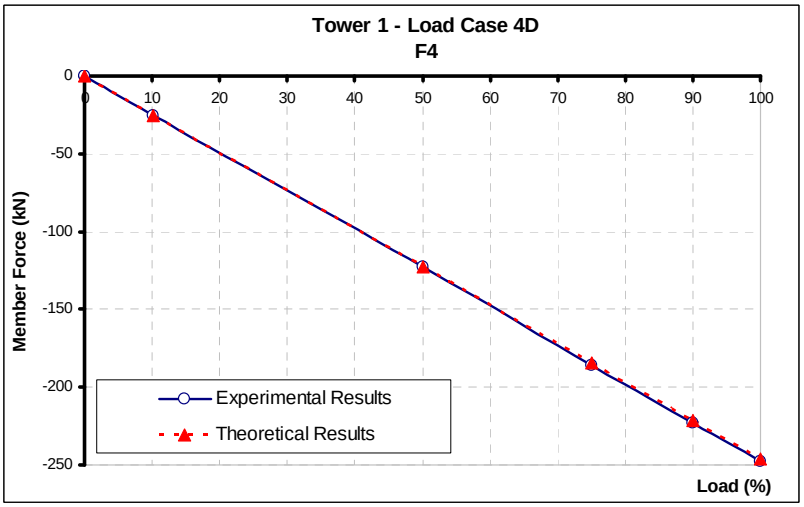

Figure 54: Comparison force (kN) on bar F4 - Prototype 1 for load case 4D

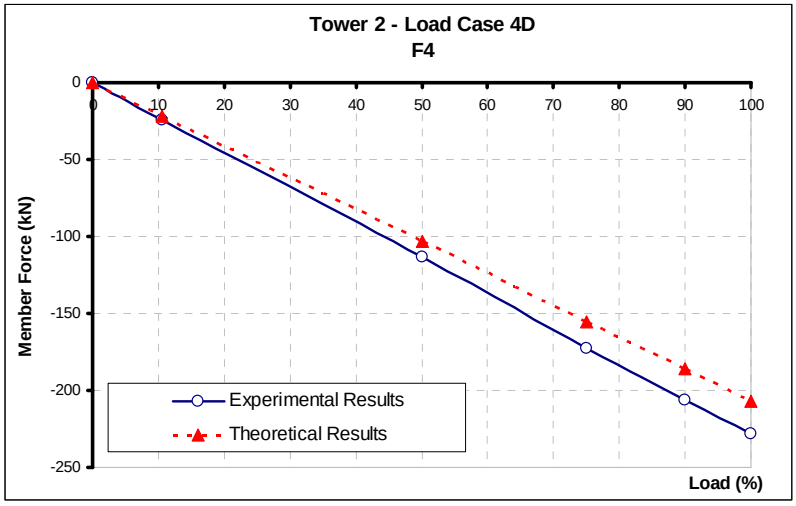

Figure 55: Comparison force (kN) on bar F4 - Prototype 2 for load case 4D

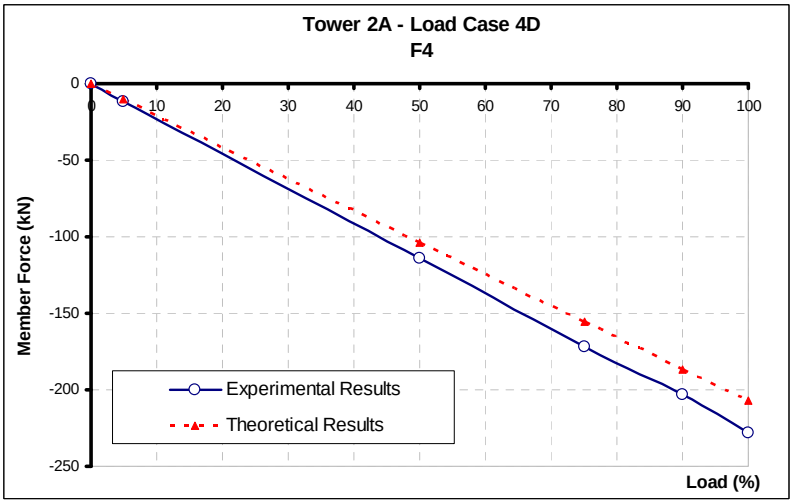

Figure 56: Comparison force (kN) on bar F4 - Prototype 2A for load case 4D

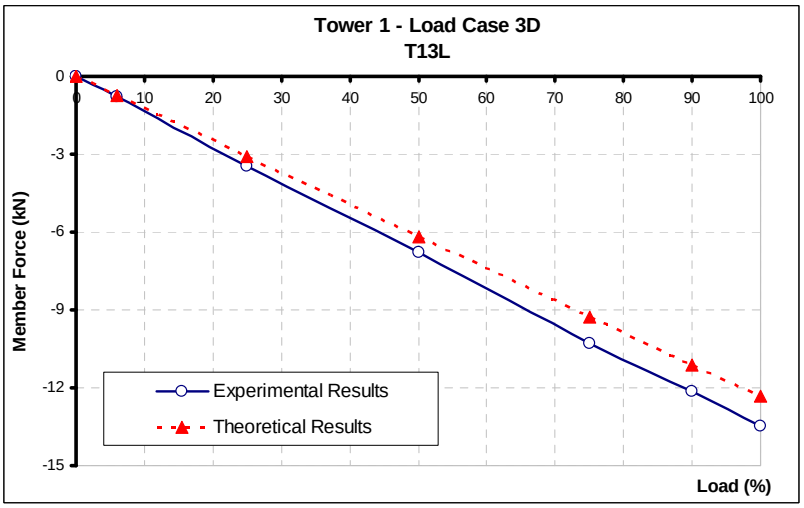

Figure 57: Comparison force (kN) on bar T13L - Prototype 1 for load case 3D

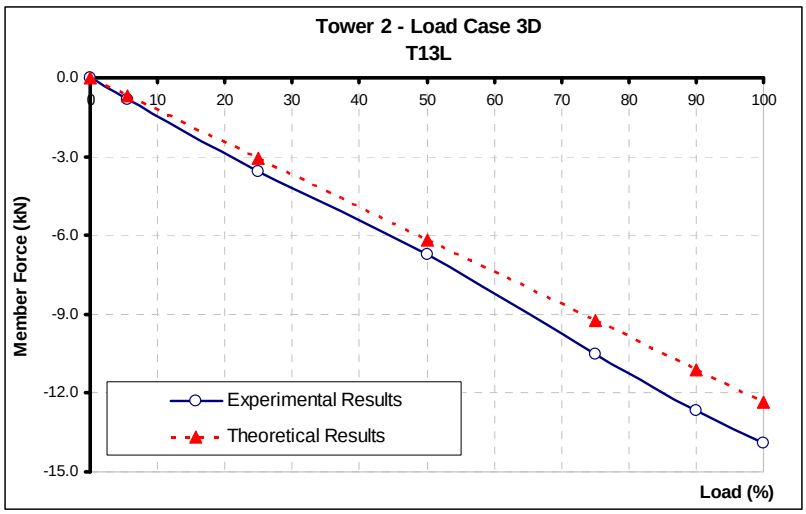

Figure 58: Comparison force (kN) on bar T13L - Prototype 2 for load case 3D

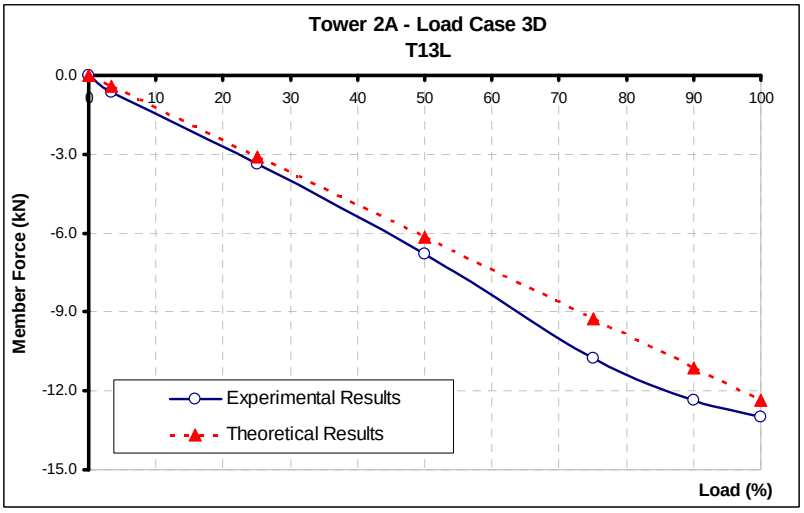

Figure 59: Comparison force (kN) on bar T13L - Prototype 2A for load case 3D

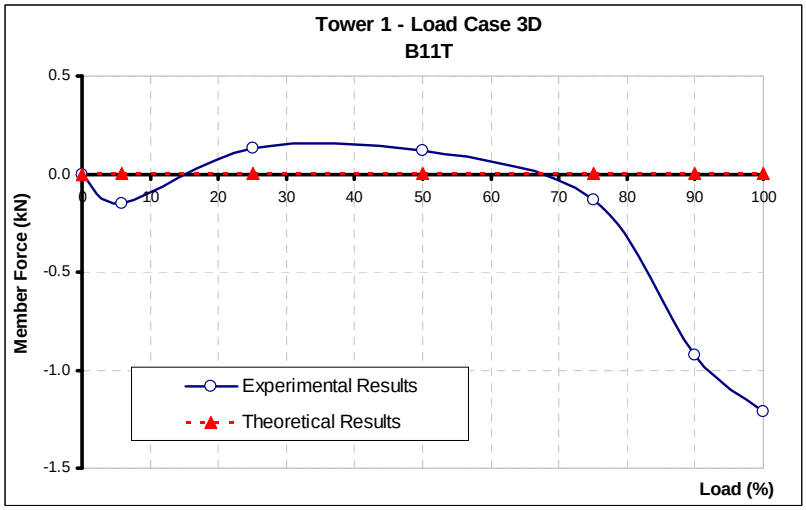

Figure 60: Comparison force (kN) on bar B11T - Prototype 1 for load case 3D

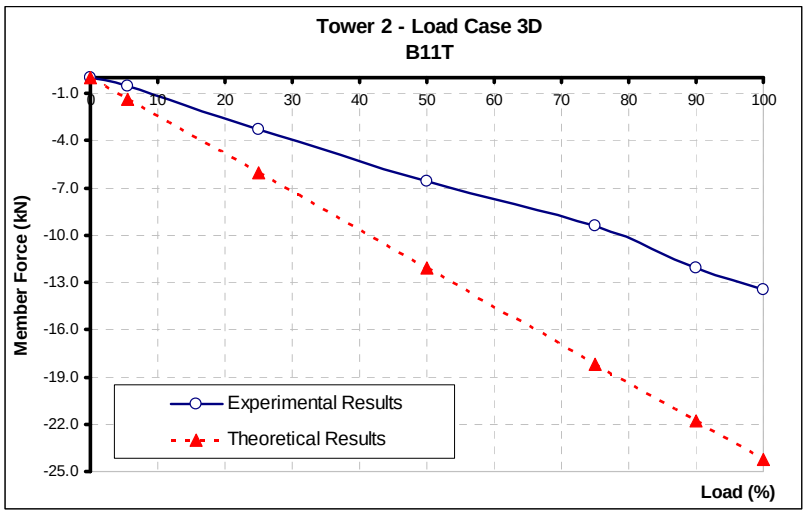

Figure 61: Comparison force (kN) on bar B11T - Prototype 2 for load case 3D

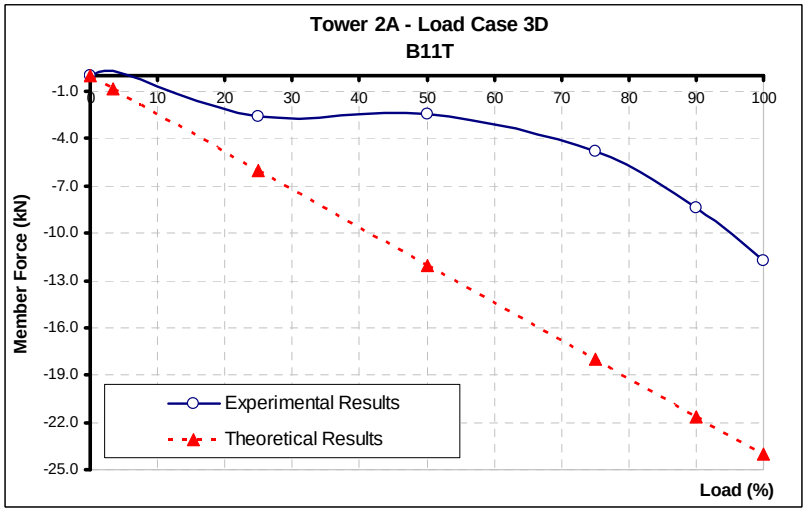

Figure 62: Comparison force (kN) on bar B11T - Prototype 2A for load case 3D

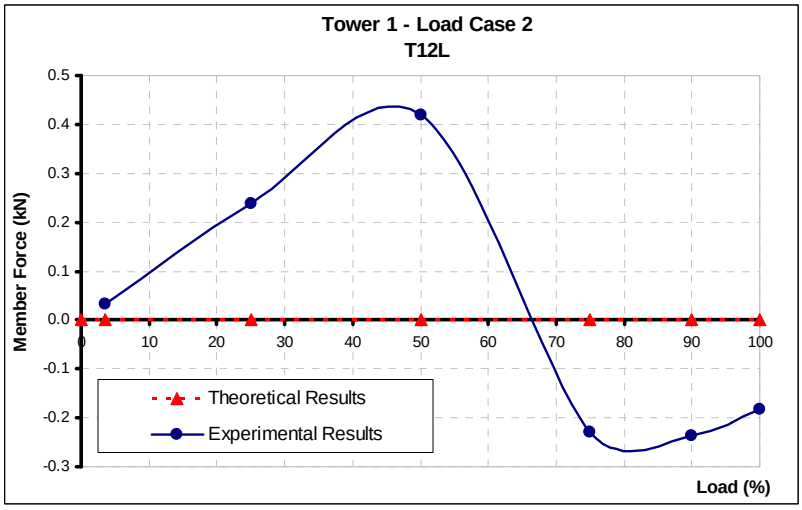

Figure 63: Comparison force (kN) on bar T12L - Prototype 1 for load case 2

From observing the graphs, it may be seen that for main members the predictions have almost the same behaviour as that of the experimental results. However, for diagonals, the experimental structural behaviour presented differences when compared with the theoretical results. Actually, this occurs for longitudinal diagonals when the structures are subjected to transverse loads only, or to transverse diagonals when the structures are subjected only to longitudinal loads, which is in accordance with the former Cigré experiment [1].

7.5 Destructive Tests / Description and Analysis of the failures

After the normal tests, all the three prototypes were destructively tested based on increments of loads of load case 4D. The prototypes failed very similarly and with very satisfactory behaviours. During the destructive tests (Figure 64), all three ruptures occurred on the same member (bar M2), by tensile shearing of the bolts, at load stages of 102% on structure 1, 107% on structure 2 and 114% on structure 2A. After the destructive tests, those failed members were collected for further analysis and verification of the physical and geometrical properties. After the analysis carried out all the failed members were found to be adequate in their materials quality and geometrical properties.

(a) (b)

Figure 64: (a) Destructive test and (b) Failure detail – Prototype 1.

8. ANALYSIS AND RESULTS

The results of this research are very interesting and productive. Studying the behaviour predicted for the prototype structures and confirmed by the test results, the following can be concluded:

- Structures 1 is structural simpler, predictable, and shows less variation in member forces than Structures 2 and 2A. Its member force balance tends to be about the same (isostatic configuration) as predicted. The member force distribution is more concentrated on the main members and consequently the horizontal forces on the foundations are smaller and the vertical forces are larger than structures 2 and 2A. It is important to remember, however, that the horizontal diaphragms in the tower body are located at the recommended positions [6]. In order to guarantee isostatic behaviour, the erection process can become more difficult.
- Structures 2 and 2A, being more hyperstatic have a more complex behaviour (multiple possibility of member force balance), therefore are more susceptible to discrepancies in the member force predictions. The diagonal members have larger forces, therefore having more responsibility for the member force balance. For this reason, the main members are in many circumstances less loaded than in Structure 1. On the other hand, forces in diagonal members are more sensitive to dispersion in the structure behaviour. The structural configurations of Structures 2 and 2A (more hyperstatic than Structure 1) tend to offer other possibilities of member force balance.

At the level of structural analysis, all the member force predictions made by the participants were very close. This is significant, when considering the diversity of the engineers involved and the analysis tools employed. The small differences may be easily explained by the various methodologies of the software programs used. In addition, three participants used more sophisticated softwares: MORENA, PBA/CVA, and AK Tower. MORENA and PBA/CVA use probabilistic base concepts. This allows for example, knowing the statistical distribution of the properties of members, to consider the distribution of member parameters in the structural analysis. AK Tower uses an advanced finite element non-linear analysis to predict member behaviour.

As far as the results of the tests are concerned, some important conclusions are:

- For main members, in addition to the good agreement between the member force predictions of the participants, there was also a good comparison between the participants predictions and the results achieved during the tests (Figures 54 to 56). This occurred for all three structures, thus supporting the results of the prior Cigré experiment [1].
- There was also good agreement for the diagonal members, provided that, those diagonal members had the same orientation as the test loads. This corresponds to having diagonal members in the transverse face and transverse structure loads, and longitudinal diagonal members in the longitudinal face, with longitudinal loads (Figures 57 to 59).
- For the lightly loaded diagonal members (transverse and longitudinal), however, the agreement was not as good between the member forces obtained from the tests and the member force predictions. This emphasizes the influence of structure modelling. Transverse diagonal members responding to only longitudinal loads or longitudinal diagonal members responding to only transverse loads, experience a larger influence from unpredictable factors, as discussed in the Chapter 3 (Figures 60 to 63).

The above conclusions have justified the experiment. For the first time, such variations of member force behaviour are confirmed, thus responding to the questions proposed in the 1991 Cigré´s report [1].

It is confirmed that for many members, when the loads are small, the behaviour is influenced by factors (specially the bolts slippage) that are not currently considered in a linear elastic analysis and therefore the behaviour can be different from the expected. Observing the graph of the Figure 63, which is similarly repeated for several other members and under various circumstances during the experiment, one can conclude that even the static loading can provoke a nonlinear behaviour on the static force balance. That means, in the particular case of the graph in Figure 63, that the force on diagonal T12L goes to zero when the test loading achieves about 65% of the specified test loading. Then, the member force changes from tension to compression. This can be explained due to the accommodation of elastic deformations of the structure member connections not predicted by the analysis and also due to the small magnitude of the member forces (see graph ordinate). Again, this addresses questions launched by a previous Cigré experiment [1] about diagonal member behaviour.

9. ADVANCED MODELLING STUDIES AFTER THE TESTS

Aiming to study the uncertainties of different analysis models for the proposed structures of this research, and in order to know how they can be of influence in the estimate of reliability, Kaminski Jr. (2007) [7] prepared a study evaluating the use of simplified analysis for self-supporting towers as currently adopted by the industry, up to more improved models. The differences in the numeric results between the models were used to quantify the uncertainties related to the mechanical model, and the available results of static tests of prototypes were used to develop models which results came closest to the experimental values.

The models constructed by Kaminski Jr. (2005) [7] are presented and discussed below.
At first, six basic models were constructed to evaluate the response of each tower, where eight load cases were applied, as shown in Section 4.3. These models were prepared in accordance with the usual practice of design, that is, elastic linear or non-linear geometric analysis with spatial frame and/or truss elements and unmovable supports, in order to determine the displacements and loads in the bars. The models are identified as:

- Model “0”: All bars are modeled with spatial truss elements. In the bars that have “plain nodes”, fictitious bars are introduced in order to eliminate the internal hipostaticities;
- Model “A”: All bars are modeled with spatial truss elements, except those ones that have “plain nodes”, where spatial frame elements are used.
- Model “B”: The main bars and all bars that have “plain nodes” are modeled with spatial frame elements, and all the others with spatial truss elements;
- Model “C”: All bars are modeled with spatial frame elements;
- Model “C1”: All bars are modeled with spatial frame elements and the crossing points of the diagonals are considered nodes;
- Model “C_{nl}”: All bars are modeled with spatial frame elements and the analysis is non-linear geometric.

The numeric results obtained in these five basic models, which follows, show a small dispersion for the three towers when the eight load cases are applied, which are due exclusively to:

a) the number of bars modeled with spatial frame or truss elements;
b) the insertion or not of all redundant bars in the model;
c) the way to characterize the crossing point of two diagonals;
d) the consideration or not of geometric non-linearity.

Regarding the linear analysis, it is relevant to note that either by the stiffness method or by finite elements, it is normally assumed that the displacements and rotations of the nodes are infinitely small, the material is linearly elastic, the outline conditions do not change during the application of the load and the loads are conservative, that is, they maintain their original directions when the structure deforms. This way, the equilibrium equations are formulated for the undeformed configuration of the structure and the displacements are obtained in only one step of solution of the equations system. Many practical problems can be solved with this simple formulation; however, a non-linear analysis must be used when this is not possible.

Several sources of non linearity can be present by a structural system, which have influence in the response. In lattice steel towers of transmission lines, the main causes of a non-linear behaviour are:

a) geometrical non-linearity: associated to the change in geometry of the structure due to large displacements and to alterations in the axial and flexural stiffness of the bars as function of the axial load.
b) physical non-linearity: related to the non-linear behaviour of the tension versus steel deformation ratio;
c) sliding and rotational rigidity in the connections, which present non-linear characteristics;
d) flexibility of the foundations, which behaviour of load versus vertical displacement is non-linear.

In order to take into account the effects of non-linearity in structures, several techniques can be used. In this research the intention is not to detail their applications, but to evaluate their effects in the structural response of steel towers. Details and description of the procedures can be found at [8], [9], [10], [11] and [12].

It is relevant to point out that these small differences between the above models are, basically, the same ones encountered by all professionals' analysis. However, with such considerations, few discrepancies were found between the loads in some bars, calculated using the basic

models, and the values obtained experimentally, such as in the study prepared by EPRI [13], suggesting that some aspects must be incorporated to the model in order to reach more precise results. Among them, the flexibility to translation, the rotational rigidity in the connections and the eccentricity of the connections. Such aspects are described below.

9.1 Flexibility to translation in the bolted connections

The total deformation of translation in a bolted connection is measured by the relative displacement among the connected bars. The sliding deformation, which is part of the total deformation, occurs because the holes for the bolts have a diameter which is larger than the nominal diameter of the bolts, in order to guarantee a tolerance for the assembly, specified at 1.6mm (ASCE 10-97) [14].

In steel towers for transmission lines, the connections are of contact type, also known as contact type, made with galvanized bolts of the metric system (classes 5.8 or 8.8) or imperial system. Even though minimum and maximum tightening torques are recommended for the bolts, the resistance to the sliding between the connected parts is not considered in the dimensioning of the connection.

In this type of structure, the contact type connections are preferred over the friction types due to:

a) easiness to assemble at great heights;

b) application of high assembly torques in the friction type connections could peel the galvanization, leading to corrosion;

c) the friction type connections would have their efficiency reduced due to the galvanization of the angles.

The total translation deformation in a bolted connection includes the deformation of the connector, that is, of the bolt rod, the deformation of sliding and the deformation of the angle at the bolt hole. Of all these deformations, the sliding one has a significant importance, as it occurs with a low level of load, besides increasing the structure capacity to support differential movements at the foundations. It also allows a redistribution of the loads of the bars.

A curve that represents the behaviour of the total deformation of bolted connections (δ) as a function of the applied loads (F), obtained from the experimental results [15], and used in this research is shown in Figure 65.

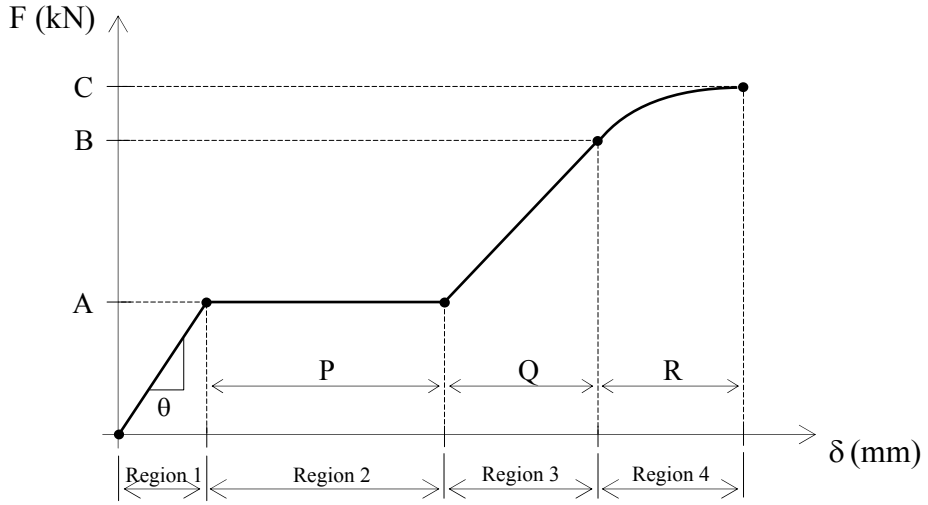

Figure 65: Applied load versus Connection Displacement (Ungkurapinan et al., 2003).

In the graph of Figure 65 it can be observed the existence of four regions:

Region 1: the applied load (F) does not surpass the sliding resistance. Only displacements occur due to the elastic deformation of the angles. Even though there is no specification for the assembly torque (bolt tightening) in the contact type connections, there is always a sliding resistance between the connected angles at the beginning of load application.

Region 2: the applied load (F) surpasses the sliding resistance. A rough displacement occurs caused by the sliding between the angles until the accommodation of the bolts at their respective holes.

Region 3: The hole is elastically deformed, and consequently the load-displacement ratio remains linear.

Region 4: An inelastic deformation of the bolts and angles occurs, culminating in a failure of the connection.

According to [16] the sliding deformation has little influence in the last resistance of the tower, but has a great effect over the displacements, becoming then an important aspect to be studied in the evaluation of uncertainties of the mechanical model.

9.2 Rotational stiffness of the connections

The rotational stiffness of a connection is defined as its capacity to avoid the relative rotation among the connected members, determining the outline conditions of these members, which are responsible for the behaviour of the structure, as they have direct influence upon the rotations and node displacements and, consequently upon the internal loads of the structure.

A connection can be classified according to the impediment degree of the relative rotation among the members, into three different categories: rigid, semi-rigid and flexible, as illustrated in Figure 66 [17], as a function of the moment behaviour (M) versus relative rotation (ϕ).

The connection is considered rigid when it has enough stiffness to maintain practically constant the angle between the connected members, that is, the relative rotation (ϕ) is almost null, for any level of load, until it reaches the resistant moment (M_s) of the connection, defined as the one that causes the rotational displacement between the members in contact. The flexible connection is the one that allows a relative rotation between the members, with a behaviour similar to a pinned connection, conducting a very small bending moment. The semi-rigid connection corresponds to an intermediate situation. In this case the rotational stiffness of the connections must be taken into consideration in the analysis of the structure.

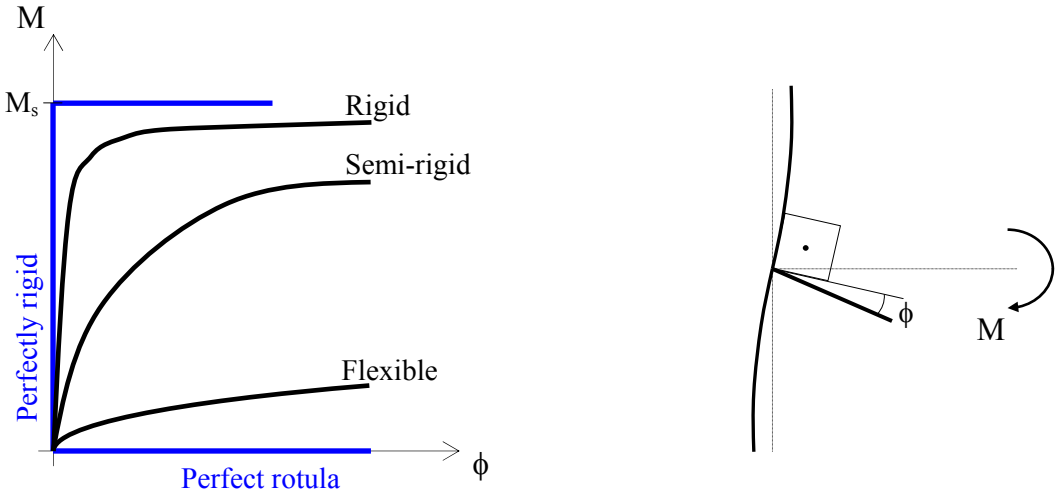

Figure 66: Rigidity classification of connections.

Perfectly rigid connections and perfect pinned connections are idealized outline conditions, hardly found in real steel structures. The behaviour study of the connections and its influence

upon the stability of framed steel structures has received a considerable attention during the last years, through a large number of published papers, such as [18], [19], among others. [20] and [21] present moment versus relative rotation curves, from experimental data, in connections with steel angles.

Figure 67 illustrates a simple connection with only one bolt connecting the angles, typical in towers for transmission lines, where the outline condition is generally modeled as a perfect pinned connection. However, variables such as the tightening strength of the bolt, the total contact surface between the angles and the roughness of this surface can make the connection behave as semi-rigid.

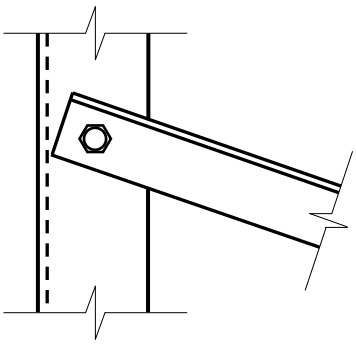

Figure 67: Single bolt connection detailing.

According to [22], for low levels of load, the connection of Figure 67 is done by friction between the surfaces of the angles, that is, the relative rotation (ϕ) is almost null, not being totally null due to the non-uniform distribution of normal tensions among the surfaces in contact as represented in Figure 68. At extreme load conditions, after reaching the resistant moment (M_s), the connection is done by contact between the bolt and the hole in the angles, which means that no additional moment is transmitted.

In this type of connection the parameters that have influence upon the outline conditions in the bars can be represented by the resistant moment (M_s) and by the initial stiffness (K_I) of the connection, which present uncertainties related to the variability in the torque used to tighten the bolt, in the total contact surface between the angles and the roughness of the surface. Reference [22] quantifies such uncertainties and introduce them in the load evaluation of the failure of a steel tower that presents this type of connection, concluding that the variability of the outline conditions practically does not affect the load of failure.

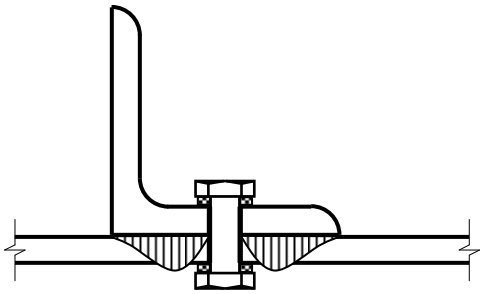

Figure 68: Normal stress distribution on XX surfaces.

The connections with more than one bolt offer a rotation restriction degree much higher than those with only one bolt, in some cases being able to admit that the restriction offered is enough to consider the connection as rigid.

9.3 Eccentricity in the connections

Steel lattice towers are constructed with angle type profiles, which can be directly connected, without the use of connection plates (gusset plates). In this case, the longitudinal axis of the connected members do not converge at one unique point, that is, eccentricity exists in the connection. The connections where gusset plates are used are detailed in order to minimize these eccentricities.

In the simple cut connections, such as the one in Figure 69, the load transmission is made with one eccentricity (e), which produces bending stresses in the bars and traction in the bolts. The usual technique for tower analysis considers the bars axially loaded, disregarding the eccentricities. However, measurements performed by [23] at tower prototype testing indicates that the normal bending tensions, introduced in the bars due to the eccentricities, can be significant. This fact suggests that the eccentricity of the bars at the connections is an important factor to be considered in the evaluation of uncertainties of a mechanical model in this type of structure.

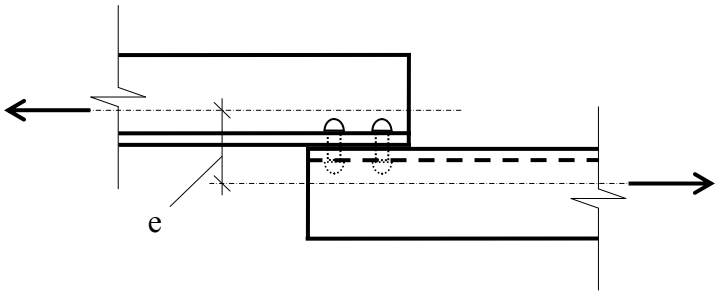

Figure 69: Eccentric connection on angles.

9.4 Description of Complementary Models

Some of the factors discussed in the previous items were now introduced in the analysis of all the three towers, among them, flexibility to translation in the connections. These complementary models were subjected to the same eight load hypotheses as described at Section 4.2, in order to determine displacements and loads in the bars. These models were identified as:

- Models "G" and "GM": All bars are modeled with spatial frame elements and the deformation (translation) in the bolted connections is considered through non-linear springs between the nodes of the elements. The analysis is linear, physical and geometrical; however an iterative incremental procedure is necessary, once the deformation behaviour is non-linear.

In the elaboration of models "G" and "GM" the deformation (translation) of the connections is introduced by means of springs between the elements, which are curves of load versus displacement, as a function of the angle and number of bolts in the connection. Normally the deformations are determined from the experimental results of [15], presented in Figure 70 and valid for connections between equal leg profile angles L 102 x 102 x 6,4mm, with 1 to 4 aligned bolts of 16mm of diameter, tightening torque of 114,27kN.mm and assembly clearance of 1,6mm between the diameter of the holes and the diameter of the bolts.

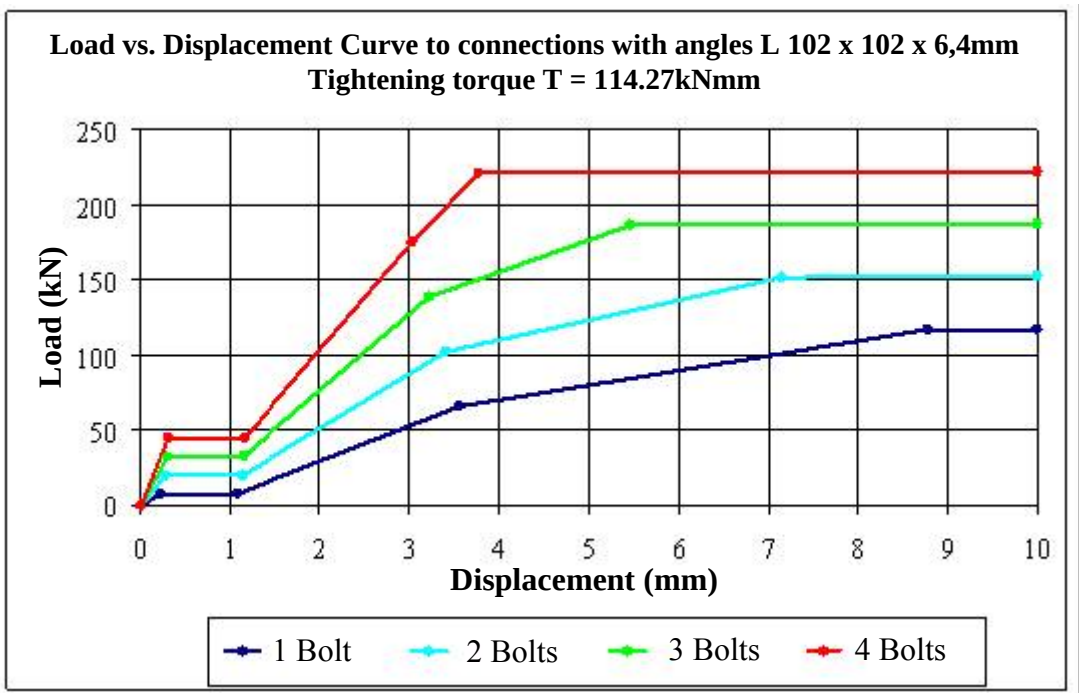

Figure 70: Behaviour on bolted connections of L 102 x 102 x 6,4 mm angles (Ungkurapinan et al., 2003).

For the angles and bolts used in the towers, the curves were adjusted taking into consideration the section area of these angles, the contact area between the bolts and the angles, the number of bolts in the connection, the clearance between the diameter of the holes and the diameter of the bolts and the tightening torque of the bolts.

The models “G30” and “GM30” were elaborated considering a tightening torque of 30kN.mm in each bolt. For models “G45” and “GM45” the torque is 45kN.mm.

The “GM” models are identical to the “G” models, adding the splice connections of the main members, with eight (8) or ten (10) bolts each. All mentioned models were analyzed with the version 9.0 of the software ANSYS, available at the Federal University of Rio Grande do Sul, Brazil.

At last, the towers were analyzed with the direct integration method of movement equations, of explicit form, using central finite differences. This method of solution is normally adopted to solve dynamic problems; however, the response of structures subjected to static loads can also be evaluated.

To apply this method in a structure with static loads, or “almost static,” the loads must be increased from zero up to its final value, during a relatively large time period (not less than five times the largest period of vibration of the structure) and from that value be maintained constant for a period of time sufficient for the structure to stop oscillating. This way, the results converge to the static response.

This approach is known as the dynamic relaxation technique and, even not being very attractive for the solution of linear problems, due to its high number of steps of integration needed in the analysis, it was adopted as another model for the prediction of the linear static response of towers “1”, “2” and “2A”. The advantage of applying the numeric direct integration of movement equations, of explicit form is that it does not require the use of the global stiffness matrix, once the integration is made at the element level. It is important to note that the analysis is restricted to the structures that can be discretized with bar elements, in this case, spatial lattice structures.

To assure the stability of the method, the time interval between the integration steps (Δt) must be small (from the order of 10^{-5} to 10^{-6} s), which requires at least 100000 integration steps for

each second of analysis of the problem; in order that the dynamic amplifications of response do not reach significant values, the loads must also be applied during a period of time not less than five times the fundamental vibration period (largest period) of the structure, which results in a few seconds of analysis, depending mainly on the height of the structure (the towers in this case). Therefore, a linear static analysis requires a few hundreds of thousands of integration steps.

For the three analyzed towers, that have small heights, the fundamental frequencies of vibration are high (around 17Hz), which means that the fundamental periods are short (around 0,06s). In this case, the load application period must be higher than 0,30s. In the analysis it was used a period of 1s for the application of each load hypothesis in the towers and a total analysis period of 10s with an integration time interval (Δt) of $2{,}5 \times 10^{-05}$s.

The model in which the direct integration method was used is here identified as:

- Model "MID": The bars are modeled with spatial lattice elements and the problem is solved using the direct integration method of movement equations, of explicit form. The constitutive law of the material, that is, the load versus axial displacement of the bars of the tower ratio is considered linear.

The results obtained with this model are also presented and discussed at Section 9.6.

9.5 Model's details

In this section all the mechanical models used in the static analysis of towers "1", "2" and "2A" are detailed and the numeric results are presented and discussed.

All the basic models were analyzed using the software ANSYS version 9.0, which are formed only by spatial lattice elements (LINK8) and/or spatial frame (BEAM4) elements. In the more improved models analyzed by ANSYS, linear spring (COMBIN40) and non-linear spring (COMBIN39) elements were used, in addition to LINK8 and BEAM4 elements. In Figures 68 to 71, LINK8 elements are represented by the blue color, while BEAM4 are represented by red color.

In all cases the self weight of the towers was not considered, in order that the loads on the bars can be compared with the experimental values, which begun to be measured from the external application of loads or from the support displacements, that is, with the structure assembled and under action of its own weight. The basic models identified as "0", "A", "B", "C", "C1" and "C_{1n}", are following detailed. The more advanced models that take into account flexibility to translation in the connections are described from pages 77 to 82

Model "0": all bars of towers "1", "2" and "2A" were modeled with spatial lattice elements, the supports were unmovable and the analysis was linear, physical and geometrical.

Fictitious bars were introduced at the spots where "plain nodes" existed, in order to eliminate the internal hipostaticities. These fictitious bars presented an axial stiffness 100 times lower than the lowest stiffness between the real bars, so that they didn't lead to significant alterations in the results.

The quantity of nodes and of LINK8 elements at each tower are indicated at Table 4. At Figure 71 the model "0" of tower "1" is illustrated, including the fictitious bars.

Table 4: Nodes and elements of model "0" for towers 1, 2 and 2A

Tower	Qty. of nodes	Qty. of real bars	Qty. of fictitious bars	Qty of LINK8 elements
"1"	74	196	23	219
"2"	58	170	14	184
"2A"	66	182	19	201

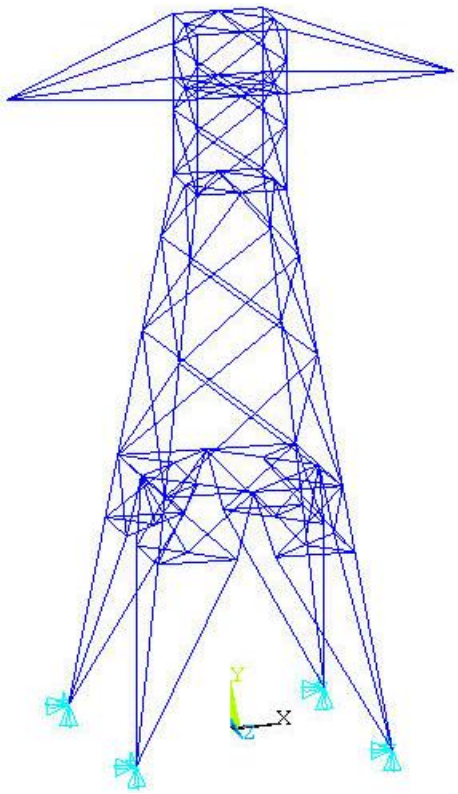

Figure 71: Structural modelling "0" on prototype 1.

Model "A": the bars on all three towers were modeled with spatial lattice elements, except those ones that present "plain nodes," where spatial frame elements were used. This way, the "plain nodes" were eliminated, not being necessary to introduce fictitious bars. The analysis was linear, physical and geometrical, and the supports were unmovable.

The quantity of nodes and elements (BEAM4 and LINK8) in each tower are indicated at Table 5. Figure 72 shows model "A" of tower "1", identifying the elements LINK8 in blue and BEAM4 in red.

Table 5: Nodes and elements of model "A" for towers 1, 2 and 2A

Tower	Qty. of nodes	Qty. of real bars	Qty. of fictitious bars	Qty of LINK8 elements	Qty of BEAM4 elements
"1"	74	196		156	40
"2"	58	170		138	32
"2A"	66	182		142	40

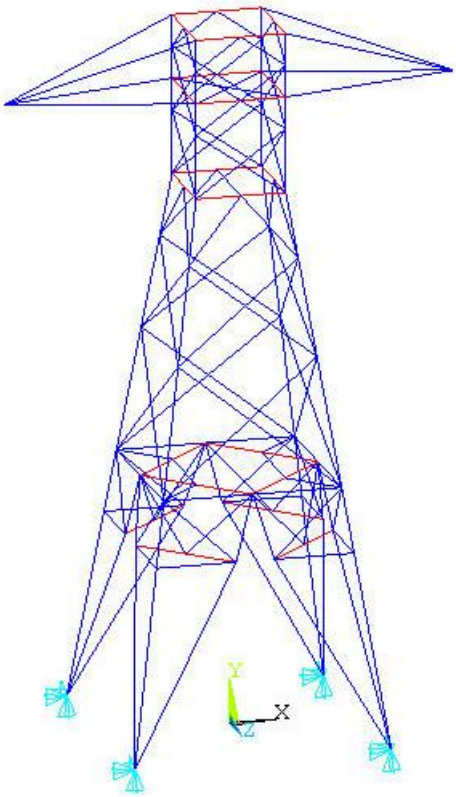

Figure 72: Structural modelling "A" on prototype 1.

Model "B": the main bars and all those ones that present "plain nodes" were modeled with spatial frame elements, and the rest with spatial truss elements, not being necessary to introduce fictitious bars. The analysis was linear, physical and geometrical, and the supports were unmovable.

The quantity of nodes and elements (BEAM4 and LINK8) in each tower are indicated at Table 6. Figure 73 shows model "B" of tower "1", identifying the elements LINK8 in blue and BEAM4 in red.

Table 6: Nodes and elements of model "B" for towers 1, 2 and 2A

Tower	Qty. of nodes	Qty. of real bars	Qty. of fictitious bars	Qty of LINK8 elements	Qty of BEAM4 elements
"1"	74	196		120	76
"2"	58	170		70	100
"2A"	66	182		78	104

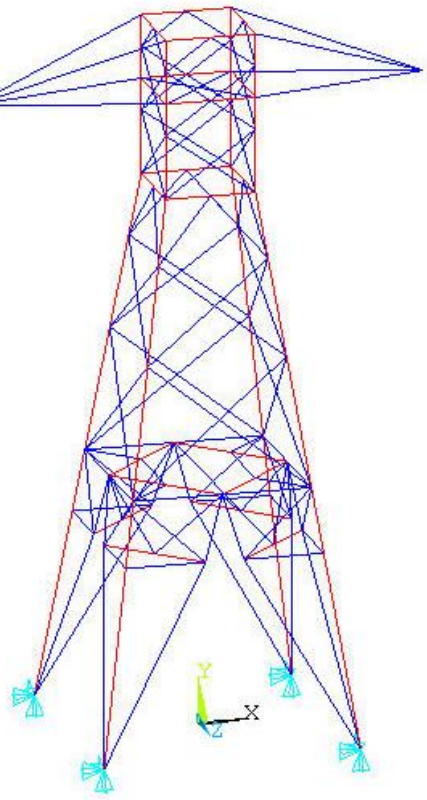

Figure 73: Structural modelling "B" on prototype 1.

Model "C": all bars for the three towers were modeled with frame spatial elements, the supports were unmovable and the analysis was linear, physical and geometrical.

The quantity of nodes and BEAM4 elements in each tower are indicated at Table 7. Figure 74 shows model "C" of tower "1".

Table 7: Nodes and elements of model "C" for towers 1, 2 and 2A

Tower	Qty. of nodes	Qty. of real bars	Qty. of fictitious bars	Qty of BEAM4 elements
"1"	74	196		196
"2"	58	170		170
"2A"	66	182		182

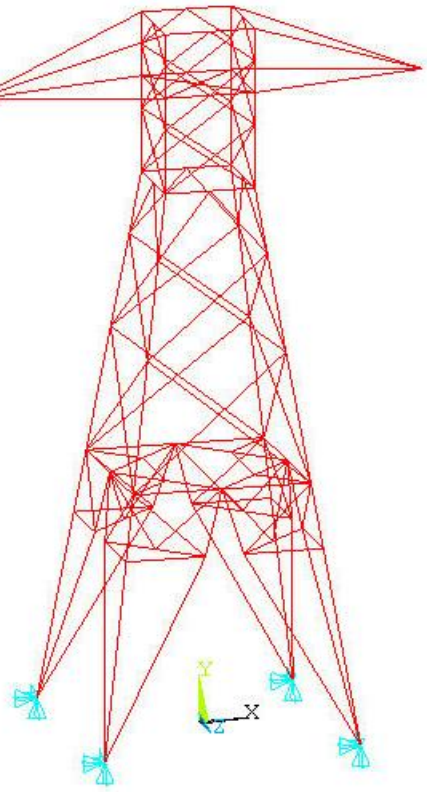

Figure 74: Structural modelling "C" on prototype 1.

Model "C1": all bars were modeled with spatial frame elements and "nodes" were created at the crossing point of the diagonals, in order to take into account the bolt which is inserted at this spot. Actually, two coincident nodes were created at each crossing point of two diagonals and the freedom degree to translation at "x", "y" and "z" directions of these two nodes were coupled (DOF coupling), thus allowing the relative rotation between the two diagonal bars. The analysis was linear, physical and geometrical, and the supports were unmovable. Table 8 indicates the quantities of nodes and elements (BEAM4) in each tower.

Table 8: Nodes and elements of model "C1" for towers 1, 2 and 2A

Tower	Qty. of nodes	Qty. of real bars	Qty. of fictitious bars	Qty of BEAM4 elements
"1"	100	222		222
"2"	100	212		212
"2A"	100	216		216

Model "C_{nl}": all bars are modeled with spatial frame elements and the supports were unmovable, as in model "C," however the analysis was geometrical non-linear. The quantities of nodes and elements (BEAM4) in each tower are identical to the ones for model "C," indicated at Table 7.

The numeric results for all six basic models, subject to all eight load cases described on Section 4.3, presented a very small dispersion as for displacements and loads in the bars. However, a considerable discrepancy is found between the loads in some bars and the values that were experimentally obtained, suggesting that some aspects must be incorporated to the model, in order to obtain better results.

Among the aspects discussed above, models that consider flexibility to translation in the connections were elaborated. Such models, identified as "G", "GM" and "MID" are hereafter detailed:

Models "G30" and "G45": all bars were modeled with spatial frame elements and the deformation (translation) in the bolted connections was introduced through non-linear spring

elements (COMBIN39), each element with only one degree of freedom to translation. These elements connect two coincident nodes, introduced in all connections between:

- diagonals and main bars;
- diagonals and horizontal bars;
- horizontal bars and main bars.

The load versus displacement curves of these elements were determined from the experimental results of [15], presented in Figure 70 and valid for connections between equal leg angles L102 x 102 x 6.4mm, with 1 to 4 aligned bolts of 16mm of diameter, tightening torque of 114.27kN.mm and assembly gap of 1.6mm between the diameters of the holes and the diameters of the bolts.

At the connections of towers "1", "2" and "2A", the load versus displacement curves are adjusted for each one of all six angles used, with 1 to 10 bolts of 12mm diameters, tightening torque of 30 and 45kN.mm and assembly gap of 1.6mm, taking into account:

- the transversal section area of the angles;
- the contact area between the bolts and the angles;
- the number of bolts in the connection;
- the assembly tolerance;
- the tightening torque of the bolts.

The maximum tightening torque values are determined with equation 4 (Brazilian Standard NBR 8850), which correlates the torque with the tension produced in the bolt, at the elastic regimen:

$$T = KPd \tag{4}$$

Where T is the tightening torque in the bolt (kN.mm), K is the proportionality coefficient which depends on the inclination angle of the fillets and of the friction coefficient between the bolt and the nut (K≅0,20 usually adopted), P is the tension produced by the torque applied to the bolt (in kN), d is the nominal diameter of the bolt (in mm).

This way, the minimum and maximum specified values (see detailing drawings) for the tightening torque of 12mm bolts, induce tension values of 12.5kN and 18.75kN, respectively.

The tension acting in 16mm bolts, with a tightening torque of 114.27kN.mm, as used in the research described in [15], is 35,71kN, which is the maximum specified tension limit at NBR 8850 [24] for this type of bolt.

Figures 75 to 77 show the load versus axial displacement curves in the connections for some of the angles used on towers "1", "2" and "2A", with 1 to 10 bolts of 12mm, tightening torque of 45kN.mm and assembly gap of 1.6mm.

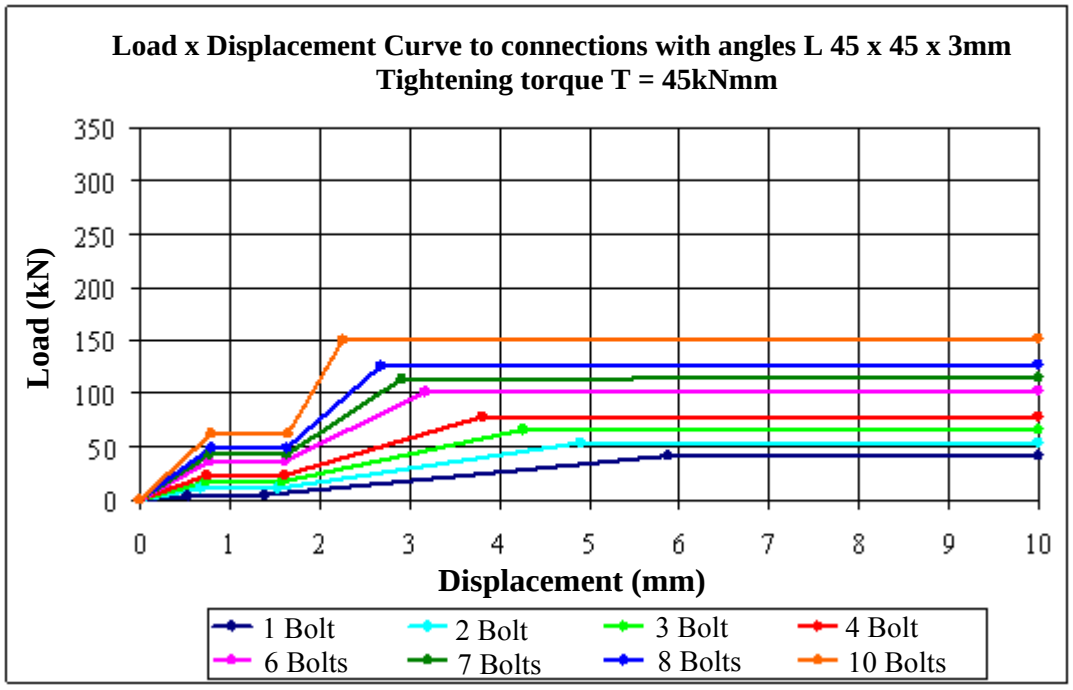

Figure 75: Load x axial displacement curve on connections L 45 x 45 x 3.0mm and assembly torque of 45kNmm.

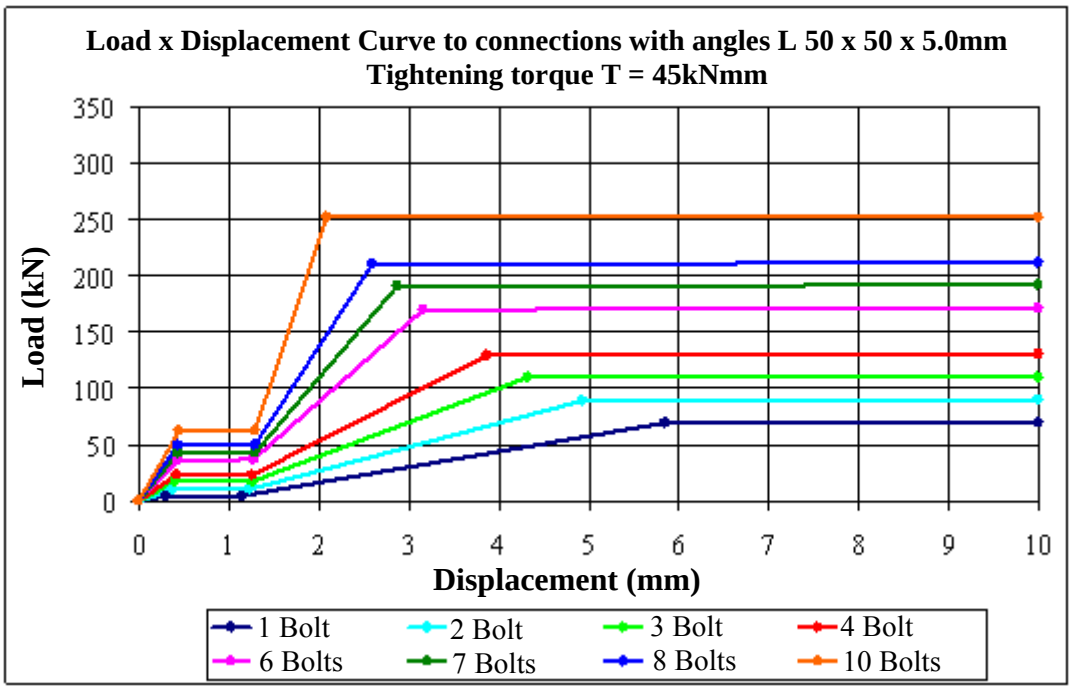

Figure 76: Load x axial displacement curve on connections L 50 x 50 x 5.0mm and assembly torque of 45kNmm.

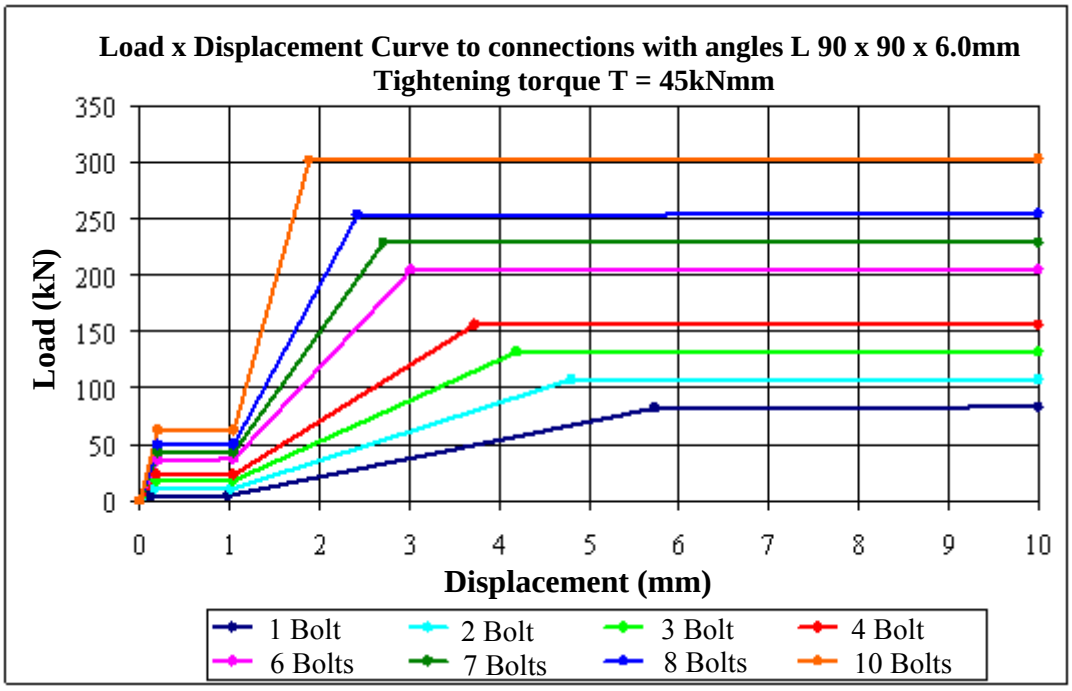

Figure 77: Load x axial displacement curve on connections L 90 x 90 x 6.0mm and assembly torque of 45kNmm.

The number of nodes and elements (BEAM4 and COMBIN39) in each tower are indicated at Table 9.

Table 9: Nodes and elements of models “G30” and “G45” for towers 1, 2 and 2A

Tower	Qty. of nodes	Qty. of real bars	Qty. of BEAM4 elements	Qty. of COMBIN39 elements
“1”	266	196	196	576
“2”	242	170	170	552
“2A”	258	182	182	576

Models “GM30” and “GM45”: these are equal to models “G30” and “G45,” having the only difference in the consideration of the connections in the main bar splices, which have ten 12mm bolts for tower “1” and eight for towers “2” and “2A.” Model “GM30” was designed considering a tightening torque of 30kN.mm, and “GM45” a torque of 45kN.mm. In the connections of the main bar splices, the freedom degrees to rotation of the coincident nodes are coupled, avoiding the relative rotation between these nodes.

Figure 78 (a) illustrates the detail of one of the main bar splices of tower “2.” Each main member has two splices throughout the structure, shown in Figure 78 (b), and each splice is represented in the models through two connections with eight bolts.

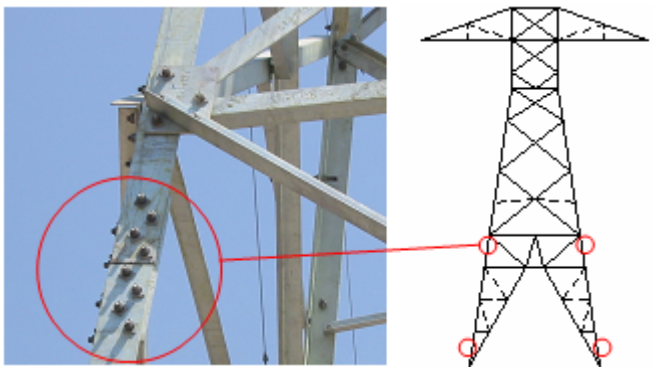

(a) (b)

Figure 78: (a) Main bar splice detailing of tower “2”and (b) Splice localization on the tower.

The load versus axial displacement ratios for each COMBIN39 element in each direction “x”, “y” or “z” are established by multiplying the respective load versus displacement curve of the angle by the directing cosine of the bar, in the corresponding direction. This is done for the directions in which the bar can slide. In the directions where the deformation cannot occur, the degrees of freedom are coupled, that is, the coincident nodes have the same displacement in these directions. The quantity of nodes and elements (BEAM4 and COMBIN39) in each tower is indicated at Table 10.

Table 10: Nodes and elements of models “GM30” and “GM45” for towers 1, 2 and 2A

Tower	Qty. of nodes	Qty. of real bars	Qty. of BEAM4 elements	Qty. of COMBIN39 elements
“1”	302	196	212	696
“2”	278	186	186	672
“2A”	294	182	198	696

For models “G30”, “G45”, “GM30” and “GM45” the analysis was linear, physical and geometrical, however an incremental procedure was necessary, once the behaviour of the deformation in the connections is non-linear.

Model “MID”: all bars of the three towers were modeled with spatial lattice elements, the supports were unmovable and the problem was solved using the direct integration method of movement equations, of explicit form, using central finite differences. The analysis was non-linear geometric, once the coordinates of the nodes were updated at each integration step. This was the only model of the static analysis that was not solved in the ANSYS software.

This solution method is normally adopted to solve dynamic problems; however, it can also be used to evaluate the response of structures subjected to static loads. In order to eliminate the internal hipostaticities originated by the use of spatial lattice elements, fictitious bars were introduced, which had axial stiffness 100 times lower than the lowest stiffness between real bars, just like in model “0”. This way, the quantity of nodes and spatial lattice elements in each tower were identical to model “0” and are indicated at Table 4.

9.6 Numeric Results

The numeric results for the comparison among the models are the axial forces in the selected bars, identified in Figures 54 to 63. Such results are presented for all models mentioned in the previous item, subjected to the eight load cases of Section 4.3. Figures 79 to 87 present the resulting axial forces on all selected bars of the prototypes 1, 2 and 2A, subjected to load case “4D,” for all studied models.

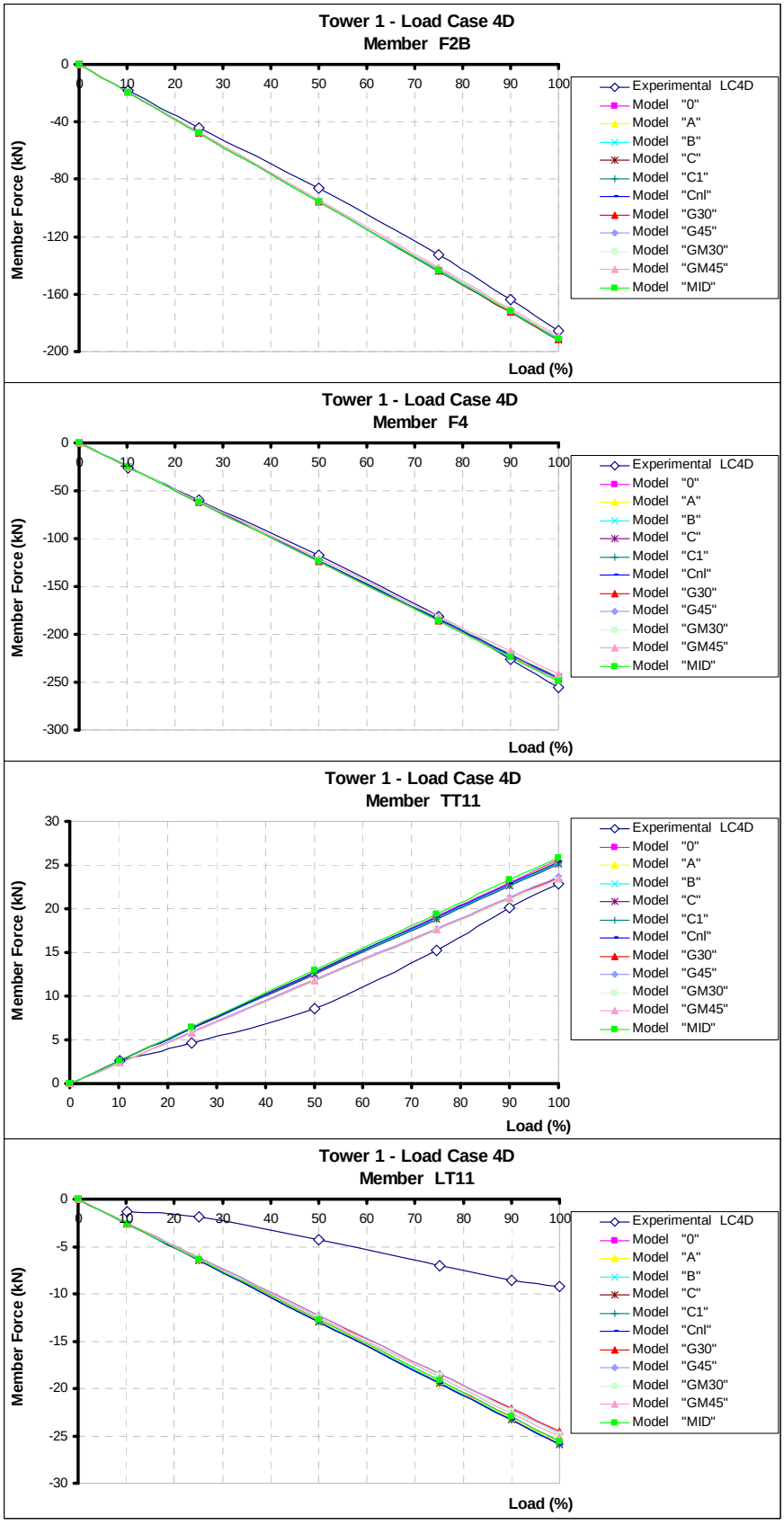

Figure 79: Axial forces on bars F2B, F4, TT11 and LT11 of prototype “1” – LC 4D.

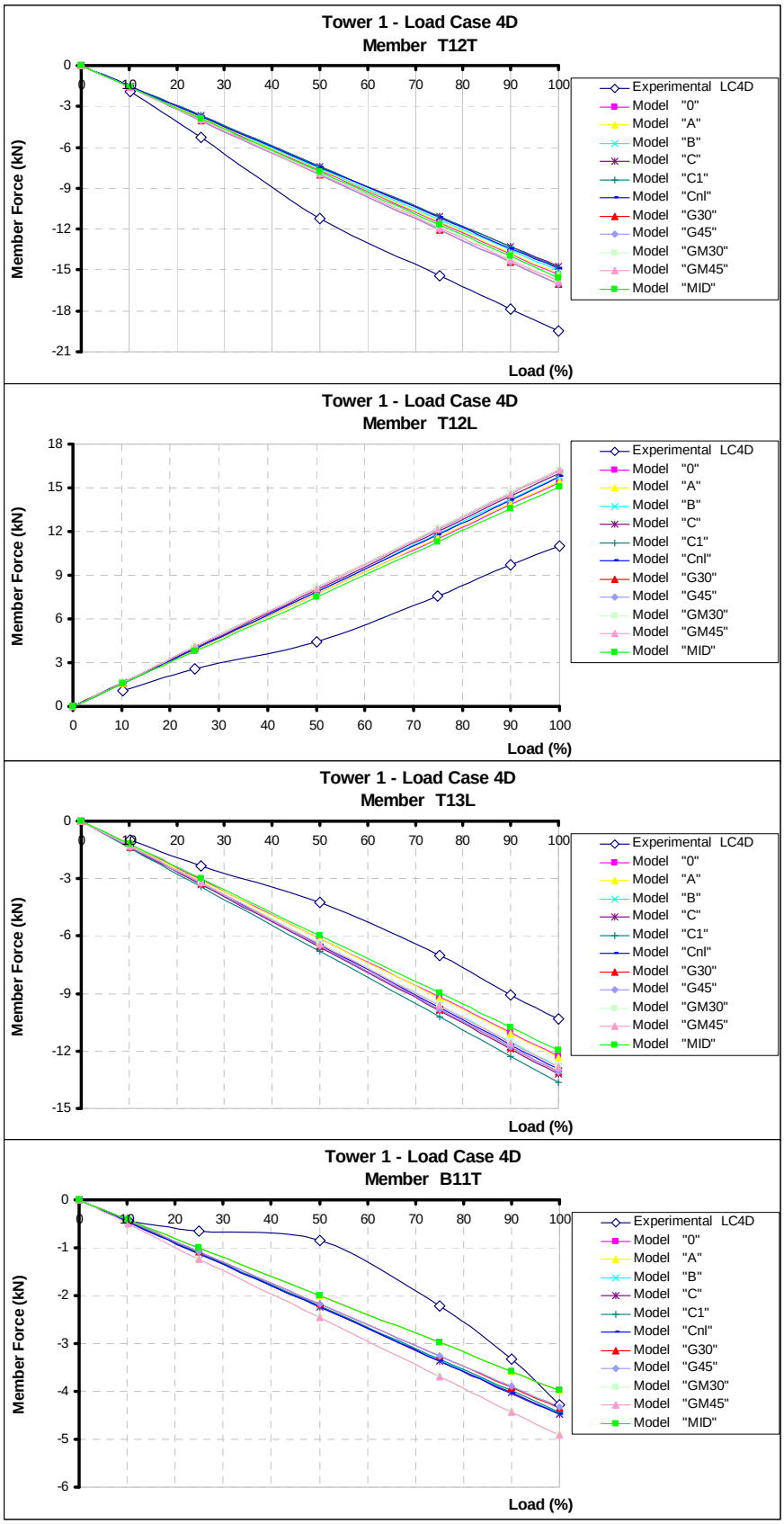

Figure 80: Axial forces on bars T12T, T12L, T13L and B11T of prototype "1" – LC 4D.

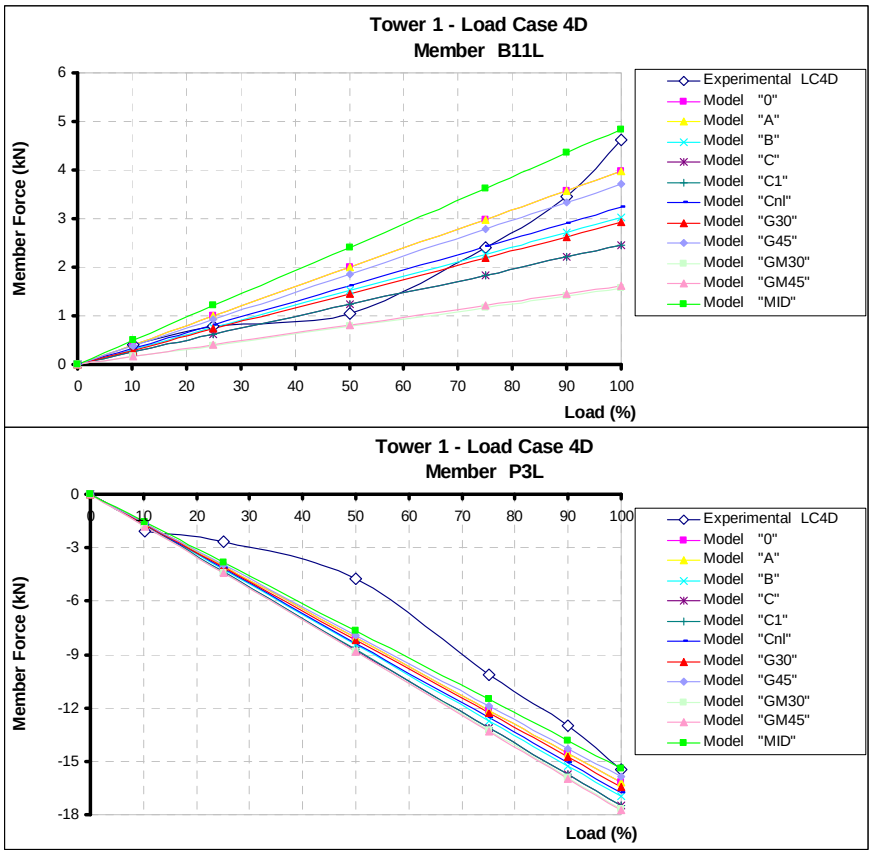

Figure 81: Axial forces on bars B11L and P3L of prototype "1" – LC 4D.

Figures 82 to 84 show the numeric results of the axial forces on the selected bars of tower "2", subjected to load case "4D", for all models.

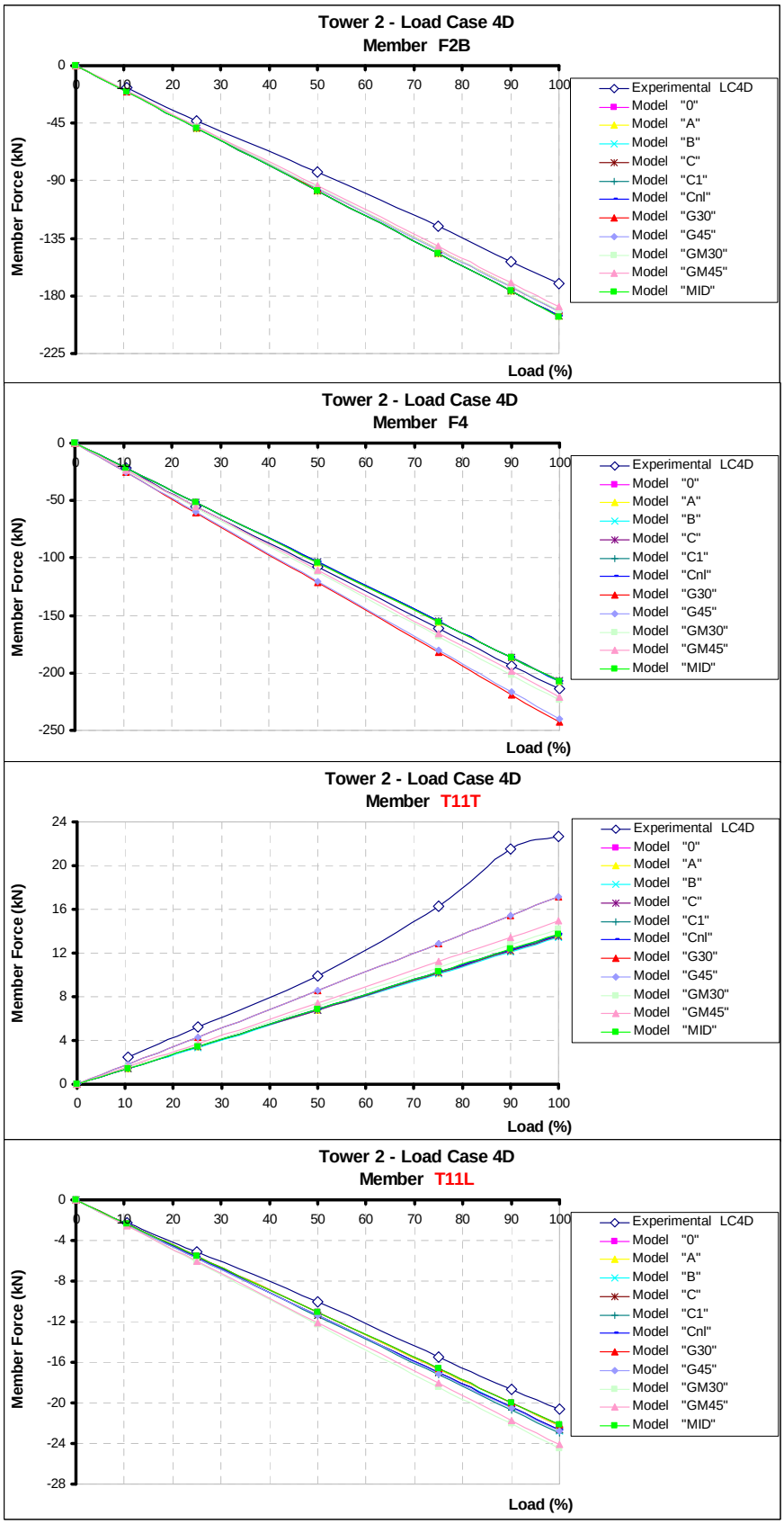

Figure 82: Axial forces on bars F2B, F4, T11T and T11L of prototype "2" – LC 4D.

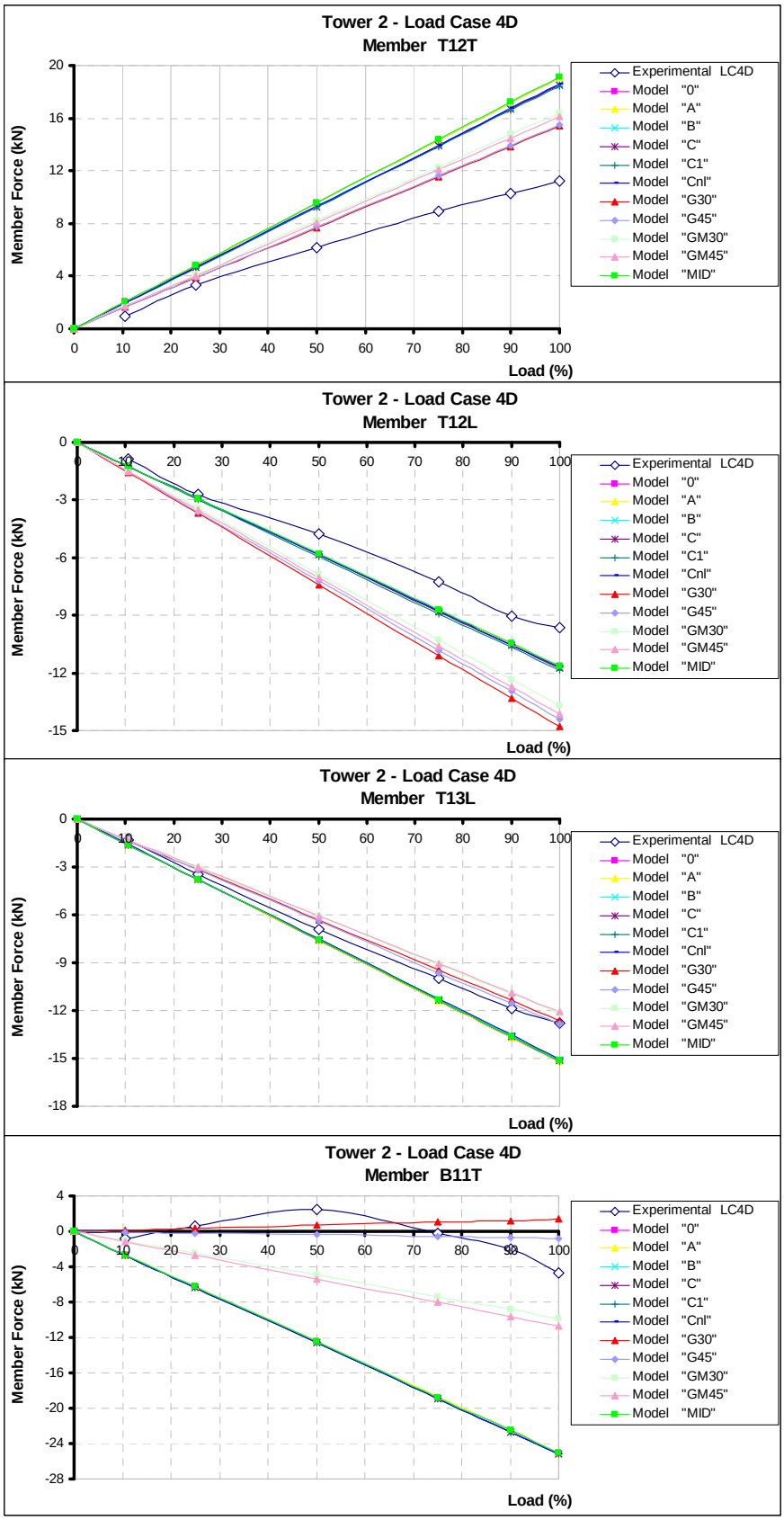

Figure 83: Axial forces on bars T12T, T12L, T13L and B11T of prototype “2” – LC 4D.

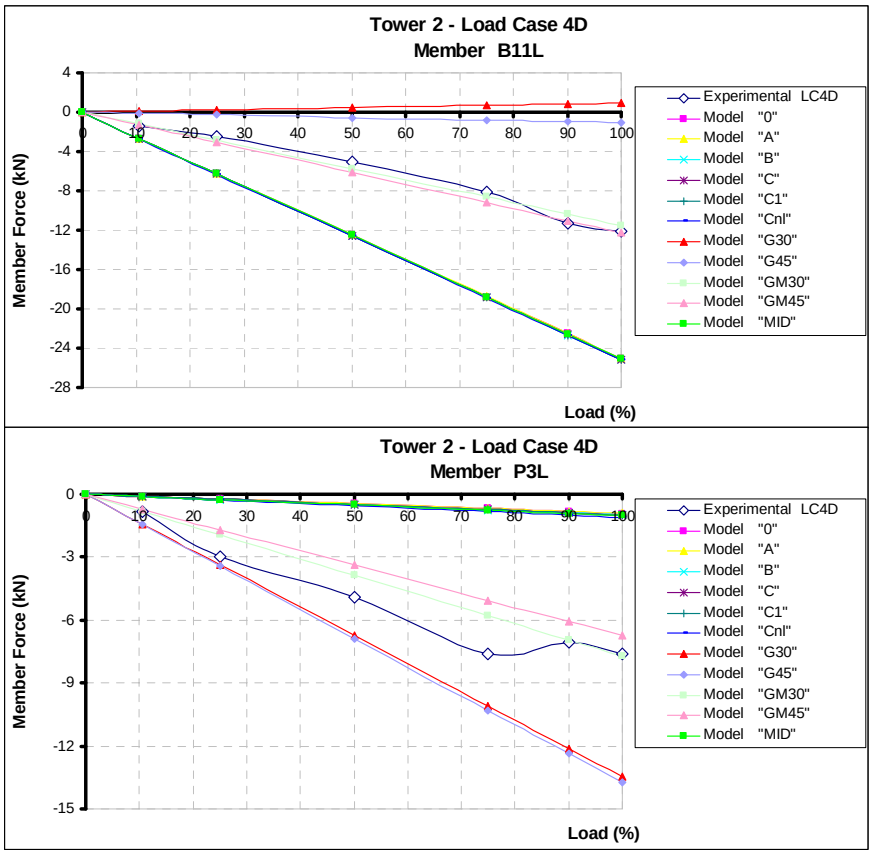

Figure 84: Axial forces on bars B11L and P3L of prototype "2" – LC 4D.

Figures 85 to 87 show the numeric results of the axial forces on the selected bars of tower "2A", subjected to load case "4D", for all models.

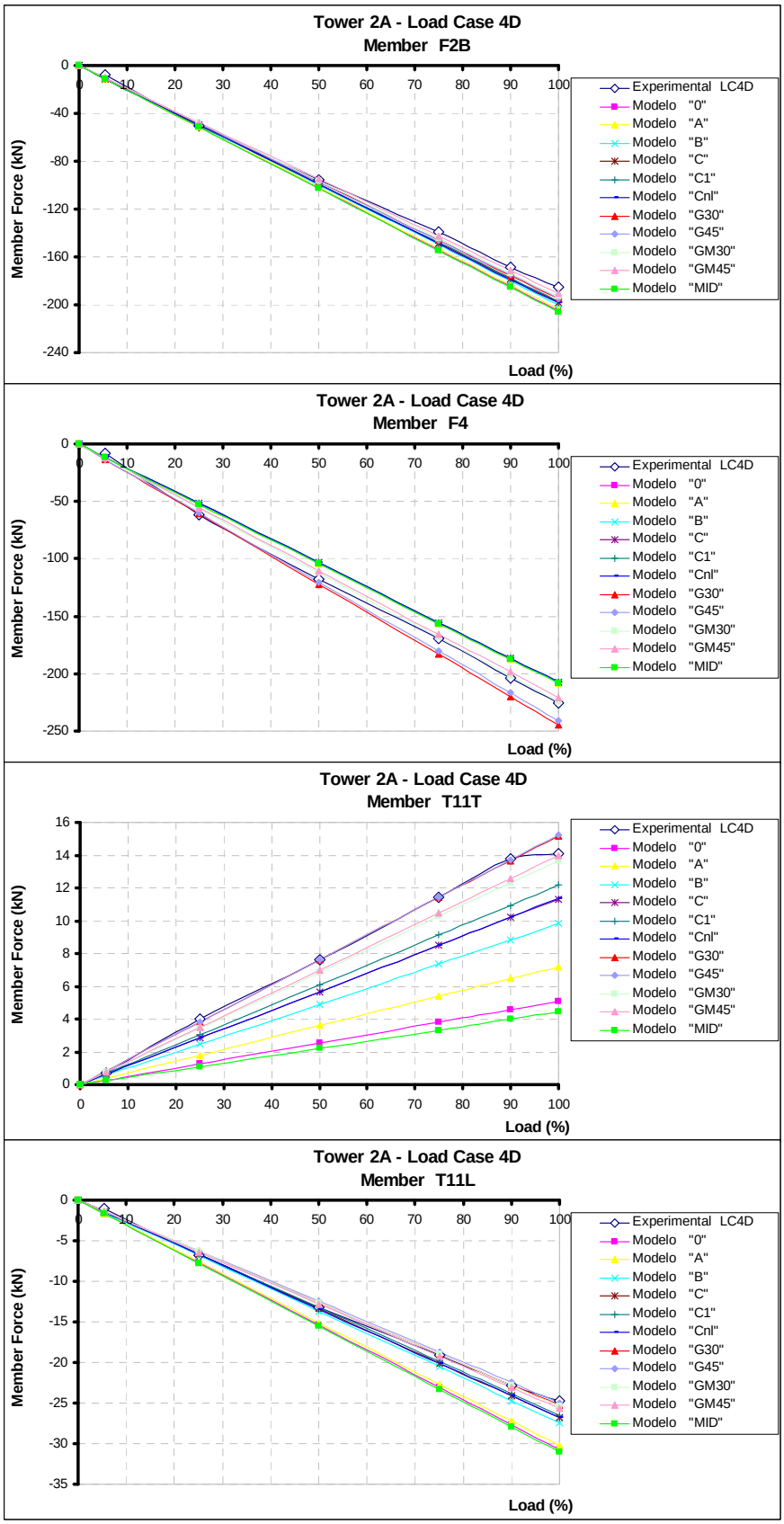

Figure 85: Axial forces on bars F2B, F4, T11T and T11L of prototype “2A” – LC 4D.

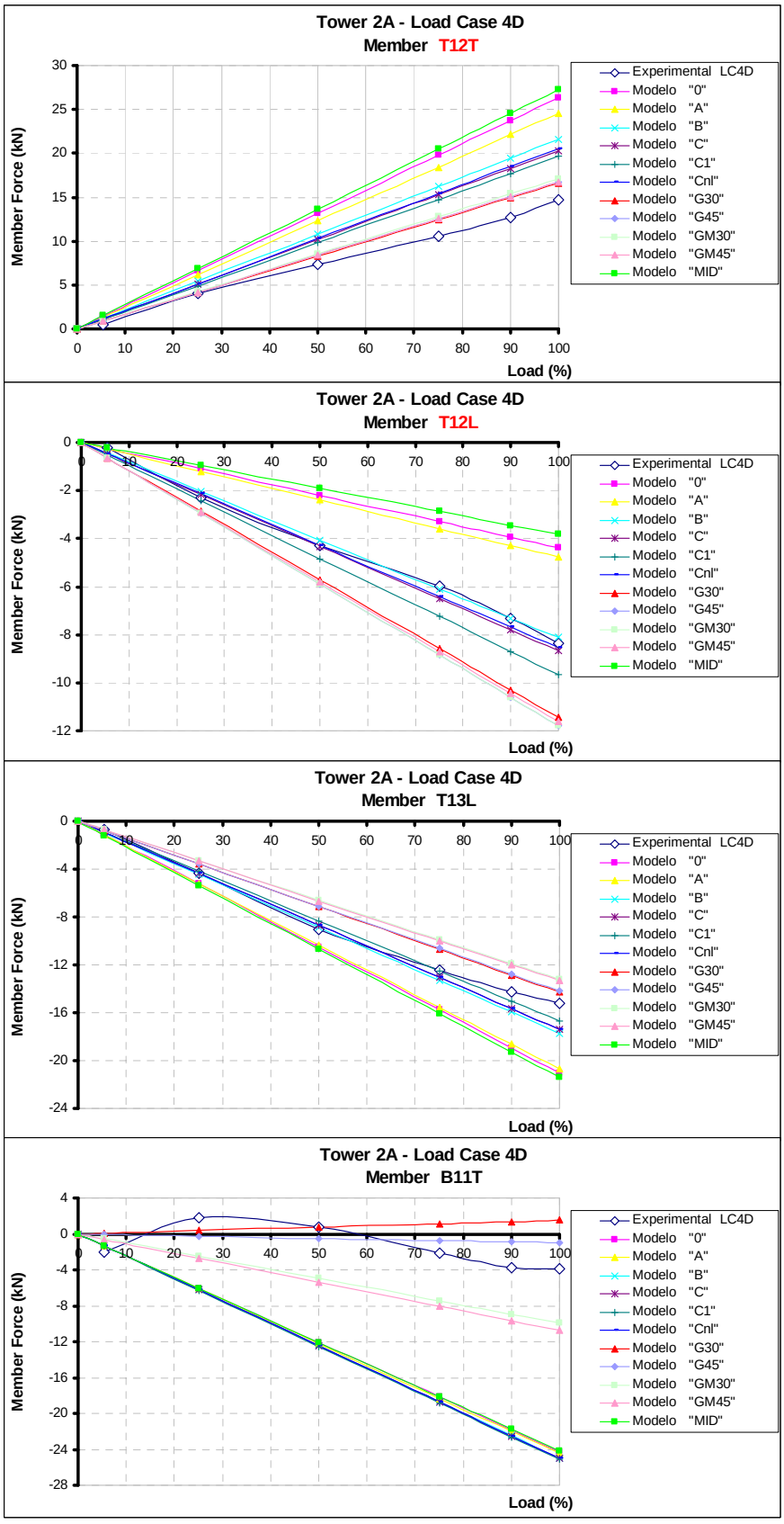

Figure 86: Axial forces on bars T12T, T12L, T13L and B11T of prototype "2A" – LC 4D.

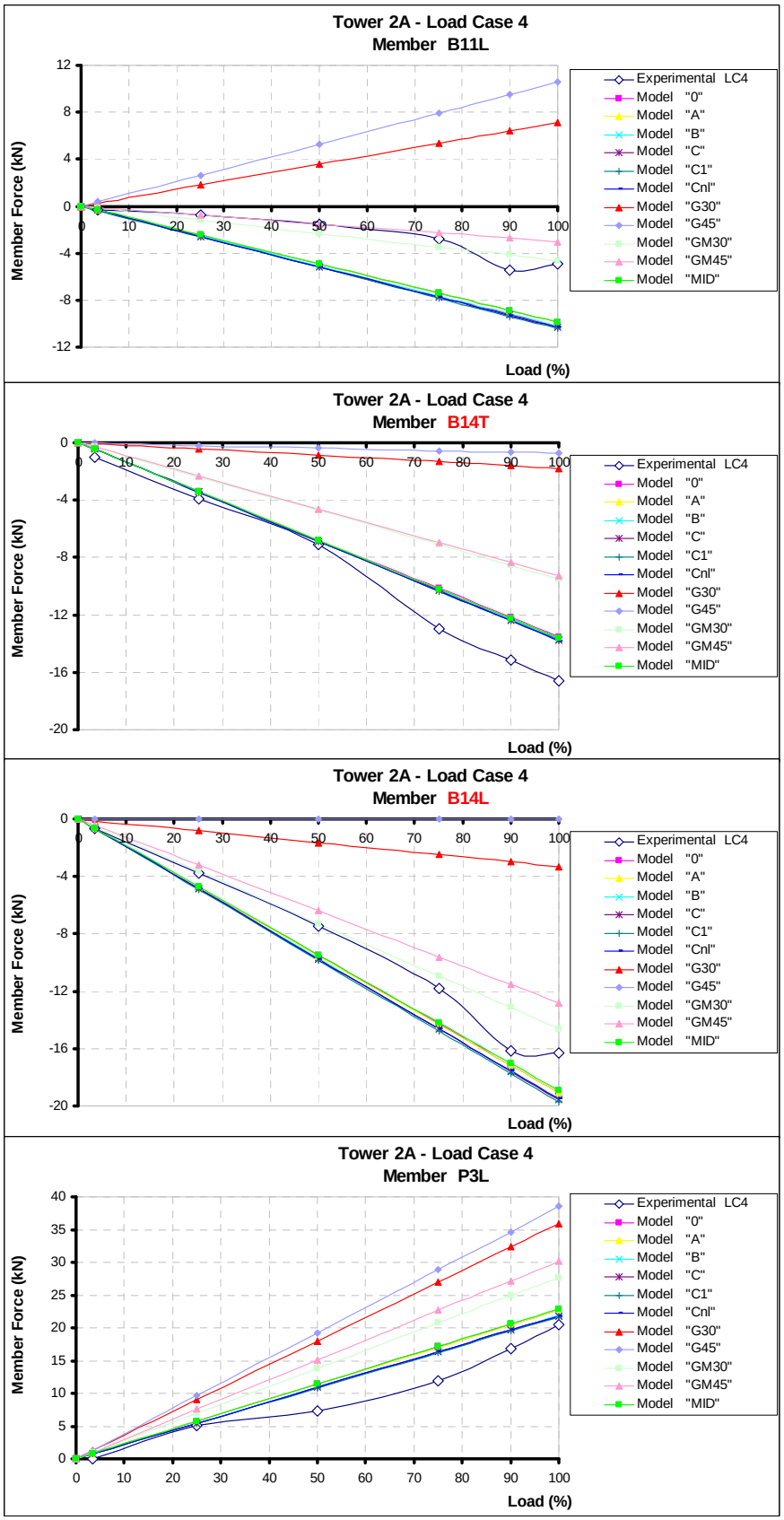

Figure 87: Axial forces on bars B11L, B14T, B14L and P3L of prototype "2A" – LC 4D.

The numeric results of the axial forces on the selected bars of the three towers for all models, subjected to all load cases, are presented in the attachment of this research (Annex 6). Observing these results it can be noted that the models which take into account the flexibility of the connections present values closer to the experimental ones.

It is important to note that when a test of a certain load case was finished, a residual displacement remained at the measuring points. When starting the next test, with a new load case, this displacement was disregarded, and this was not taken into consideration in the models.

9.7 Analysis of the results

In order to evaluate the accuracy of the distinct models, the axial forces of each model were compared with those experimentally obtained and an error index was introduced.

This index was defined as the sum for each tested bar of the difference between the model axial force and the experimental axial force, normalized for the element capacity. Figure 88 shows this index for each studied model.

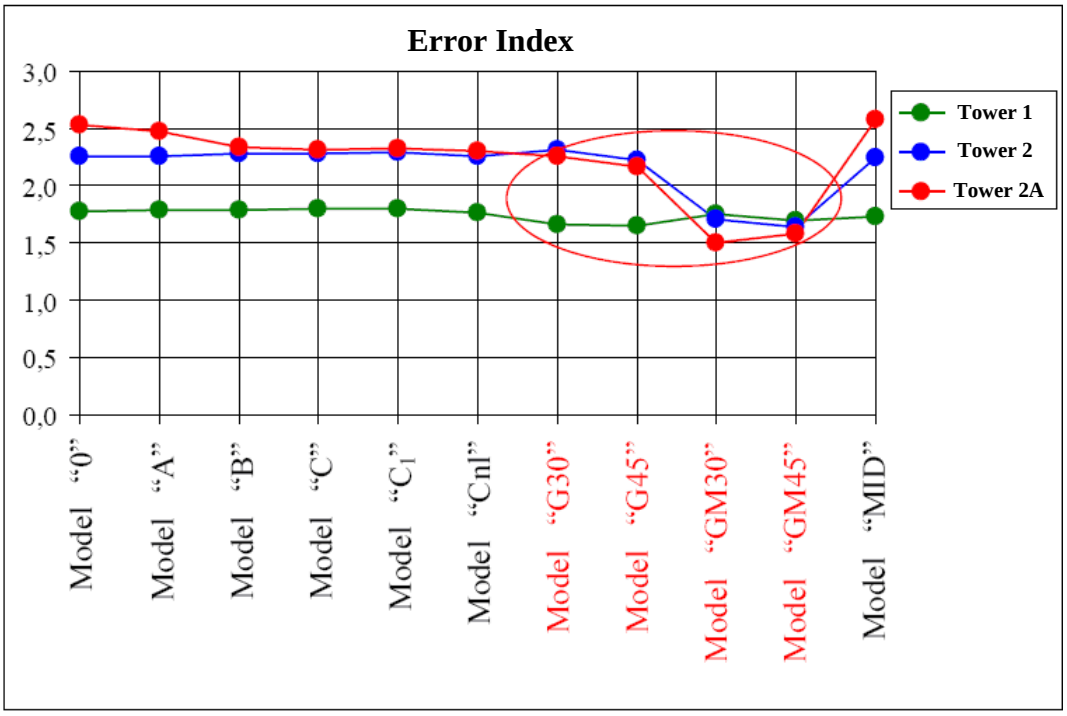

Figure 88: Error index for measured bars.

Figure 88 shows that the error indices are smaller in models which the bolt slippage was considered. On the other hand, Tower "1" value presented an index error practically constant, which is due to the fact that this structure is less hyperstatic than the others (this tower has less options of force balance, so it is less sensitive to the mechanical model).

It is important to point out that the experimental results do not represent the "real structural behaviour," since there are two main uncertainties that should be considered: (i) the uncertainty related to the method used to monitor the structures during testing, (ii) the statistical uncertainties related to the limited measured samples (it was measured just one sample for each case). However, the tests showed a clear tendency on structural behaviour.

10. CONCLUSIONS

The results of this experiment demonstrate that member force predictions using industry standard softwares can provide member forces different than actual structure behaviour. These differences can be caused by the structural system modeled, variation in material properties, and tolerances in manufacturing processes and erection practices. This experiment investigated the influence of different structural system models. It should be emphasized, however, that the "current industry practice on how to design OHL supports" has been confirmed as valid. Uncertainties can be controlled and kept under acceptable levels.

The prototype Structures (1, 2, and 2A) (Figures 3, 4 and 5) represent both isostatic and hyperstatic behaviour. Structure 1 (isostatic) test results and predicted member forces gave better agreement than Structures 2 and 2A (hyperstatic). The hyperstatic structures provided the potential for more member force balance options than for isostatic Structure 1. The isostatic configuration (Structure 1) is simpler, predictable, and less sensitive to all kinds of distortions on the member force balance.

Members with larger forces showed good agreement between test results and member force predictions. These members typically are the main support members. Lightly loaded members, such as diagonal members not in the plane of the structure loads, showed larger differences between actual and predicted member forces.

As a complement of the former Cigré studies [1], the accuracy on predictions for main member forces (typical coefficients of variation of about 3%) were again proved. Discrepancies in the prediction of diagonal member forces, were studied and now explained. Coefficients of variation for diagonal member forces could be reduced from around 30% as per Cigré former document [1] to 10% according to this experiment.

Discrepancies such as those shown in Figure 63 occurred in many members and in different circumstances during the experience. It is important to stress, however, that they are not relevant from the practical point of view, since in all those load cases the members were not critical (see graph ordinate). For their critical load conditions, the diagonal members behaved as predicted.

Regarding specifically structural modelling, Prototypes 2 and 2A (hyperstatic) could also be adequately modeled, by using refined analysis methods as done here in this exercise. The member forces obtained from the refined analysis show better agreement with the test results.

As an extension of this Cigré experiment, Kaminski Jr [7], taking the data and results of this B2.08TF4 study, carried out sophisticated analysis, not currently performed by the industry, aiming to approach the member force predictions to those measured during the tests. As an example, the method of analysis that take into account 'bolts slippage' showed the best comparison between the calculated versus measured member force curves. Using the sophisticated analysis mentioned above, it was possible to confirm that Structures 1, 2, and 2A, with the design and fabrication tolerances as well as the hyperstaticity level, was able to develop structural force balance similar to that of the test results, that is the "principle of minimum energy level." This can be seen in the chapter 9 of this technical brochure.

This experiment supports the argument for prototype testing. Until the transmission tower industry has software tools available with significantly advanced analysis capabilities (such as non-linear material and geometry, non-linear member connection modelling, probabilistic analysis, etc.) real-scale testing will continue to be an important tool for the design engineer. Therefore, when, for any reason, a prototype test can not be performed, it is recommended that an appropriate (reduced) value of $Ø_R$ (strength factor) be used for member strength calculations. As example, values of $Ø_R = 0.93$ and $Ø_R = 0.90$ have been adopted for suspension towers, of which the design will be calibrated by testing or not respectively. For anchor towers not tested, $Ø_R = 0.85$ has been suggested [24].

In conclusion, this experiment provides a better understanding of the structural behaviour of transmission line towers and the potential variations in member force predictions. Working Group 08 believes that the information presented in this document will help to advance the transmission line tower industry by providing more reliable structures.

11. ACKNOWLEDGEMENTS

WG08 acknowledges the support received from: Eskom, ABB, Roy Macey, Mark Newby, S.J. Madibu, and the contributors Leandro F. Fadel Miguel, J. Kaminski Jr, Márcia A. M. Cadete.

The Convener also thanks the reviewers R. Stephen, P. Riisiö and H. Øbro for their contributions and comments.

12. BIBLIOGRAPHIC REFERENCES

[1] CIGRÉ SCB2 WG08, An Experiment to measure the Variation in Lattice Tower Strength due to local design Practice, Electra nº 138, October, 1991.

[2] IEC 60826, Loading and Strength of Overhead Transmission Line, Second edition, October, 2003.

[3] SILVA, J.B.G.F.; RIEIRA, J.D.; MENEZES, R.C.R.; SILVA, V.R., Evaluation of the probability distribution of the strength of transmission line steel tower based on tower test results, Bienal Cigré, Paris, 1990.

[4] CIGRÉ SCB2 WG08, Variability on the Mechanical Properties of Materials, Electra nº 189, April, 2000.

[5] CIGRÉ SCB2 WG08, Statistical Analysis on the Material, Electra nº 208, June, 2003.

[6] CIGRÉ SCB2 WG08, Diaphragms in lattice steel tower, Electra nº 199, December, 2001 & Technical Brochure nº 196.

[7] KAMINSKI Jr., J. Incerteza de modelo na análise de torres metálicas treliçadas de linhas de transmissão, Post Graduation Program in Civil Engineering, Federal University of Rio Grande do Sul (UFRGS), Brazil, 2007 (in portuguese).

[8] PRZEMIENIECHI, J. S. Theory of matrix structural analysis. New York: McGraw-Hill Book Company, 1968.

[9] ORAN, C. Tangent stiffness in space frames. Journal of Structural Division - ASCE, v. 99, n. ST5, p. 987-1001, 1973.

[10] ARGYRIS, J. H.; HILPERT, O.; MALEJANNAKIS, G. A.; SCHARPF, D. W. On the

geometric stiffness of a beam in space – A consistent virtual work approach. Computer Methods in Applied Mechanics and Engineering, v. 20, p. 105-131, 1979.

[11] BATHE, K. J.; BOLOURCHI, S. Large displacement analysis of three-dimensional beam structures. International Journal for Numerical Methods in Engineering, v. 14, p. 961-986, 1979.

[12] COOK, R. D. Finite element modelling for stress analysis. New York: John Wiley & Sons, 1995.

[13] ELECTRIC POWER RESEARCH INSTITUTE (EPRI). Structural development studies at the EPRI transmission line mechanical research facility. Interim Report, n. 1, EL-4756, 1986.

[14] AMERICAN SOCIETY OF CIVIL ENGINEERS (ASCE). ASCE Standard 10-97: design of latticed steel transmission structures, 2000.

[15] UNGKURAPINAN, N.; CHANDRAKEERTHY, S. R. De S.; RAJAPAKSE, R. K. N. D.; YUE, S. B. Joint slip in steel electric transmission towers. Engineering Structures, v. 25, n. 6, p. 779-788, 2003.

[16] KITIPORNCHAI, S.; AL-BERMANI, F. G. A.; PEYROT, A. H. Effect of bolt slippage on ultimate behaviour of lattice structures. Journal of Structural Engineering, ASCE, v. 120, n. 8, p. 2281-2287, 1994.

[17] PFEIL, W.; PFEIL, M. Estruturas de aço – Dimensionamento prático. 7ª edição. Rio de Janeiro: Livros Técnicos e Científicos Editora, 2000 (in Portuguese).

[18] CHEN, W. F.; LUI, E. M. Effects of joint flexibility on the behaviour of steel frames. Computers and Structures, v. 26, n. 5, p. 719-732, 1987.

[19] NETHERCOT, D. A. Stability and connections: their interaction as it affects the behaviour and design of steel frames. Fifth International Colloquium on Structural Stability, Rio de Janeiro, Brasil, 1996.

[20] WILHOITE, G.; ZANDONINI, R.; ZAVELANI, A. Behaviour and strength of angles in compression: An experimental investigation. Annual Convention and Structures Congress, ASCE, San Francisco, 1984

[21] KISHI, N.; CHEN, W. F. Moment-rotation relations of semirigid connections with angles. Journal of Structural Engineering, ASCE, v. 116, n. 7, p. 1813-1834, 1990.

[22] MENEZES, R. C. R. Failure-data based reliability assessment considering mechanical model uncertainties. 1992. Ph.D. Thesis - Institut für Mechanik, Universität Innsbruck, Austria.

[23] ROY, S.; FANG, S.; ROSSOW, E. Secondary stresses on transmission tower structures. Journal of Energy Engineering, ASCE, v. 110, n. 2, p. 157-172, 1984.

[24] ABNT NBR 8850: Execução de Suportes Metálicos Treliçados para Linhas de Transmissão – Procedimento. Rio de Janeiro, 2003 (in Portuguese).

ANNEX A:

BASIC DESIGN INFORMATION

WORKING GROUP SCB2.08

TF4 – INFLUENCE OF THE HYPERSTATIC MODELLING ON THE BEHAVIOUR OF TRANSMISSION LINE LATTICE STRUCTURES

BASIC DESIGN INFORMATION STRUCTURES 1, 2, 2A

A	04/02/2004	Information to calculate structures 1, 2 and 2A
REVISION	**DATE**	**DESCRIPTION**

SUMÁRIO

1. STRUCTURE OUTLINE

1.1. STRUCTURE 1

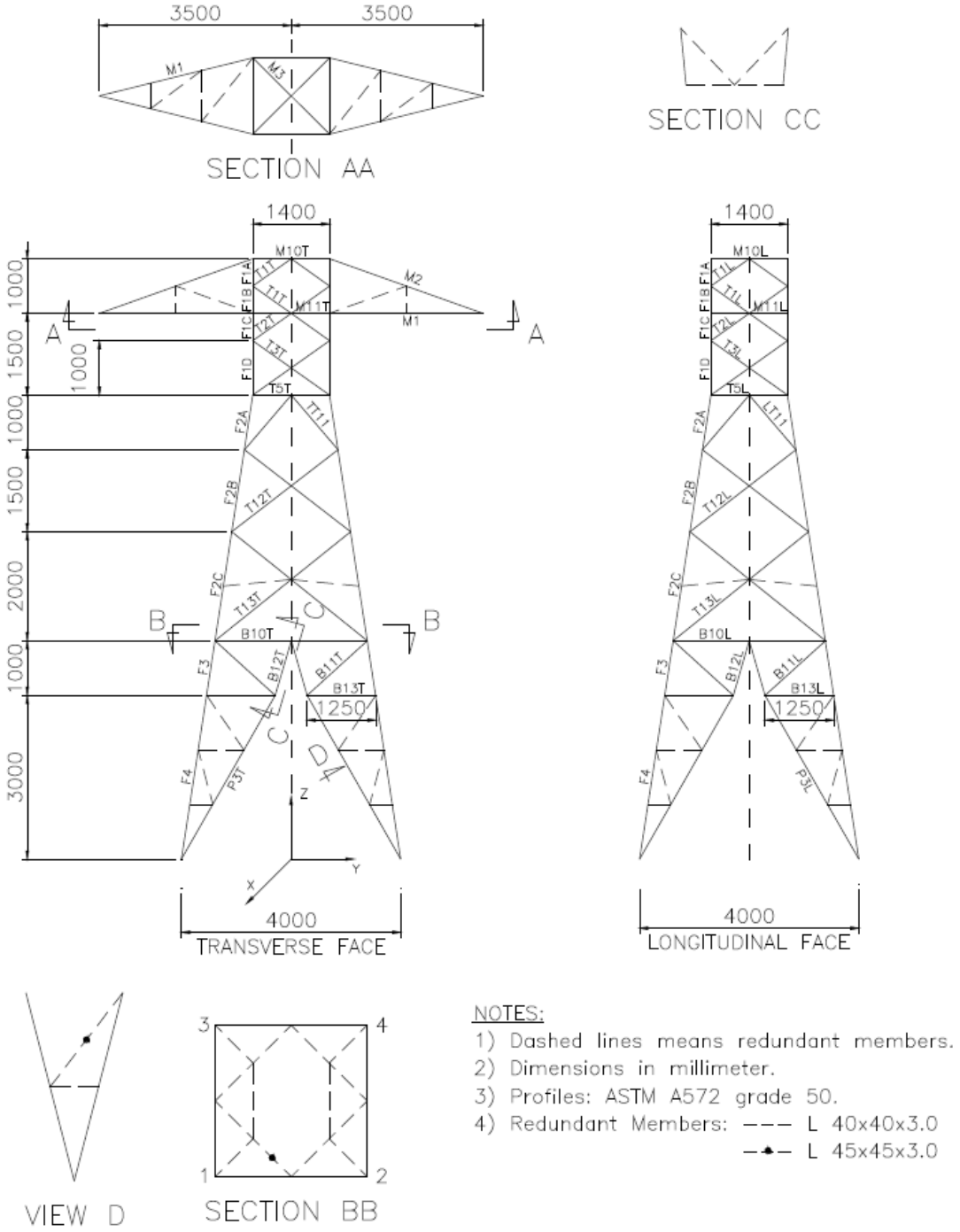

NOTES:
1) Dashed lines means redundant members.
2) Dimensions in millimeter.
3) Profiles: ASTM A572 grade 50.
4) Redundant Members: --- L 40x40x3.0
-•- L 45x45x3.0

1.2. STRUCTURE 2

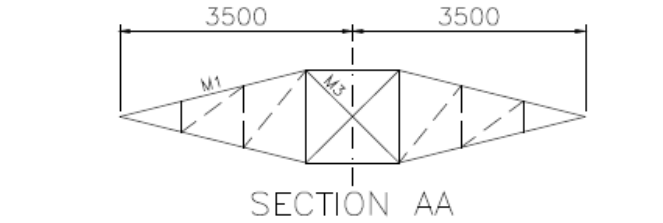

SECTION AA

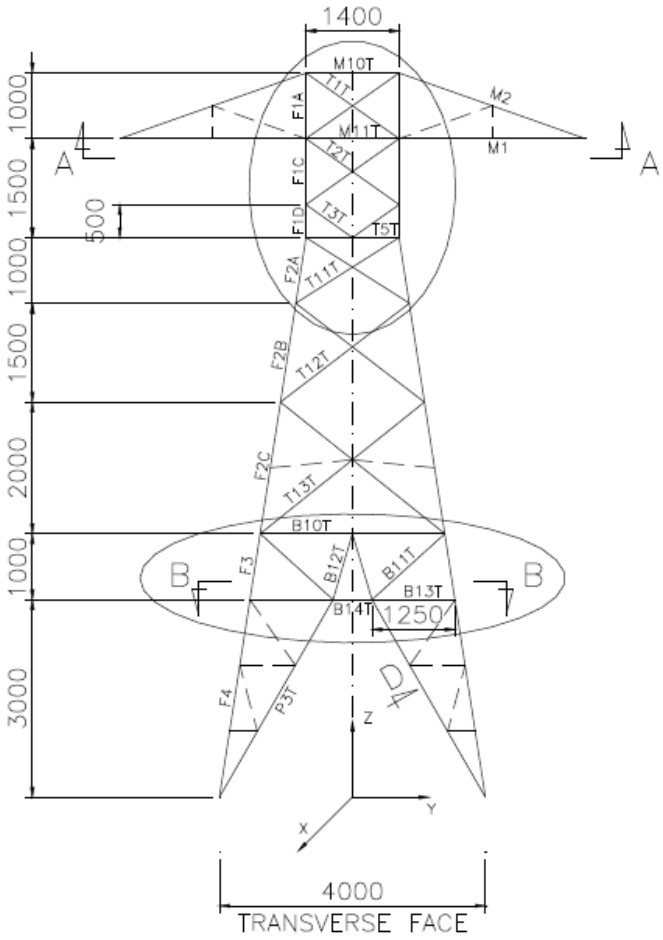

TRANSVERSE FACE

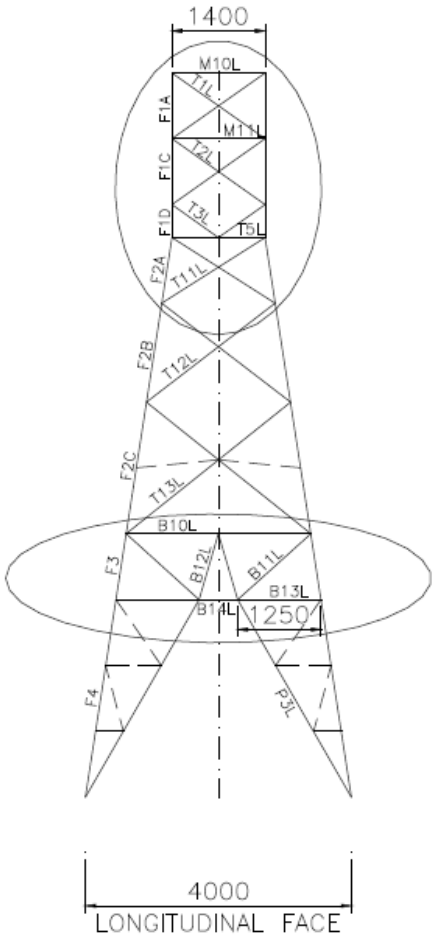

LONGITUDINAL FACE

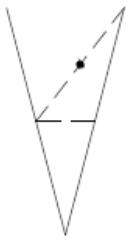

VIEW D

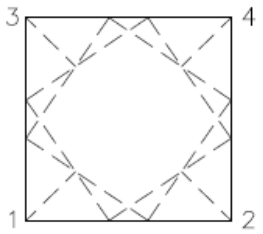

SECTION BB

NOTES:
1) Dashed lines means redundant members.
2) Dimensions in millimeter.
3) Profiles: ASTM A572 grade 50.
4) Redundant Members: --- L 40x40x3.0
-•- L 45x45x3.0

1.3. STRUCTURE 2A

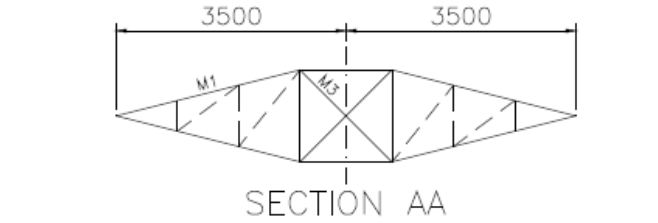

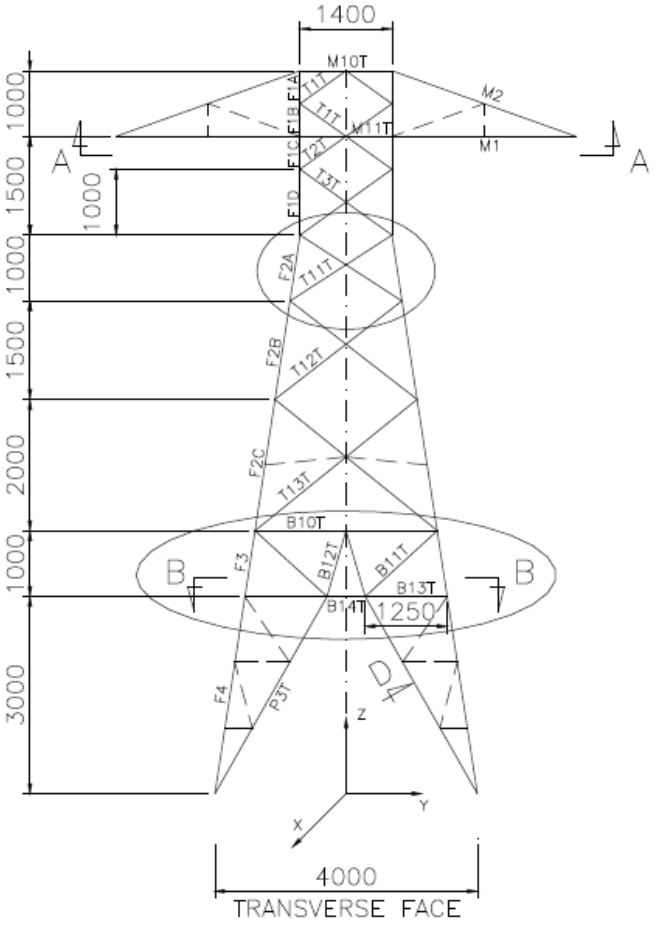

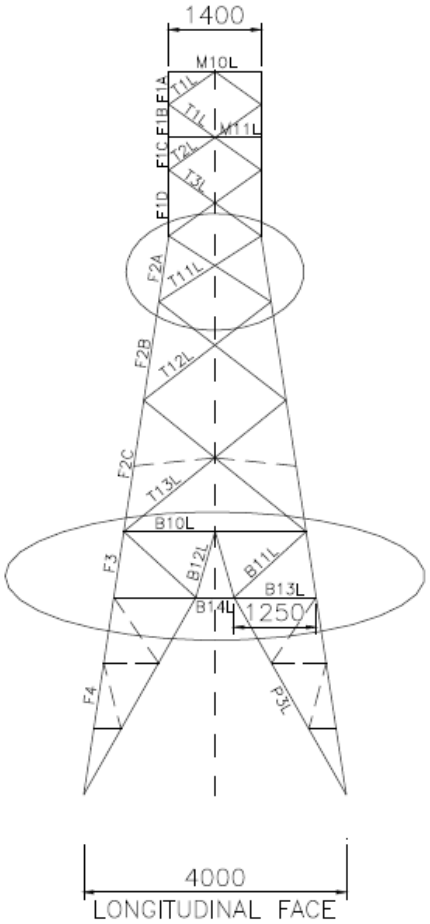

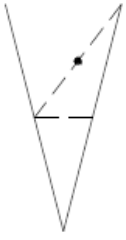
VIEW D

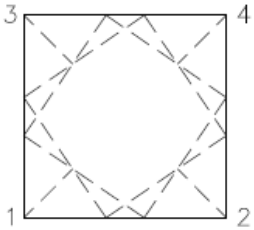

SECTION BB

NOTES:
1) Dashed lines means redundant members.
2) Dimensions in millimeter.
3) Profiles: ASTM A572 grade 50.
4) Redundant Members: ––– L 40x40x3.0
–•– L 45x45x3.0

2. LOADING CASES

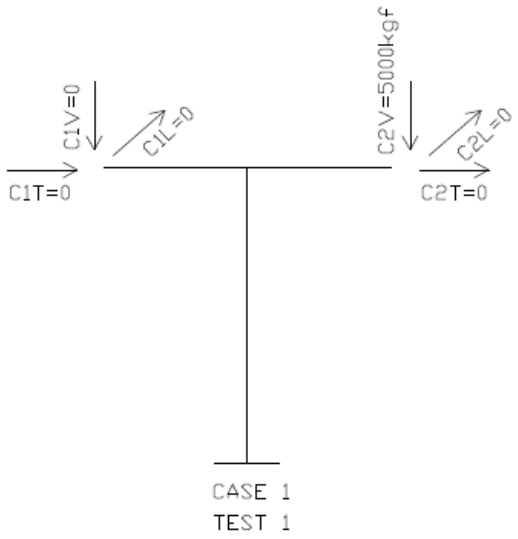

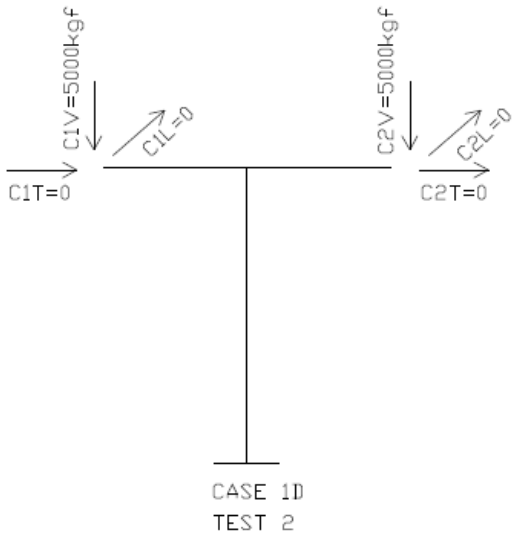

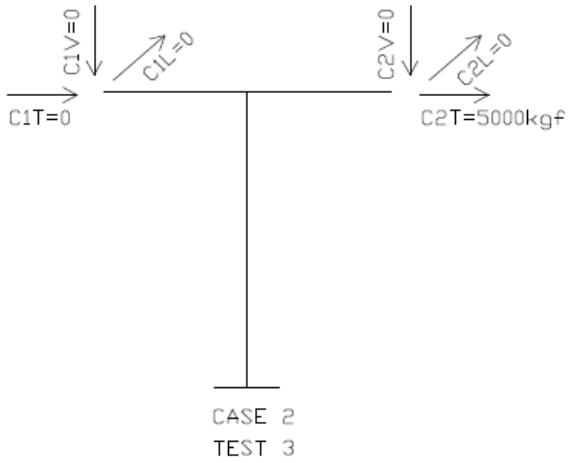

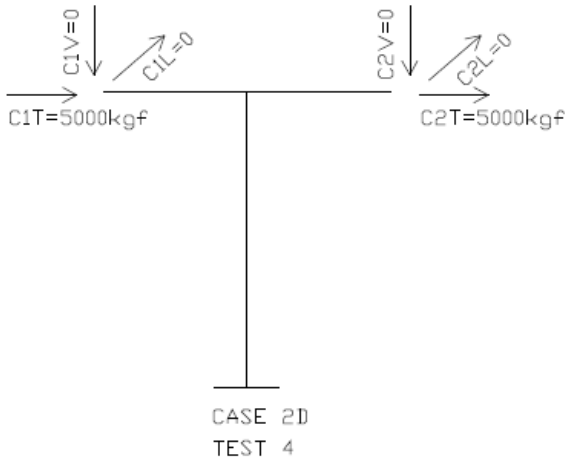

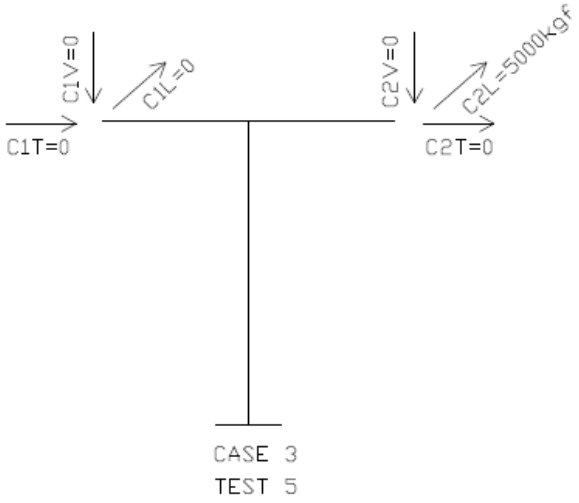
C1V=0
C1L=0
C2V=0
C2L=5000kgf
C1T=0
C2T=0
CASE 3
TEST 5

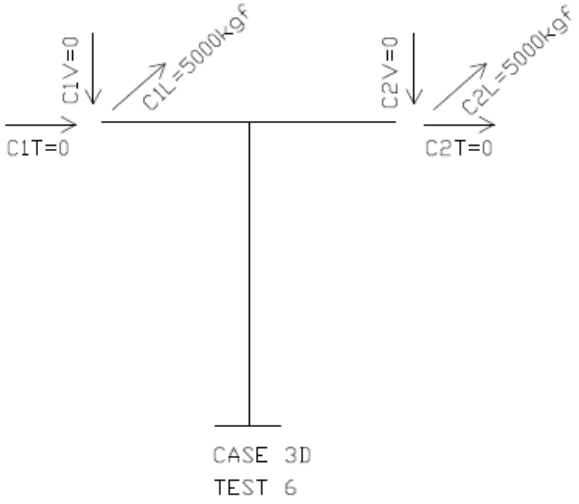
C1V=0
C1L=5000kgf
C2V=0
C2L=5000kgf
C1T=0
C2T=0
CASE 3D
TEST 6

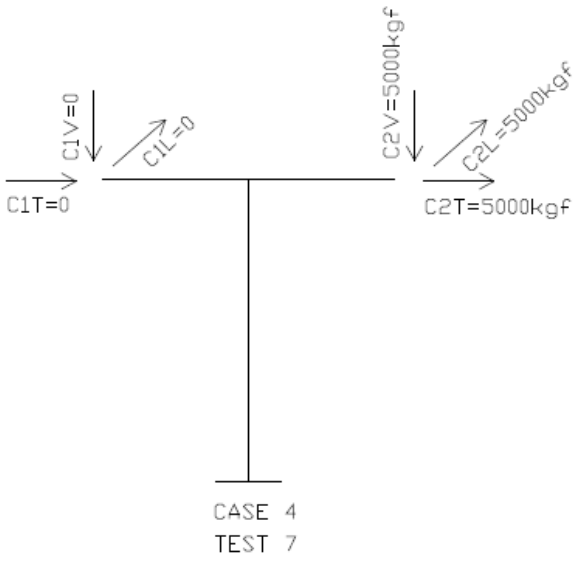
C1V=0
C1L=0
C2V=5000kgf
C2L=5000kgf
C1T=0
C2T=5000kgf
CASE 4
TEST 7

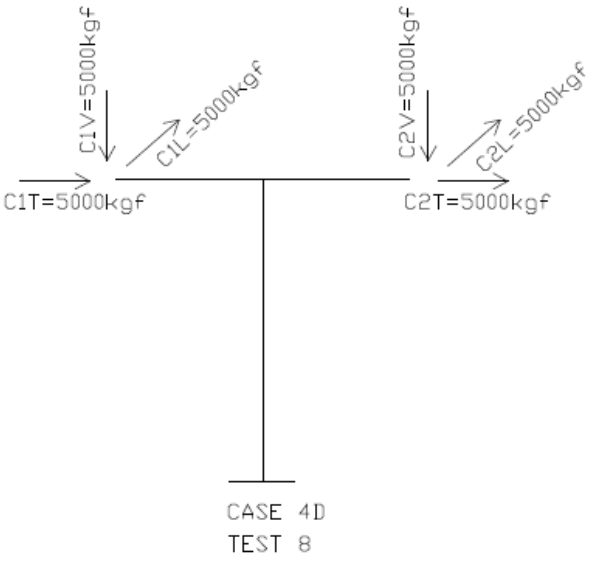
C1V=5000kgf
C1L=5000kgf
C2V=5000kgf
C2L=5000kgf
C1T=5000kgf
C2T=5000kgf
CASE 4D
TEST 8

3. MEMBERS MEASURED WITH STRAIN GAGE - ORIENTATION AND ATTACHMENT POINT IDENTIFICATION

3.1. STRUCTURE 1

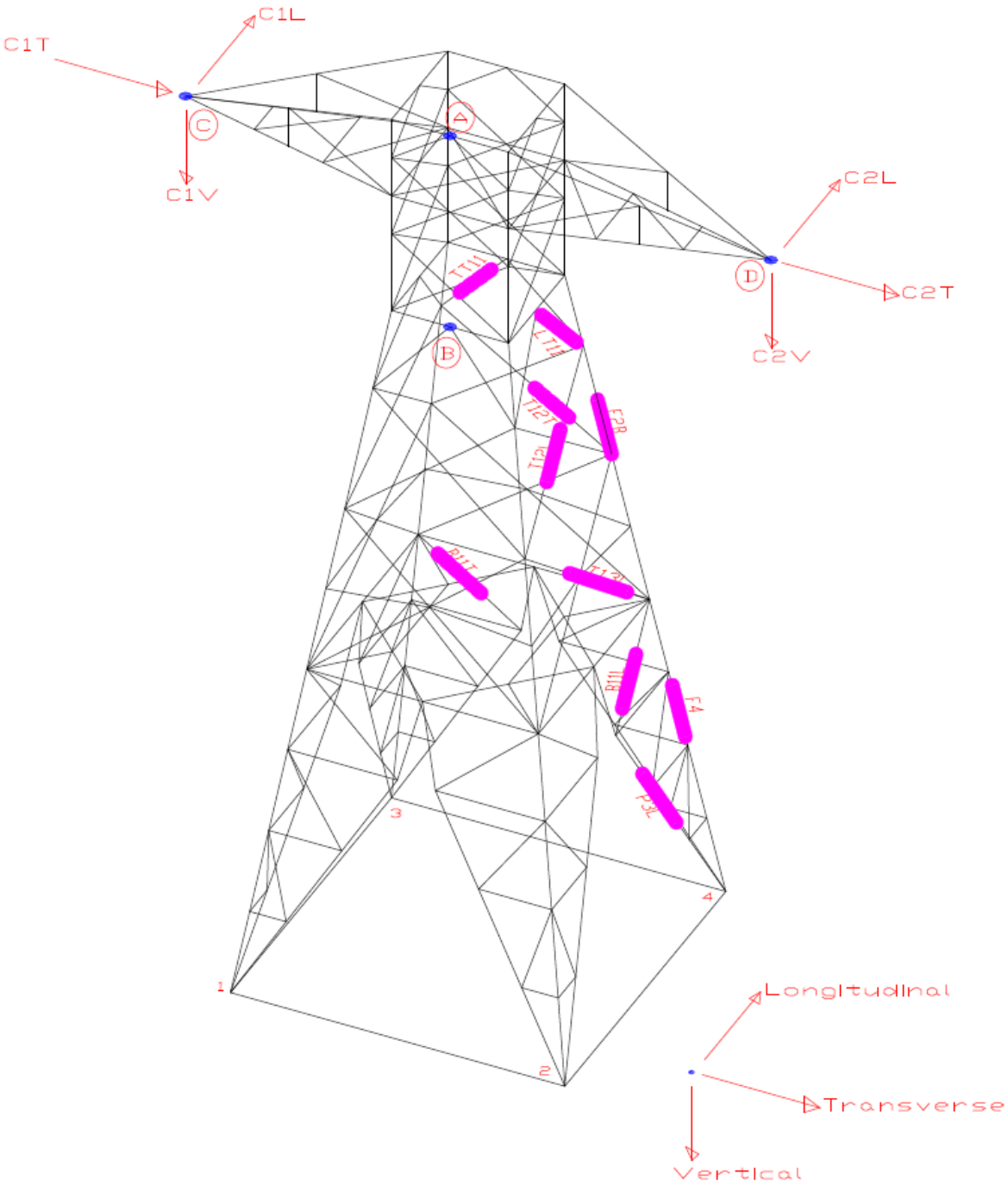

3.2. STRUCTURE 2

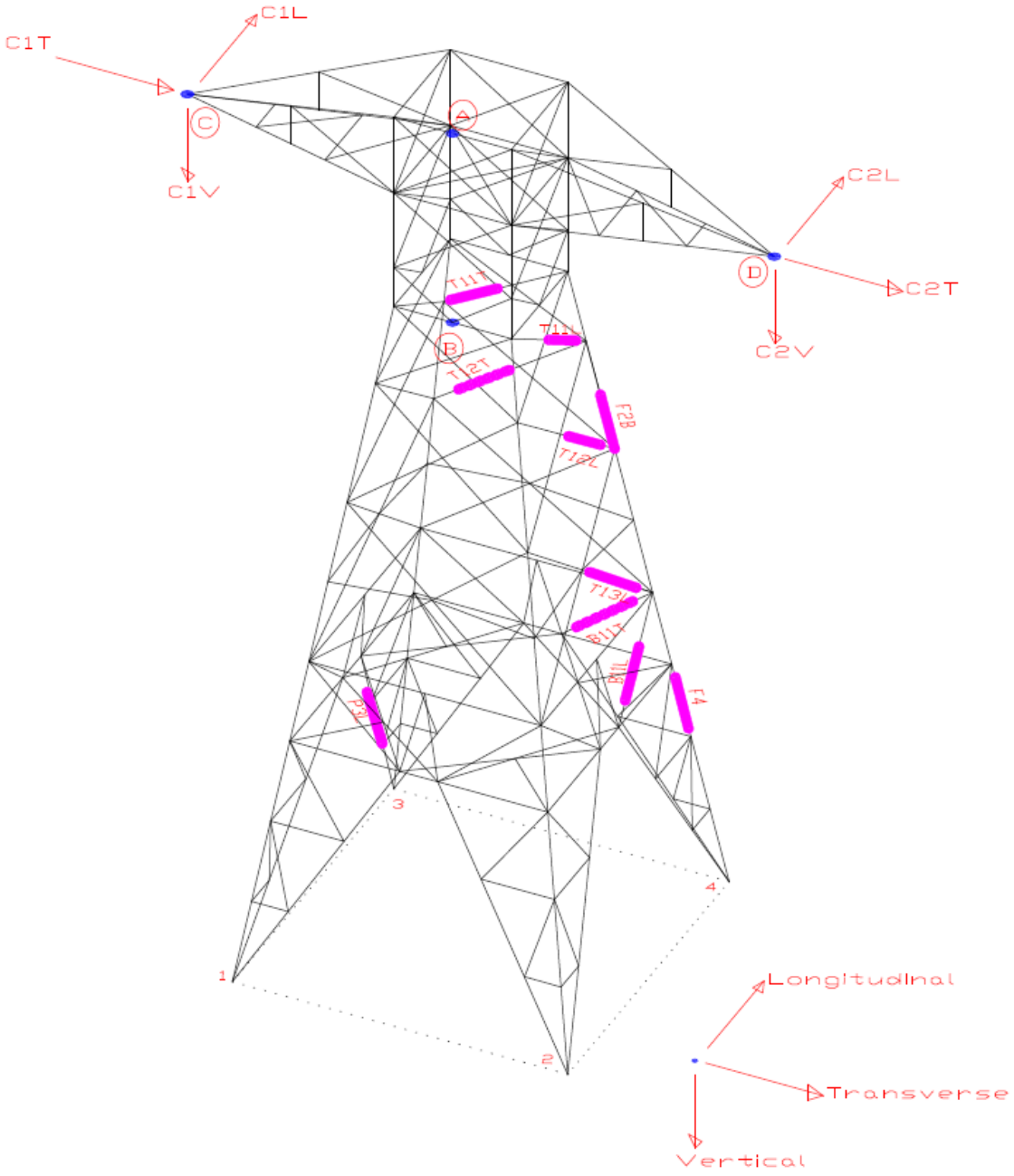

3.3. STRUCTURE 2A

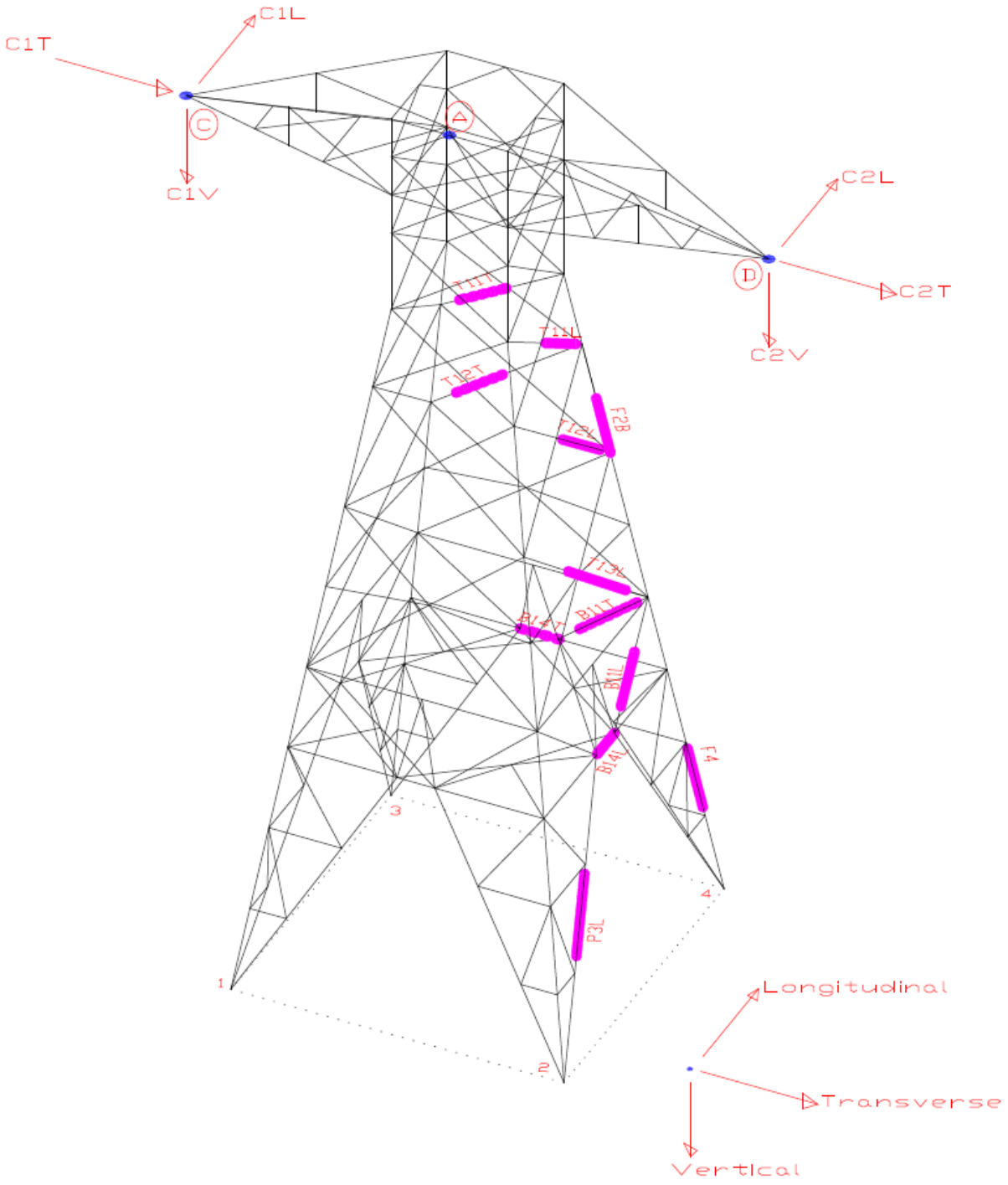

4. LIST OF MEMBERS, PROFILES AND BOLTS

MEMBERS	ANGLE SIZE STRUCTURES 1, 2, 2A	NUMBER OF BOLTS		
		STRUCTURE 1	STRUCTURE 2	STRUCTURE 2A
B10L	L 50 x 50 x 5.0 H	1	2	2
B10T	L 50 x 50 x 5.0 H	1	2	2
B11L	L 50 x 50 x 5.0 H	1	2	2
B11T	L 50 x 50 x 5.0 H	1	2	2
B12L	2L 50 x 50 x 5.0 H	2	2	2
B12T	2L 50 x 50 x 5.0 H	2	2	2
B13L	L 50 x 50 x 5.0 H	1	1	1
B13T	L 50 x 50 x 5.0 H	1	1	1
B14L	L 50 x 50 x 5.0 H	Not Applicable	1	1
B14T	L 50 x 50 x 5.0 H	Not Applicable	1	1
F 1A	L 65 x 65 x 5.0 H	4	4	4
F 1B	L 65 x 65 x 5.0 H	-	-	-
F 1C	L 65 x 65 x 5.0 H	-	-	-
F 1D	L 65 x 65 x 5.0 H	4	6	4
F 2A	L 90 x 90 x 6.0 H	6	6	6
F 2B	L 90 x 90 x 6.0 H	-	-	-
F 2C	L 90 x 90 x 6.0 H	-	-	-
F 3	L 90 x 90 x 6.0 H	10	8	8
F 4	L 90 x 90 x 6.0 H	10	8	8
M 1	L 90 x 90 x 6.0 H	7	7	7
M 2	L 50 x 50 x 5.0 H	3	3	3
M 3	L 45 x 45 x 3.0 H	2	2	2
M10L	L 45 x 45 x 3.0 H	2	2	2
M10T	L 50 x 50 x 5.0 H	3	3	3
M11L	L 50 x 50 x 5.0 H	2	2	2
M11T	L 90 x 90 x 6.0 H	7	7	7
P 3L	L 50 x 50 x 5.0 H	2	3	3
P 3T	L 50 x 50 x 5.0 H	2	2	2
T 1L	L 45 x 45 x 3.0 H	1	1	1
T 1T	L 45 x 45 x 5.0 H	2	2	2
T 2L	L 45 x 45 x 5.0 H	3	3	3
T 2T	L 45 x 45 x 5.0 H	2	2	2
T 3L	L 45 x 45 x 5.0 H	3	3	3
T 3T	L 45 x 45 x 5.0 H	2	2	2
T 5L	L 50 x 50 x 5.0 H	3	3	Not Applicable
T 5T	L 50 x 50 x 5.0 H	2	2	Not Applicable
LT11	L 65 x 65 x 5.0 H	3	Not Applicable	Not Applicable
T11L	L 65 x 65 x 5.0 H	Not Applicable	2	3
TT11	L 65 x 65 x 5.0 H	2	Not Applicable	Not Applicable
T11T	L 65 x 65 x 5.0 H	Not Applicable	2	2
T12L	L 50 x 50 x 5.0 H	2	2	2
T12T	L 50 x 50 x 5.0 H	2	2	2
T13L	L 65 x 65 x 5.0 H	2	2	2
T13T	L 65 x 65 x 5.0 H	1	1	2

Notes:

a) Steel for plates: ASTM A36 (YIELD STRESS : 2530 kgf / cm^2).

b) Steel for profiles: ASTM A572 GRADE 50 (YIELD STRESS : 3515 kgf / cm^2).

c) Bolt diameter is 12mm (M12).

d) Shear on bolts should be taken through their bodies.

5. ANGLE PROPERTIES

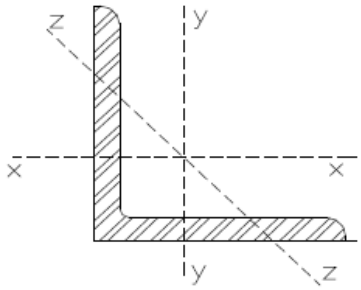

Size and Thickness (mm)	Weight	Area	Axis X-X / Y-Y				Axis Z-Z	B/T
			I	S	r	x-y	r	
	kg/m	cm2	cm4	cm3	cm	cm	cm	
L 40 X 40 X 3.0	1.84	2.35	3.45	1.18	1.21	1.07	0.78	10.33
L 40 X 40 X 5.0	2.97	3.79	5.43	1.91	1.20	1.16	0.77	5.80
L 45 X 45 X 3.0	2.09	2.66	4.93	1.49	1.36	1.18	0.88	11.67
L 45 X 45 X 5.0	3.38	4.30	7.84	2.43	1.35	1.28	0.87	6.60
L 50 X 50 X 5.0	3.77	4.80	11.00	3.05	1.51	1.40	0.97	7.60
L 50 X 50 X 6.0	4.47	5.69	12.80	3.61	1.50	1.45	0.97	6.17
L 65 X 65 X 5.0	4.95	6.31	24.70	5.21	1.98	1.76	1.28	10.20
L 65 X 65 X 6.0	5.91	7.53	29.20	6.21	1.97	1.80	1.27	8.33
L 75 X 75 X 5.0	5.78	7.36	38.60	7.01	2.29	1.99	1.48	12.00
L 75 X 75 X 6.0	6.87	8.75	45.60	8.35	2.28	2.04	1.47	9.83
L 75 X 75 X 8.0	9.03	11.50	58.90	11.00	2.26	2.13	1.45	7.12
L 90 X 90 X 6.0	8.30	10.60	80.30	12.20	2.76	2.41	1.78	12.17
L 90 X 90 X 7.0	9.58	12.20	92.40	14.10	2.75	2.46	1.77	10.28

6. MEMBER FORCE TABLE (RESULTS)

MEMBER FORCE TABLE (kN)															
CASE	STRUCTURE	F2B*	F4*	TT11	T11T**	LT11	T11L**	T12T**	T12L**	T13L*	B11T**	B11L*	B14T	B14L	P3L
1	1				-		-						-	-	
	2			-		-							-	-	
	2A			-		-									
1D	1				-		-						-	-	
	2			-		-							-	-	
	2A			-		-									
2	1				-		-						-	-	
	2			-		-							-	-	
	2A			-		-									
2D	1				-		-						-	-	
	2			-		-							-	-	
	2A			-		-									
3	1				-		-						-	-	
	2			-		-							-	-	
	2A			-		-									
3D	1				-		-						-	-	
	2			-		-							-	-	
	2A			-		-									
4	1				-		-						-	-	
	2			-		-							-	-	
	2A			-		-									
4D	1				-		-						-	-	
	2			-		-							-	-	
	2A			-		-									

Notes:

a) Tension Force (+).

b) Compression Force (-).

c) * - Strain gage fixed in the same position in structures 1, 2 and 2A.

d) ** - Strain gage fixed in the same position in structures 2 and 2A.

ANNEX B:

EXPERIMENTAL DATA

&

TEST REPORTS

B.1 EXPERIMENTAL DATA

The values presented below are those obtained from the application of the equations 1, 2 and 3 shown on Chapter 7 (pages 50 and 51) over the experimental readings obtained from the "strain-gage systems" during the tests.

B.1.1. PROTOTYPE 1

Load Case 1

	F2B			P3L			F4			T12L		
Load	M11	M22	Axial	M11	M22	Axial	M11	M22	Axial	M11	M22	Axial
(%)	Nm	Nm	N	Nm	Nm	N	Nm	Nm	N	Nm	Nm	N
0.4	0	0	0	0	0	0	0	0	0	-1	0	32
25	-53	-22	-14176	-8	0	-442	-23	-24	-11536	11	-3	-72
50	-104	-53	-26931	-20	5	-584	-36	-28	-19014	16	-4	-212
75	-210	-95	-40798	-30	6	-1650	-53	-33	-28718	14	-4	-253
90	-256	-114	-50239	-38	8	-2343	-66	-37	-36423	17	-5	-79
100	-298	-127	-57766	-45	8	-2704	-80	-38	-42356	16	-5	127
0.4	-111	-3	-1710	-20	9	12	-13	-31	-1867	-2	2	615

	T13L			T12T			B11L			T11T		
Load	M11	M22	Axial	M11	M22	Axial	M11	M22	Axial	M11	M22	Axial
(%)	Nm	Nm	N	Nm	Nm	N	Nm	Nm	N	Nm	Nm	N
0.4	0	0	0	0	0	0	0	0	0	0	0	0
25	-15	-10	-523	23	-6	1943	-7	-2	-365	-49	23	-3216
50	-11	-13	-347	51	-13	4547	-8	-1	-248	-127	58	-7106
75	-21	-17	-565	80	-21	7343	-10	-1	-66	-183	96	-10645
90	-26	-20	-885	93	-24	8504	-12	1	37	-207	111	-12358
100	-31	-23	-858	106	-27	9463	-13	2	251	-231	124	-13787
0.4	-20	-10	-705	1	0	-69	-15	3	13	-4	-4	-15

	B11T			T11L		
Load	M11	M22	Axial	M11	M22	Axial
(%)	Nm	Nm	N	Nm	Nm	N
0.4	0	0	0	0	0	0
25	28	-2	1269	10	-1	-291
50	42	0	1815	18	-19	438
75	41	-1	2041	22	-31	849
90	40	-1	2122	26	-25	974
100	42	-1	2251	27	-25	1194
0.4	-5	2	-455	-7	25	173

Load Case 1D

	F2B			P3L			F4			T12L		
Load	M11	M22	Axial	M11	M22	Axial	M11	M22	Axial	M11	M22	Axial
(%)	Nm	Nm	N	Nm	Nm	N	Nm	Nm	N	Nm	Nm	N
0.4	0	0	0	0	0	0	0	0	0	-1	0	32
25	-2	-8	-5872	-2	1	-189	0	7	-5962	3	-1	-120
50	-16	-20	-11785	-6	1	-96	-8	8	-11451	4	-2	-94
75	-16	-29	-15810	-9	1	-257	-13	10	-16233	10	-3	-20
90	-18	-31	-18885	-10	2	-376	-13	13	-19440	9	-4	60
100	-21	-34	-21325	-11	2	-359	-19	13	-21827	10	-3	-20
0.4	-9	-6	1508	0	-1	-105	8	1	1510	5	-1	201

	T13L			T12T			B11L			T11T		
Load	M11	M22	Axial	M11	M22	Axial	M11	M22	Axial	M11	M22	Axial
(%)	Nm	Nm	N	Nm	Nm	N	Nm	Nm	N	Nm	Nm	N
0.4	0	0	0	0	0	0	0	0	0	0	0	0
25	-4	0	-161	0	-1	-51	-1	0	-273	-2	-1	-186
50	-6	-1	192	2	-1	54	-2	0	-143	-4	1	-110
75	-8	-2	128	-1	0	-174	-2	0	-143	-4	-2	43
90	-11	-2	189	-1	-1	-225	-2	0	-143	-8	-1	72
100	-11	-2	189	-1	-1	-214	-2	0	-159	-9	-1	48
0.4	0	1	62	-1	2	91	-1	0	-210	-7	4	-66

	B11T			T11L		
Load	M11	M22	Axial	M11	M22	Axial
(%)	Nm	Nm	N	Nm	Nm	N
0.4	0	0	0	0	0	0
25	-1	0	-63	4	4	-189
50	-1	0	131	5	-1	115
75	-1	0	131	9	3	57
90	-1	0	131	12	2	63
100	-1	0	131	12	1	132
0.4	1	0	113	5	2	-161

Load Case 2

	F2B			P3L			F4			T12L		
Load	M11	M22	Axial	M11	M22	Axial	M11	M22	Axial	M11	M22	Axial
(%)	Nm	Nm	N	Nm	Nm	N	Nm	Nm	N	Nm	Nm	N
3.6	0	0	0	0	0	0	0	0	0	-1	0	32
25	-14	0	-7435	-2	1	397	-25	3	-10745	-19	6	239
50	16	8	-17189	-1	0	407	-42	26	-24835	-29	9	418
75	288	77	-29045	-1	-4	-4	-44	39	-41765	-27	8	-229
90	321	93	-36316	-1	-8	-227	-51	31	-52701	-29	8	-237
100	353	107	-42612	-3	-10	-385	-57	28	-61611	-27	7	-183
3.6	265	78	-6466	3	-8	-285	32	16	-10796	-8	5	329

	T13L			T12T			B11L			T11T		
Load	M11	M22	Axial	M11	M22	Axial	M11	M22	Axial	M11	M22	Axial
(%)	Nm	Nm	N	Nm	Nm	N	Nm	Nm	N	Nm	Nm	N
3.6	0	0	0	0	0	0	0	0	0	0	0	0
25	0	-4	286	-35	1	-2315	1	0	16	64	-17	3925
50	1	0	679	-67	4	-4295	12	1	112	117	-45	7617
75	-21	2	987	-97	13	-7083	14	-1	106	156	-41	9424
90	-40	-1	972	-131	21	-9079	11	-1	28	179	-36	10460
100	-51	-4	857	-157	26	-10437	10	-1	-2	216	-23	11318
3.6	-19	2	905	-56	-3	-2059	10	-2	337	-23	45	-1555

	B11T			T11L		
Load	M11	M22	Axial	M11	M22	Axial
(%)	Nm	Nm	N	Nm	Nm	N
3.6	0	0	0	0	0	0
25	-4	1	-345	-9	-7	420
50	-4	4	-678	-13	-6	393
75	-10	2	-1174	-8	19	115
90	-14	3	-1601	-9	26	56
100	-17	2	-1775	-6	35	-184
3.6	11	-4	373	3	17	-279

Load Case 2D

	F2B			P3L			F4			T12L		
Load	M11	M22	Axial	M11	M22	Axial	M11	M22	Axial	M11	M22	Axial
(%)	Nm	Nm	N	Nm	Nm	N	Nm	Nm	N	Nm	Nm	N
7.4	0	0	0	0	0	0	0	0	0	-1	0	32
25	21	10	-13962	-2	1	104	-36	5	-19498	-7	1	-162
50	48	21	-32380	0	-6	206	-85	13	-45874	-17	2	-438
75	81	49	-50914	5	-21	-2258	-87	46	-73900	-29	4	-662
90	18	40	-63070	-23	-26	-3347	-78	225	-90060	-31	4	-549
100	9	44	-71216	-40	-32	-4042	30	317	-101436	-36	5	-764
7	-39	18	-972	-34	-17	-4197	161	242	-1276	2	0	194

	T13L			T12T			B11L			T11T		
Load	M11	M22	Axial	M11	M22	Axial	M11	M22	Axial	M11	M22	Axial
(%)	Nm	Nm	N	Nm	Nm	N	Nm	Nm	N	Nm	Nm	N
7.4	0	0	0	0	0	0	0	0	0	0	0	0
25	-14	-1	49	-40	12	-3130	-1	1	-174	98	-25	5036
50	-33	-6	1	-102	29	-7452	-1	2	-496	235	-45	11505
75	-69	-14	-62	-233	16	-12371	-4	0	-479	341	-81	17470
90	-85	-23	-482	-313	-3	-14848	-11	0	-759	407	-117	22438
100	-96	-27	-417	-339	2	-16449	-15	0	-816	443	-137	25184
7	-24	-8	-570	-109	-53	-452	-18	-5	-238	-22	-13	-420

	B11T			T11L		
Load	M11	M22	Axial	M11	M22	Axial
(%)	Nm	Nm	N	Nm	Nm	N
7.4	0	0	0	0	0	0
25	-10	3	-914	-6	4	172
50	-23	6	-2012	-12	11	328
75	-54	7	-3750	-12	16	365
90	-76	3	-4594	-14	23	478
100	-83	0	-4979	-17	29	710
7	-24	-7	-1253	1	5	-134

Load Case 3

	F2B			P3L			F4			T12L		
Load	M11	M22	Axial	M11	M22	Axial	M11	M22	Axial	M11	M22	Axial
(%)	Nm	Nm	N	Nm	Nm	N	Nm	Nm	N	Nm	Nm	N
5.5	0	0	0	0	0	0	0	0	0	-1	0	32
25	-385	0	-5789	-49	-16	-8754	32	-63	-12747	95	-31	8089
50	-884	-43	-10315	-175	-21	-18025	104	-141	-22435	188	-38	16259
75	-1061	-24	-20709	-250	-71	-24986	167	-187	-38351	275	-47	25144
90	-1315	28	-24298	-359	-116	-29854	406	-126	-44760	334	-54	31325
100	-1412	32	-24798	-396	-135	-31102	482	-86	-45269	354	-55	32986
5.4	-1110	68	6612	-77	45	1882	9	41	9029	62	5	1140

	T13L			T12T			B11L			T11T		
Load	M11	M22	Axial	M11	M22	Axial	M11	M22	Axial	M11	M22	Axial
(%)	Nm	Nm	N	Nm	Nm	N	Nm	Nm	N	Nm	Nm	N
5.5	0	0	0	0	0	0	0	0	0	0	0	0
25	-78	-6	-6326	47	-6	5302	29	-2	2388	-70	71	-5449
50	-109	-21	-12093	154	2	11953	73	10	4735	-201	146	-13826
75	-246	-51	-18335	275	31	17637	106	10	6847	-402	223	-25036
90	-306	-48	-23208	270	15	20656	136	4	8514	-504	263	-30153
100	-306	-48	-24434	289	12	22540	139	3	8990	-526	281	-31507
5.4	42	-52	2043	116	63	-440	25	-4	-534	128	21	5300

	B11T			T11L		
Load	M11	M22	Axial	M11	M22	Axial
(%)	Nm	Nm	N	Nm	Nm	N
5.5	0	0	0	0	0	0
25	50	0	2414	114	210	-3887
50	70	5	3203	152	400	-10014
75	98	3	5118	123	683	-18976
90	129	-8	6064	115	852	-23548
100	132	-8	6481	114	902	-24807
5.4	-11	10	-1035	-125	-111	-1829

Load Case 3D

	F2B			P3L			F4			T12L		
Load	M11	M22	Axial	M11	M22	Axial	M11	M22	Axial	M11	M22	Axial
(%)	Nm	Nm	N	Nm	Nm	N	Nm	Nm	N	Nm	Nm	N
5.9	0	0	0	0	0	0	0	0	0	-1	0	32
25	-185	31	-15422	-20	-4	-2565	25	4	-21467	39	-10	3487
50	-316	60	-36919	-62	-5	-6352	46	11	-51987	85	-22	7355
75	-390	74	-60123	-120	-5	-11041	99	22	-85360	133	-33	11666
90	-432	76	-72390	-171	-9	-15078	186	36	-104131	163	-38	13867
100	-480	69	-80414	-223	-7	-17973	298	62	-116387	182	-42	15525
5.3	-171	33	-5361	-53	6	-3487	241	25	-10610	8	-1	783

	T13L			T12T			B11L			T11T		
Load	M11	M22	Axial	M11	M22	Axial	M11	M22	Axial	M11	M22	Axial
(%)	Nm	Nm	N	Nm	Nm	N	Nm	Nm	N	Nm	Nm	N
5.9	0	0	0	0	0	0	0	0	0	0	0	0
25	-39	1	-2680	-11	0	27	5	-1	701	-4	2	-45
50	-90	6	-5970	-26	2	-800	16	-2	1764	9	-4	880
75	-146	15	-9506	-35	4	-1965	40	-2	3584	12	-6	1106
90	-181	20	-11319	-46	6	-2503	57	-1	4981	9	-8	1385
100	-205	23	-12669	-55	7	-2794	67	0	5920	-6	-5	1186
5.3	-23	6	-69	-10	1	-1904	20	3	1589	35	-20	1335

	B11T			T11L		
Load	M11	M22	Axial	M11	M22	Axial
(%)	Nm	Nm	N	Nm	Nm	N
5.9	0	0	0	0	0	0
25	4	-1	282	-20	67	-3406
50	5	-1	264	-12	180	-6480
75	-5	1	15	23	327	-9385
90	-16	7	-775	50	403	-10390
100	-19	12	-1065	68	458	-11179
5.3	-16	16	-1089	-60	-38	-133

Load Case 4

	F2B			P3L			F4			T12L		
Load	M11	M22	Axial	M11	M22	Axial	M11	M22	Axial	M11	M22	Axial
(%)	Nm	Nm	N	Nm	Nm	N	Nm	Nm	N	Nm	Nm	N
5.3	0	0	0	0	0	0	0	0	0	-1	0	32
25	-535	-95	-28020	-91	-10	-9917	120	16	-34843	76	-20	8334
50	-699	-102	-57880	-255	-12	-18683	271	62	-67965	155	-37	16026
75	-870	-125	-90740	-346	-70	-26140	423	115	-102976	231	-52	23759
90	-958	-127	-110709	-411	-131	-30713	583	192	-124624	273	-59	28159
100	-1031	-131	-124599	-468	-187	-34304	714	267	-140647	303	-63	31168
4.7	-429	-98	-270	-44	17	165	228	124	5314	-2	2	-192

	T13L			T12T			B11L			T11T		
Load	M11	M22	Axial	M11	M22	Axial	M11	M22	Axial	M11	M22	Axial
(%)	Nm	Nm	N	Nm	Nm	N	Nm	Nm	N	Nm	Nm	N
5.3	0	0	0	0	0	0	0	0	0	0	0	0
25	-83	2	-6747	12	-22	4623	24	-4	2651	-100	79	-7706
50	-168	-5	-13125	57	-34	11297	51	1	5187	-265	155	-17020
75	-264	-13	-19695	109	-45	18367	83	5	7325	-464	237	-27298
90	-327	-17	-23417	141	-51	22588	104	8	8673	-575	289	-33195
100	-372	-19	-26050	160	-55	25172	114	12	9632	-657	328	-37252
4.7	8	-12	1062	-21	-6	967	-3	10	-346	13	54	-266

	B11T			T11L		
Load	M11	M22	Axial	M11	M22	Axial
(%)	Nm	Nm	N	Nm	Nm	N
5.3	0	0	0	0	0	0
25	42	-3	2195	64	180	-5924
50	62	-5	3515	152	425	-11121
75	95	-8	5563	229	699	-16456
90	112	-9	6660	255	870	-19600
100	135	-16	7408	266	986	-21777
4.7	2	-6	77	-16	-41	505

Load Case 4D

	F2B			P3L			F4			T12L		
Load	M11	M22	Axial	M11	M22	Axial	M11	M22	Axial	M11	M22	Axial
(%)	Nm	Nm	N	Nm	Nm	N	Nm	Nm	N	Nm	Nm	N
10.2	0	0	0	0	0	0	0	0	0	-1	0	32
25	-16	25	-26091	-15	0	-562	-28	20	-33985	-12	2	1598
50	113	118	-68465	-47	-2	-2618	-53	46	-91262	10	-4	3401
75	16	150	-114195	-89	-24	-8055	-106	65	-155867	56	-16	6536
90	-104	164	-145480	-108	-49	-10885	-205	145	-199949	87	-23	8715
100	-185	163	-167153	-144	-68	-13367	-190	257	-229953	102	-27	9985
9.2	166	71	-2842	-10	-18	-1088	-156	4	-8253	-29	10	-735

	T13L			T12T			B11L			T11T		
Load	M11	M22	Axial	M11	M22	Axial	M11	M22	Axial	M11	M22	Axial
(%)	Nm	Nm	N	Nm	Nm	N	Nm	Nm	N	Nm	Nm	N
10.2	0	0	0	0	0	0	0	0	0	0	0	0
25	-31	-2	-1358	-53	0	-3366	8	1	392	42	3	2032
50	-113	5	-3236	-152	15	-9324	12	0	644	125	-1	5947
75	-182	2	-6012	-270	1	-13532	23	1	2001	222	-45	12691
90	-238	-3	-8095	-322	14	-15985	38	1	3058	290	-75	17546
100	-271	-8	-9348	-364	26	-17572	53	-1	4211	319	-90	20292
9.2	-24	10	809	-106	-39	-2227	-10	-1	-116	-75	21	-4347

	B11T			T11L		
Load	M11	M22	Axial	M11	M22	Axial
(%)	Nm	Nm	N	Nm	Nm	N
10.2	0	0	0	0	0	0
25	-5	1	-214	7	54	-448
50	-21	-10	-410	28	175	-2879
75	-40	-6	-1789	66	319	-5681
90	-59	-5	-2884	91	419	-7201
100	-76	-8	-3847	105	471	-7850
9.2	8	-14	932	-14	8	687

Load Case 4D (collapse)

	F2B			P3L			F4			T12L		
Load	M11	M22	Axial	M11	M22	Axial	M11	M22	Axial	M11	M22	Axial
(%)	Nm	Nm	N	Nm	Nm	N	Nm	Nm	N	Nm	Nm	N
10.2	0	0	0	0	0	0	0	0	0	-1	0	32
50	-150	31	-72438	-47	-20	-5658	-57	61	-96944	55	-17	4873
75	-265	57	-119470	-85	-35	-9159	-63	136	-160477	94	-27	7880
90	-339	72	-146612	-112	-46	-11098	-38	210	-197660	118	-33	9584
100	-385	79	-164519	-139	-51	-12619	-4	278	-222232	130	-37	10739
101	-402	77	-167194	-145	-52	-12809	4	291	-225271	131	-37	10719

	T13L			T12T			B11L			T11T		
Load	M11	M22	Axial	M11	M22	Axial	M11	M22	Axial	M11	M22	Axial
(%)	Nm	Nm	N	Nm	Nm	N	Nm	Nm	N	Nm	Nm	N
10.2	0	0	0	0	0	0	0	0	0	0	0	0
50	-101	-4	-4599	-107	24	-6916	25	-2	1798	182	-49	10950
75	-170	-9	-7429	-182	45	-11221	45	-2	3123	295	-81	17980
90	-212	-11	-9133	-228	58	-13684	55	-3	3914	355	-100	21948
100	-243	-11	-10408	-261	68	-15274	62	-3	4531	389	-112	24512
101	-245	-13	-10471	-264	68	-15344	54	-1	5099	-325	204	-18217

	B11T			T11L		
Load	M11	M22	Axial	M11	M22	Axial
(%)	Nm	Nm	N	Nm	Nm	N
10.2	0	0	0	0	0	0
50	-31	4	-2165	56	198	-4044
75	-56	6	-3554	90	331	-6377
90	-71	7	-4365	110	412	-7691
100	-83	6	-4960	124	463	-8490
101	83	-8	3365	260	677	-15162

B.1.2. PROTOTYPE 2

Load Case 1

	F2B			P3L			F4			T12L		
Load	M11	M22	Axial	M11	M22	Axial	M11	M22	Axial	M11	M22	Axial
(%)	Nm	Nm	N	Nm	Nm	N	Nm	Nm	N	Nm	Nm	N
0	0.0	0.0	0.0	0.0	0.0	0.0	0.0	0.0	0.0	-0.6	0.2	32.3
25	7.0	-10.6	-15643.6	-6.2	-2.7	218.9	18.8	11.7	-8383.8	10.3	-2.6	923.7
50	9.3	-16.5	-30978.2	-15.6	-5.1	462.8	39.8	29.5	-17539.9	14.5	-3.7	1526.1
75	23.3	-23.6	-44849.2	-28.7	-7.1	957.3	79.6	47.1	-26352.5	6.6	-2.2	2176.1
90	58.4	-17.1	-53854.0	-33.0	-7.5	1235.0	113.0	63.1	-31545.7	9.1	-2.9	3335.8
100	65.4	-15.4	-59777.0	-33.0	-7.0	1095.2	138.2	74.6	-34507.1	10.3	-2.1	4837.2
0	39.7	17.6	-1946.0	-6.2	-4.9	-752.1	52.3	24.2	1321.7	-3.6	2.5	3279.6

	T13L			T12T			B11L			T11T		
Load	M11	M22	Axial	M11	M22	Axial	M11	M22	Axial	M11	M22	Axial
(%)	Nm	Nm	N	Nm	Nm	N	Nm	Nm	N	Nm	Nm	N
0	0.0	0.0	0.0	0.0	0.0	0.0	0.0	0.0	0.0	0.0	0.0	0.0
25	-2.0	-0.9	212.7	-37.3	7.7	-2392.5	-27.1	8.7	-1294.2	63.9	17.3	-2951.9
50	-8.1	1.5	-4.2	-68.3	14.3	-4413.9	-52.9	17.1	-2465.4	121.1	31.6	-5673.3
75	-18.2	3.6	-451.2	-96.2	19.1	-5949.8	-81.2	26.1	-3601.3	171.6	44.3	-8304.1
90	-25.3	4.9	-1150.0	-112.6	21.6	-6534.7	-95.4	31.7	-4209.5	209.7	53.6	-10269.1
100	-30.3	4.8	-2256.0	-118.3	21.4	-5994.5	-97.2	33.2	-4293.6	240.2	60.9	-12950.2
0	2.0	-2.1	-1780.8	-5.7	-2.3	2241.7	9.8	-0.7	904.2	29.6	9.7	-3637.5

	B11T			T11L		
Load	M11	M22	Axial	M11	M22	Axial
(%)	Nm	Nm	N	Nm	Nm	N
0	0.0	0.0	0.0	0.0	0.0	0.0
25	-16.5	3.4	-1151.3	-6.8	-9.4	-178.4
50	-24.8	5.1	-1956.8	-4.9	-15.0	-809.1
75	-17.7	5.2	-2056.3	13.7	-18.1	-2266.7
90	-7.7	5.0	-1806.1	32.2	-21.2	-3986.1
100	2.4	4.3	-1325.5	47.8	-25.0	-6236.1
0	46.6	-6.0	2547.8	37.1	-7.0	-4284.8

Load Case 1D

	F2B			P3L			F4			T12L		
Load	M11	M22	Axial	M11	M22	Axial	M11	M22	Axial	M11	M22	Axial
(%)	Nm	Nm	N	Nm	Nm	N	Nm	Nm	N	Nm	Nm	N
1.2	0.0	0.0	0.0	0.0	0.0	0.0	0.0	0.0	0.0	-0.6	0.2	32.3
25	-11.7	-3.9	-5327.7	4.4	-0.6	-476.3	-4.2	2.9	-5096.3	-3.0	0.3	23.1
50	-23.3	-9.6	-10535.3	7.5	-0.9	-788.1	-10.5	8.2	-10892.3	-12.1	2.1	-183.0
75	-39.7	-15.8	-16974.4	11.2	-1.9	-1090.2	-10.5	13.3	-16786.0	-15.1	2.3	-67.9
90	-49.0	-20.4	-20253.2	13.7	-2.0	-1176.3	-14.7	16.3	-19759.2	-17.5	2.4	107.0
100	-51.4	-23.3	-22906.7	14.9	-2.3	-1245.2	-14.7	18.0	-22006.9	-16.9	2.8	213.2
1	4.7	-6.5	1289.8	0.0	0.0	478.1	-10.5	-2.1	-166.3	-6.0	1.0	-367.7

	T13L			T12T			B11L			T11T		
Load	M11	M22	Axial	M11	M22	Axial	M11	M22	Axial	M11	M22	Axial
(%)	Nm	Nm	N	Nm	Nm	N	Nm	Nm	N	Nm	Nm	N
1.2	0.0	0.0	0.0	0.0	0.0	0.0	0.0	0.0	0.0	0.0	0.0	0.0
25	-8.1	3.0	-267.1	5.7	-1.4	354.2	-11.7	4.3	-599.8	-3.8	-5.2	258.3
50	-20.2	4.9	-698.4	15.2	-3.2	837.3	-20.9	7.0	-960.2	-12.4	-12.6	662.6
75	-29.3	6.7	-924.0	17.7	-4.4	932.3	-33.8	11.7	-1589.3	-7.6	-16.9	624.8
90	-32.3	7.6	-1195.7	19.0	-5.3	906.2	-40.6	13.6	-1891.1	-6.7	-21.4	746.6
100	-34.4	8.2	-1245.9	18.3	-5.6	889.2	-46.8	15.3	-2131.3	-1.9	-22.8	689.7
1	-4.0	1.9	-166.6	8.2	-1.5	75.6	0.0	0.0	281.3	-7.6	-7.0	819.2

	B11T			T11L		
Load	M11	M22	Axial	M11	M22	Axial
(%)	Nm	Nm	N	Nm	Nm	N
1.2	0.0	0.0	0.0	0.0	0.0	0.0
25	-9.4	2.5	-697.9	7.8	1.3	-394.5
50	-16.5	3.9	-1197.8	21.5	3.9	-1036.9
75	-27.7	6.4	-1847.8	28.3	3.3	-1444.0
90	-33.6	8.0	-2180.6	30.3	2.8	-1651.0
100	-39.0	9.4	-2452.4	30.3	3.5	-1721.4
1	-0.6	-0.3	-14.3	8.8	1.1	-39.8

Load Case 2

Load	**M11**	**M22**	**Axial**	**M11**	**M22**	**Axial**	**M11**	**M22**	**Axial**	**M11**	**M22**	**Axial**
(%)	**Nm**	**Nm**	**N**	**Nm**	**Nm**	**N**	**Nm**	**Nm**	**N**	**Nm**	**Nm**	**N**
3.2	0.0	0.0	0.0	0.0	0.0	0.0	0.0	0.0	0.0	-0.6	0.2	32.3
25	0.0	0.0	-9505.7	-7.5	0.9	501.2	-16.7	4.9	-12031.6	-3.0	0.3	391.4
50	-2.3	-1.1	-20517.6	-14.3	0.5	673.7	-37.7	12.7	-25974.8	-6.6	1.7	723.8
75	-11.7	-3.9	-31521.2	-23.7	0.3	932.4	-56.5	23.3	-41078.2	-7.9	1.5	834.1
90	-35.0	-8.3	-37347.4	-28.0	0.9	930.6	-83.7	31.2	-50252.7	-13.9	3.1	881.1
100	-60.7	-17.3	-40214.6	-34.9	0.5	1294.3	-111.0	30.6	-54770.6	-17.5	4.0	1167.1
3.4	-70.0	-25.4	-371.8	-6.2	-3.2	-1649.4	-64.9	-1.7	-5505.0	-3.0	-1.3	160.0

	T13L			**T12T**			**B11L**			**T11T**		
Load	**M11**	**M22**	**Axial**	**M11**	**M22**	**Axial**	**M11**	**M22**	**Axial**	**M11**	**M22**	**Axial**
(%)	**Nm**	**Nm**	**N**	**Nm**	**Nm**	**N**	**Nm**	**Nm**	**N**	**Nm**	**Nm**	**N**
3.2	0.0	0.0	0.0	0.0	0.0	0.0	0.0	0.0	0.0	0.0	0.0	0.0
25	-19.2	5.4	-281.2	23.4	-5.3	1910.9	-30.2	9.6	-1320.6	-48.6	-11.2	2345.6
50	-39.4	11.1	-653.0	49.3	-11.2	3682.3	-57.8	19.5	-2669.6	-107.7	-23.5	5132.4
75	-61.6	18.0	-1272.0	84.1	-17.7	5025.5	-84.9	28.7	-3819.8	-181.1	-37.2	8911.7
90	-78.8	22.9	-1372.0	102.5	-20.7	5123.9	-103.4	35.0	-4440.1	-222.1	-42.1	11683.6
100	-84.9	22.3	-1455.6	113.9	-23.0	5120.6	-112.0	38.4	-4826.0	-244.1	-46.3	13466.6
3.4	-12.1	-1.8	-362.8	18.3	-1.4	-2800.2	16.0	-5.6	1124.4	-44.8	-1.7	4148.3

	B11T			**T11L**		
Load	**M11**	**M22**	**Axial**	**M11**	**M22**	**Axial**
(%)	**Nm**	**Nm**	**N**	**Nm**	**Nm**	**N**
3.2	0.0	0.0	0.0	0.0	0.0	0.0
25	8.3	-2.2	392.3	10.7	1.2	-186.3
50	14.8	-5.4	833.5	26.4	3.9	-582.5
75	22.4	-10.4	1260.2	47.8	5.6	-753.7
90	34.8	-19.6	2269.1	49.8	5.1	-698.9
100	33.1	-22.1	2365.7	44.9	2.2	-740.9
3.4	0.6	-16.4	952.9	6.8	-4.8	15.2

Load Case 2D

	F2B			P3L			F4			T12L		
Load	M11	M22	Axial	M11	M22	Axial	M11	M22	Axial	M11	M22	Axial
(%)	Nm	Nm	N	Nm	Nm	N	Nm	Nm	N	Nm	Nm	N
6.6	0.0	0.0	0.0	0.0	0.0	0.0	0.0	0.0	0.0	-0.6	0.2	32.3
25	-2.3	4.1	-16442.2	-13.7	2.0	1367.6	-18.8	10.6	-20835.9	-5.4	1.9	337.3
50	-9.3	7.7	-36017.0	-26.8	4.9	2516.9	-50.2	28.3	-45583.6	-15.1	4.4	946.5
75	-149.4	-16.7	-57786.1	-94.7	19.0	10497.5	-87.9	44.4	-73930.6	-18.7	6.4	1693.7
90	-224.1	-33.9	-66749.9	-92.2	18.4	13993.5	-113.0	56.9	-86088.3	-22.4	7.8	2486.5
100	-235.7	-51.8	-67102.7	-81.6	13.4	14732.4	-119.3	81.0	-89644.7	-23.6	10.2	3105.3
5.8	-156.4	-37.7	7549.3	-34.3	6.9	5607.3	16.7	29.4	6356.4	9.1	2.8	900.4

	T13L			T12T			B11L			T11T		
Load	M11	M22	Axial	M11	M22	Axial	M11	M22	Axial	M11	M22	Axial
(%)	Nm	Nm	N	Nm	Nm	N	Nm	Nm	N	Nm	Nm	N
0.0	0.0	0.0	0.0	0.0	0.0	0.0	0.0	0.0	0.0	0.0	0.0	0.0
-663.4	8.2	3329.1	-29.3	-10.4	-2429.4	41.8	17.7	3750.7	-51.7	-20.7	-663.4	-85.8
-1079.2	18.8	6942.1	-69.7	-20.8	-5426.3	89.8	40.0	8778.1	-115.7	-42.5	-1079.2	-185.0
-1605.9	27.7	11922.6	-104.1	-21.6	-8433.5	157.5	68.5	12868.0	-196.3	-57.4	-1605.9	-268.8
-1835.1	34.0	13856.1	-113.2	-31.2	-9489.4	172.7	80.5	16714.7	-231.4	-75.8	-1835.1	-328.9
-1415.7	39.6	12482.3	-117.2	-26.7	-10500.1	197.4	89.8	21556.4	-264.0	-111.5	-1415.7	-287.0
1151.6	4.7	-1265.5	28.3	17.3	1015.8	20.9	0.2	1970.9	-6.2	-48.9	1151.6	137.3

	B11T			T11L		
Load	M11	M22	Axial	M11	M22	Axial
(%)	Nm	Nm	N	Nm	Nm	N
6.6	0.0	0.0	0.0	0.0	0.0	0.0
25	15.3	-2.6	615.1	21.5	5.3	-523.1
50	33.1	-6.3	1520.3	34.2	6.7	-986.8
75	95.6	-25.0	5858.8	29.3	4.5	-1753.7
90	112.2	-33.8	7521.9	17.6	0.0	-1570.2
100	135.8	-44.5	9547.6	9.8	-7.7	-1458.6
5.8	62.6	-32.4	6009.4	-23.4	-12.6	718.9

Load Case 3

	F2B			P3L			F4			T12L		
Load	M11	M22	Axial	M11	M22	Axial	M11	M22	Axial	M11	M22	Axial
(%)	Nm	Nm	N	Nm	Nm	N	Nm	Nm	N	Nm	Nm	N
6	0.0	0.0	0.0	0.0	0.0	0.0	0.0	0.0	0.0	-0.6	0.2	32.3
25	-21.0	12.5	-8781.3	-24.3	-5.5	4607.7	104.7	10.7	-12663.7	-67.1	0.7	-6737.6
50	-14.0	49.2	-19642.8	-68.5	-15.5	9867.5	347.5	11.9	-28255.1	-133.6	19.9	-18832.9
75	51.4	46.0	-29775.2	-88.5	-22.1	13469.3	579.9	26.5	-43859.6	-284.1	4.8	-29886.6
90	179.7	15.8	-35830.9	-89.1	-24.7	14393.7	707.6	40.8	-54766.3	-394.0	-7.2	-36834.2
100	217.1	-4.6	-39716.7	-85.3	-27.3	14606.4	795.5	51.1	-60829.1	-451.5	-13.2	-40041.0
5.2	289.4	30.7	-2529.1	-2.5	-16.7	-3901.2	278.4	23.5	-7331.8	-112.4	-39.4	-7485.0

	T13L			T12T			B11L			T11T		
Load	M11	M22	Axial	M11	M22	Axial	M11	M22	Axial	M11	M22	Axial
(%)	Nm	Nm	N	Nm	Nm	N	Nm	Nm	N	Nm	Nm	N
6	0.0	0.0	0.0	0.0	0.0	0.0	0.0	0.0	0.0	0.0	0.0	0.0
25	-63.6	5.2	-6415.5	-46.2	7.8	-4020.3	64.6	-11.0	3694.8	101.1	18.4	-6258.7
50	-185.9	20.9	-12975.2	-133.5	17.7	-11990.8	58.5	2.6	3109.6	164.0	35.2	-12237.5
75	-189.9	63.8	-18082.4	-212.6	1.0	-17644.2	168.0	-14.9	7585.5	230.7	67.9	-20962.3
90	-253.6	62.2	-21286.1	-252.4	-12.1	-20538.0	225.8	-31.3	10837.9	296.5	103.0	-26986.6
100	-296.0	53.3	-24157.1	-282.8	-18.9	-22553.3	270.8	-43.0	13555.0	344.2	139.2	-31224.9
5.2	1.0	-7.7	3499.3	-87.9	-56.8	-0.5	126.1	-15.5	1820.1	-152.5	30.1	-2976.4

	B11T			T11L		
Load	M11	M22	Axial	M11	M22	Axial
(%)	Nm	Nm	N	Nm	Nm	N
6	0.0	0.0	0.0	0.0	0.0	0.0
25	-35.4	9.9	-2502.8	182.6	34.3	-7776.4
50	-43.1	37.5	-5897.8	373.9	88.1	-11662.6
75	-73.8	49.2	-9296.5	558.4	133.9	-19140.7
90	-113.3	49.9	-11064.1	708.8	169.5	-23185.6
100	-141.1	51.3	-12262.6	796.6	193.6	-27146.1
5.2	24.8	25.4	-1480.3	32.2	3.0	10638.7

Load Case 3D

	F2B			P3L			F4			T12L		
Load	M11	M22	Axial	M11	M22	Axial	M11	M22	Axial	M11	M22	Axial
(%)	Nm	Nm	N	Nm	Nm	N	Nm	Nm	N	Nm	Nm	N
5.6	0.0	0.0	0.0	0.0	0.0	0.0	0.0	0.0	0.0	-0.6	0.2	32.3
25	-49.0	-4.6	-17321.3	13.7	-2.0	-1941.3	18.8	9.9	-21635.1	-39.3	6.0	-3150.5
50	-116.7	-11.3	-38090.0	39.2	-8.2	-3396.5	35.6	20.5	-47879.2	-91.9	13.8	-6926.3
75	-184.4	-18.0	-59915.0	110.3	-19.4	-6694.3	41.9	51.2	-78456.3	-134.2	22.1	-9591.7
90	-212.4	-22.9	-73521.0	165.7	-27.0	-13773.1	104.7	80.9	-96113.2	-167.4	29.1	-11728.4
100	-254.4	-31.1	-82674.3	216.1	-20.8	-17957.6	186.3	124.0	-106991.9	-194.6	35.6	-12898.4
5	-35.0	-8.3	-3126.8	77.2	6.1	-3751.6	117.2	84.1	-6536.7	-4.8	5.4	1366.7

	T13L			T12T			B11L			T11T		
Load	M11	M22	Axial	M11	M22	Axial	M11	M22	Axial	M11	M22	Axial
(%)	Nm	Nm	N	Nm	Nm	N	Nm	Nm	N	Nm	Nm	N
5.6	0.0	0.0	0.0	0.0	0.0	0.0	0.0	0.0	0.0	0.0	0.0	0.0
25	-26.3	5.9	-2746.2	-10.1	2.0	219.9	12.3	-1.9	1100.1	11.4	0.2	-408.6
50	-61.6	11.3	-5912.6	-19.0	4.2	517.2	30.8	-5.6	2440.5	28.6	-2.1	-841.5
75	-49.5	1.2	-9728.1	-24.7	6.7	648.4	177.8	-46.7	10352.1	61.0	-1.0	-1469.8
90	-56.6	-2.0	-11862.9	-29.1	7.8	510.8	244.9	-63.7	13321.7	98.2	2.2	-1852.4
100	-77.8	1.0	-13108.1	-32.3	8.6	876.0	272.6	-69.9	14178.4	122.0	7.2	-2414.0
5	46.5	-24.2	-1125.2	12.7	0.6	237.8	188.3	-54.4	8320.1	68.6	13.0	-900.2

	B11T			T11L		
Load	M11	M22	Axial	M11	M22	Axial
(%)	Nm	Nm	N	Nm	Nm	N
5.6	0.0	0.0	0.0	0.0	0.0	0.0
25	-48.4	9.5	-2733.7	76.2	19.6	-3777.1
50	-109.2	22.2	-6009.9	175.7	41.9	-8465.9
75	-182.4	37.8	-8862.3	273.4	61.9	-13582.4
90	-239.7	52.0	-11546.1	346.6	76.6	-16551.4
100	-267.4	57.9	-12887.6	398.3	88.3	-18684.7
5	-18.3	3.4	-91.8	32.2	0.8	-1455.4

Load Case 4

	F2B			P3L			F4			T12L		
Load	M11	M22	Axial	M11	M22	Axial	M11	M22	Axial	M11	M22	Axial
(%)	Nm	Nm	N	Nm	Nm	N	Nm	Nm	N	Nm	Nm	N
5.4	0.0	0.0	0.0	0.0	0.0	0.0	0.0	0.0	0.0	-0.6	0.2	32.3
25	-16.3	-13.2	-32996.8	-48.0	-1.4	4561.9	144.4	35.1	-33439.4	-69.5	7.5	-6419.2
50	-21.0	-27.7	-63896.4	-104.6	-6.5	7604.7	291.0	69.5	-64817.5	-158.9	17.6	-14213.9
75	-63.0	-50.0	-100816.6	-165.1	-8.9	11486.6	483.6	106.0	-97191.2	-234.5	23.6	-19852.0
90	-65.4	-66.8	-122365.0	-192.5	-14.7	13677.1	669.9	178.5	-117007.8	-285.9	26.5	-23834.2
100	-7.0	-90.9	-137504.2	-204.3	-20.2	16471.2	816.5	278.1	-129763.3	-315.5	25.8	-25479.5
4.6	51.4	-22.3	-6076.8	-78.5	-10.1	348.4	201.0	135.1	7377.9	-6.6	-2.4	3298.6

	T13L			T12T			B11L			T11T		
Load	M11	M22	Axial	M11	M22	Axial	M11	M22	Axial	M11	M22	Axial
(%)	Nm	Nm	N	Nm	Nm	N	Nm	Nm	N	Nm	Nm	N
5.4	0.0	0.0	0.0	0.0	0.0	0.0	0.0	0.0	0.0	0.0	0.0	0.0
25	-84.9	17.1	-7144.4	-41.1	5.4	-4880.1	-27.7	10.4	201.7	90.6	25.0	-6327.2
50	-180.8	35.9	-14367.7	-91.7	11.6	-10156.0	-30.8	14.4	1039.5	179.2	50.5	-12579.4
75	-287.9	57.7	-21932.9	-148.7	15.1	-14352.3	-36.3	20.6	1312.9	282.2	83.9	-22544.4
90	-355.6	74.5	-25839.9	-180.9	16.2	-17542.0	-55.4	29.2	644.5	375.6	105.2	-27789.6
100	-403.1	84.1	-28457.7	-208.1	15.4	-20394.3	-68.3	38.0	42.2	446.2	119.8	-30672.8
4.6	-9.1	-1.9	-157.2	-17.1	-9.1	1078.0	-32.0	10.1	-2536.8	-42.9	-1.5	-2265.6

	B11T			T11L		
Load	M11	M22	Axial	M11	M22	Axial
(%)	Nm	Nm	N	Nm	Nm	N
5.4	0.0	0.0	0.0	0.0	0.0	0.0
25	-37.8	8.1	-3157.3	202.1	38.0	-9714.1
50	-131.6	32.1	-9062.8	421.8	76.7	-20152.4
75	-253.8	53.8	-15487.6	635.6	114.1	-31128.1
90	-322.3	54.9	-18343.9	779.1	138.2	-37496.6
100	-370.1	49.9	-20218.9	927.5	153.0	-43019.3
4.6	-158.8	11.3	-7094.7	103.5	-18.0	-2933.4

Load Case 4D

	F2B			P3L			F4			T12L		
Load	M11	M22	Axial	M11	M22	Axial	M11	M22	Axial	M11	M22	Axial
(%)	Nm	Nm	N	Nm	Nm	N	Nm	Nm	N	Nm	Nm	N
10.6	0.0	0.0	0.0	0.0	0.0	0.0	0.0	0.0	0.0	-0.6	0.2	32.3
25	-44.3	-9.3	-26502.4	17.4	-1.9	-2140.4	18.8	40.8	-34279.9	-32.6	5.8	-1801.5
50	-301.1	-74.9	-66574.4	62.9	-4.2	-4108.1	52.3	96.1	-86710.9	-84.0	16.4	-3890.1
75	-574.2	-165.9	-109017.5	90.9	-4.5	-6804.0	77.5	164.2	-139853.9	-148.7	28.4	-6374.1
90	-679.2	-213.5	-136480.8	99.0	-1.2	-6258.1	142.4	296.1	-172687.6	-189.8	36.9	-8137.0
100	-751.6	-245.3	-153207.4	110.9	-1.1	-6794.2	79.6	341.8	-192569.2	-203.7	39.0	-8729.9
10	-378.1	-117.7	12724.2	34.3	-7.4	-973.3	-50.2	98.6	10032.7	8.5	2.0	1576.4

	T13L			T12T			B11L			T11T		
Load	M11	M22	Axial	M11	M22	Axial	M11	M22	Axial	M11	M22	Axial
(%)	Nm	Nm	N	Nm	Nm	N	Nm	Nm	N	Nm	Nm	N
10.6	0.0	0.0	0.0	0.0	0.0	0.0	0.0	0.0	0.0	0.0	0.0	0.0
25	-46.5	8.6	-2199.5	22.8	-3.0	2343.9	-32.6	11.3	-1091.1	-51.5	-14.6	2748.0
50	-125.3	24.0	-5659.5	87.9	2.2	5214.3	-103.4	36.5	-3632.9	-103.0	-37.6	7381.6
75	-211.1	41.4	-8706.5	159.4	10.6	7915.9	-178.5	63.0	-6793.0	-48.6	-86.9	13761.7
90	-267.7	53.5	-10569.0	200.5	23.9	9264.7	-248.0	92.0	-9935.1	-60.1	-109.7	19024.7
100	-291.0	58.6	-11473.0	218.9	31.6	10208.4	-259.7	100.5	-10695.7	-41.0	-128.0	20189.0
10	1.0	-5.5	1468.9	101.9	56.0	-2702.8	-34.5	16.5	-729.8	245.0	-53.0	4795.4

	B11T			T11L		
Load	M11	M22	Axial	M11	M22	Axial
(%)	Nm	Nm	N	Nm	Nm	N
10.6	0.0	0.0	0.0	0.0	0.0	0.0
25	21.3	-8.1	1320.2	60.5	12.7	-2958.6
50	49.0	-27.3	3182.5	123.0	22.7	-7876.6
75	-3.0	-25.3	506.8	223.6	35.4	-13259.3
90	-24.2	-21.1	-1176.7	290.0	42.9	-16486.9
100	-73.8	-10.8	-3894.8	321.2	45.4	-18437.8
10	129.9	-39.0	7555.1	-59.6	-20.1	-41.0

Load Case 4D (collapse)

	F2B			P3L			F4			T12L		
Load	M11	M22	Axial	M11	M22	Axial	M11	M22	Axial	M11	M22	Axial
(%)	Nm	Nm	N	Nm	Nm	N	Nm	Nm	N	Nm	Nm	N
10.5	0.0	0.0	0.0	0.0	0.0	0.0	0.0	0.0	0.0	-0.6	0.2	32.3
50	-130.7	-46.2	-72454.3	21.2	-1.3	-2479.3	18.8	92.2	-88334.2	-88.8	15.1	-4692.4
75	-242.7	-86.7	-120789.0	41.1	0.0	-3918.7	41.9	166.0	-147946.0	-153.5	27.1	-7728.8
90	-312.8	-110.3	-148108.2	54.2	0.3	-4950.2	56.5	221.7	-181399.9	-189.8	34.3	-9382.0
100	-371.1	-135.2	-165936.8	62.3	0.3	-5669.7	58.6	265.7	-203595.4	-212.7	39.2	-10456.4
105	-403.8	-152.9	-176764.6	67.9	-0.1	-6067.6	52.3	277.8	-215409.6	-217.0	40.3	-10598.5
107.3	-417.8	-161.5	-181034.6	71.0	-0.3	-6188.2	44.0	283.7	-219232.8	-213.3	39.4	-10424.1

	T13L			T12T			B11L			T11T		
Load	M11	M22	Axial	M11	M22	Axial	M11	M22	Axial	M11	M22	Axial
(%)	Nm	Nm	N	Nm	Nm	N	Nm	Nm	N	Nm	Nm	N
10.5	0.0	0.0	0.0	0.0	0.0	0.0	0.0	0.0	0.0	0.0	0.0	0.0
50	-120.2	24.8	-5666.5	47.4	-14.0	5671.2	-94.8	35.1	-4171.4	-122.0	-36.9	6793.8
75	-207.1	42.5	-9458.5	81.6	-19.8	8818.9	-160.0	58.8	-7003.4	-203.1	-60.5	11803.1
90	-254.6	52.8	-11488.0	105.0	-24.0	11119.7	-192.0	72.0	-8488.4	-243.1	-74.2	14072.4
100	-284.9	59.9	-12764.2	118.3	-26.2	12495.2	-210.5	80.3	-9376.6	-266.0	-83.0	15599.9
105	-294.0	63.2	-13252.8	119.6	-25.5	12815.4	-224.6	85.9	-10078.6	-265.0	-85.4	16033.8
107.3	-296.0	63.0	-13237.0	113.9	-23.5	12703.8	-230.8	88.7	-10405.9	-254.5	-84.3	15853.9

	B11T			T11L		
Load	M11	M22	Axial	M11	M22	Axial
(%)	Nm	Nm	N	Nm	Nm	N
10.5	0.0	0.0	0.0	0.0	0.0	0.0
50	-93.3	16.0	-5743.8	168.9	31.7	-8312.1
75	-155.3	25.6	-9183.8	285.1	49.3	-13778.5
90	-187.7	31.8	-11011.0	352.4	59.3	-16802.1
100	-211.9	35.3	-12215.6	395.4	66.4	-18805.5
105	-232.0	39.2	-13317.6	407.1	65.2	-19473.2
107.3	-243.2	41.7	-13875.7	406.1	62.6	-19546.4

B.1.3. PROTOTYPE 2A

Load Case 1

	F2B			P3L			F4			T12T		
Load	M11	M22	Axial	M11	M22	Axial	M11	M22	Axial	M11	M22	Axial
(%)	Nm	Nm	N	Nm	Nm	N	Nm	Nm	N	Nm	Nm	N
1.0	0.0	0.0	0.0	0.0	0.0	0.0	0.0	0.0	0.0	0.0	0.0	0.0
25.0	-41.5	-25.4	-17947.1	-4.9	-1.4	303.5	17.1	18.6	-7633.6	-49.5	9.3	-3192.4
50.0	-48.5	8.2	-31458.9	-6.2	-2.1	653.1	41.6	26.1	-10924.6	-86.3	16.5	-4086.8
75.0	-53.1	7.7	-48563.5	-10.5	-3.6	1595.6	71.0	43.1	-19242.7	-124.4	23.0	-6362.3
90.0	-60.0	-8.0	-58532.8	-12.3	-4.2	2171.8	93.0	55.0	-25244.9	-146.6	24.9	-7726.0
100.0	-50.8	-35.2	-63828.6	-14.8	-4.6	2301.4	124.8	62.3	-29090.0	-169.4	24.3	-9601.8
1.0	96.9	11.8	2664.6	2.5	-0.1	10.9	36.7	-4.8	4811.3	-22.8	-2.7	-254.2

	T13L			T12L			B11L			T11L		
Load	M11	M22	Axial	M11	M22	Axial	M11	M22	Axial	M11	M22	Axial
(%)	Nm	Nm	N	Nm	Nm	N	Nm	Nm	N	Nm	Nm	N
1.0	0.0	0.0	0.0	0.0	0.0	0.0	0.0	0.0	0.0	0.0	0.0	0.0
25.0	9.6	-0.6	-70.8	25.5	-7.2	2389.8	-27.5	4.3	-1913.0	0.0	-17.4	-1061.4
50.0	3.8	1.0	-3012.0	47.1	-15.5	7242.5	-57.5	9.8	-3238.9	74.0	-64.0	-6752.2
75.0	1.9	3.0	-3571.9	49.7	-22.5	8537.5	-94.5	16.1	-5468.2	175.1	-92.9	-7935.2
90.0	-3.8	4.7	-3848.8	45.2	-27.2	8890.9	-120.7	19.6	-6813.8	225.1	-109.6	-8663.3
100.0	-3.8	5.4	-3786.6	39.5	-30.5	8927.3	-138.6	21.5	-7773.1	259.1	-120.7	-8758.6
1.0	2.9	2.0	-1008.3	-10.2	-16.0	1074.9	-45.3	4.7	-2143.0	195.1	-74.6	-1298.0

	B11T			T11T			B14L			B14T		
Load	M11	M22	Axial	M11	M22	Axial	M11	M22	Axial	M11	M22	Axial
(%)	Nm	Nm	N	Nm	Nm	N	Nm	Nm	N	Nm	Nm	N
1.0	0.0	0.0	0.0	0.0	0.0	0.0	0.0	0.0	0.0	0.0	0.0	0.0
25.0	-15.0	5.0	-1430.0	95.8	29.7	-3592.3	11.1	2.2	-1644.2	4.3	-1.1	-144.8
50.0	-27.0	7.6	-2301.3	119.8	76.5	-7501.0	25.2	8.3	-3182.6	0.6	1.4	-73.8
75.0	-42.6	9.6	-3615.5	181.2	104.7	-10203.8	48.0	15.2	-5274.5	-9.8	7.0	47.8
90.0	-54.5	8.5	-4359.9	223.9	119.5	-11522.2	63.4	20.5	-6740.0	-18.4	11.2	-132.7
100.0	-61.4	9.2	-4970.6	262.4	125.1	-11432.3	75.1	23.1	-7784.7	-20.9	14.4	-413.8
1.0	-12.5	-5.3	-337.1	-35.4	35.2	-37.4	42.5	9.9	-2351.4	-30.1	13.7	567.2

7L	
Load	Axial
(%)	N
1.0	0.0
25.0	1.8
50.0	1.2
75.0	3.7
90.0	4.4
100.0	4.6
1.0	-0.3

Load Case 1D

	F2B			P3L			F4			T12T		
Load	M11	M22	Axial	M11	M22	Axial	M11	M22	Axial	M11	M22	Axial
(%)	Nm	Nm	N	Nm	Nm	N	Nm	Nm	N	Nm	Nm	N
2.2	0.0	0.0	0.0	0.0	0.0	0.0	0.0	0.0	0.0	0.0	0.0	0.0
25.0	11.5	-19.0	-5772.6	1.2	-0.3	-549.5	0.0	7.2	-4179.8	2.5	0.9	112.7
50.0	-16.2	-18.4	-11971.1	1.9	-0.5	-968.5	0.0	14.4	-9503.7	3.2	0.8	78.1
75.0	-23.1	-18.2	-19783.1	3.7	-1.0	-1456.1	14.7	19.3	-14433.3	2.5	0.9	112.7
90.0	-36.9	-30.2	-22875.6	4.9	-0.8	-1665.2	22.0	24.4	-17207.0	3.2	1.3	129.7
100.0	-43.8	-16.0	-26645.9	6.2	-0.6	-1778.0	26.9	28.4	-19099.3	0.6	1.4	120.3
1.9	23.1	-8.2	366.9	1.2	0.7	516.1	17.1	-1.2	1572.5	3.2	1.8	277.6

	T13L			T12L			B11L			T11L		
Load	M11	M22	Axial	M11	M22	Axial	M11	M22	Axial	M11	M22	Axial
(%)	Nm	Nm	N	Nm	Nm	N	Nm	Nm	N	Nm	Nm	N
2.2	0.0	0.0	0.0	0.0	0.0	0.0	0.0	0.0	0.0	0.0	0.0	0.0
25.0	-8.6	1.8	-223.9	-1.9	-0.6	590.7	-10.9	2.2	-640.6	11.0	-1.5	-838.6
50.0	-15.3	3.0	-651.4	-3.8	-1.1	1280.1	-21.7	3.9	-1235.4	27.0	-2.3	-1949.5
75.0	-14.4	4.8	-883.8	1.3	-2.5	1886.9	-35.1	6.3	-1985.9	35.0	-6.5	-2590.7
90.0	-16.3	5.4	-933.8	1.9	-2.6	2344.7	-43.4	7.8	-2372.2	41.0	-8.1	-2961.7
100.0	-18.2	5.9	-857.0	3.2	-3.0	2767.5	-51.1	8.7	-2649.0	43.0	-10.0	-3168.4
1.9	-1.9	1.3	646.6	-1.3	0.3	464.4	-7.7	1.4	268.7	-3.0	0.1	583.4

	B11T			T11T			B14L			B14T		
Load	M11	M22	Axial	M11	M22	Axial	M11	M22	Axial	M11	M22	Axial
(%)	Nm	Nm	N	Nm	Nm	N	Nm	Nm	N	Nm	Nm	N
2.2	0.0	0.0	0.0	0.0	0.0	0.0	0.0	0.0	0.0	0.0	0.0	0.0
25.0	-8.1	2.1	-633.2	-1.0	-1.9	113.6	4.3	2.0	-701.2	6.1	1.5	-808.7
50.0	-17.5	4.6	-1295.1	-5.2	-3.7	282.8	9.8	4.7	-1463.3	12.9	2.9	-1555.5
75.0	-27.0	7.1	-2056.3	-4.2	-4.8	40.4	17.8	6.1	-2414.7	17.8	3.7	-2301.2
90.0	-32.0	8.4	-2468.8	-3.1	-5.1	-0.2	22.8	8.5	-2904.1	20.9	4.4	-2705.5
100.0	-37.0	9.2	-2735.7	-1.0	-4.2	51.0	27.7	9.8	-3207.3	23.9	5.2	-3013.5
1.9	1.3	0.2	180.7	-8.3	0.8	192.2	6.2	2.5	75.9	1.2	0.7	226.1

7L	
Load	Axial
(%)	N
2.2	0.0
25.0	13.0
50.0	23.4
75.0	44.8
90.0	56.5
100.0	63.3
1.9	-1.9

Load Case 2

	F2B			P3L			F4			T12T		
Load	M11	M22	Axial	M11	M22	Axial	M11	M22	Axial	M11	M22	Axial
(%)	Nm	Nm	N	Nm	Nm	N	Nm	Nm	N	Nm	Nm	N
2.8	0.0	0.0	0.0	0.0	0.0	0.0	0.0	0.0	0.0	0.0	0.0	0.0
25.0	-2.3	-6.4	-10416.7	-5.6	0.4	-83.7	-36.7	13.8	-13010.8	28.6	-4.6	1973.0
50.0	-4.6	-9.3	-20866.6	-6.2	2.2	490.9	-53.8	27.6	-26245.8	61.6	-10.3	4281.1
75.0	-30.0	1.3	-30964.3	-4.9	4.0	725.9	-71.0	36.0	-38634.3	93.9	-15.3	7156.6
90.0	-13.8	-6.7	-37091.1	-2.5	5.5	1084.8	-80.7	42.3	-46184.1	111.7	-16.1	8377.6
100.0	4.6	-17.1	-41177.6	1.9	7.0	1296.5	-85.6	45.4	-51904.1	122.5	-18.8	8944.2
3.6	60.0	-13.1	-2572.6	8.0	1.6	-178.8	-24.5	1.4	-3993.2	22.8	0.0	765.8

	T13L			T12L			B11L			T11L		
Load	M11	M22	Axial	M11	M22	Axial	M11	M22	Axial	M11	M22	Axial
(%)	Nm	Nm	N	Nm	Nm	N	Nm	Nm	N	Nm	Nm	N
2.8	0.0	0.0	0.0	0.0	0.0	0.0	0.0	0.0	0.0	0.0	0.0	0.0
25.0	-22.0	5.6	-66.5	-8.3	1.1	-44.6	-20.4	3.6	-1206.8	1.0	-0.3	-435.4
50.0	-40.2	10.1	-159.8	-18.5	3.2	-226.8	-44.7	8.2	-2795.1	-13.0	-3.5	-908.5
75.0	-55.6	14.5	-179.3	-25.5	4.5	-485.7	-71.5	12.3	-4348.7	-13.0	-3.5	-1040.3
90.0	-67.1	17.1	-414.7	-35.0	7.5	-498.6	-88.8	15.6	-5283.5	-8.0	-3.4	-1112.5
100.0	-74.7	20.7	-617.2	-40.1	8.9	-514.0	-102.8	17.6	-5953.1	-10.0	-5.7	-1155.1
3.6	-20.1	4.4	-332.4	-22.9	6.0	-808.6	3.8	-1.0	282.9	-49.0	-6.5	305.0

	B11T			T11T			B14L			B14T		
Load	M11	M22	Axial	M11	M22	Axial	M11	M22	Axial	M11	M22	Axial
(%)	Nm	Nm	N	Nm	Nm	N	Nm	Nm	N	Nm	Nm	N
2.8	0.0	0.0	0.0	0.0	0.0	0.0	0.0	0.0	0.0	0.0	0.0	0.0
25.0	14.4	-2.2	935.0	-52.1	-15.2	2369.1	9.8	4.7	-1754.0	6.1	-1.0	-4.3
50.0	16.3	-2.7	928.4	-112.5	-29.5	4659.0	20.9	9.0	-3673.4	21.5	-2.9	-950.2
75.0	18.2	-3.2	1120.3	-171.8	-43.3	6295.7	35.7	13.3	-5500.0	36.2	-6.1	-1725.9
90.0	23.8	-3.6	1404.7	-209.3	-55.9	7470.5	44.9	14.5	-6520.0	42.3	-8.1	-1928.9
100.0	34.5	-4.3	1909.3	-229.1	-64.5	8477.8	56.0	13.1	-7173.6	44.8	-10.8	-1693.0
3.6	38.2	0.6	1682.4	-26.0	-8.3	-781.9	-1.8	-11.5	353.2	15.3	-17.6	1323.7

7L	
Load	Axial
(%)	N
2.8	0.0
25.0	-0.3
50.0	-1.0
75.0	-1.5
90.0	-1.6
100.0	-1.6
3.6	-0.6

Load Case 2D

	F2B			P3L			F4			T12T		
Load	M11	M22	Axial	M11	M22	Axial	M11	M22	Axial	M11	M22	Axial
(%)	Nm	Nm	N	Nm	Nm	N	Nm	Nm	N	Nm	Nm	N
3.8	0.0	0.0	0.0	0.0	0.0	0.0	0.0	0.0	0.0	0.0	0.0	0.0
25.0	-20.8	0.5	-19041.3	-4.3	2.8	587.9	-22.0	24.1	-23363.6	48.2	-8.5	3698.1
50.0	-41.5	-7.8	-38548.7	-4.3	6.6	1912.8	-44.0	41.0	-46895.2	102.2	-17.3	7861.6
75.0	6.9	-17.7	-58820.0	25.3	16.3	5345.0	-73.4	58.2	-72847.6	185.9	-17.9	13391.2
90.0	-69.2	10.4	-69084.2	22.8	27.8	12194.2	-83.2	71.7	-85492.5	203.1	-27.5	16752.0
100.0	-133.8	24.8	-75832.4	3.1	26.1	14925.4	-29.4	96.2	-93440.3	226.5	-30.3	19149.5
5.4	-30.0	31.2	-1034.3	9.9	16.2	8768.9	122.3	23.4	2659.7	34.9	-0.9	3682.8

	T13L			T12L			B11L			T11L		
Load	M11	M22	Axial	M11	M22	Axial	M11	M22	Axial	M11	M22	Axial
(%)	Nm	Nm	N	Nm	Nm	N	Nm	Nm	N	Nm	Nm	N
3.8	0.0	0.0	0.0	0.0	0.0	0.0	0.0	0.0	0.0	0.0	0.0	0.0
25.0	-28.7	8.3	-242.7	-10.2	2.7	67.8	-48.5	8.6	-2736.4	18.0	0.8	-868.1
50.0	-54.6	17.1	-603.2	-19.1	3.4	301.1	-107.9	17.9	-5877.1	42.0	2.1	-1652.7
75.0	-99.6	33.6	-516.0	-40.1	8.9	373.1	-203.1	29.5	-10010.0	72.0	6.6	-1836.2
90.0	-105.4	45.2	-175.6	-49.0	11.7	423.7	-244.6	31.1	-11587.9	109.0	14.2	-1590.0
100.0	-112.1	52.1	148.3	-51.6	11.3	556.6	-266.3	33.0	-12541.1	143.0	19.0	-1542.0
5.4	15.3	19.1	1945.8	-11.5	4.6	-590.6	-24.9	-7.2	192.5	50.0	18.7	2249.2

	B11T			T11T			B14L			B14T		
Load	M11	M22	Axial	M11	M22	Axial	M11	M22	Axial	M11	M22	Axial
(%)	Nm	Nm	N	Nm	Nm	N	Nm	Nm	N	Nm	Nm	N
3.8	0.0	0.0	0.0	0.0	0.0	0.0	0.0	0.0	0.0	0.0	0.0	0.0
25.0	6.3	-4.3	673.7	-96.8	-28.6	4649.2	31.4	10.8	-3591.3	8.6	2.4	-889.5
50.0	2.5	-4.4	283.6	-201.0	-55.3	9039.4	64.6	21.7	-7330.0	27.6	2.7	-2699.0
75.0	70.8	-6.3	3579.5	-336.4	-72.4	11997.8	131.7	26.1	-12110.2	14.7	-7.8	113.2
90.0	74.6	-5.2	3479.6	-429.0	-78.4	13578.6	159.4	26.9	-13881.1	42.9	-20.5	-299.5
100.0	78.3	-5.1	3572.0	-483.2	-82.5	14782.9	168.6	30.2	-14982.5	61.4	-28.1	-194.3
5.4	31.3	4.6	594.2	-72.9	26.4	-3282.9	41.8	-13.4	-19.7	15.3	-31.3	2641.4

7L	
Load	Axial
(%)	N
3.8	0.0
25.0	0.3
50.0	0.5
75.0	1.1
90.0	2.2
100.0	2.6
5.4	1.9

Load Case 3

	F2B			P3L			F4			T12T		
Load	M11	M22	Axial	M11	M22	Axial	M11	M22	Axial	M11	M22	Axial
(%)	Nm	Nm	N	Nm	Nm	N	Nm	Nm	N	Nm	Nm	N
1.0	0.0	0.0	0.0	0.0	0.0	0.0	0.0	0.0	0.0	0.0	0.0	0.0
25.0	85.4	-39.5	-6497.7	-10.5	-2.5	5739.0	149.2	10.5	-11398.9	-59.0	8.6	-6639.5
50.0	-76.2	-66.8	-14858.3	-53.7	-8.6	11140.4	430.6	-3.2	-26083.1	-123.7	12.2	-13298.6
75.0	0.0	-161.8	-23077.8	-83.3	-20.5	16157.3	792.7	-32.3	-40463.4	-201.8	-11.4	-19434.7
90.0	48.5	-159.4	-29512.7	-85.8	-20.3	17781.5	932.2	-47.8	-47468.0	-241.1	-11.5	-22312.1
100.0	122.3	-149.9	-34586.0	-88.3	-19.7	18495.7	1032.5	-50.6	-51728.0	-272.9	-13.0	-24783.1
1.0	-36.9	-77.7	-123.2	-96.3	-11.5	-4245.5	457.5	-91.6	-1288.3	-33.0	-39.8	-1840.2

	T13L			T12L			B11L			T11L		
Load	M11	M22	Axial	M11	M22	Axial	M11	M22	Axial	M11	M22	Axial
(%)	Nm	Nm	N	Nm	Nm	N	Nm	Nm	N	Nm	Nm	N
1.0	0.0	0.0	0.0	0.0	0.0	0.0	0.0	0.0	0.0	0.0	0.0	0.0
25.0	-69.0	14.1	-6611.9	-91.0	4.0	-7000.8	19.2	2.4	2349.2	133.0	34.2	-8832.9
50.0	-196.4	27.2	-15353.2	-170.6	-21.5	-16587.2	76.0	6.7	6256.8	308.1	60.0	-16580.2
75.0	-286.4	26.8	-19879.1	-354.6	-12.4	-29050.8	162.2	13.4	10541.1	521.2	60.5	-24734.9
90.0	-362.1	29.3	-24739.8	-410.6	-10.0	-33393.9	195.4	20.5	12273.0	638.2	84.3	-32155.3
100.0	-424.3	30.8	-28747.9	-434.8	-11.1	-35168.7	217.1	27.5	13234.6	700.2	106.7	-37922.8
1.0	-74.7	-33.3	-778.4	-73.8	-69.0	-2449.5	100.3	30.0	930.2	65.0	-67.2	1535.7

	B11T			T11T			B14L			B14T		
Load	M11	M22	Axial	M11	M22	Axial	M11	M22	Axial	M11	M22	Axial
(%)	Nm	Nm	N	Nm	Nm	N	Nm	Nm	N	Nm	Nm	N
1.0	0.0	0.0	0.0	0.0	0.0	0.0	0.0	0.0	0.0	0.0	0.0	0.0
25.0	-23.2	-1.9	-1868.3	118.7	21.0	-4411.6	-16.6	5.5	545.3	-26.4	8.7	240.5
50.0	-105.9	-4.7	-5693.2	227.0	50.9	-9924.7	-60.3	14.2	2179.7	-87.1	44.8	-2443.7
75.0	-196.8	-4.9	-10197.9	366.6	48.3	-17684.9	-112.0	19.3	4265.6	-122.1	79.0	-5054.6
90.0	-238.2	3.9	-12844.9	439.5	61.3	-22978.0	-112.0	18.2	4742.4	-95.7	80.0	-7021.8
100.0	-261.4	20.1	-15102.9	450.9	69.3	-25689.9	-103.4	14.9	5030.2	-65.0	80.9	-9128.0
1.0	-87.7	4.9	-4001.4	-67.7	-62.1	1807.9	-19.7	6.9	1738.0	-23.9	57.9	-5775.9

7L	
Load	Axial
(%)	N
1.0	0.0
25.0	1.1
50.0	1.6
75.0	4.9
90.0	6.7
100.0	7.8
1.0	1.1

Load Case 3D

	F2B			P3L			F4			T12T		
Load	M11	M22	Axial	M11	M22	Axial	M11	M22	Axial	M11	M22	Axial
(%)	Nm	Nm	N	Nm	Nm	N	Nm	Nm	N	Nm	Nm	N
3.4	0.0	0.0	0.0	0.0	0.0	0.0	0.0	0.0	0.0	0.0	0.0	0.0
25.0	36.9	-10.2	-19699.0	11.7	-1.6	-1361.4	31.8	12.7	-23455.9	-5.1	3.9	727.2
50.0	85.4	-18.4	-39657.3	19.1	-3.6	-4754.5	90.5	43.1	-50588.1	-22.8	11.6	1331.9
75.0	140.8	-40.8	-63975.4	26.5	-14.2	-11478.1	144.3	105.3	-85285.3	-38.7	17.7	2018.3
90.0	203.1	-40.4	-77072.5	60.5	-8.4	-14027.6	210.4	146.2	-99332.9	-42.5	21.3	1906.6
100.0	230.8	-62.2	-80562.1	92.0	-3.5	-14960.5	293.6	227.3	-103347.4	-51.4	24.6	1724.4
4.9	41.5	-8.0	-963.0	71.6	2.1	-844.4	134.6	162.0	-2414.0	-10.2	15.8	15.7

	T13L			T12L			B11L			T11L		
Load	M11	M22	Axial	M11	M22	Axial	M11	M22	Axial	M11	M22	Axial
(%)	Nm	Nm	N	Nm	Nm	N	Nm	Nm	N	Nm	Nm	N
3.4	0.0	0.0	0.0	0.0	0.0	0.0	0.0	0.0	0.0	0.0	0.0	0.0
25.0	-26.8	6.3	-2727.7	-36.3	8.4	-3037.1	4.5	-0.1	846.2	74.0	17.2	-3931.4
50.0	-67.1	14.3	-6119.1	-86.6	19.4	-6887.6	31.3	-2.2	3399.2	162.1	39.7	-8912.9
75.0	-83.3	11.1	-10083.2	-136.9	30.3	-10639.6	139.8	-14.6	10609.3	258.1	64.2	-14622.9
90.0	-98.7	13.4	-11684.9	-168.7	37.0	-13186.3	166.7	-17.2	12321.0	307.1	74.1	-17247.0
100.0	-112.1	15.1	-12348.6	-193.5	41.9	-15132.7	167.9	-16.0	12113.3	345.1	75.2	-18139.9
4.9	40.2	-14.4	801.5	-2.5	1.2	-1778.4	77.9	-10.8	4413.4	8.0	-19.5	1388.5

	B11T			T11T			B14L			B14T		
Load	M11	M22	Axial	M11	M22	Axial	M11	M22	Axial	M11	M22	Axial
(%)	Nm	Nm	N	Nm	Nm	N	Nm	Nm	N	Nm	Nm	N
3.4	0.0	0.0	0.0	0.0	0.0	0.0	0.0	0.0	0.0	0.0	0.0	0.0
25.0	-48.3	9.0	-2913.5	16.7	-1.7	-248.7	-6.8	-0.3	555.3	35.0	-0.2	-2443.7
50.0	-50.1	7.9	-2767.4	57.3	-0.4	-842.2	-27.1	-1.6	2362.7	52.8	-7.7	-2496.9
75.0	-107.2	21.3	-5075.3	96.8	3.4	-1196.6	-95.4	-11.8	9490.9	132.5	-16.1	-6185.1
90.0	-169.2	40.3	-8663.9	144.8	16.0	-1426.6	-123.1	-5.4	11025.2	174.8	-12.5	-10214.5
100.0	-222.5	60.2	-12032.9	172.9	22.2	-1808.2	-137.2	0.5	10665.8	217.8	-11.1	-13711.9
4.9	19.4	12.0	991.8	85.4	27.4	422.6	-81.8	2.3	5961.1	97.5	-39.3	845.1

7L	
Load	Axial
(%)	N
3.4	0.0
25.0	5.0
50.0	9.6
75.0	14.7
90.0	16.0
100.0	17.2
4.9	-2.5

Load Case 4

	F2B			P3L			F4			T12T		
Load	M11	M22	Axial	M11	M22	Axial	M11	M22	Axial	M11	M22	Axial
(%)	Nm	Nm	N	Nm	Nm	N	Nm	Nm	N	Nm	Nm	N
3.4	0.0	0.0	0.0	0.0	0.0	0.0	0.0	0.0	0.0	0.0	0.0	0.0
25.0	4.6	-99.7	-30397.0	-29.0	3.0	5088.1	176.2	53.3	-32679.3	-54.6	6.4	-5734.1
50.0	6.9	-68.7	-69653.2	-53.1	1.5	7378.5	340.1	110.1	-64345.9	-106.0	5.1	-11253.7
75.0	0.0	-133.6	-110358.1	-79.6	-3.1	11943.8	562.7	173.8	-99491.7	-181.5	7.8	-16820.1
90.0	16.2	-176.8	-133730.3	-90.7	-3.3	16866.5	866.1	335.4	-116412.5	-226.5	8.0	-19874.2
100.0	-6.9	-219.6	-149325.1	-96.9	-6.0	20545.6	986.0	397.2	-133114.3	-254.5	6.6	-21776.1
4.9	53.1	-44.6	-11183.4	-83.9	-2.5	-2872.7	227.5	168.4	1241.1	-2.5	-15.2	1380.1

	T13L			T12L			B11L			T11L		
Load	M11	M22	Axial	M11	M22	Axial	M11	M22	Axial	M11	M22	Axial
(%)	Nm	Nm	N	Nm	Nm	N	Nm	Nm	N	Nm	Nm	N
3.4	0.0	0.0	0.0	0.0	0.0	0.0	0.0	0.0	0.0	0.0	0.0	0.0
25.0	-78.5	19.0	-7182.8	-69.4	12.8	-6073.9	-35.1	8.3	-493.6	176.1	27.6	-11156.2
50.0	-176.2	41.4	-14671.9	-139.4	23.0	-11687.2	-68.3	16.7	-1236.7	369.1	48.7	-22916.8
75.0	-296.0	67.9	-22605.5	-216.4	32.5	-17968.2	-102.2	25.2	-2536.3	595.2	77.6	-35917.4
90.0	-365.9	88.7	-26589.1	-263.5	36.2	-21544.4	-157.1	38.0	-5152.2	730.2	95.3	-42995.6
100.0	-380.3	94.3	-28933.2	-303.0	37.5	-24411.2	-153.9	41.4	-4610.0	830.3	102.1	-47885.3
4.9	27.8	7.7	1903.7	-19.1	-5.1	-1136.7	-83.0	5.9	-5455.6	24.0	-14.0	585.9

	B11T			T11T			B14L			B14T		
Load	M11	M22	Axial	M11	M22	Axial	M11	M22	Axial	M11	M22	Axial
(%)	Nm	Nm	N	Nm	Nm	N	Nm	Nm	N	Nm	Nm	N
3.4	0.0	0.0	0.0	0.0	0.0	0.0	0.0	0.0	0.0	0.0	0.0	0.0
25.0	-52.0	9.9	-4289.9	131.2	39.1	-6509.8	11.7	10.9	-3114.9	-11.7	11.6	-2909.3
50.0	-121.6	21.3	-8802.0	256.2	71.8	-14318.1	38.2	24.2	-6811.9	-22.7	32.1	-6088.9
75.0	-250.7	49.4	-16606.5	393.6	106.9	-22219.9	73.2	35.6	-11130.2	12.9	52.7	-11963.7
90.0	-295.8	74.1	-20244.5	496.7	132.3	-27109.0	116.3	42.2	-15477.2	30.1	55.0	-14094.7
100.0	-311.5	100.7	-22109.4	572.8	147.5	-29815.9	121.8	39.2	-15651.8	38.0	58.0	-15573.2
4.9	-51.4	43.5	-5170.1	-17.7	-11.4	-2394.2	71.4	7.9	-6196.7	-12.9	35.3	-5499.4

7L	
Load	Axial
(%)	N
3.4	0.0
25.0	4.1
50.0	8.4
75.0	12.0
90.0	14.9
100.0	16.7
4.9	7.2

Load Case 4D

	F2B			P3L			F4			T12T		
Load	M11	M22	Axial	M11	M22	Axial	M11	M22	Axial	M11	M22	Axial
(%)	Nm	Nm	N	Nm	Nm	N	Nm	Nm	N	Nm	Nm	N
5.5	0.0	0.0	0.0	0.0	0.0	0.0	0.0	0.0	0.0	0.0	0.0	0.0
25.0	53.1	-48.1	-42571.8	26.5	0.9	-2812.3	56.3	88.5	-53411.5	36.8	-0.8	3534.4
50.0	230.8	-150.1	-88298.9	53.1	-3.1	-5802.8	88.1	173.1	-108825.5	57.7	8.7	6917.2
75.0	295.4	-226.0	-131616.1	75.9	-5.0	-8195.3	73.4	276.1	-161100.7	133.3	28.7	10084.7
90.0	325.4	-260.7	-160871.4	87.6	-6.1	-9216.3	-68.5	365.9	-195043.0	165.0	30.8	12222.5
100.0	253.8	-274.3	-177362.5	102.5	-4.2	-9949.6	-217.7	405.7	-216564.0	177.0	28.8	14266.4
5.2	94.6	-59.6	8135.5	109.2	2.6	2526.0	-389.0	25.8	86.0	28.6	49.9	-2236.0

	T13L			T12L			B11L			T11L		
Load	M11	M22	Axial	M11	M22	Axial	M11	M22	Axial	M11	M22	Axial
(%)	Nm	Nm	N	Nm	Nm	N	Nm	Nm	N	Nm	Nm	N
5.5	0.0	0.0	0.0	0.0	0.0	0.0	0.0	0.0	0.0	0.0	0.0	0.0
25.0	-65.1	15.9	-3598.7	-47.7	9.8	-2072.2	-55.6	12.4	-2140.6	104.0	14.1	-5736.7
50.0	-142.7	36.0	-8285.0	-120.3	26.0	-4059.3	-113.0	23.8	-4531.5	194.1	18.7	-12122.9
75.0	-206.9	52.3	-11733.0	-178.2	37.4	-5775.2	-179.4	36.9	-7470.8	307.1	29.0	-18081.7
90.0	-243.3	67.0	-13578.8	-215.2	43.8	-7116.0	-224.1	44.1	-9385.5	401.1	39.5	-21750.5
100.0	-256.7	77.3	-14510.7	-239.4	49.1	-8157.4	-235.0	44.2	-9546.7	478.2	52.4	-23614.2
5.2	35.4	12.6	696.0	-21.0	8.1	-353.5	-17.2	-12.7	882.5	1.0	3.2	1332.6

	B11T			T11T			B14L			B14T		
Load	M11	M22	Axial	M11	M22	Axial	M11	M22	Axial	M11	M22	Axial
(%)	Nm	Nm	N	Nm	Nm	N	Nm	Nm	N	Nm	Nm	N
5.5	0.0	0.0	0.0	0.0	0.0	0.0	0.0	0.0	0.0	0.0	0.0	0.0
25.0	62.0	-17.4	3746.9	-48.9	-27.2	3291.6	18.5	10.2	-3484.1	-4.9	-13.5	2743.9
50.0	47.0	-16.1	2741.7	-28.1	-77.7	6928.3	46.8	21.8	-7291.7	46.6	-24.4	536.2
75.0	15.0	-4.5	-204.6	-92.7	-74.4	10699.6	83.1	34.5	-11909.2	133.1	-39.1	-3509.4
90.0	1.3	3.4	-1785.6	-206.2	-42.6	13084.8	108.3	39.7	-14921.1	182.8	-47.0	-5454.4
100.0	12.5	8.5	-1927.0	-281.2	-20.9	13356.6	113.2	41.0	-15709.0	195.7	-50.2	-5214.2
5.2	193.7	-20.5	9079.3	-64.6	93.2	371.1	-13.5	-8.9	758.1	4.9	-73.4	11833.7

7L	
Load	Axial
(%)	N
5.5	0.0
25.0	20.5
50.0	46.3
75.0	78.0
90.0	93.6
100.0	102.0
5.2	3.3

Load Case 4D (collapse)

	F2B			P3L			F4			T12T		
Load	M11	M22	Axial	M11	M22	Axial	M11	M22	Axial	M11	M22	Axial
(%)	Nm	Nm	N	Nm	Nm	N	Nm	Nm	N	Nm	Nm	N
4.9	0.0	0.0	0.0	0.0	0.0	0.0	0.0	0.0	0.0	0.0	0.0	0.0
50.0	57.7	-84.6	-87191.8	-8.6	-2.5	-6238.7	31.8	158.3	-102375.8	64.7	-12.6	7705.9
75.0	94.6	-138.7	-137127.0	-5.6	-2.8	-8666.7	58.7	262.2	-160786.2	106.0	-19.4	12265.5
90.0	99.2	-180.5	-162909.9	-1.9	-2.7	-10307.6	78.3	325.0	-191633.9	129.5	-22.7	14707.6
100.0	115.4	-216.6	-183711.9	4.9	-3.0	-11490.9	83.2	381.1	-216278.1	147.9	-25.2	16508.9
105.0	85.4	-222.3	-193515.4	14.8	-2.4	-11632.1	78.3	405.9	-227672.5	156.1	-26.2	17220.9
110.0	60.0	-243.4	-203093.6	23.5	-2.1	-12045.1	80.7	433.9	-238964.9	162.5	-26.2	17414.7

	T13L			T12L			B11L			T11L		
Load	M11	M22	Axial	M11	M22	Axial	M11	M22	Axial	M11	M22	Axial
(%)	Nm	Nm	N	Nm	Nm	N	Nm	Nm	N	Nm	Nm	N
4.9	0.0	0.0	0.0	0.0	0.0	0.0	0.0	0.0	0.0	0.0	0.0	0.0
50.0	-130.3	31.0	-7005.9	-103.8	20.1	-4241.9	-93.9	23.6	-4515.9	226.1	29.0	-11814.1
75.0	-206.9	50.9	-11096.3	-163.0	31.8	-6479.1	-154.5	37.9	-7309.7	363.1	43.3	-18567.0
90.0	-248.1	61.3	-13247.6	-193.5	38.2	-7518.8	-185.2	45.6	-8685.7	437.1	50.1	-22001.3
100.0	-276.8	69.6	-14885.9	-217.7	42.9	-8415.9	-204.3	50.4	-9508.7	501.2	56.0	-24695.8
105.0	-288.3	72.9	-15439.7	-227.3	43.8	-8739.0	-215.8	52.8	-10015.8	533.2	59.4	-25945.3
110.0	-296.0	75.8	-15831.3	-233.6	44.9	-8934.4	-228.0	55.9	-10632.3	561.2	60.3	-26825.8

	B11T			T11T			B14L			B14T		
Load	M11	M22	Axial	M11	M22	Axial	M11	M22	Axial	M11	M22	Axial
(%)	Nm	Nm	N	Nm	Nm	N	Nm	Nm	N	Nm	Nm	N
4.9	0.0	0.0	0.0	0.0	0.0	0.0	0.0	0.0	0.0	0.0	0.0	0.0
50.0	-79.0	10.6	-4696.5	-115.6	-51.7	6259.8	49.8	21.5	-7507.6	70.6	10.7	-7651.8
75.0	-134.1	20.9	-8168.0	-182.2	-80.6	9645.8	84.9	35.0	-11907.3	125.8	13.6	-12727.3
90.0	-159.8	27.1	-9851.3	-216.6	-94.0	11513.3	102.8	41.2	-14031.3	154.6	14.5	-15263.1
100.0	-179.3	30.6	-11000.3	-251.0	-99.3	12886.6	114.5	44.8	-15455.9	176.7	14.5	-17001.0
105.0	-193.0	33.7	-11865.1	-267.6	-101.3	13619.1	120.6	46.8	-16207.6	189.6	14.8	-17848.4
110.0	-204.3	36.1	-12573.2	-274.9	-104.5	14661.8	128.0	49.0	-17072.4	200.6	14.6	-18598.4

7L	
Load	Axial
(%)	N
4.9	0.0
50.0	45.1
75.0	71.7
90.0	86.3
100.0	97.7
105.0	103.4
110.0	112.0

B.2 TEST REPORT

B.2.1. PROTOTYPE 1 TEST REPORT

LINE ENGINEERING SERVICES
TOWER TESTING STATION, ROSHERVILLE
JOHANNESBURG , GAUTENG PROVINCE
SOUTH AFRICA

TEST REPORT NUMBER :	SC 00 / 542
PROJECT NUMBER:	RO - 423

TOWER TYPE : " STRUCTURE 1 "

TOWER DETAIL : ABB DRAWINGS: (T - 47787 TRANSVERSAL FACE)
(T - 47788 LONGITUDINAL FACE)

MANUFACTURER : ABB Asea Brown Boveri

CLIENT : CIGRE

PROJECT: WORKING GROUP 08 - TASK FORCE 4
INFLUENCE OF HYPERSTATIC MODELLING

CONSULTANT : CIGRE

TABLE OF CONTENTS

1 . INTRODUCTION

ALL TESTS WERE :

(a) In accordance with the Contract , the Test Schedules SC 00 / 542 and our General Conditions of Test (Annexure " A ").

(b) Reported in chronological order in which they were performed .

(c) Conducted by : Mr JA Meintjes & Mr DL Stevens.

(d) Witnessed by :

Joao Batista Ferreira	~	ABB
David Hughes	~	PB Power
Leon Kempner	~	BPA
Ruy C. Menezes	~	UFRGS / Engelieas - Brazil
S. Kitipornchai	~	Citi Uni - Hong Kong
Geir Nesgaard	~	Norconsult
J. Diez-Serrano	~	Eskom Enterprises TSI
Pierre Dalleves	~	Energie Quest Suisse
Fabiana Camcugo	~	UFRGS / Engelieas - Brazil
Rania Peixoto	~	ABB Ltda
S.J. Madibu	~	Eskom Enterprises TSI
Mark Newby	~	Eskom Enterprises TSI
Dan Dukhan	~	Eskom

TEST SCHEDULES

TEST SEQUENCE : 1, 2, 3, 4, 5, 6, 7, 8.

REVISION 2 **8th Oct 2001**

CALCULATION OF TEST LOADS AND ANGLES

TOWER TYPE : " CIGRE "
INFLUENCE OF HYPERSTATIC MODELLING ON SELF SUPPORTING STRUCTURES

TEST NUMBER ONE

LOAD CONDITION : 1

VERTICAL LOADING

ATT POINT	V VERT	H TRANS	H LONG	LOAD CELL	Vr (kN.)	Vr 1 (kN.)	Vr 2 (kN.)	h (m)	R (kN.)	ANGLE DEG	MASS (kg)
C2V	49,05			120~2	0,20				48,85		

NOTES : **(g = 9.80665)**

1) LOADS IN KILONEWTONS EXCEPT FOR MASS WHICH HAS BEEN CONVERTED TO KILOGRAM

2) ANGLES ARE IN DEGREES , NEGATIVE ANGLES SLOPE ABOVE HORIZONTAL FROM TOWER

REVISION 2 8th Oct 2001

CALCULATION OF TEST LOADS AND ANGLES

TOWER TYPE : " CIGRE "
INFLUENCE OF HYPERSTATIC MODELLING ON SELF SUPPORTING STRUCTURES

TEST NUMBER TWO

LOAD CONDITION : 1D
VERTICAL LOADING

ATT POINT	V VERT	H TRANS	H LONG	LOAD CELL	Vr (kN.)	Vr 1 (kN.)	Vr 2 (kN.)	h (m)	R (kN.)	ANGLE DEG	MASS (kg)
C1V	49,05			120~1	0,20				48,85		
C2V	49,05			120~2	0,20				48,85		

NOTES : (g = 9.80665)

1) LOADS IN KILONEWTONS EXCEPT FOR MASS WHICH HAS BEEN CONVERTED TO KILOGRAM
2) ANGLES ARE IN DEGREES , NEGATIVE ANGLES SLOPE ABOVE HORIZONTAL FROM TOWER

REVISION 2 8th Oct 2001

CALCULATION OF TEST LOADS AND ANGLES

TOWER TYPE : " CIGRE "
INFLUENCE OF HYPERSTATIC MODELLING ON SELF SUPPORTING STRUCTURES

TEST NUMBER THREE

LOAD CONDITION : 2

TRANSVERSE LOADING

ATT POINT	V VERT	H TRANS	H LONG	LOAD CELL	Vr (kN.)	Vr 1 (kN.)	Vr 2 (kN.)	h (m)	R (kN.)	ANGLE DEG	MASS (kg)
C2T		49,05		120~2	0,20	0,70		-0,80	49,05	-0,82	

NOTES : (g = 9.80665)

1) LOADS IN KILONEWTONS EXCEPT FOR MASS WHICH HAS BEEN CONVERTED TO KILOGRAM
2) ANGLES ARE IN DEGREES , NEGATIVE ANGLES SLOPE ABOVE HORIZONTAL FROM TOWER

REVISION 2 8th Oct 2001

CALCULATION OF TEST LOADS AND ANGLES

TOWER TYPE : " CIGRE "
INFLUENCE OF HYPERSTATIC MODELLING ON SELF SUPPORTING STRUCTURES

TEST NUMBER FOUR

LOAD CONDITION : 2D
TRANSVERSE LOADING

ATT POINT	V VERT	H TRANS	H LONG	LOAD CELL	Vr (kN.)	Vr 1 (kN.)	Vr 2 (kN.)	h (m)	R (kN.)	ANGLE DEG	MASS (kg)
C1T		49,05		120~1	0,20	0,76		-0,98	49,05	-0,89	
C2T		49,05		120~2	0,20	0,70		-0,80	49,05	-0,82	

NOTES : (g = 9.80665)

1) LOADS IN KILONEWTONS EXCEPT FOR MASS WHICH HAS BEEN CONVERTED TO KILOGRAM
2) ANGLES ARE IN DEGREES , NEGATIVE ANGLES SLOPE ABOVE HORIZONTAL FROM TOWER

REVISION 2 **8th Oct 2001**

CALCULATION OF TEST LOADS AND ANGLES

TOWER TYPE : " CIGRE "
INFLUENCE OF HYPERSTATIC MODELLING ON SELF SUPPORTING STRUCTURES

TEST NUMBER FIVE

LOAD CONDITION : 3

LONGITUDINAL LOADING

ATT POINT	V VERT	H TRANS	H LONG	LOAD CELL	Vr (kN.)	Vr 1 (kN.)	Vr 2 (kN.)	h (m)	R (kN.)	ANGLE DEG	MASS (kg)
C2L			49,05	120~4	0,20	0,74		-0,91	49,05	-0,86	

NOTES : **(g = 9.80665)**

1) LOADS IN KILONEWTONS EXCEPT FOR MASS WHICH HAS BEEN CONVERTED TO KILOGRAM
2) ANGLES ARE IN DEGREES , NEGATIVE ANGLES SLOPE ABOVE HORIZONTAL FROM TOWER

REVISION 2 8th Oct 2001

CALCULATION OF TEST LOADS AND ANGLES

TOWER TYPE : " CIGRE "
INFLUENCE OF HYPERSTATIC MODELLING ON SELF SUPPORTING STRUCTURES

TEST NUMBER **SIX**

LOAD CONDITION : 3D

LONGITUDINAL LOADING

ATT POINT	V VERT	H TRANS	H LONG	LOAD CELL	Vr (kN.)	Vr 1 (kN.)	Vr 2 (kN.)	h (m)	R (kN.)	ANGLE DEG	MASS (kg)
C1L			49,05	120~3	0,20	0,74		-0,91	49,05	-0,86	
C2L			49,05	120~4	0,20	0,74		-0,91	49,05	-0,86	

NOTES : (g = 9.80665)

1) LOADS IN KILONEWTONS EXCEPT FOR MASS WHICH HAS BEEN CONVERTED TO KILOGRAM

2) ANGLES ARE IN DEGREES , NEGATIVE ANGLES SLOPE ABOVE HORIZONTAL FROM TOWER

TEST SEQUENCE : 1, 2, 3, 4, 5, 6, 7, 8.

REVISION 2 8th Oct 2001

CALCULATION OF TEST LOADS AND ANGLES

TOWER TYPE : **" CIGRE "**
INFLUENCE OF HYPERSTATIC MODELLING ON SELF SUPPORTING STRUCTURES

TEST NUMBER
SEVEN

LOAD CONDITION : **4**
VERTICAL LOADING, TRANSVERSE AND LONGITUDINAL LOADING

ATT POINT	V VERT	H TRANS	H LONG	LOAD CELL	Vr (kN.)	Vr 1 (kN.)	Vr 2 (kN.)	h (m)	R (kN.)	ANGLE DEG	MASS (kg)
C2T	49,05	49,05		120~2	0,20	0,20			69,23	44,88	
C2L			49,05	120~4	0,20	0,74		-0,91	49,05	-0,86	

NOTES : **(g = 9.80665)**

1) LOADS IN KILONEWTONS EXCEPT FOR MASS WHICH HAS BEEN CONVERTED TO KILOGRAM
2) ANGLES ARE IN DEGREES , NEGATIVE ANGLES SLOPE ABOVE HORIZONTAL FROM TOWER
3) WHERE HORIZONTAL AND VERTICAL LOADS ARE COMBINED , ANGLE CONTROL IS EMPLOYED .

REVISION 2 8th Oct 2001

CALCULATION OF TEST LOADS AND ANGLES

TOWER TYPE : **" CIGRE "**
INFLUENCE OF HYPERSTATIC MODELLING ON SELF SUPPORTING STRUCTURES

TEST NUMBER
EIGHT

LOAD CONDITION : **4D**
VERTICAL LOADING, TRANSVERSE AND LONGITUDINAL LOADING

ATT POINT	V VERT	H TRANS	H LONG	LOAD CELL	Vr (kN.)	Vr 1 (kN.)	Vr 2 (kN.)	h (m)	R (kN.)	ANGLE DEG	MASS (kg)
C1T	49,05	49,05		120~1	0,20	0,20			69,23	44,88	
C2T	49,05	49,05		120~2	0,20	0,20			69,23	44,88	
C1L			49,05	120~3	0,20	0,74		-0,91	49,05	-0,86	
C2L			49,05	120~4	0,20	0,74		-0,91	49,05	-0,86	

NOTES : **(g = 9.80665)**

1) LOADS IN KILONEWTONS EXCEPT FOR MASS WHICH HAS BEEN CONVERTED TO KILOGRAM
2) ANGLES ARE IN DEGREES , NEGATIVE ANGLES SLOPE ABOVE HORIZONTAL FROM TOWER
3) WHERE HORIZONTAL AND VERTICAL LOADS ARE COMBINED , ANGLE CONTROL IS EMPLOYED .

TEST RESULTS

TEST 1	STRUCTURE 1	LOADCASE 1

See applied loads relative to this test in SECTION 3 Page 1 and the photograph of this structure showing rigging for Test 1 Run 1 in SECTION 5 Page 1 of this report.

RUN 1 - 10th October 2001

One hundred percent of the applied loads was held satisfactorily for 60 seconds.
No visual damage to the structure was detected after the test.

DEFLECTION READINGS

Transverse deflection readings taken in the centre at the tip of the earth peak **(A)** and at the joint between the body and the waist **(B)** . As well as, **Longitudinal** deflection readings taken at the tip of the cross ams , E1 **(C)** and E2 **(D)** , in millimeters , are tabulated below:

Loading Stage:	0,40%	25%	50%	75%	90%	100%	0,40%	RESIDUAL
TRANSVERSE (A)	0	0	10	32	54	65	0	0
TRANSVERSE (B)	0	0	0	0	0	0	0	0
LONGITUDINAL (C)	0	0	0	0	0	0	0	0
LONGITUDINAL (D)	0	0	0	0	0	0	0	0

ORIENTATION

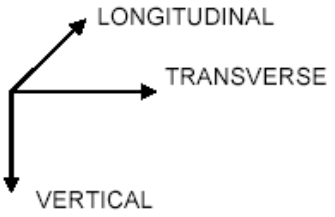

MEMBER FORCES RECORDED ON THE STRAIN GAUGES

Summary of the internal member forces monitored during the test.

Loading Stage:	0,40%	25%	50%	75%	90%	100%	0,40%
Strain Gauge ID:	Strain Gauge reading in (N)						
F2B	0	-14176	-26931	-40798	-50239	-57766	-1710
P3L	0	-442	-585	-1650	-2343	-2704	12
F4	0	-11536	-19014	-28718	-36423	-42356	-1867
T11L	0	-291	438	849	974	1194	173
T12L	32	-72	-212	-253	-79	127	615
T13L	0	-523	-347	-565	-885	-858	-705
B11L	0	-365	-248	-66	37	251	13
T11T	0	-3216	-7106	-10645	-12358	-13787	-15
T12T	0	1943	4547	7343	8504	9463	-69
B11T	0	1269	1815	2041	2122	2251	-455

TEST RESULTS

TEST 2	STRUCTURE 1	LOADCASE 1D

See applied loads relative to this test in SECTION 3 Page 2 and the photograph of this structure showing rigging for Test 2 Run 1 in SECTION 5 Page 2 of this report.

RUN 1 - 10th October 2001

One hundred percent of the applied loads was held satisfactorily for 60 seconds.
No visual damage to the structure was detected after the test.

DEFLECTION READINGS

Transverse deflection readings taken in the centre at the tip of the earth peak **(A)** and at the joint between the body and the waist **(B)** . As well as, **Longitudinal** deflection readings taken at the tip of the cross ams , E1 **(C)** and E2 **(D)** , in millimeters , are tabulated below:

Loading Stage:	0,40%	25%	50%	75%	90%	100%	0,40%	RESIDUAL
TRANSVERSE (A)	0	10	21	30	30	31	0	0
TRANSVERSE (B)	0	0	0	0	0	0	0	0
LONGITUDINAL (C)	0	0	0	0	0	0	0	0
LONGITUDINAL (D)	0	0	0	0	0	0	0	0

ORIENTATION

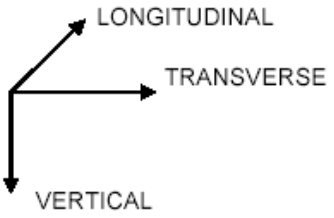

MEMBER FORCES RECORDED ON THE STRAIN GAUGES

Summary of the internal member forces monitored during the test.

Loading Stage:	0,40%	25%	50%	75%	90%	100%	0,40%
Strain Gauge ID:	Strain Gauge reading in (N)						
F2B	0	-5872	-11785	-15810	-18885	-21325	1508
P3L	0	-189	-96	-257	-376	-359	-105
F4	0	-5962	-11451	-16233	-19440	-21827	1510
T11L	0	-189	115	57	63	132	-161
T12L	32	-120	-94	-20	60	-20	201
T13L	0	-161	192	128	189	189	62
B11L	0	-273	-143	-143	-143	-159	-210
T11T	0	-186	-110	43	72	48	-66
T12T	0	-51	54	-174	-225	-214	91
B11T	0	-63	131	131	131	131	113

TEST RESULTS

TEST 3	STRUCTURE 1	LOADCASE 2

See applied loads relative to this test in SECTION 3 Page 3 and the photograph of this structure showing rigging for Test 3 Run 1 in SECTION 5 Page 3 of this report.

RUN 1 - 10th October 2001

One hundred percent of the applied loads was held satisfactorily for 60 seconds.
No visual damage to the structure was detected after the test.

DEFLECTION READINGS

Transverse deflection readings taken in the centre at the tip of the earth peak **(A)** and at the joint between the body and the waist **(B)** . As well as, **Longitudinal** deflection readings taken at the tip of the cross ams , E1 **(C)** and E2 **(D)** , in millimeters , are tabulated below:

Loading Stage:	0,36%	25%	50%	75%	90%	100%	0,36%	RESIDUAL
TRANSVERSE (A)	0	10	20	30	30	40	0	0
TRANSVERSE (B)	0	10	20	30	30	40	0	0
LONGITUDINAL (C)	0	0	0	0	0	0	0	0
LONGITUDINAL (D)	0	0	0	0	0	0	0	0

ORIENTATION

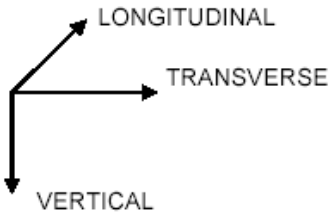

MEMBER FORCES RECORDED ON THE STRAIN GAUGES

Summary of the internal member forces monitored during the test.

Loading Stage:	0,36%	25%	50%	75%	90%	100%	0,36%
Strain Gauge ID:	Strain Gauge reading in (N)						
F2B	0	-7435	-17189	-29045	-36316	-42612	-6466
P3L	0	397	407	-4	-227	-385	-285
F4	0	-10745	-24835	-41765	-52701	-61611	-10796
T11L	0	420	393	115	56	-184	-279
T12L	32	239	418	-229	-237	-183	329
T13L	0	286	679	987	972	857	905
B11L	0	16	112	106	28	-2	337
T11T	0	3925	7617	9424	10460	11318	-1555
T12T	0	-2315	-4295	-7083	-9079	-10437	-2059
B11T	0	-345	-678	-1174	-1601	-1775	373

TEST RESULTS

TEST 4	STRUCTURE 1	LOADCASE 2D

See applied loads relative to this test in SECTION 3 Page 4 and the photograph of this structure showing rigging for Test 4 Run 1 in SECTION 5 Page 4 of this report.

RUN 1 - 10th October 2001

One hundred percent of the applied loads was held satisfactorily for 60 seconds.
No visual damage to the structure was detected after the test.

DEFLECTION READINGS

Transverse deflection readings taken in the centre at the tip of the earth peak **(A)** and at the joint between the body and the waist **(B)** . As well as, **Longitudinal** deflection readings taken at the tip of the cross ams , E1 **(C)** and E2 **(D)** , in millimeters , are tabulated below:

Loading Stage:	7,40%	25%	50%	75%	90%	100%	7,00%	RESIDUAL
TRANSVERSE (A)	0	10	30	50	70	80	20	20
TRANSVERSE (B)	0	10	30	50	70	80	20	20
LONGITUDINAL (C)	0	0	0	0	0	0	0	0
LONGITUDINAL (D)	0	0	0	0	0	0	0	0

ORIENTATION

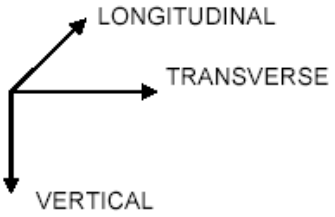

MEMBER FORCES RECORDED ON THE STRAIN GAUGES

Summary of the internal member forces monitored during the test.

Loading Stage:	7,40%	25%	50%	75%	90%	100%	7,00%
Strain Gauge ID:	Strain Gauge reading in (N)						
F2B	0	-13962	-32380	-50914	-63070	-71216	-972
P3L	0	104	206	-2258	-3347	-4042	-4197
F4	0	-19498	-45874	-73900	-90060	-1E+05	-1276
T11L	0	172	328	365	478	710	-134
T12L	32	-162	-438	-662	-549	-764	194
T13L	0	49	1	-62	-482	-417	-570
B11L	0	-174	-496	-479	-759	-816	-238
T11T	0	5036	11505	17470	22438	25184	-420
T12T	0	-3130	-7452	-12371	-14848	-16449	-452
B11T	0	-914	-2012	-3750	-4594	-4979	-1253

TEST RESULTS

TEST 5	STRUCTURE 1	LOADCASE 3

See applied loads relative to this test in SECTION 3 Page 5 and the photograph of this structure showing rigging for Test 5 Run 1 in SECTION 5 Page 5 of this report.

RUN 1 - 10th October 2001

One hundred percent of the applied loads was held satisfactorily for 60 seconds.
No visual damage to the structure was detected after the test.

DEFLECTION READINGS

Transverse deflection readings taken in the centre at the tip of the earth peak **(A)** and at the joint between the body and the waist **(B)** . As well as, **Longitudinal** deflection readings taken at the tip of the cross ams , E1 **(C)** and E2 **(D)** , in millimeters , are tabulated below:

Loading Stage:	5,50%	25%	50%	75%	90%	100%	5,40%	RESIDUAL
TRANSVERSE (A)	0	10	20	30	40	50	0	0
TRANSVERSE (B)	0	10	20	20	20	20	0	0
LONGITUDINAL (C)	0	0	-30	-90	-100	-120	-80	-80
LONGITUDINAL (D)	0	0	30	90	100	120	80	80

ORIENTATION

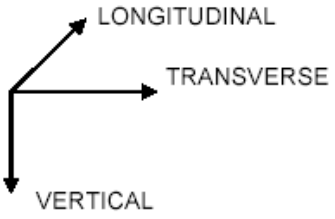

MEMBER FORCES RECORDED ON THE STRAIN GAUGES

Summary of the internal member forces monitored during the test.

Loading Stage:	5,50%	25%	50%	75%	90%	100%	5,40%
Strain Gauge ID:	Strain Gauge reading in (N)						
F2B	0	-5789	-10315	-20709	-24298	-24798	6612
P3L	0	-8754	-18025	-24986	-29854	-31102	1882
F4	0	-12747	-22435	-38351	-44760	-45269	9029
T11L	0	-3887	-10014	-18976	-23548	-24807	-1829
T12L	32	8089	16259	25144	31325	32986	1140
T13L	0	-6326	-12093	-18335	-23208	-24434	2043
B11L	0	2388	4735	6847	8514	8990	-534
T11T	0	-5449	-13826	-25036	-30153	-31507	5300
T12T	0	5302	11953	17637	20656	22540	-440
B11T	0	2414	3203	5118	6064	6481	-1035

TEST RESULTS

TEST 6	STRUCTURE 1	LOADCASE 3D

See applied loads relative to this test in SECTION 3 Page 6 and the photograph of this structure showing rigging for Test 6 Run 1 in SECTION 5 Page 6 of this report.

RUN 1 - 10th October 2001

One hundred percent of the applied loads was held satisfactorily for 60 seconds.
No visual damage to the structure was detected after the test.

DEFLECTION READINGS

Transverse deflection readings taken in the centre at the tip of the earth peak **(A)** and at the joint between the body and the waist **(B)** . As well as, **Longitudinal** deflection readings taken at the tip of the cross ams , E1 **(C)** and E2 **(D)** , in millimeters , are tabulated below:

Loading Stage:	5,90%	25%	50%	75%	90%	100%	5,30%	RESIDUAL
TRANSVERSE (A)	0	10	20	20	0	0	0	0
TRANSVERSE (B)	0	10	20	10	0	0	0	0
LONGITUDINAL (C)	0	0	20	20	20	20	0	0
LONGITUDINAL (D)	0	0	20	20	20	20	0	0

ORIENTATION

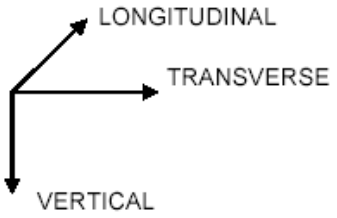

MEMBER FORCES RECORDED ON THE STRAIN GAUGES

Summary of the internal member forces monitored during the test.

Loading Stage:	5,90%	25%	50%	75%	90%	100%	5,30%
Strain Gauge ID:	Strain Gauge reading in (N)						
F2B	0	-15422	-36919	-60123	-72390	-80414	-5361
P3L	0	-2565	-6352	-11041	-15078	-17973	-3487
F4	0	-21467	-51987	-85360	-1E+05	-1E+05	-10610
T11L	0	-3406	-6480	-9385	-10390	-11179	-133
T12L	32	3487	7355	11666	13867	15525	783
T13L	0	-2680	-5970	-9506	-11319	-12669	-69
B11L	0	701	1764	3584	4981	5920	1589
T11T	0	-45	880	1106	1385	1186	1335
T12T	0	27	-800	-1965	-2503	-2794	-1904
B11T	0	282	264	15	-775	-1065	-1089

TEST RESULTS

TEST 7	STRUCTURE 1	LOADCASE 4

See applied loads relative to this test in SECTION 3 Page 7 and the photograph of this structure showing rigging for Test 7 Run 1 in SECTION 5 Page 7 of this report.

RUN 1 - 10th October 2001

One hundred percent of the applied loads was held satisfactorily for 60 seconds.
No visual damage to the structure was detected after the test.

DEFLECTION READINGS

Transverse deflection readings taken in the centre at the tip of the earth peak **(A)** and at the joint between the body and the waist **(B)** . As well as, **Longitudinal** deflection readings taken at the tip of the cross ams , E1 **(C)** and E2 **(D)** , in millimeters , are tabulated below:

Loading Stage:	5,30%	25%	50%	75%	90%	100%	4,70%	RESIDUAL
TRANSVERSE (A)	0	10	30	40	50	60	0	0
TRANSVERSE (B)	0	0	10	20	20	30	0	0
LONGITUDINAL (C)	0	0	30	50	60	90	20	20
LONGITUDINAL (D)	0	0	30	50	60	90	20	20

ORIENTATION

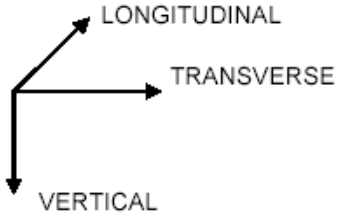

MEMBER FORCES RECORDED ON THE STRAIN GAUGES

Summary of the internal member forces monitored during the test.

Loading Stage:	5,30%	25%	50%	75%	90%	100%	4,70%
Strain Gauge ID:	Strain Gauge reading in (N)						
F2B	0	-28020	-57880	-90740	-1E+05	-1E+05	-270
P3L	0	-9917	-18683	-26140	-30713	-34304	165
F4	0	-34843	-67965	-1E+05	-1E+05	-1E+05	5314
T11L	0	-5924	-11121	-16456	-19600	-21777	505
T12L	32	8334	16026	23759	28159	31168	-192
T13L	0	-6747	-13125	-19695	-23417	-26050	1062
B11L	0	2651	5187	7325	8673	9632	-346
T11T	0	-7706	-17020	-27298	-33195	-37252	-266
T12T	0	4623	11297	18367	22588	25172	967
B11T	0	2195	3515	5563	6660	7408	77

TEST RESULTS

TEST 8	STRUCTURE 1	LOADCASE 4D

See applied loads relative to this test in SECTION 3 Page 8 and the photograph of this structure showing rigging for Test 8 Run 1 in SECTION 5 Page 8 of this report.

RUN 1 - 10th October 2001

One hundred percent of the applied loads was held satisfactorily for 60 seconds.
No visual damage to the structure was detected after the test.

DEFLECTION READINGS

Transverse deflection readings taken in the centre at the tip of the earth peak **(A)** and at the joint between the body and the waist **(B)** . As well as, **Longitudinal** deflection readings taken at the tip of the cross ams , E1 **(C)** and E2 **(D)** , in millimeters , are tabulated below:

Loading Stage:	######	25%	50%	75%	90%	100%	9,20%	RESIDUAL
TRANSVERSE (A)	0	10	20	30	40	50	0	0
TRANSVERSE (B)	0	10	20	30	30	40	0	0
LONGITUDINAL (C)	0	0	20	30	30	30	0	0
LONGITUDINAL (D)	0	0	20	30	30	30	0	0

ORIENTATION

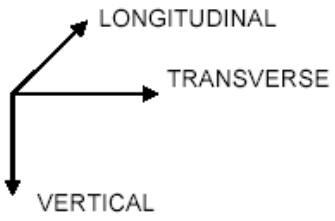

MEMBER FORCES RECORDED ON THE STRAIN GAUGES

Summary of the internal member forces monitored during the test.

Loading Stage:	######	25%	50%	75%	90%	100%	9,20%
Strain Gauge ID:	Strain Gauge reading in (N)						
F2B	0	-26091	-68465	-1E+05	-1E+05	-2E+05	-2842
P3L	0	-562	-2618	-8055	-10885	-13367	-1088
F4	0	-33985	-91262	-2E+05	-2E+05	-2E+05	-8253
T11L	0	-448	-2879	-5681	-7201	-7850	687
T12L	32	1598	3401	6536	8715	9985	-735
T13L	0	-1358	-3236	-6012	-8095	-9348	809
B11L	0	392	644	2001	3058	4211	-116
T11T	0	2032	5947	12691	17546	20292	-4347
T12T	0	-3366	-9324	-13532	-15985	-17572	-2227
B11T	0	-214	-410	-1789	-2884	-3847	932

TEST RESULTS

TEST 9	STRUCTURE 1	LOADCASE 4D - DESTRUCTION

See applied loads relative to this test in SECTION 3 Page 8 and the photograph of this structure showing rigging for Test 8 Run 1 in SECTION 5 Page 8 of this report.

RUN 1 - 10th October 2001

After successful completion of Test 8 , the same test was used to do a Destruction Test and the structure was again loaded up to 100% , then the loading targets were set to increase in increments of 5% beyond 100% until failure occurred.

Failure of the Left Cross Arm (C1) occurred at 101,4% of the applied load.

Unfortunately no photograph of this failure is available.

DEFLECTION READINGS

No deflection readings additional to the readings taken during the first loading could be taken.

MEMBER FORCES RECORDED ON THE STRAIN GAUGES

Summary of the internal member forces monitored during the test.

Loading Stage:	######	25%	50%	75%	90%	100%	######
Strain Gauge ID:	Strain Gauge reading in (N)						
F2B	0	n/a	-72438	-1E+05	-1E+05	-2E+05	-167194
P3L	0	n/a	-5658	-9159	-11098	-12619	-12809
F4	0	n/a	-96944	-2E+05	-2E+05	-2E+05	-225271
T11L	0	n/a	-4044	-6377	-7691	-8490	-15162
T12L	32	n/a	4873	7880	9584	10739	10719
T13L	0	n/a	-4599	-7429	-9133	-10408	-10471
B11L	0	n/a	1798	3123	3914	4531	5099
T11T	0	n/a	10950	17980	21948	24512	-18217
T12T	0	n/a	-6916	-11221	-13684	-15274	-15344
B11T	0	n/a	-2165	-3554	-4365	-4960	3365

B.2.2. PROTOTYPE 2 TEST REPORT

Technology Services International

LINE ENGINEERING SERVICES
TOWER TESTING STATION, ROSHERVILLE
JOHANNESBURG, GAUTENG PROVINCE
SOUTH AFRICA

TEST REPORT NUMBER :	SC 00 / 542
PROJECT NUMBER:	RO - 423

TOWER TYPE : " STRUCTURE 2 "

TOWER DETAIL : ABB DRAWINGS: (T - 47792 TRANSVERSAL FACE)
(T - 47793 LONGITUDINAL FACE)

MANUFACTURER : ABB Asea Brown Boveri

CLIENT : CIGRÉ

PROJECT: WORKING GROUP 08 - TASK FORCE 4
INFLUENCE OF HYPERSTATIC MODELLING

CONSULTANT : CIGRÉ

TABLE OF CONTENTS

1 . INTRODUCTION

ALL TESTS WERE :

(a) In accordance with the Contract , the Test Schedules SC 00 / 542 and our General Conditions of Test (Annexure " A ").

(b) Reported in chronological order in which they were performed .

(c) Conducted by : Mr JA Meintjes & Mr DL Stevens.

(d) Witnessed by :

Joao Batista Ferreira	~	ABB
David Hughes	~	PB Power
Leon Kempner	~	BPA
Ruy C. Menezes	~	UFRGS / Engelieas - Brazil
S. Kitipornchai	~	Citi Uni - Hong Kong
Geir Nesgaard	~	Norconsult
J. Diez-Serrano	~	Eskom Enterprises TSI
Pierre Dalleves	~	Energie Quest Suisse
Fabiana Camcugo	~	UFRGS / Engelieas - Brazil
Rania Peixoto	~	ABB Ltda
S.J. Madibu	~	Eskom Enterprises TSI
Mark Newby	~	Eskom Enterprises TSI
Dan Dukhan	~	Eskom

TEST SCHEDULES

TEST SEQUENCE : 1, 2, 3, 4, 5, 6, 7, 8.

REVISION 2 8th Oct 2001

CALCULATION OF TEST LOADS AND ANGLES

TOWER TYPE : **" CIGRE "** " HYPOSTATIC MODELLING INFLUEN SELF SUPPORTING STRUCTURE	TEST NUMBER ONE	***LOAD CONDITION :*** **1** *VERTICAL LOADING*

ATT POINT	V VERT	H TRANS	H LONG	LOAD CELL	Vr (kN.)	Vr 1 (kN.)	Vr 2 (kN.)	h (m)	R (kN.)	ANGLE DEG	MASS (kg)
C2V	49,05			120~2	0,20				48,85		

NOTES : **(g = 9.80665)**

1) LOADS IN KILONEWTONS EXCEPT FOR MASS WHICH HAS BEEN CONVERTED TO KILOGRAM
2) ANGLES ARE IN DEGREES , NEGATIVE ANGLES SLOPE ABOVE HORIZONTAL FROM TOWER

TEST SEQUENCE : 1, 2, 3, 4, 5, 6, 7, 8.

REVISION 2 8th Oct 2001

CALCULATION OF TEST LOADS AND ANGLES

TOWER TYPE : " CIGRE " " HYPOSTATIC MODELLING INFLUEN SELF SUPPORTING STRUCTURE	TEST NUMBER TWO	***LOAD CONDITION :*** 1D *VERTICAL LOADING*

ATT POINT	V VERT	H TRANS	H LONG	LOAD CELL	Vr (kN.)	Vr 1 (kN.)	Vr 2 (kN.)	h (m)	R (kN.)	ANGLE DEG	MASS (kg)
C1V	49,05			120~1	0,20				48,85		
C2V	49,05			120~2	0,20				48,85		

NOTES : **(g = 9.80665)**

1) LOADS IN KILONEWTONS EXCEPT FOR MASS WHICH HAS BEEN CONVERTED TO KILOGRAM
2) ANGLES ARE IN DEGREES , NEGATIVE ANGLES SLOPE ABOVE HORIZONTAL FROM TOWER

REVISION 2 8th Oct 2001

CALCULATION OF TEST LOADS AND ANGLES

TOWER TYPE : " CIGRE "
" HYPOSTATIC MODELLING INFLUEN-
SELF SUPPORTING STRUCTURE

TEST NUMBER THREE

LOAD CONDITION : 2

TRANSVERSE LOADING

ATT POINT	V VERT	H TRANS	H LONG	LOAD CELL	Vr (kN.)	Vr 1 (kN.)	Vr 2 (kN.)	h (m)	R (kN.)	ANGLE DEG	MASS (kg)
C2T		49,05		120~2	0,20	0,70		-0,80	49,05	-0,82	

NOTES : **(g = 9.80665)**

1) LOADS IN KILONEWTONS EXCEPT FOR MASS WHICH HAS BEEN CONVERTED TO KILOGRAM
2) ANGLES ARE IN DEGREES , NEGATIVE ANGLES SLOPE ABOVE HORIZONTAL FROM TOWER

TEST SEQUENCE : 1, 2, 3, 4, 5, 6, 7, 8.

REVISION 2 8th Oct 2001

CALCULATION OF TEST LOADS AND ANGLES

TOWER TYPE : " CIGRE " " HYPOSTATIC MODELLING INFLUEN SELF SUPPORTING STRUCTURE	TEST NUMBER FOUR	***LOAD CONDITION :*** 2D *TRANSVERSE LOADING*

ATT POINT	V VERT	H TRANS	H LONG	LOAD CELL	Vr (kN.)	Vr 1 (kN.)	Vr 2 (kN.)	h (m)	R (kN.)	ANGLE DEG	MASS (kg)
C1T		49,05		120~1	0,20	0,76		-0,98	49,05	-0,89	
C2T		49,05		120~2	0,20	0,70		-0,80	49,05	-0,82	

NOTES : **(g = 9.80665)**

1) LOADS IN KILONEWTONS EXCEPT FOR MASS WHICH HAS BEEN CONVERTED TO KILOGRAM

2) ANGLES ARE IN DEGREES , NEGATIVE ANGLES SLOPE ABOVE HORIZONTAL FROM TOWER

TEST SEQUENCE : 1, 2, 3, 4, 5, 6, 7, 8.

REVISION 2 8th Oct 2001

CALCULATION OF TEST LOADS AND ANGLES

TOWER TYPE : **" CIGRE "**
" HYPOSTATIC MODELLING INFLUEN
SELF SUPPORTING STRUCTURE

TEST NUMBER FIVE

LOAD CONDITION : **3**
LONGITUDINAL LOADING

ATT POINT	V VERT	H TRANS	H LONG	LOAD CELL	Vr (kN.)	Vr 1 (kN.)	Vr 2 (kN.)	h (m)	R (kN.)	ANGLE DEG	MASS (kg)
C2L			49,05	120~4	0,20	0,74		-0,91	49,05	-0,86	

NOTES : **(g = 9.80665)**

1) LOADS IN KILONEWTONS EXCEPT FOR MASS WHICH HAS BEEN CONVERTED TO KILOGRAM
2) ANGLES ARE IN DEGREES , NEGATIVE ANGLES SLOPE ABOVE HORIZONTAL FROM TOWER

REVISION 2 8th Oct 2001

CALCULATION OF TEST LOADS AND ANGLES

TOWER TYPE : " CIGRE "
" HYPOSTATIC MODELLING INFLUEN
SELF SUPPORTING STRUCTURE

TEST NUMBER SIX

LOAD CONDITION : 3D

LONGITUDINAL LOADING

ATT POINT	V VERT	H TRANS	H LONG	LOAD CELL	Vr (kN.)	Vr 1 (kN.)	Vr 2 (kN.)	h (m)	R (kN.)	ANGLE DEG	MASS (kg)
C1L			49,05	120~3	0,20	0,74		-0,91	49,05	-0,86	
C2L			49,05	120~4	0,20	0,74		-0,91	49,05	-0,86	

NOTES : **(g = 9.80665)**

1) LOADS IN KILONEWTONS EXCEPT FOR MASS WHICH HAS BEEN CONVERTED TO KILOGRAM
2) ANGLES ARE IN DEGREES , NEGATIVE ANGLES SLOPE ABOVE HORIZONTAL FROM TOWER

REVISION 2 8th Oct 2001

CALCULATION OF TEST LOADS AND ANGLES

TOWER TYPE : " CIGRE " " HYPOSTATIC MODELLING INFLUEN SELF SUPPORTING STRUCTURE	TEST NUMBER SEVEN	*LOAD CONDITION :* 4 *VERTICAL LOADING, TRANSVERSE AND LONGITUDINAL LOADING*

ATT POINT	V VERT	H TRANS	H LONG	LOAD CELL	Vr (kN.)	Vr 1 (kN.)	Vr 2 (kN.)	h (m)	R (kN.)	ANGLE DEG	MASS (kg)
C2T	49,05	49,05		120~2	0,20	0,20			69,23	44,88	
C2L			49,05	120~4	0,20	0,74		-0,91	49,05	-0,86	

NOTES : **(g = 9.80665)**

1) LOADS IN KILONEWTONS EXCEPT FOR MASS WHICH HAS BEEN CONVERTED TO KILOGRAM
2) ANGLES ARE IN DEGREES , NEGATIVE ANGLES SLOPE ABOVE HORIZONTAL FROM TOWER
3) WHERE HORIZONTAL AND VERTICAL LOADS ARE COMBINED , ANGLE CONTROL IS EMPLOYED .

REVISION 2 8th Oct 2001

CALCULATION OF TEST LOADS AND ANGLES

TOWER TYPE : **" CIGRE "**
" HYPOSTATIC MODELLING INFLUEN
SELF SUPPORTING STRUCTURE

TEST NUMBER
EIGHT

LOAD CONDITION : **4D**
VERTICAL LOADING, TRANSVERSE AND LONGITUDINAL LOADING

ATT POINT	V VERT	H TRANS	H LONG	LOAD CELL	Vr (kN.)	Vr 1 (kN.)	Vr 2 (kN.)	h (m)	R (kN.)	ANGLE DEG	MASS (kg)
C1T	49,05	49,05		120~1	0,20	0,20			69,23	44,88	
C2T	49,05	49,05		120~2	0,20	0,20			69,23	44,88	
C1L			49,05	120~3	0,20	0,74		-0,91	49,05	-0,86	
C2L			49,05	120~4	0,20	0,74		-0,91	49,05	-0,86	

NOTES : **(g = 9.80665)**

1) LOADS IN KILONEWTONS EXCEPT FOR MASS WHICH HAS BEEN CONVERTED TO KILOGRAM
2) ANGLES ARE IN DEGREES , NEGATIVE ANGLES SLOPE ABOVE HORIZONTAL FROM TOWER
3) WHERE HORIZONTAL AND VERTICAL LOADS ARE COMBINED , ANGLE CONTROL IS EMPLOYED .

TEST RESULTS

TEST 1	STRUCTURE 2	LOADCASE 1

See applied loads relative to this test in SECTION 3 Page 1 and the photograph of this structure showing rigging for Test 1 Run 2 in SECTION 5 Page 1 of this report.

RUN 2 - 15th October 2001

One hundred percent of the applied loads was held satisfactorily for 60 seconds.
No visual damage to the structure was detected after the test.

DEFLECTION READINGS

Transverse deflection readings taken in the centre at the tip of the earth peak **(A)** and at the joint between the body and the waist **(B)** . As well as, **Longitudinal** deflection readings taken at the tip of the cross ams , E1 **(C)** and E2 **(D)** , in millimeters , are tabulated below:

Loading Stage:	0,40%	25%	50%	75%	90%	100%	0,40%	RESIDUAL
TRANSVERSE (A)	0	10	15	20	30	40	0	0
TRANSVERSE (B)	0	0	0	0	0	0	0	0
LONGITUDINAL (C)	0	0	0	0	0	0	0	0
LONGITUDINAL (D)	0	0	0	0	0	0	0	0

ORIENTATION

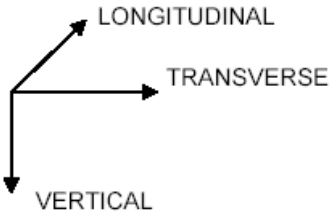

MEMBER FORCES RECORDED ON THE STRAIN GAUGES

Summary of the internal member forces monitored during the test.

Loading Stage:	0,40%	25%	50%	75%	90%	100%	0,40%
Strain Gauge ID:	Strain Gauge reading in (N)						
F2B	0	-15644	-30978	-44849	-53854	-59777	-1946
P3L	0	219	463	957	1235	1095	-752
F4	0	-8384	-17540	-26352	-31546	-34507	1322
T11L	0	-2952	-5673	-8304	-10269	-12950	-3637
T12L	32	924	1526	2176	3336	4837	3280
T13L	0	213	-4	-451	-1150	-2256	-1781
B11L	0	-1294	-2465	-3601	-4209	-4294	904
T11T	0	-178	-809	-2267	-3986	-6236	-4285
T12T	0	-2393	-4414	-5950	-6535	-5994	-2242
B11T	0	-1151	-1957	-2056	-1806	-1325	2548

TEST RESULTS

TEST 2	STRUCTURE 2	LOADCASE 1D

See applied loads relative to this test in SECTION 3 Page 2 and the photograph of this structure showing rigging for Test 2 Run 2 in SECTION 5 Page 2 of this report.

RUN 2 - 15th October 2001

One hundred percent of the applied loads was held satisfactorily for 60 seconds.
No visual damage to the structure was detected after the test.

DEFLECTION READINGS

Transverse deflection readings taken in the centre at the tip of the earth peak **(A)** and at the joint between the body and the waist **(B)** . As well as, **Longitudinal** deflection readings taken at the tip of the cross ams , E1 **(C)** and E2 **(D)** , in millimeters , are tabulated below:

Loading Stage:	1,20%	25%	50%	75%	90%	100%	1,15%	RESIDUAL
TRANSVERSE (A)	0	0	0	0	0	0	0	0
TRANSVERSE (B)	0	0	0	0	0	0	0	0
LONGITUDINAL (C)	0	0	0	0	0	0	0	0
LONGITUDINAL (D)	0	0	0	0	0	0	0	0

ORIENTATION

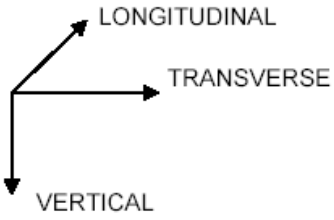

MEMBER FORCES RECORDED ON THE STRAIN GAUGES

Summary of the internal member forces monitored during the test.

Loading Stage:	1,20%	25%	50%	75%	90%	100%	1,15%
Strain Gauge ID:	Strain Gauge reading in (N)						
F2B	0	-5328	-10535	-16974	-20253	-22907	1290
P3L	0	-476	-788	-1090	-1176	-1245	478
F4	0	-5096	-10892	-16786	-19759	-22007	-166
T11L	0	258	663	625	747	690	819
T12L	32	23	-183	-68	107	213	-368
T13L	0	-267	-698	-924	-1196	-1246	-167
B11L	0	-600	-960	-1589	-1891	-2131	281
T11T	0	-394	-1037	-1444	-1651	-1721	-40
T12T	0	354	837	932	906	889	76
B11T	0	-698	-1198	-1848	-2181	-2452	-14

TEST RESULTS

TEST 3	STRUCTURE 2	LOADCASE 2

See applied loads relative to this test in SECTION 3 Page 3 and the photograph of this structure showing rigging for Test 3 Run 2 in SECTION 5 Page 3 of this report.

RUN 2 - 15th October 2001

One hundred percent of the applied loads was held satisfactorily for 60 seconds.
No visual damage to the structure was detected after the test.

DEFLECTION READINGS

Transverse deflection readings taken in the centre at the tip of the earth peak **(A)** and at the joint between the body and the waist **(B)** . As well as, **Longitudinal** deflection readings taken at the tip of the cross ams , E1 **(C)** and E2 **(D)** , in millimeters , are tabulated below:

Loading Stage:	3,20%	25%	50%	75%	90%	100%	3,40%	RESIDUAL
TRANSVERSE (A)	0	0	10	20	30	40	0	0
TRANSVERSE (B)	0	0	0	20	20	30	0	0
LONGITUDINAL (C)	0	0	0	0	0	0	0	0
LONGITUDINAL (D)	0	0	0	0	0	0	0	0

ORIENTATION

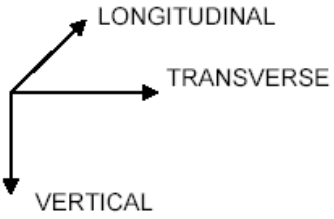

MEMBER FORCES RECORDED ON THE STRAIN GAUGES

Summary of the internal member forces monitored during the test.

Loading Stage:	3,20%	25%	50%	75%	90%	100%	3,40%
Strain Gauge ID:	Strain Gauge reading in (N)						
F2B	0	-9506	-20518	-31521	-37347	-40215	-372
P3L	0	501	674	932	931	1294	-1649
F4	0	-12032	-25975	-41078	-50253	-54771	-5505
T11L	0	2346	5132	8912	11684	13467	4148
T12L	32	391	724	834	881	1167	160
T13L	0	-281	-653	-1272	-1372	-1456	-363
B11L	0	-1321	-2670	-3820	-4440	-4826	1124
T11T	0	-186	-582	-754	-699	-741	15
T12T	0	1911	3682	5025	5124	5121	-2800
B11T	0	392	834	1260	2269	2366	953

TEST RESULTS

TEST 4	STRUCTURE 2	LOADCASE 2D

See applied loads relative to this test in SECTION 3 Page 4 and the photograph of this structure showing rigging for Test 4 Run 2 in SECTION 5 Page 4 of this report.

RUN 2 - 15th October 2001

One hundred percent of the applied loads was held satisfactorily for 60 seconds.
No visual damage to the structure was detected after the test.

DEFLECTION READINGS

Transverse deflection readings taken in the centre at the tip of the earth peak **(A)** and at the joint between the body and the waist **(B)** . As well as, **Longitudinal** deflection readings taken at the tip of the cross ams , E1 **(C)** and E2 **(D)** , in millimeters , are tabulated below:

Loading Stage:	6,60%	25%	50%	75%	90%	100%	5,80%	RESIDUAL
TRANSVERSE (A)	0	10	20	50	60	70	20	20
TRANSVERSE (B)	0	0	10	30	40	50	20	20
LONGITUDINAL (C)	0	0	0	0	0	0	0	0
LONGITUDINAL (D)	0	0	0	0	0	0	0	0

ORIENTATION

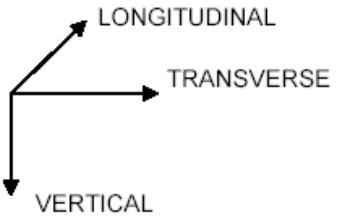

MEMBER FORCES RECORDED ON THE STRAIN GAUGES

Summary of the internal member forces monitored during the test.

Loading Stage:	6,60%	25%	50%	75%	90%	100%	5,80%
Strain Gauge ID:	Strain Gauge reading in (N)						
F2B	0	-16442	-36017	-57786	-66750	-67103	7549
P3L	0	1368	2517	10498	13994	14732	5607
F4	0	-20836	-45584	-73931	-86088	-89645	6356
T11L	0	3751	8778	12868	16715	21556	1971
T12L	32	337	947	1694	2487	3105	900
T13L	0	-663	-1079	-1606	-835	-1416	1152
B11L	0	-2429	-5426	-8434	-9489	-10500	1016
T11T	0	-523	-987	-1754	-1570	-1459	719
T12T	0	3329	6942	11923	13856	12482	-1265
B11T	0	615	1520	5859	7522	9548	6009

TEST RESULTS

TEST 5	STRUCTURE 2	LOADCASE 3

See applied loads relative to this test in SECTION 3 Page 5 and the photograph of this structure showing rigging for Test 5 Run 2 in SECTION 5 Page 5 of this report.

RUN 2 - 15th October 2001

One hundred percent of the applied loads was held satisfactorily for 60 seconds.
No visual damage to the structure was detected after the test.

DEFLECTION READINGS

Transverse deflection readings taken in the centre at the tip of the earth peak **(A)** and at the joint between the body and the waist **(B)** . As well as, **Longitudinal** deflection readings taken at the tip of the cross ams , E1 **(C)** and E2 **(D)** , in millimeters , are tabulated below:

Loading Stage:	6,00%	25%	50%	75%	90%	100%	5,20%	RESIDUAL
TRANSVERSE (A)	0	10	10	20	20	20	0	0
TRANSVERSE (B)	0	10	10	20	20	20	0	0
LONGITUDINAL (C)	0	0	-20	-50	-70	-80	-60	-60
LONGITUDINAL (D)	0	0	50	80	100	110	70	70

ORIENTATION

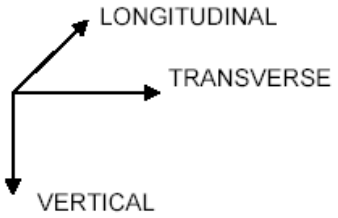

MEMBER FORCES RECORDED ON THE STRAIN GAUGES

Summary of the internal member forces monitored during the test.

Loading Stage:	6,00%	25%	50%	75%	90%	100%	5,20%
Strain Gauge ID:	Strain Gauge reading in (N)						
F2B	0	-8781	-19643	-29775	-35831	-39717	-2529
P3L	0	4608	9868	13469	14394	14606	-3901
F4	0	-12664	-28255	-43860	-54766	-60829	-7332
T11L	0	-6259	-12237	-20962	-26987	-31225	-2976
T12L	32	-6738	-18833	-29887	-36834	-40041	-7485
T13L	0	-6415	-12975	-18082	-21286	-24157	3499
B11L	0	3695	3110	7586	10838	13555	1820
T11T	0	-7776	-11663	-19141	-23186	-2746	10639
T12T	0	-4020	-11991	-17644	-20538	-22553	0
B11T	0	-2503	-5898	-9296	-11064	-12263	-1480

TEST RESULTS

TEST 6	STRUCTURE 2	LOADCASE 3D

See applied loads relative to this test in SECTION 3 Page 6 and the photograph of this structure showing rigging for Test 6 Run 2 in SECTION 5 Page 6 of this report.

RUN 2 - 15th October 2001

One hundred percent of the applied loads was held satisfactorily for 60 seconds.
No visual damage to the structure was detected after the test.

DEFLECTION READINGS

Transverse deflection readings taken in the centre at the tip of the earth peak **(A)** and at the joint between the body and the waist **(B)** . As well as, **Longitudinal** deflection readings taken at the tip of the cross ams , E1 **(C)** and E2 **(D)** , in millimeters , are tabulated below:

Loading Stage:	5,60%	25%	50%	75%	90%	100%	5,00%	RESIDUAL
TRANSVERSE (A)	0	0	0	10	20	20	20	20
TRANSVERSE (B)	0	0	0	0	10	10	10	10
LONGITUDINAL (C)	0	0	0	20	30	40	0	0
LONGITUDINAL (D)	0	0	0	20	30	40	0	0

ORIENTATION

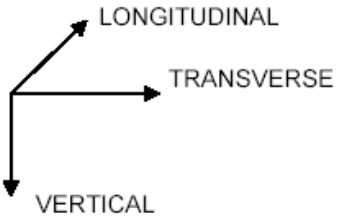

MEMBER FORCES RECORDED ON THE STRAIN GAUGES

Summary of the internal member forces monitored during the test.

Loading Stage:	5,60%	25%	50%	75%	90%	100%	5,00%
Strain Gauge ID:	Strain Gauge reading in (N)						
F2B	0	-17321	-38090	-59915	-73521	-82674	-3127
P3L	0	-1941	-3396	-6694	-13773	-17958	-3752
F4	0	-21635	-47879	-78456	-96113	-1E+05	-6537
T11L	0	-409	-841	-1470	-1852	-2414	-900
T12L	32	-3151	-6926	-9592	-11728	-12898	1367
T13L	0	-2746	-5913	-9728	-11863	-13108	-1125
B11L	0	1100	2440	10352	13322	14178	8320
T11T	0	-3777	-8466	-13582	-16551	-18685	-1455
T12T	0	220	517	648	511	876	238
B11T	0	-2734	-6010	-8862	-11546	-12888	-92

TEST RESULTS

TEST 7	STRUCTURE 2	LOADCASE 4

See applied loads relative to this test in SECTION 3 Page 7 and the photograph of this structure showing rigging for Test 7 Run 2 in SECTION 5 Page 7 of this report.

RUN 2 - 15th October 2001

One hundred percent of the applied loads was held satisfactorily for 60 seconds.
No visual damage to the structure was detected after the test.

DEFLECTION READINGS

Transverse deflection readings taken in the centre at the tip of the earth peak **(A)** and at the joint between the body and the waist **(B)** . As well as, **Longitudinal** deflection readings taken at the tip of the cross ams , E1 **(C)** and E2 **(D)** , in millimeters , are tabulated below:

Loading Stage:	5,40%	25%	50%	75%	90%	100%	4,60%	RESIDUAL
TRANSVERSE (A)	0	0	10	20	40	50	0	0
TRANSVERSE (B)	0	0	10	20	20	30	0	0
LONGITUDINAL (C)	0	0	0	20	30	50	0	0
LONGITUDINAL (D)	0	0	0	20	30	50	0	0

ORIENTATION

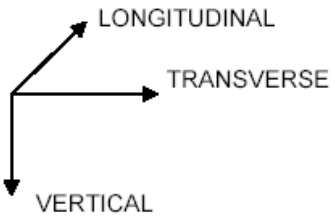

MEMBER FORCES RECORDED ON THE STRAIN GAUGES

Summary of the internal member forces monitored during the test.

Loading Stage:	5,40%	25%	50%	75%	90%	100%	4,60%
Strain Gauge ID:	Strain Gauge reading in (N)						
F2B	0	-32997	-63896	-1E+05	-1E+05	-1E+05	-6077
P3L	0	4562	7605	11487	13677	16471	348
F4	0	-33439	-64817	-97191	-1E+05	-1E+05	7378
T11L	0	-6327	-12579	-22544	-27790	-30673	-2266
T12L	32	-6419	-14214	-19852	-23834	-25480	3299
T13L	0	-7144	-14368	-21933	-25840	-28458	-157
B11L	0	202	1039	1313	645	42	-2537
T11T	0	-9714	-20152	-31128	-37497	-43019	-2933
T12T	0	-4880	-10156	-14352	-17542	-20394	1078
B11T	0	-3157	-9063	-15488	-18344	-20219	-7095

TEST RESULTS

TEST 8	STRUCTURE 2	LOADCASE 4D

See applied loads relative to this test in SECTION 3 Page 8 and the photograph of this structure showing rigging for Test 8 Run 2 in SECTION 5 Page 8 of this report.

RUN 2 - 15th October 2001

One hundred percent of the applied loads was held satisfactorily for 60 seconds.
No visual damage to the structure was detected after the test.

DEFLECTION READINGS

Transverse deflection readings taken in the centre at the tip of the earth peak **(A)** and at the joint between the body and the waist **(B)** . As well as, **Longitudinal** deflection readings taken at the tip of the cross ams , E1 **(C)** and E2 **(D)** , in millimeters , are tabulated below:

Loading Stage:	10,60%	25%	50%	75%	90%	100%	10,00%	RESIDUAL
TRANSVERSE (A)	0	10	30	40	50	60	0	0
TRANSVERSE (B)	0	10	20	30	40	50	0	0
LONGITUDINAL (C)	0	0	20	30	50	80	50	50
LONGITUDINAL (D)	0	0	20	50	70	80	60	60

ORIENTATION

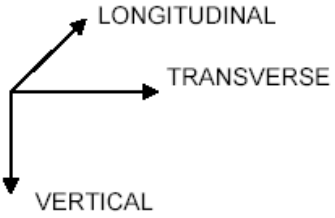

MEMBER FORCES RECORDED ON THE STRAIN GAUGES

Summary of the internal member forces monitored during the test.

Loading Stage:	10,60%	25%	50%	75%	90%	100%	10,00%
Strain Gauge ID:	Strain Gauge reading in (N)						
F2B	0	-26502	-66574	-1E+05	-1E+05	-2E+05	12724
P3L	0	-2140	-4108	-6804	-6258	-6794	-973
F4	0	-34280	-86711	-1E+05	-2E+05	-2E+05	10033
T11L	0	2748	7382	13762	19025	20189	4795
T12L	32	-1801	-3890	-6374	-8137	-8730	1576
T13L	0	-2199	-5660	-8707	-10569	-11473	1469
B11L	0	-1091	-3633	-6793	-9935	-10696	-730
T11T	0	-2959	-7877	-13259	-16487	-18438	-41
T12T	0	2344	5214	7916	9265	10208	-2703
B11T	0	1320	3182	507	-1177	-3895	7555

TEST RESULTS

TEST 9	STRUCTURE 2	LOADCASE 4D - DESTRUCTION

See applied loads relative to this test in SECTION 3 Page 8 and the photograph of this structure showing rigging for Test 8 Run 2 in SECTION 5 Page 8 of this report.

RUN 2 - 15th October 2001

After successful completion of Test 8 , the same test was used to do a Destruction Test and the structure was again loaded up to 100% , then the loading targets were set to increase in increments of 5% beyond 100% until failure occurred.

Failure of the Left Cross Arm (C1) occurred at 107,3% of the applied load.

Unfortunately no photograph of this failure is available.

DEFLECTION READINGS

At 105% of the applied load there was an additional 10mm deflection on all four the deflection scales compared to the previous 100% load application.

MEMBER FORCES RECORDED ON THE STRAIN GAUGES

Summary of the internal member forces monitored during the test.

Loading Stage:	10,50%	25%	50%	75%	90%	100%	105%	107,30%
Strain Gauge ID:	Strain Gauge reading in (N)							
F2B	0	n/a	-72454	-1E+05	-1E+05	-2E+05	-176765	-181035
P3L	0	n/a	-2479	-3919	-4950	-5670	-6068	-6188
F4	0	n/a	-88334	-1E+05	-2E+05	-2E+05	-215410	-219233
T11L	0	n/a	6794	11803	14072	15600	16034	15854
T12L	32	n/a	-4692	-7729	-9382	-10456	-10598	-10424
T13L	0	n/a	-5667	-9458	-11488	-12764	-13253	-13237
B11L	0	n/a	-4171	-7003	-8488	-9377	-10079	-10406
T11T	0	n/a	-8312	-13779	-16802	-18806	-19473	-19546
T12T	0	n/a	5671	8819	11120	12495	12815	12704
B11T	0	n/a	-5744	-9184	-11011	-12216	-13318	-13876

B.2.3. PROTOTYPE 2A TEST REPORT

LINE ENGINEERING SERVICES
TOWER TESTING STATION, ROSHERVILLE
JOHANNESBURG, GAUTENG PROVINCE
SOUTH AFRICA

TEST REPORT NUMBER :	**SC 00 / 542**
PROJECT NUMBER:	**RO - 423**

TOWER TYPE :	" STRUCTURE 2A "	
TOWER DETAIL :	ABB DRAWINGS:	(T - 47797 TRANSVERSAL FACE) (T - 47798 LONGITUDINAL FACE)
MANUFACTURER :	ABB Asea Brown Boveri	
CLIENT :	CIGRÉ	
PROJECT:	WORKING GROUP 08 - TASK FORCE 4 INFLUENCE OF HYPERSTATIC MODELLING	
CONSULTANT :	CIGRÉ	

TABLE OF CONTENTS

1 . INTRODUCTION

ALL TESTS WERE :

(a) In accordance with the Contract , the Test Schedules SC 00 / 542 and our General Conditions of Test (Annexure " A ").

(b) Reported in chronological order in which they were performed .

(c) Conducted by : Mr JA Meintjes & Mr DL Stevens.

(d) Witnessed by :

Joao Batista Ferreira	~	ABB
David Hughes	~	PB Power
Leon Kempner	~	BPA
Ruy C. Menezes	~	UFRGS / Engelieas - Brazil
S. Kitipornchai	~	Citi Uni - Hong Kong
Geir Nesgaard	~	Norconsult
J. Diez-Serrano	~	Eskom Enterprises TSI
Pierre Dalleves	~	Energie Quest Suisse
Fabiana Camcugo	~	UFRGS / Engelieas - Brazil
Rania Peixoto	~	ABB Ltda
S.J. Madibu	~	Eskom Enterprises TSI
Mark Newby	~	Eskom Enterprises TSI
Dan Dukhan	~	Eskom

TEST SCHEDULES

TEST SEQUENCE : 1, 2, 3, 4, 5, 6, 7, 8.

REVISION 2 8th Oct 2001

CALCULATION OF TEST LOADS AND ANGLES

TOWER TYPE : **" CIGRE "**
" HYPOSTATIC MODELLING INFLUEN
SELF SUPPORTING STRUCTURE

TEST NUMBER ONE

LOAD CONDITION : 1

VERTICAL LOADING

ATT POINT	V VERT	H TRANS	H LONG	LOAD CELL	Vr (kN.)	Vr 1 (kN.)	Vr 2 (kN.)	h (m)	R (kN.)	ANGLE DEG	MASS (kg)
C2V	49,05			120~2	0,20				48,85		

NOTES : **(g = 9.80665)**

1) LOADS IN KILONEWTONS EXCEPT FOR MASS WHICH HAS BEEN CONVERTED TO KILOGRAM
2) ANGLES ARE IN DEGREES , NEGATIVE ANGLES SLOPE ABOVE HORIZONTAL FROM TOWER

TEST SEQUENCE : *1, 2, 3, 4, 5, 6, 7, 8.*

REVISION 2 8th Oct 2001

CALCULATION OF TEST LOADS AND ANGLES

TOWER TYPE : " CIGRE "
" HYPOSTATIC MODELLING INFLUEN
SELF SUPPORTING STRUCTURE

TEST NUMBER TWO

LOAD CONDITION : 1D

VERTICAL LOADING

ATT POINT	V VERT	H TRANS	H LONG	LOAD CELL	Vr (kN.)	Vr 1 (kN.)	Vr 2 (kN.)	h (m)	R (kN.)	ANGLE DEG	MASS (kg)
C1V	49,05			120~1	0,20				48,85		
C2V	49,05			120~2	0,20				48,85		

NOTES : **(g = 9.80665)**

1) LOADS IN KILONEWTONS EXCEPT FOR MASS WHICH HAS BEEN CONVERTED TO KILOGRAM
2) ANGLES ARE IN DEGREES , NEGATIVE ANGLES SLOPE ABOVE HORIZONTAL FROM TOWER

TEST SEQUENCE : 1, 2, 3, 4, 5, 6, 7, 8.

REVISION 2 8th Oct 2001

CALCULATION OF TEST LOADS AND ANGLES

TOWER TYPE : " CIGRE " " HYPOSTATIC MODELLING INFLUEN SELF SUPPORTING STRUCTURE	TEST NUMBER THREE	*LOAD CONDITION :* 2 *TRANSVERSE LOADING*

ATT POINT	V VERT	H TRANS	H LONG	LOAD CELL	Vr (kN.)	Vr 1 (kN.)	Vr 2 (kN.)	h (m)	R (kN.)	ANGLE DEG	MASS (kg)
C2T		49,05		120~2	0,20	0,70		-0,80	49,05	-0,82	

NOTES : (g = 9.80665)

1) LOADS IN KILONEWTONS EXCEPT FOR MASS WHICH HAS BEEN CONVERTED TO KILOGRAM
2) ANGLES ARE IN DEGREES , NEGATIVE ANGLES SLOPE ABOVE HORIZONTAL FROM TOWER

REVISION 2 8th Oct 2001

CALCULATION OF TEST LOADS AND ANGLES

TOWER TYPE : " CIGRE " " HYPOSTATIC MODELLING INFLUENC SELF SUPPORTING STRUCTURE	TEST NUMBER FOUR	*LOAD CONDITION :* 2D *TRANSVERSE LOADING*

ATT POINT	V VERT	H TRANS	H LONG	LOAD CELL	Vr (kN.)	Vr 1 (kN.)	Vr 2 (kN.)	h (m)	R (kN.)	ANGLE DEG	MASS (kg)
C1T		49,05		120~1	0,20	0,76		-0,98	49,05	-0,89	
C2T		49,05		120~2	0,20	0,70		-0,80	49,05	-0,82	

NOTES : **(g = 9.80665)**

1) LOADS IN KILONEWTONS EXCEPT FOR MASS WHICH HAS BEEN CONVERTED TO KILOGRAM
2) ANGLES ARE IN DEGREES , NEGATIVE ANGLES SLOPE ABOVE HORIZONTAL FROM TOWER

REVISION 2 8th Oct 2001

CALCULATION OF TEST LOADS AND ANGLES

TOWER TYPE : " CIGRE " " HYPOSTATIC MODELLING INFLUEN SELF SUPPORTING STRUCTURE	TEST NUMBER FIVE	*LOAD CONDITION :* 3 *LONGITUDINAL LOADING*

ATT POINT	V VERT	H TRANS	H LONG	LOAD CELL	Vr (kN.)	Vr 1 (kN.)	Vr 2 (kN.)	h (m)	R (kN.)	ANGLE DEG	MASS (kg)
C2L			49,05	120~4	0,20	0,74		-0,91	49,05	-0,86	

NOTES : (g = 9.80665)

1) LOADS IN KILONEWTONS EXCEPT FOR MASS WHICH HAS BEEN CONVERTED TO KILOGRAM
2) ANGLES ARE IN DEGREES , NEGATIVE ANGLES SLOPE ABOVE HORIZONTAL FROM TOWER

REVISION 2 8th Oct 2001

CALCULATION OF TEST LOADS AND ANGLES

TOWER TYPE : " CIGRE "
" HYPOSTATIC MODELLING INFLUEN
SELF SUPPORTING STRUCTURE

TEST NUMBER SIX

LOAD CONDITION : 3D

LONGITUDINAL LOADING

ATT POINT	V VERT	H TRANS	H LONG	LOAD CELL	Vr (kN.)	Vr 1 (kN.)	Vr 2 (kN.)	h (m)	R (kN.)	ANGLE DEG	MASS (kg)
C1L			49,05	120~3	0,20	0,74		-0,91	49,05	-0,86	
C2L			49,05	120~4	0,20	0,74		-0,91	49,05	-0,86	

NOTES : (g = 9.80665)

1) LOADS IN KILONEWTONS EXCEPT FOR MASS WHICH HAS BEEN CONVERTED TO KILOGRAM
2) ANGLES ARE IN DEGREES , NEGATIVE ANGLES SLOPE ABOVE HORIZONTAL FROM TOWER

REVISION 2 8th Oct 2001

CALCULATION OF TEST LOADS AND ANGLES

TOWER TYPE : " CIGRE "
" HYPOSTATIC MODELLING INFLUEN
SELF SUPPORTING STRUCTURE

TEST NUMBER SEVEN

LOAD CONDITION : 4

VERTICAL LOADING, TRANSVERSE AND LONGITUDINAL LOADING

ATT POINT	V VERT	H TRANS	H LONG	LOAD CELL	Vr (kN.)	Vr 1 (kN.)	Vr 2 (kN.)	h (m)	R (kN.)	ANGLE DEG	MASS (kg)
C2T	49,05	49,05		120~2	0,20	0,20			69,23	44,88	
C2L			49,05	120~4	0,20	0,74		-0,91	49,05	-0,86	

NOTES : (g = 9.80665)

1) LOADS IN KILONEWTONS EXCEPT FOR MASS WHICH HAS BEEN CONVERTED TO KILOGRAM
2) ANGLES ARE IN DEGREES , NEGATIVE ANGLES SLOPE ABOVE HORIZONTAL FROM TOWER
3) WHERE HORIZONTAL AND VERTICAL LOADS ARE COMBINED , ANGLE CONTROL IS EMPLOYED .

REVISION 2 8th Oct 2001

CALCULATION OF TEST LOADS AND ANGLES

TOWER TYPE : " CIGRE "
" HYPOSTATIC MODELLING INFLUENC
SELF SUPPORTING STRUCTURE

TEST NUMBER
EIGHT

LOAD CONDITION : 4D
VERTICAL LOADING, TRANSVERSE AND LONGITUDINAL LOADING

ATT POINT	V VERT	H TRANS	H LONG	LOAD CELL	Vr (kN.)	Vr 1 (kN.)	Vr 2 (kN.)	h (m)	R (kN.)	ANGLE DEG	MASS (kg)
C1T	49,05	49,05		120~1	0,20	0,20			69,23	44,88	
C2T	49,05	49,05		120~2	0,20	0,20			69,23	44,88	
C1L			49,05	120~3	0,20	0,74		-0,91	49,05	-0,86	
C2L			49,05	120~4	0,20	0,74		-0,91	49,05	-0,86	

NOTES : (g = 9.80665)

1) LOADS IN KILONEWTONS EXCEPT FOR MASS WHICH HAS BEEN CONVERTED TO KILOGRAM
2) ANGLES ARE IN DEGREES , NEGATIVE ANGLES SLOPE ABOVE HORIZONTAL FROM TOWER
3) WHERE HORIZONTAL AND VERTICAL LOADS ARE COMBINED , ANGLE CONTROL IS EMPLOYED .

TEST RESULTS

TEST 1	STRUCTURE 2A	LOADCASE 1

See applied loads relative to this test in SECTION 3 Page 1 and the photograph of this structure showing rigging for Test 1 Run 3 in SECTION 5 Page 1 of this report.

RUN 3 - 18th October 2001

One hundred percent of the applied loads was held satisfactorily for 60 seconds.
No visual damage to the structure was detected after the test.

DEFLECTION READINGS

Transverse deflection readings taken in the centre at the tip of the earth peak **(A)** as well as **Longitudinal** deflection readings taken at the tip of the cross arms , E1 **(C)** and E2 **(D)** , in millimeters , are tabulated below:

Loading Stage:	1,00%	25%	50%	75%	90%	100%	1,00%	RESIDUAL
TRANSVERSE (A)	0	10	20	30	30	30	0	0
LONGITUDINAL (C)	0	0	0	0	0	0	0	0
LONGITUDINAL (D)	0	0	0	0	0	0	0	0

ORIENTATION

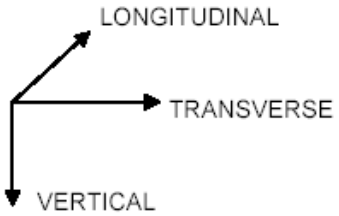

MEMBER FORCES RECORDED ON THE STRAIN GAUGES

Summary of the internal member forces monitored during the test.

Loading Stage:	1,00%	25%	50%	75%	90%	100%	1,00%
Strain Gauge ID:	Strain Gauge reading in (N)						
F2B	0	-17947	-31459	-48564	-58533	-63829	2665
P3L	0	304	653	1596	2172	2301	11
F4	0	-7634	-10925	-19243	-25245	-29090	4811
T11L	0	-1061	-6752	-7935	-8663	-8759	-1298
T12L	0	-3192	-4087	-6362	-7726	-9602	-254
T13L	0	-71	-3012	-3572	-3849	-3787	-1008
B11L	0	-1913	-3239	-5468	-6814	-7773	-2143
B13L	0	-1644	-3183	-5275	-6740	-7785	-2351
T11T	0	-3592	-7501	-10204	-11522	-11432	-37
T12T	0	2390	7242	8537	8891	8927	1075
B11T	0	-1430	-2301	-3615	-4360	-4971	-337
B13T	0	-145	-74	48	-133	-414	567

TEST RESULTS

TEST 2	STRUCTURE 2A	LOADCASE 1D

See applied loads relative to this test in SECTION 3 Page 2 and the photograph of this structure showing rigging for Test 2 Run 3 in SECTION 5 Page 2 of this report.

RUN 3 - 18th October 2001

One hundred percent of the applied loads was held satisfactorily for 60 seconds.
No visual damage to the structure was detected after the test.

DEFLECTION READINGS

Transverse deflection readings taken in the centre at the tip of the earth peak **(A)** as well as **Longitudinal** deflection readings taken at the tip of the cross arms , E1 **(C)** and E2 **(D)** , in millimeters , are tabulated below:

Loading Stage:	2,20%	25%	50%	75%	90%	100%	1,90%	RESIDUAL
TRANSVERSE (A)	0	0	0	0	0	0	0	0
LONGITUDINAL (C)	0	0	0	0	0	0	0	0
LONGITUDINAL (D)	0	0	0	0	0	0	0	0

ORIENTATION

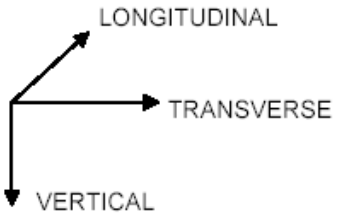

MEMBER FORCES RECORDED ON THE STRAIN GAUGES

Summary of the internal member forces monitored during the test.

Loading Stage:	2,20%	25%	50%	75%	90%	100%	1,90%
Strain Gauge ID:	Strain Gauge reading in (N)						
F2B	0	-5773	-11971	-19783	-22876	-26646	-367
P3L	0	-549	-968	-1456	-1665	-1778	516
F4	0	-4180	-9504	-14433	-17207	-19099	1573
T11L	0	-839	-1949	-2591	-2962	-3168	583
T12L	0	113	78	113	130	120	278
T13L	0	-224	-651	-884	-934	-857	647
B11L	0	-641	-1235	-1986	-2372	-2649	269
B13L	0	-701	-1463	-2415	-2904	-3207	76
T11T	0	114	283	40	0	51	192
T12T	0	591	1280	1887	2345	2767	464
B11T	0	-633	-1295	-2056	-2469	-2736	181
B13T	0	-809	-1555	-2301	-2706	-3013	226

TEST RESULTS

TEST 3	STRUCTURE 2A	LOADCASE 2

See applied loads relative to this test in SECTION 3 Page 3 and the photograph of this structure showing rigging for Test 3 Run 3 in SECTION 5 Page 3 of this report.

RUN 3 - 18th October 2001

One hundred percent of the applied loads was held satisfactorily for 60 seconds.
No visual damage to the structure was detected after the test.

DEFLECTION READINGS

Transverse deflection readings taken in the centre at the tip of the earth peak **(A)** in millimeters , are tabulated below:

Loading Stage:	2,80%	25%	50%	75%	90%	100%	3,60%	RESIDUAL
TRANSVERSE (A)	0	50	190	190	190	190	0	0

ORIENTATION

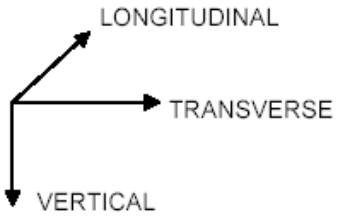

MEMBER FORCES RECORDED ON THE STRAIN GAUGES

Summary of the internal member forces monitored during the test.

Loading Stage:	2,80%	25%	50%	75%	90%	100%	3,60%
Strain Gauge ID:	Strain Gauge reading in (N)						
F2B	0	-10417	-20867	-30964	-37091	-41178	-2573
P3L	0	-84	491	726	1085	1296	-179
F4	0	-13011	-26246	-38634	-46184	-51904	-3993
T11L	0	-435	-908	-1040	-1112	-1155	305
T12L	0	1973	4281	7157	8378	8944	766
T13L	0	-66	-160	-179	-415	-617	-332
B11L	0	-1207	-2795	-4349	-5284	-5953	283
B13L	0	-1754	-3673	-5500	-6520	-7174	353
T11T	0	2369	4659	6296	7471	8478	-782
T12T	0	-45	-227	-486	-499	-514	-809
B11T	0	935	928	1120	1405	1909	1682
B13T	0	-4	-950	-1726	-1929	-1693	1324

TEST RESULTS

TEST 4	STRUCTURE 2A	LOADCASE 2D

See applied loads relative to this test in SECTION 3 Page 4 and the photograph of this structure showing rigging for Test 4 Run 3 in SECTION 5 Page 4 of this report.

RUN 3 - 18th October 2001

One hundred percent of the applied loads was held satisfactorily for 60 seconds.
No visual damage to the structure was detected after the test.

DEFLECTION READINGS

Transverse deflection readings taken in the centre at the tip of the earth peak **(A)** in millimeters , are tabulated below:

Loading Stage:	2,80%	25%	50%	75%	90%	100%	3,60%	RESIDUAL
TRANSVERSE (A)	0	10	20	30	40	40	10	10

ORIENTATION

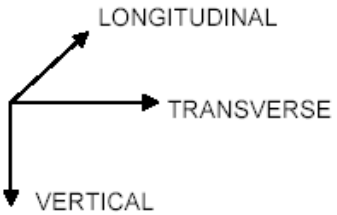

MEMBER FORCES RECORDED ON THE STRAIN GAUGES

Summary of the internal member forces monitored during the test.

Loading Stage:	3,80%	25%	50%	75%	90%	100%	5,40%
Strain Gauge ID:	Strain Gauge reading in (N)						
F2B	0	-19041	-38549	-58820	-69084	-75832	-1034
P3L	0	588	1913	5345	12194	14925	8769
F4	0	-23364	-46895	-72848	-85492	-93440	2660
T11L	0	-868	-1653	-1836	-1590	-1542	2249
T12L	0	3698	7862	13391	16752	19150	3683
T13L	0	-243	-603	-516	-176	148	1946
B11L	0	-2736	-5877	-10010	-11588	-12541	193
B13L	0	-3591	-7330	-12110	-13881	-14983	-20
T11T	0	4649	9039	11998	13579	14783	-3283
T12T	0	68	301	373	424	557	-591
B11T	0	674	284	3580	3480	3572	594
B13T	0	-889	-2699	113	-299	-194	2641

TEST RESULTS

TEST 5	STRUCTURE 2A	LOADCASE 3

See applied loads relative to this test in SECTION 3 Page 5 and the photograph of this structure showing rigging for Test 5 Run 3 in SECTION 5 Page 5 of this report.

RUN 3 - 18th October 2001

One hundred percent of the applied loads was held satisfactorily for 60 seconds.
No visual damage to the structure was detected after the test.

DEFLECTION READINGS

Transverse deflection readings taken in the centre at the tip of the earth peak **(A)** as well as **Longitudinal** deflection readings taken at the tip of the cross ams , E1 **(C)** and E2 **(D)** , in millimeters , are tabulated below:

Loading Stage:	5,70%	25%	50%	75%	90%	100%	2,30%	RESIDUAL
TRANSVERSE (A)	0	0	10	20	20	20	0	0
LONGITUDINAL (C)	0	10	20	50	80	80	40	40
LONGITUDINAL (D)	0	0	10	50	80	100	40	40

ORIENTATION

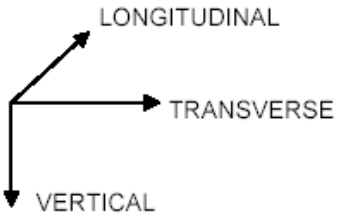

MEMBER FORCES RECORDED ON THE STRAIN GAUGES

Summary of the internal member forces monitored during the test.

Loading Stage:	5,70%	25%	50%	75%	90%	100%	2,30%
Strain Gauge ID:	Strain Gauge reading in (N)						
F2B	0	-6498	-14858	-23078	-29513	-34586	-123
P3L	0	5739	11140	16157	17781	18496	-4245
F4	0	-11399	-26083	-40463	-47468	-51728	-1288
T11L	0	-8833	-16580	-24735	-32155	-37923	1536
T12L	0	-6640	-13299	-19435	-22312	-24783	-1840
T13L	0	-6612	-15353	-19879	-24740	-28748	-778
B11L	0	2349	6257	10541	12273	13235	930
B13L	0	545	2180	4266	4742	5030	1738
T11T	0	-4412	-9925	-17685	-22978	-25690	1808
T12T	0	-7001	-16587	-29051	-33394	-35169	-2449
B11T	0	-1868	-5693	-10198	-12845	-15103	-4001
B13T	0	240	-2444	-5055	-7022	-9128	-5776

TEST RESULTS

TEST 6	STRUCTURE 2A	LOADCASE 3D

See applied loads relative to this test in SECTION 3 Page 6 and the photograph of this structure showing rigging for Test 6 Run 3 in SECTION 5 Page 6 of this report.

RUN 3 - 18th October 2001

One hundred percent of the applied loads was held satisfactorily for 60 seconds.
No visual damage to the structure was detected after the test.

DEFLECTION READINGS

Transverse deflection readings taken in the centre at the tip of the earth peak **(A)** as well as **Longitudinal** deflection readings taken at the tip of the cross arms , E1 **(C)** and E2 **(D)** , in millimeters , are tabulated below:

Loading Stage:	3,40%	25%	50%	75%	90%	100%	4,90%	RESIDUAL
TRANSVERSE (A)	0	0	0	0	0	0	0	0
LONGITUDINAL (C)	0	10	10	30	40	40	10	10
LONGITUDINAL (D)	0	10	10	20	30	30	0	0

ORIENTATION

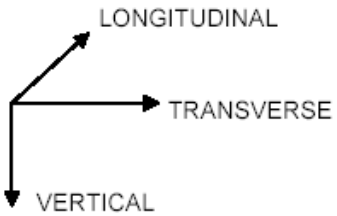

MEMBER FORCES RECORDED ON THE STRAIN GAUGES

Summary of the internal member forces monitored during the test.

Loading Stage:	3,40%	25%	50%	75%	90%	100%	4,90%
Strain Gauge ID:	Strain Gauge reading in (N)						
F2B	0	-19699	-39657	-63975	-77072	-80562	-963
P3L	0	-1361	-4755	-11478	-14028	-14960	-844
F4	0	-23456	-50588	-85285	-99333	-1E+05	-2414
T11L	0	-3931	-8913	-14623	-17247	-18140	1388
T12L	0	727	1332	2018	1907	1724	16
T13L	0	-2728	-6119	-10083	-11685	-12349	801
B11L	0	846	3399	10609	12321	12113	4413
B13L	0	555	2363	9491	11025	10666	5961
T11T	0	-249	-842	-1197	-1427	-1808	423
T12T	0	-3037	-6888	-10640	-13186	-15133	-1778
B11T	0	-2914	-2767	-5075	-8664	-12033	992
B13T	0	-2444	-2497	-6185	-10214	-13712	845

TEST RESULTS

TEST 7	STRUCTURE 2A	LOADCASE 4

See applied loads relative to this test in SECTION 3 Page 7 and the photograph of this structure showing rigging for Test 7 Run 3 in SECTION 5 Page 7 of this report.

RUN 3 - 18th October 2001

One hundred percent of the applied loads was held satisfactorily for 60 seconds.
No visual damage to the structure was detected after the test.

DEFLECTION READINGS

Transverse deflection readings taken in the centre at the tip of the earth peak **(A)** as well as **Longitudinal** deflection readings taken at the tip of the cross arms , E1 **(C)** and E2 **(D)** , in millimeters , are tabulated below:

Loading Stage:	3,40%	25%	50%	75%	90%	100%	4,90%	RESIDUAL
TRANSVERSE (A)	0	10	20	30	40	50	10	10
LONGITUDINAL (C)	0	10	30	40	50	50	10	10
LONGITUDINAL (D)	0	10	40	50	60	70	10	10

ORIENTATION

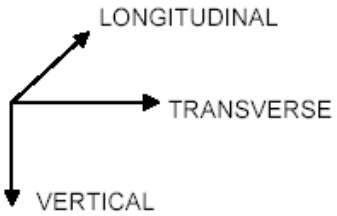

MEMBER FORCES RECORDED ON THE STRAIN GAUGES

Summary of the internal member forces monitored during the test.

Loading Stage:	3,40%	25%	50%	75%	90%	100%	4,90%
Strain Gauge ID:	Strain Gauge reading in (N)						
F2B	0	-30397	-69653	-1E+05	-1E+05	-1E+05	-11183
P3L	0	5088	7378	11944	16867	20546	-2873
F4	0	-32679	-64346	-99492	-1E+05	-1E+05	1241
T11L	0	-11156	-22917	-35917	-42996	-47885	586
T12L	0	-5734	-11254	-16820	-19874	-21776	1380
T13L	0	-7183	-14672	-22606	-26589	-28933	1904
B11L	0	-494	-1237	-2536	-5152	-4610	-5456
B13L	0	-3115	-6812	-11130	-15477	-15652	-6197
T11T	0	-6510	-14318	-22220	-27109	-29816	-2394
T12T	0	-6074	-11687	-17968	-21544	-24411	-1137
B11T	0	-4290	-8802	-16607	-20244	-22109	-5170
B13T	0	-2909	-6089	-11964	-14095	-15573	-5499

TEST RESULTS

TEST 8	STRUCTURE 2A	LOADCASE 4D

See applied loads relative to this test in SECTION 3 Page 8 and the photograph of this structure showing rigging for Test 8 Run 3 in SECTION 5 Page 8 of this report.

RUN 3 - 18th October 2001

One hundred percent of the applied loads was held satisfactorily for 60 seconds.
No visual damage to the structure was detected after the test.

DEFLECTION READINGS

Transverse deflection readings taken in the centre at the tip of the earth peak **(A)** as well as **Longitudinal** deflection readings taken at the tip of the cross arms , E1 **(C)** and E2 **(D)** , in millimeters , are tabulated below:

Loading Stage:	5,50%	25%	50%	75%	90%	100%	5,20%	RESIDUAL
TRANSVERSE (A)	0	10	20	30	40	40	0	0
LONGITUDINAL (C)	0	0	50	60	60	70	50	50
LONGITUDINAL (D)	0	0	0	10	10	10	0	0

ORIENTATION

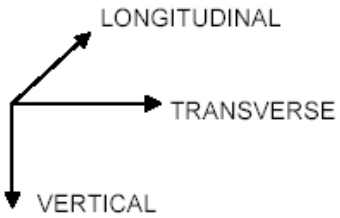

MEMBER FORCES RECORDED ON THE STRAIN GAUGES

Summary of the internal member forces monitored during the test.

Loading Stage:	5,50%	25%	50%	75%	90%	100%	5,20%
Strain Gauge ID:	Strain Gauge reading in (N)						
F2B	0	-42572	-88299	-1E+05	-2E+05	-2E+05	8135
P3L	0	-2812	-5803	-8195	-9216	-9950	2526
F4	0	-53411	-1E+05	-2E+05	-2E+05	-2E+05	86
T11L	0	-5737	-12123	-18082	-21751	-23614	1333
T12L	0	3534	6917	10085	12222	14266	-2236
T13L	0	-3599	-8285	-11733	-13579	-14511	696
B11L	0	-2141	-4531	-7471	-9385	-9547	882
B13L	0	-3484	-7292	-11909	-14921	-15709	758
T11T	0	3292	6928	10700	13085	13357	371
T12T	0	-2072	-4059	-5775	-7116	-8157	-353
B11T	0	3747	2742	-205	-1786	-1927	9079
B13T	0	2744	536	-3509	-5454	-5214	-11834

TEST RESULTS

TEST 9	STRUCTURE 2A	LOADCASE 4D - DESTRUCTION

See applied loads relative to this test in SECTION 3 Page 8 and the photograph of this structure showing rigging for Test 8 Run 3 in SECTION 5 Page 8 of this report.

RUN 3 - 18th October 2001

After successful completion of Test 8 , the same test was used to do a Destruction Test and the structure was again loaded up to 100% , then the loading targets were set to increase in increments of 5% beyond 100% until failure occurred.
Failure of the right cross arm (C2) occurred at 114.1% of the applied load.
Photographs of this failure can be seen in SECTION 5 Page 9 of this report.

DEFLECTION READINGS

Transverse deflection readings taken in the centre at the tip of the earth peak **(A)** as well as **Longitudinal** deflection readings taken at the tip of the cross ams , E1 **(C)** and E2 **(D)**, in millimeters , are tabulated below:

Loading Stage:	5,50%	25%	50%	75%	90%	100%	105%	110%
TRANSVERSE (A)	0	10	20	30	40	40	50	50
LONGITUDINAL (C)	0	0	50	60	60	70	90	100
LONGITUDINAL (D)	0	0	0	10	10	10	10	10

ORIENTATION

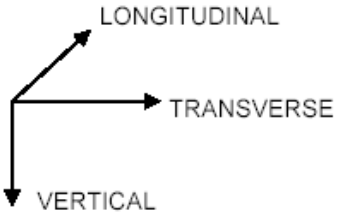

MEMBER FORCES RECORDED ON THE STRAIN GAUGES

Summary of the internal member forces monitored during the test.

Loading Stage:	4,90%	50%	75%	90%	100%	105%	110,00%	114,10%
Strain Gauge ID:	Strain Gauge reading in (N)							
F2B	0	-87192	-1E+05	-2E+05	-2E+05	-2E+05	-203094	-211165
P3L	0	-6239	-8667	-10308	-11491	-11632	-12045	-12390
F4	0	-1E+05	-2E+05	-2E+05	-2E+05	-2E+05	-238965	-247319
T11L	0	-11814	-18567	-22001	-24696	-25945	-26826	-26628
T12L	0	7706	12265	14708	16509	17221	17415	17291
T13L	0	-7006	-11096	-13248	-14886	-15440	-15831	-15884
B11L	0	-4516	-7310	-8686	-9509	-10016	-10632	-11174
B13L	0	-7508	-11907	-14031	-15456	-16208	-17072	-17444
T11T	0	6260	9646	11513	12887	13619	14662	14616
T12T	0	-4242	-6479	-7519	-8416	-8739	-8934	-9005
B11T	0	-4696	-8168	-9851	-11000	-11865	-12573	-13427
B13T	0	-7652	-12727	-15263	-17001	-17848	-18598	-9323

ANNEX C:

ESTIMATED *versus* TEST RESULTS

OF LOADS ON BARS

Prepared by Rania C. Peixoto

WORKING GROUP SCB2.08

TF4 – INFLUENCE OF THE HYPERSTATIC MODELLING

ESTIMATED *versus* TEST RESULTS OF LOADS ON BARS

NOTES:

1 - Monitored members as per item 7.1 – "Relevant test data", pages 44 and 45, chapter 7.

2 - Values of Annex C are not adjusted as per items 7.3 – "Strain gages results" and 7.4 – "Discrepancies", chapter 7, pages 51 to 59.

A	01/03/2004	Results Comparison - Structures 1, 2 and 2A
REVISION	**DATE**	**DESCRIPTION**

SUMMARY

1. STRUCTURE 1 – TEST 1 (1)

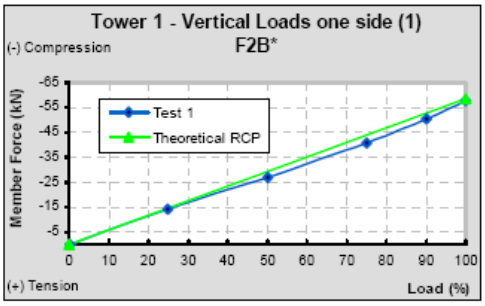

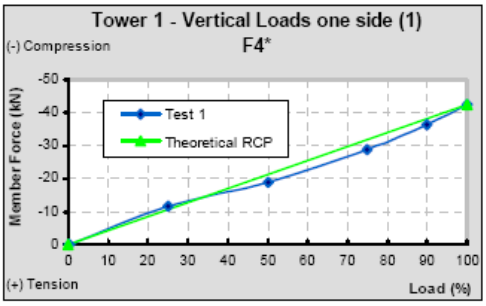

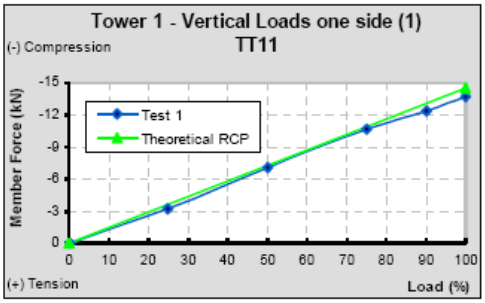

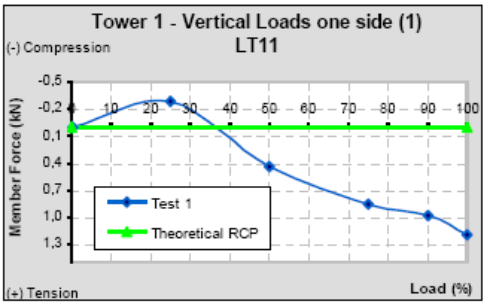

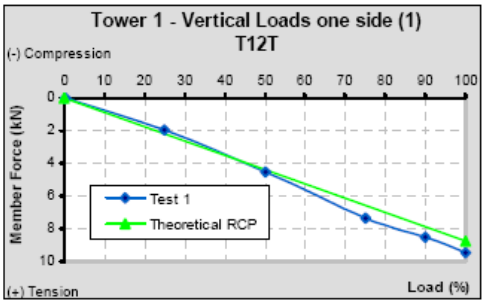

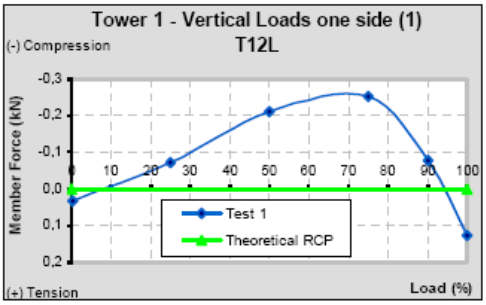

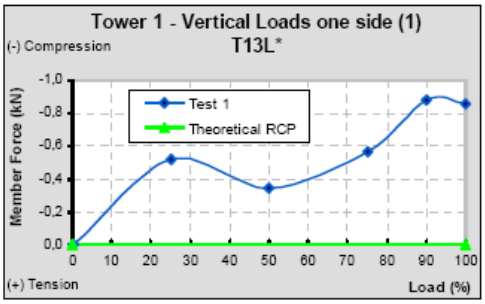

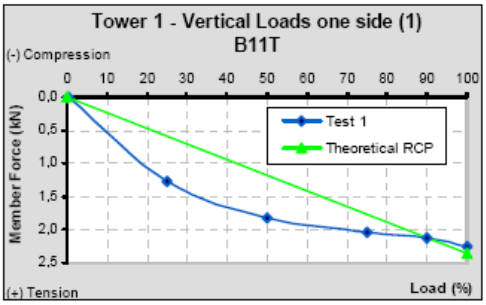

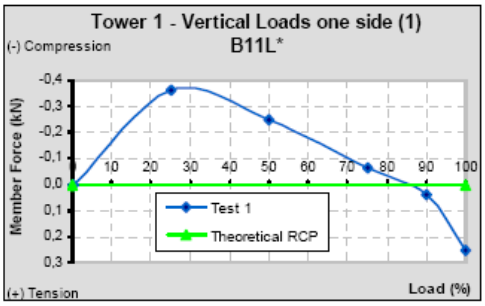

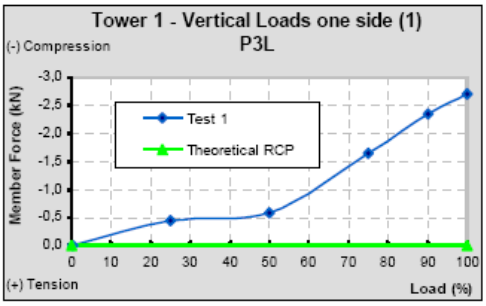

STRUCTURE 1 – TEST 2 (1D)

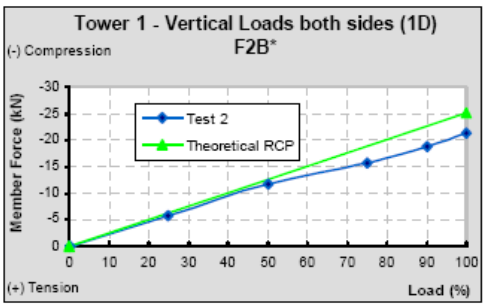

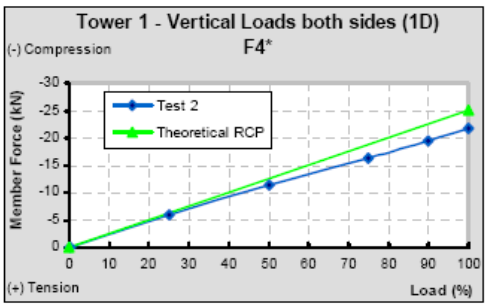

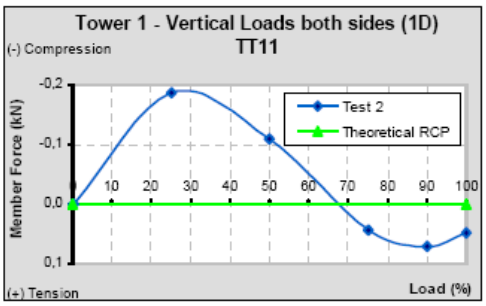

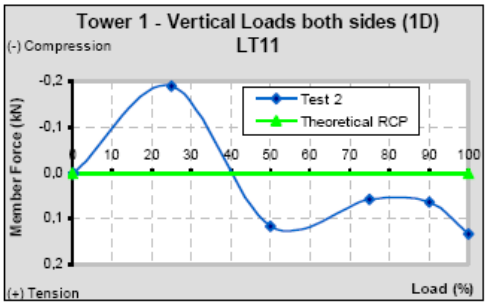

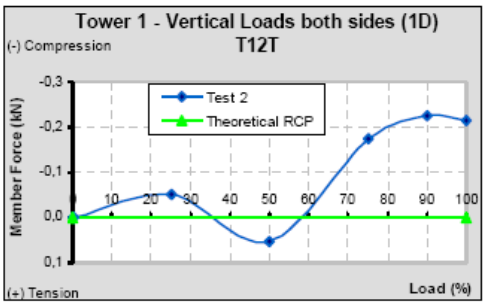

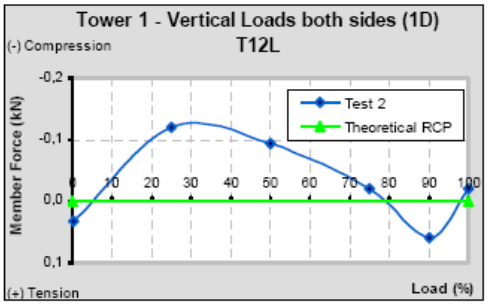

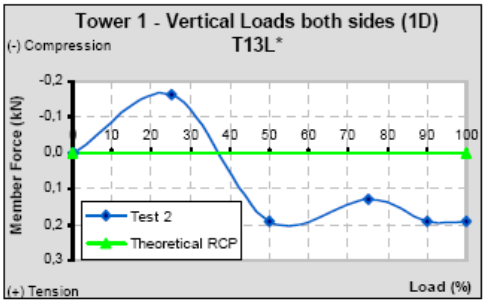

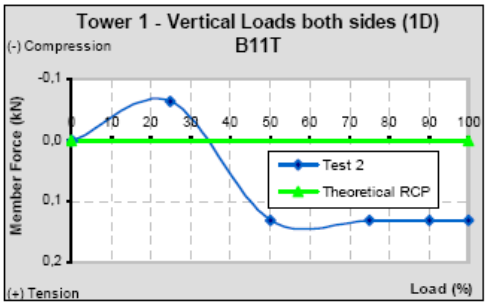

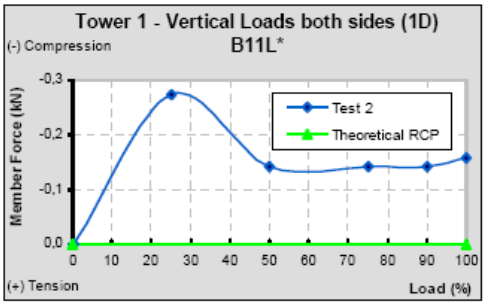

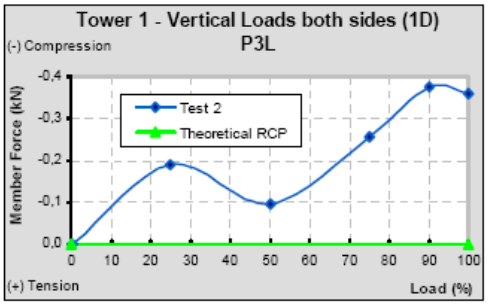

2. STRUCTURE 1 – TEST 3 (2)

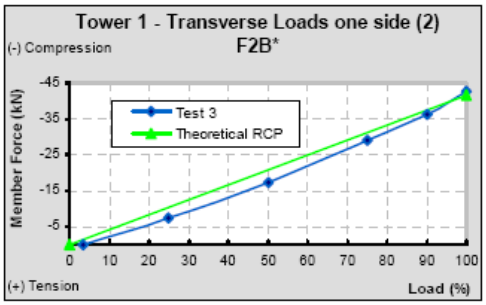

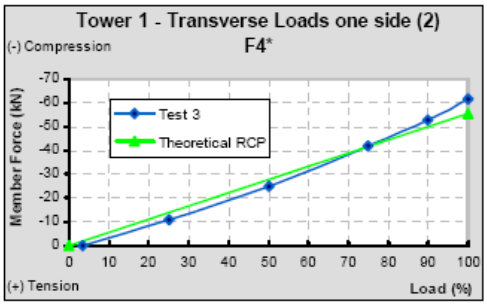

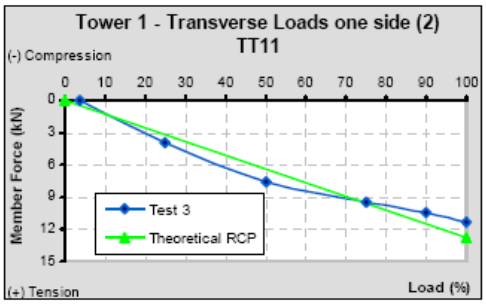

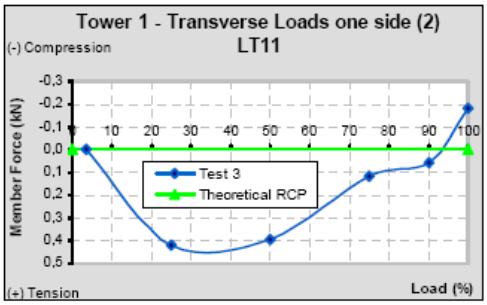

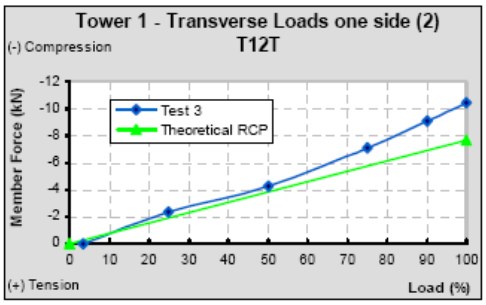

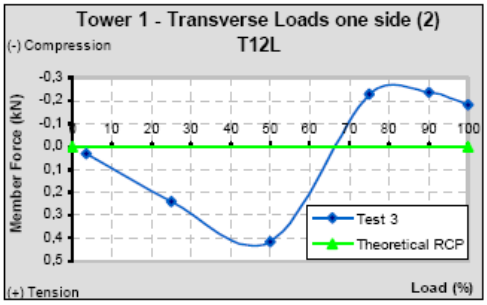

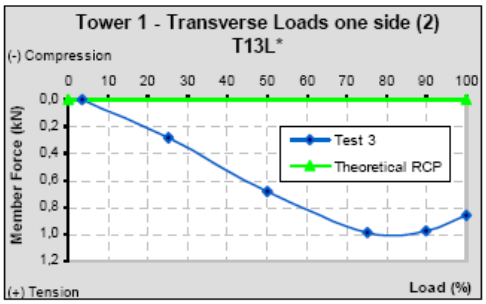

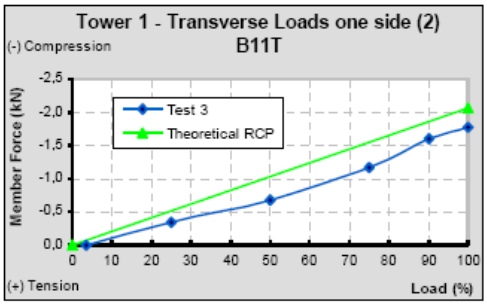

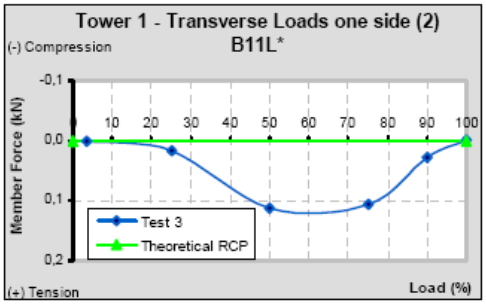

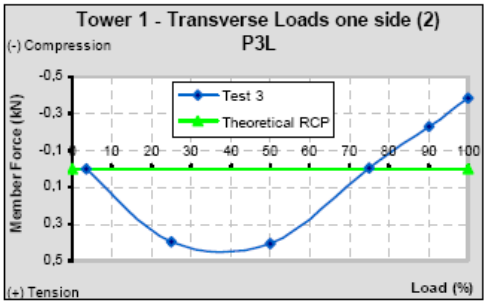

3. STRUCTURE 1 – TEST 4 (2D)

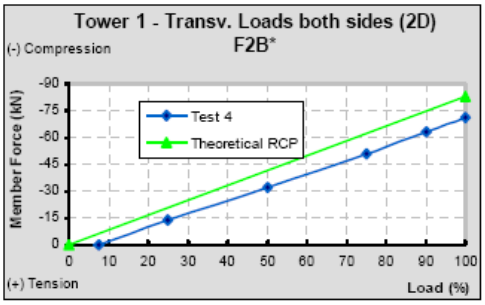

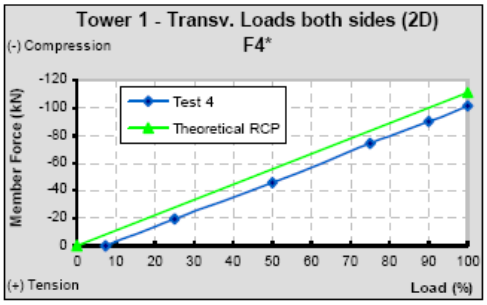

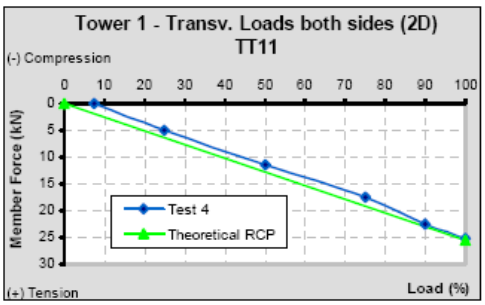

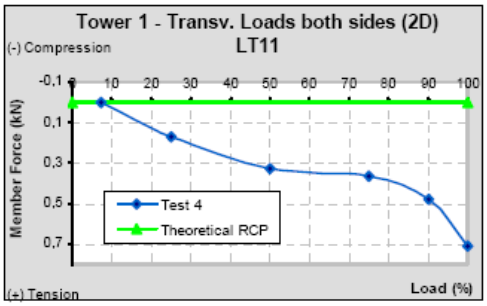

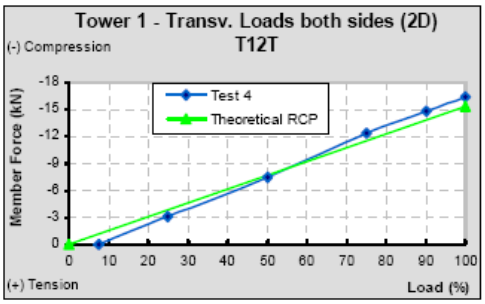

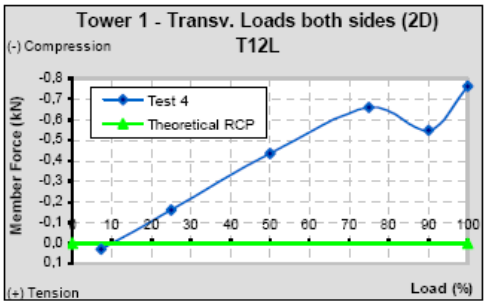

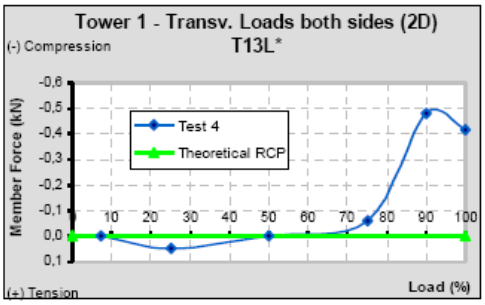

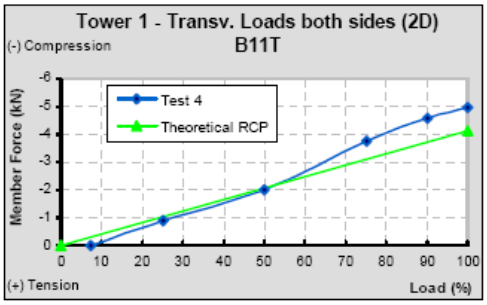

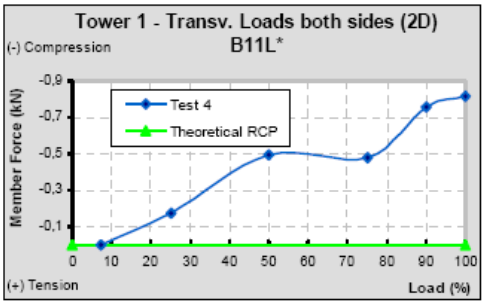

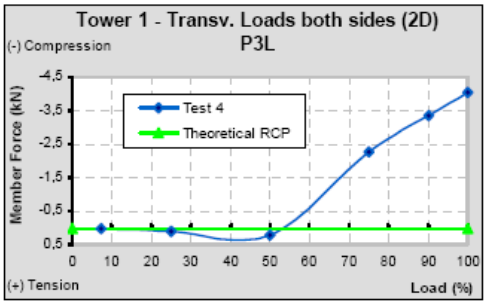

4. STRUCTURE 1 – TEST 5 (3)

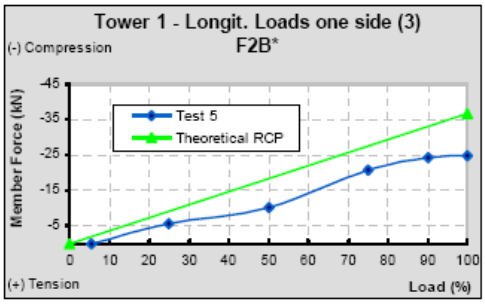

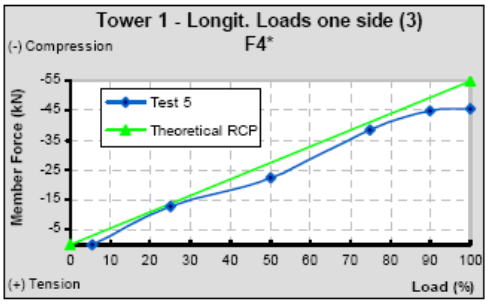

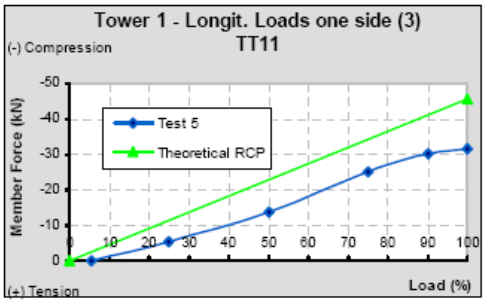

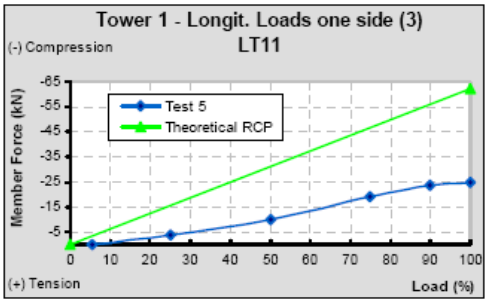

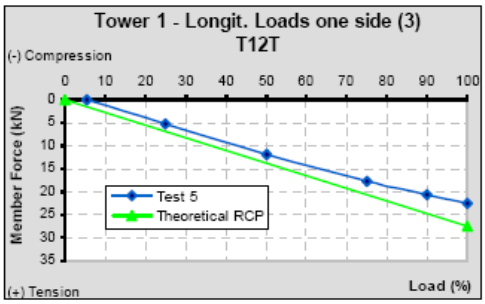

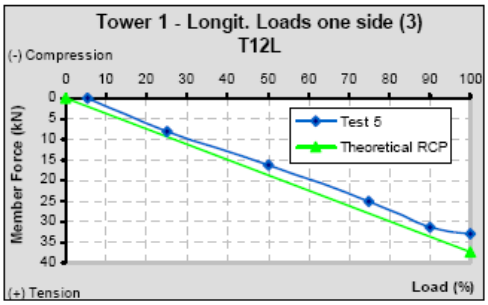

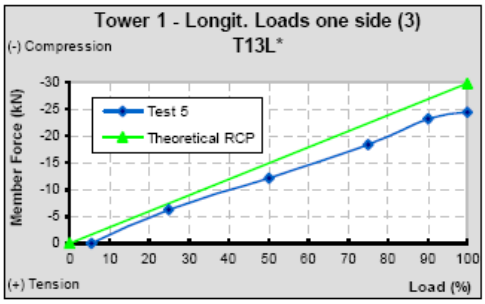

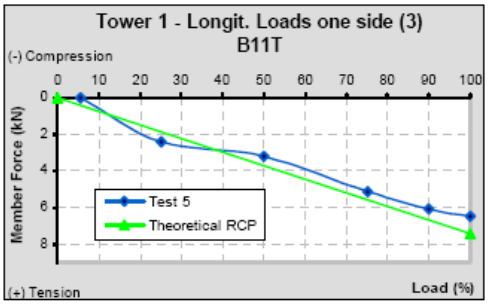

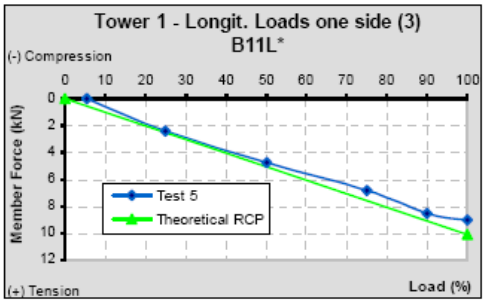

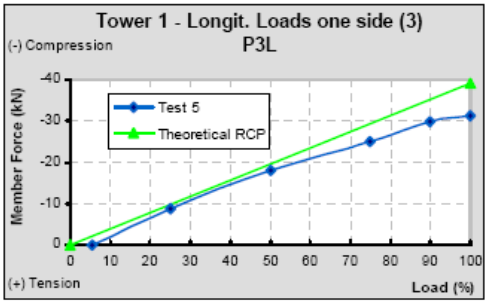

5. STRUCTURE 1 – TEST 6 (3D)

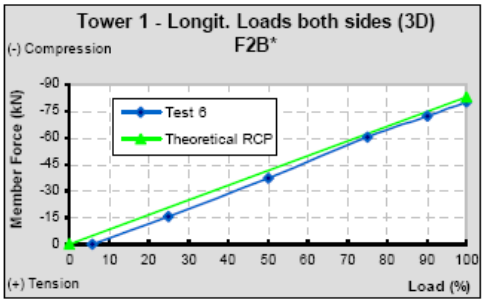

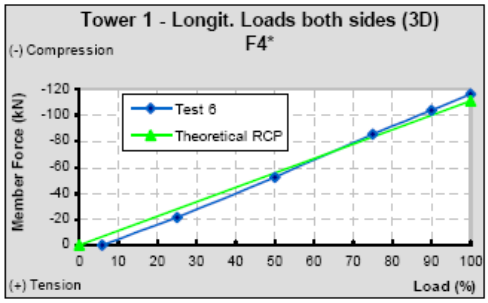

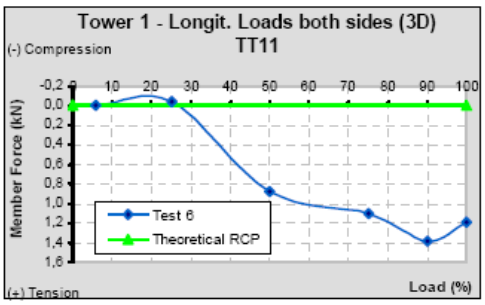

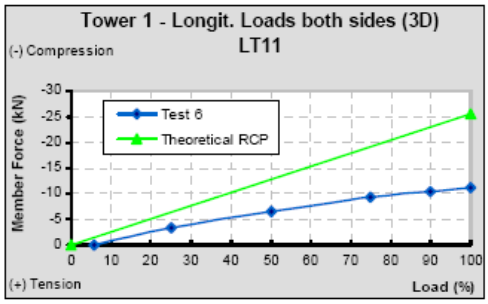

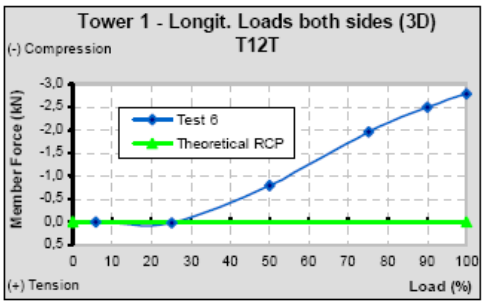

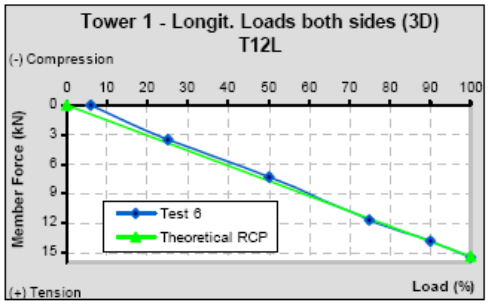

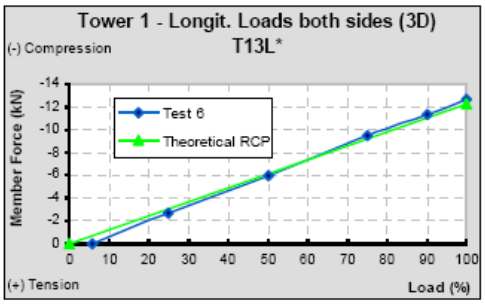

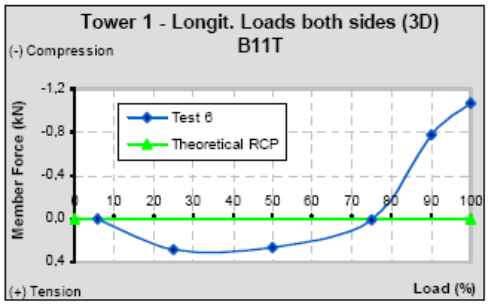

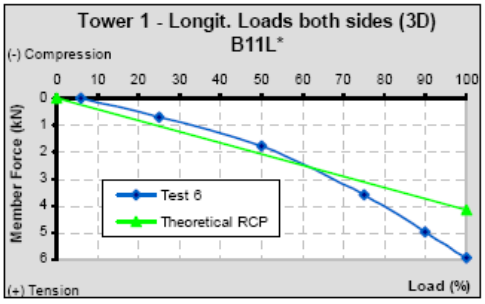

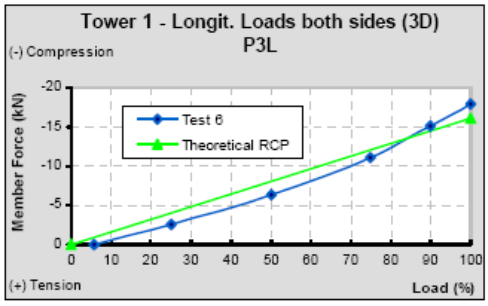

6. STRUCTURE 1 – TEST 7 (4)

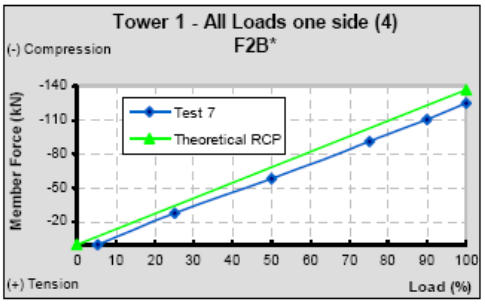

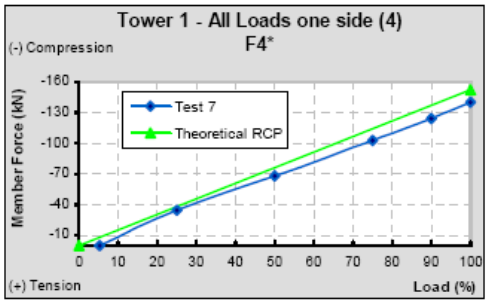

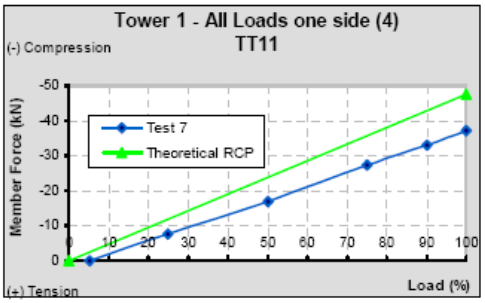

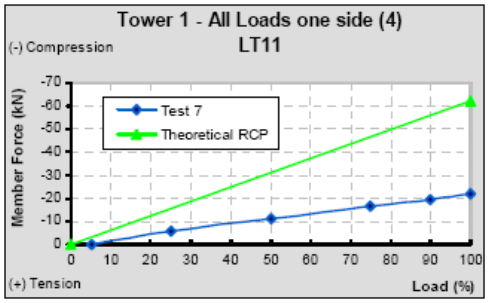

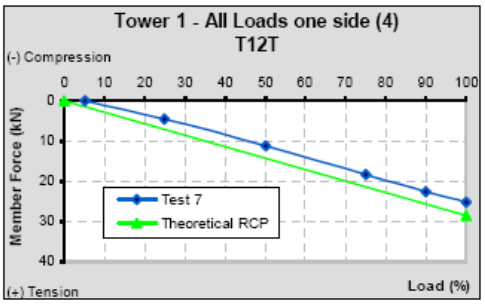

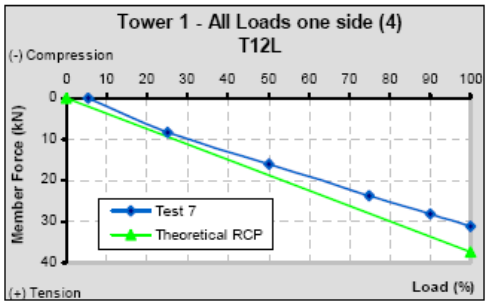

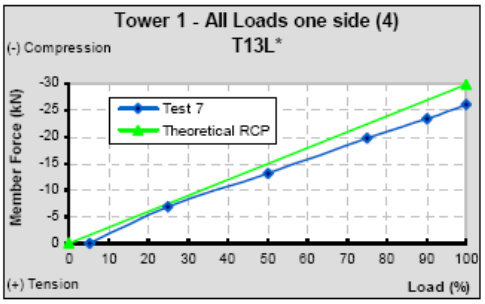

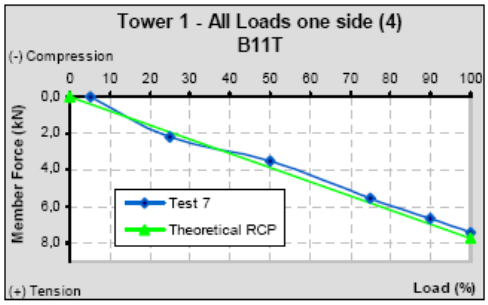

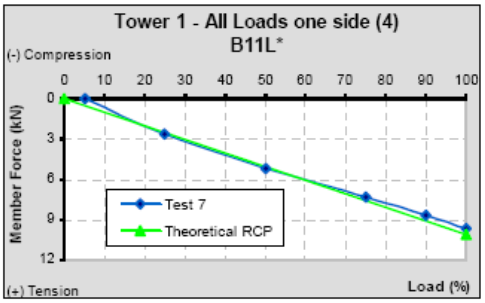

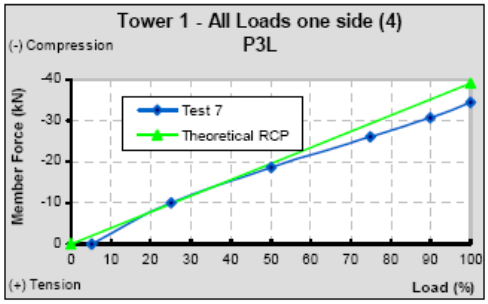

7. STRUCTURE 1 – TEST 8 (4D)

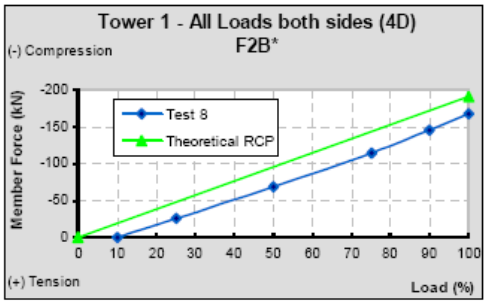

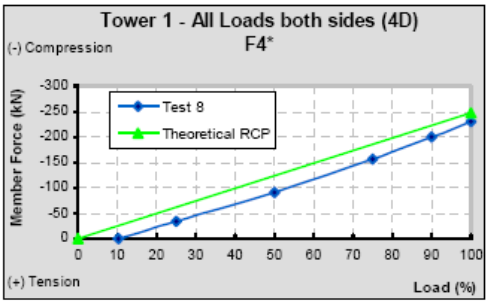

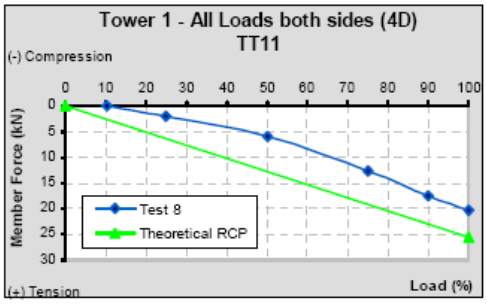

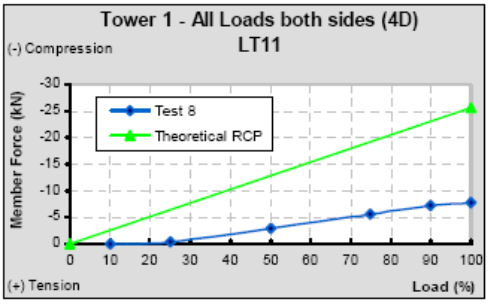

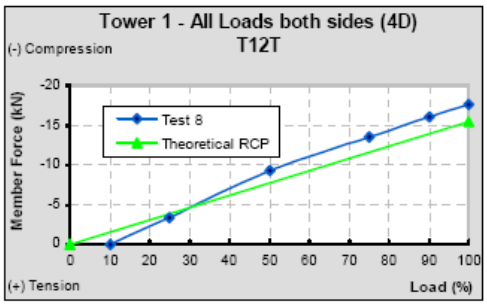

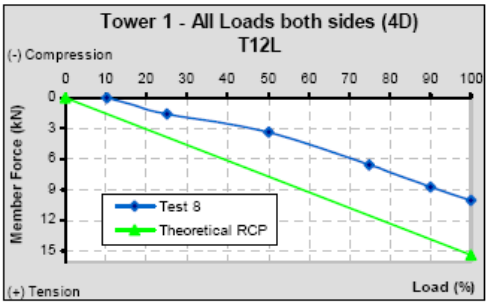

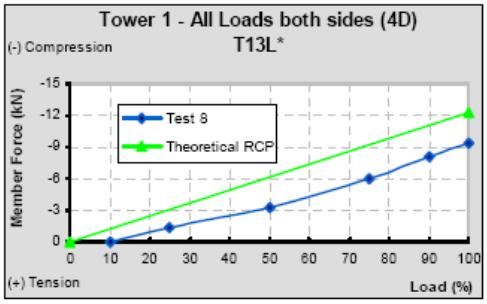

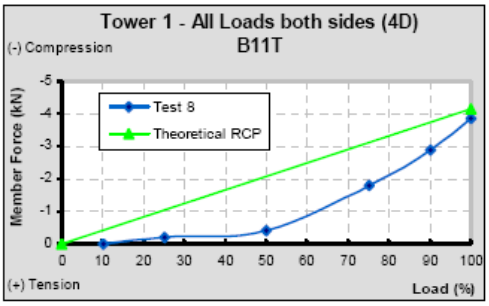

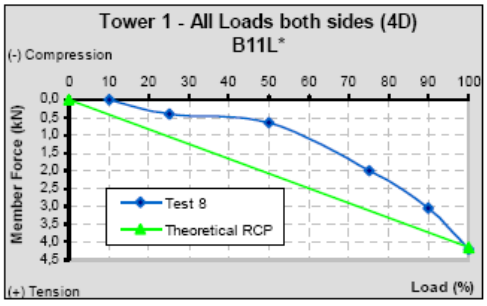

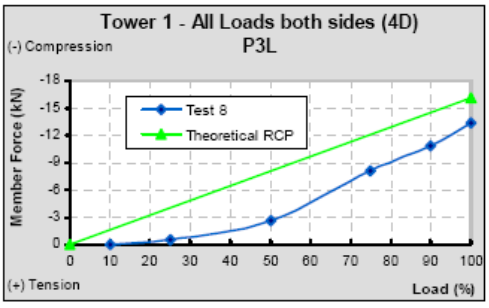

8. STRUCTURE 2 – TEST 1 (1)

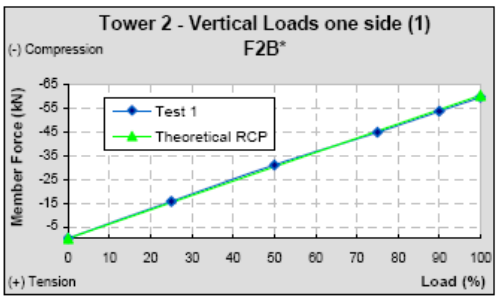

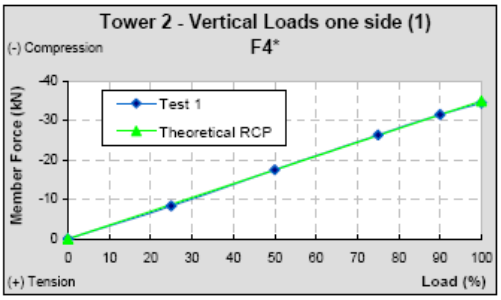

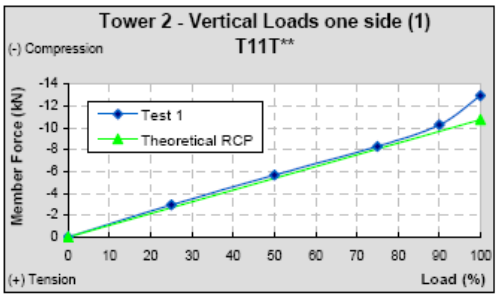

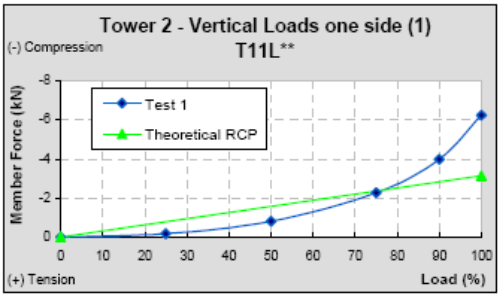

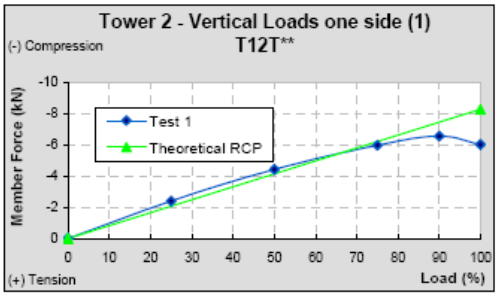

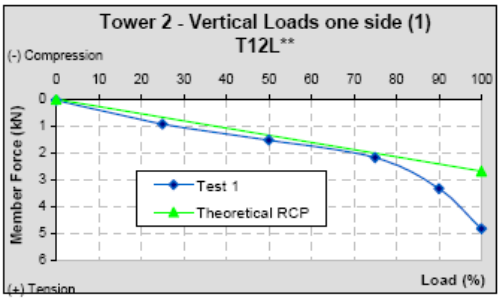

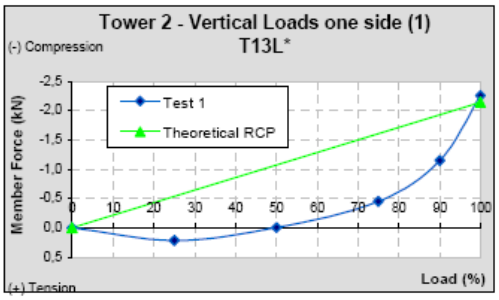

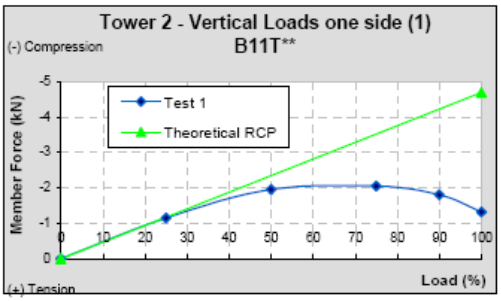

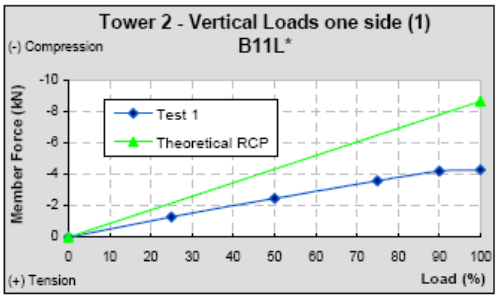

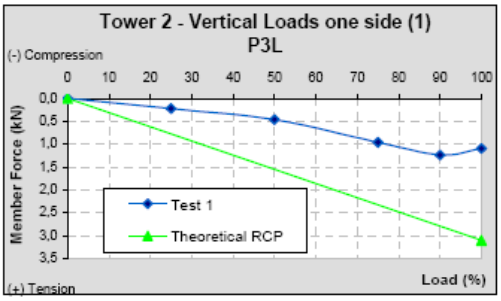

9. STRUCTURE 2 – TEST 2 (1D)

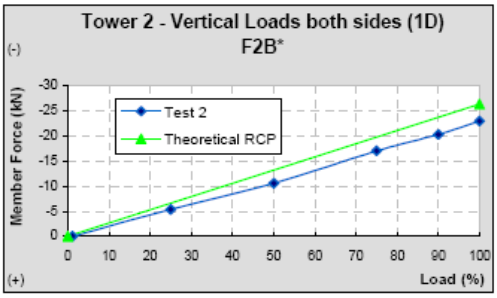

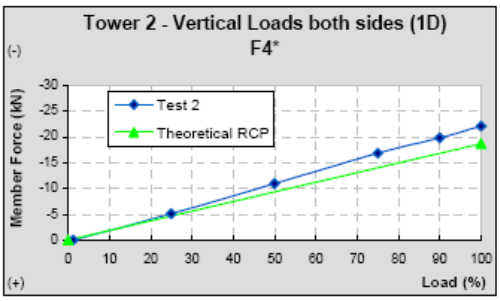

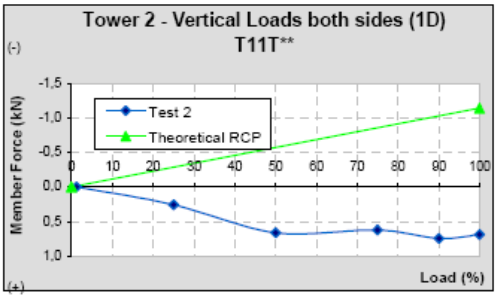

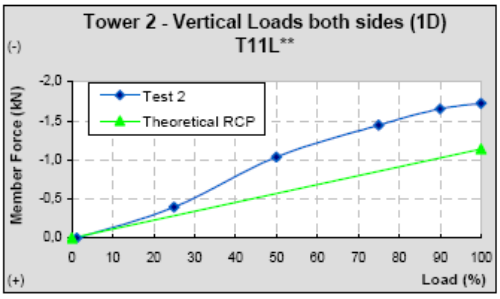

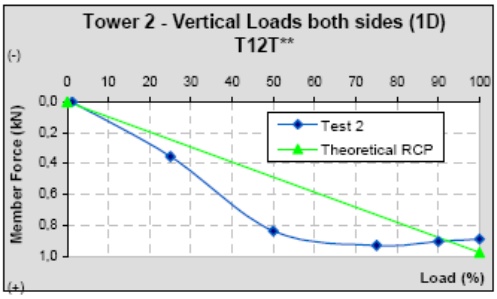

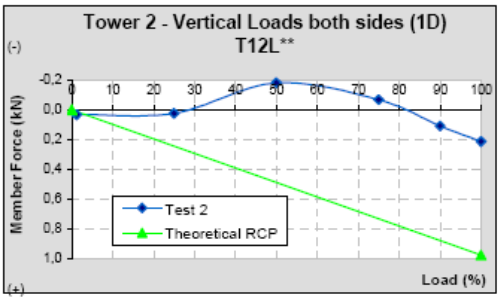

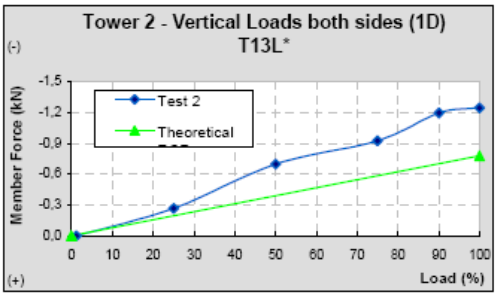

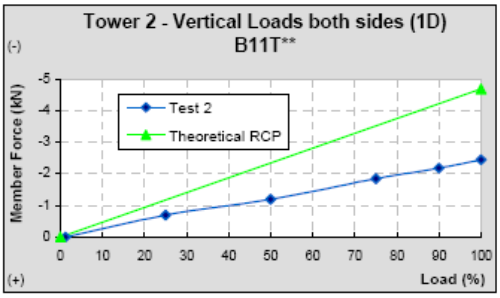

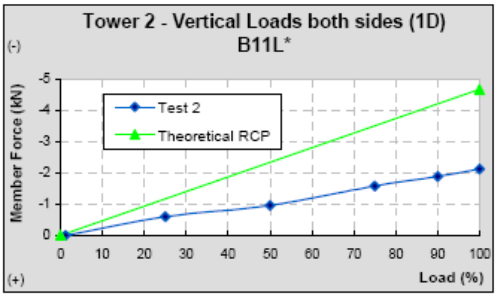

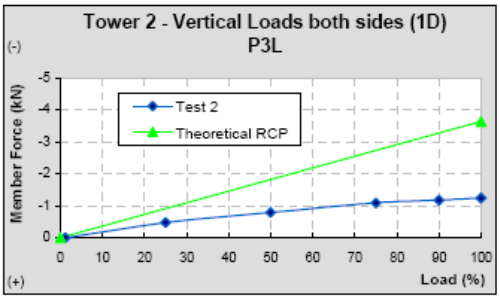

10. STRUCTURE 2 – TEST 3 (2)

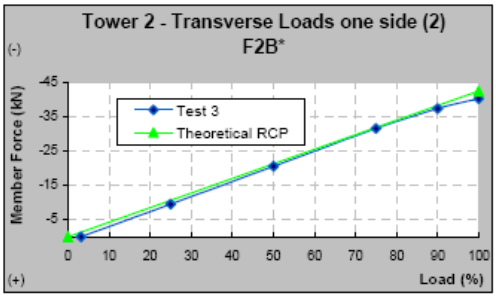

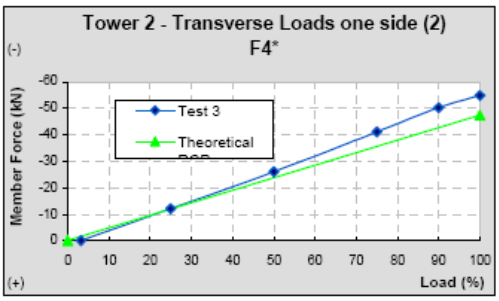

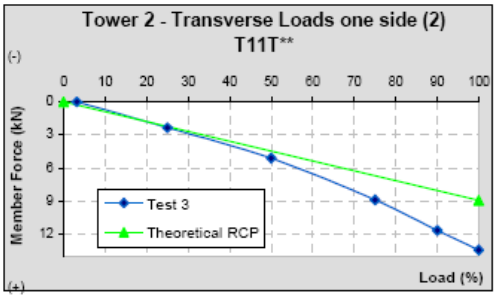

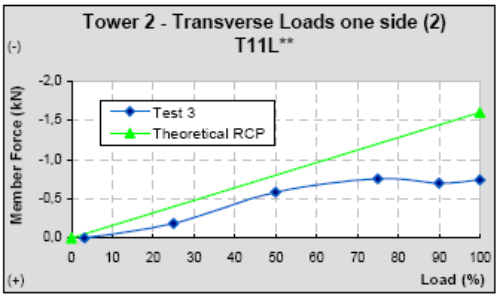

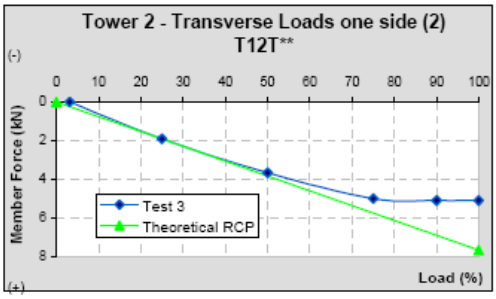

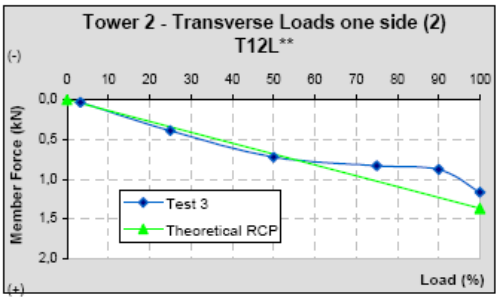

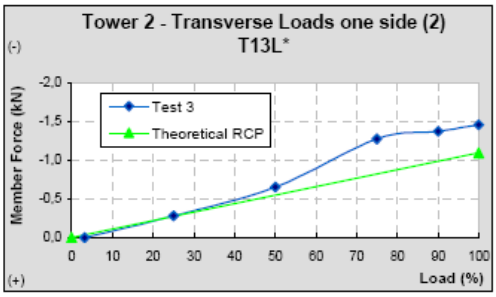

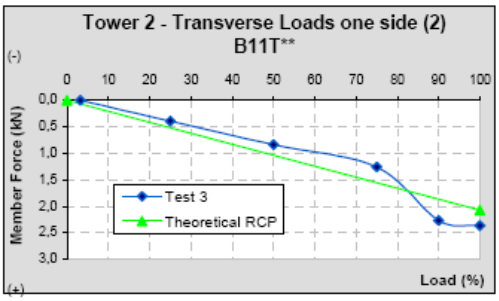

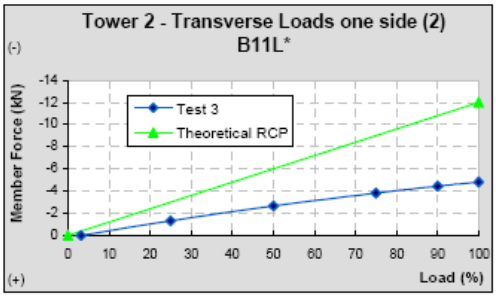

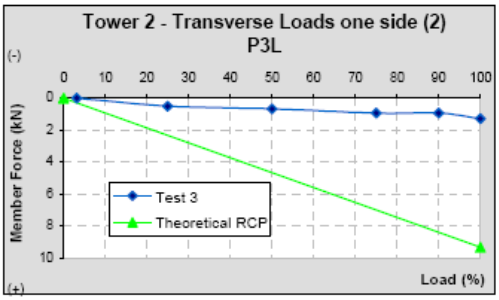

11. STRUCTURE 2 – TEST 4 (2D)

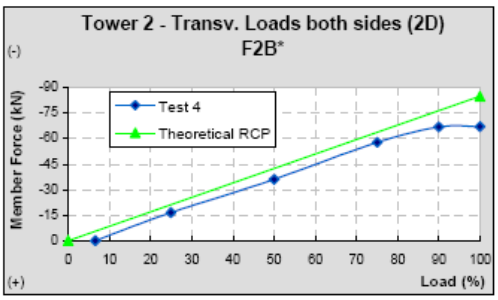

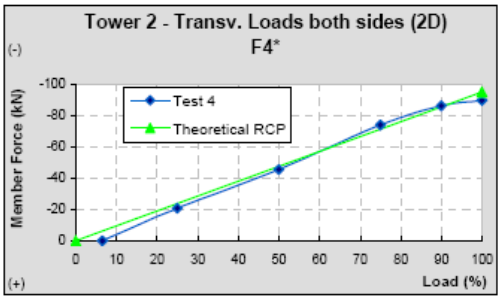

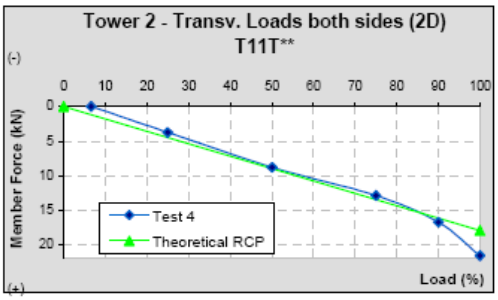

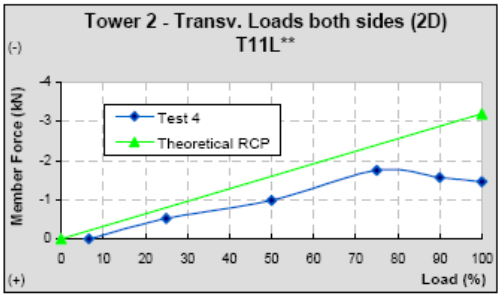

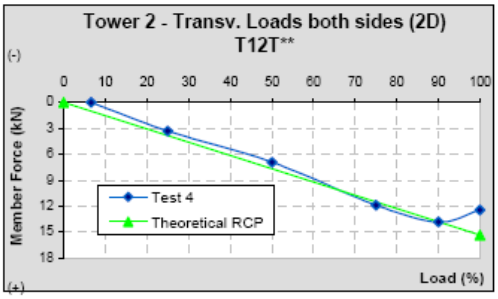

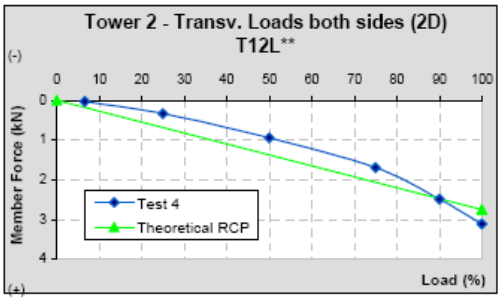

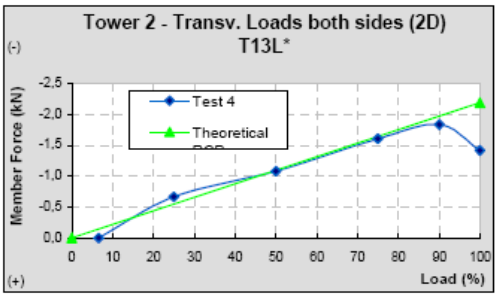

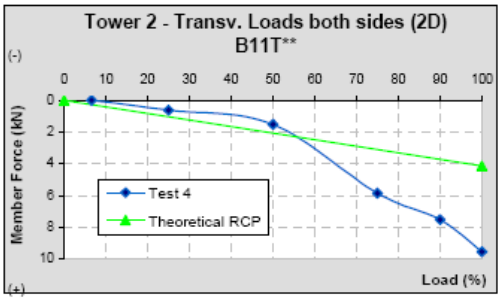

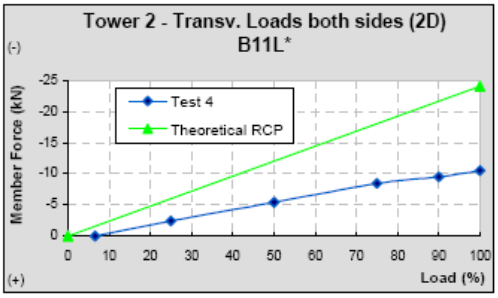

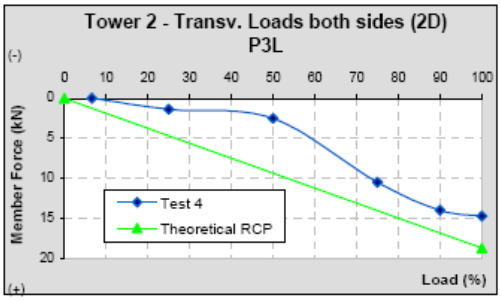

12. STRUCTURE 2 – TEST 5 (3)

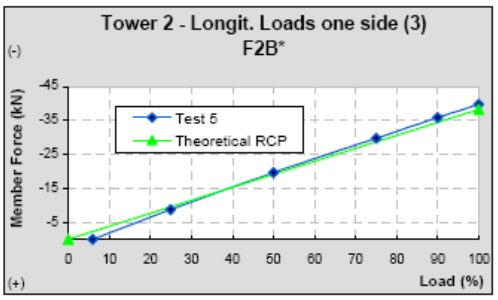

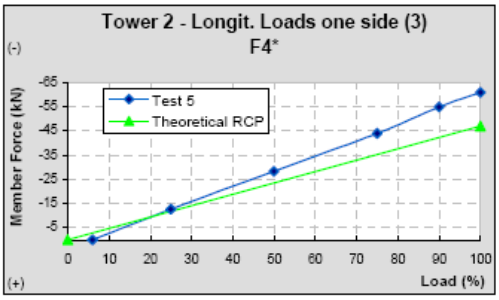

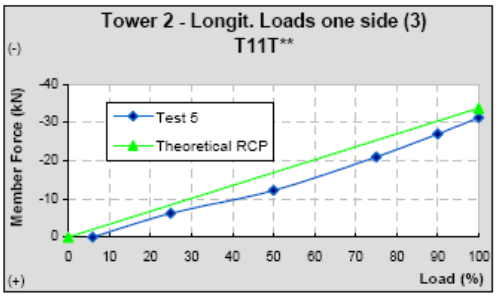

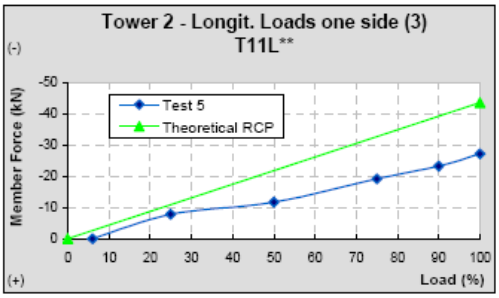

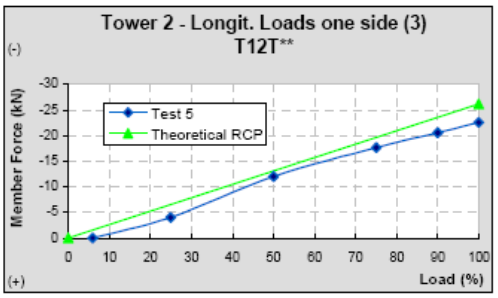

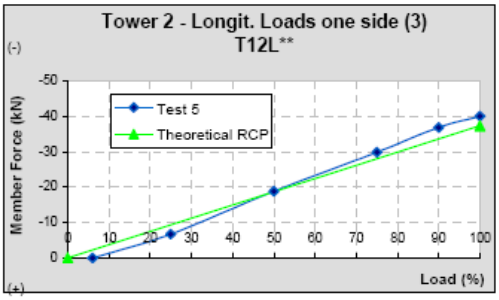

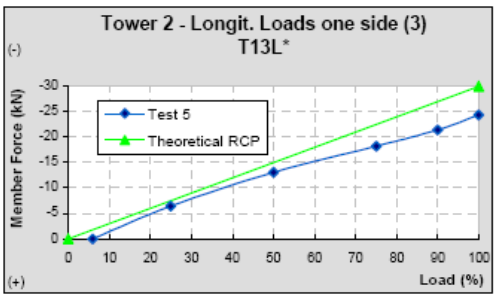

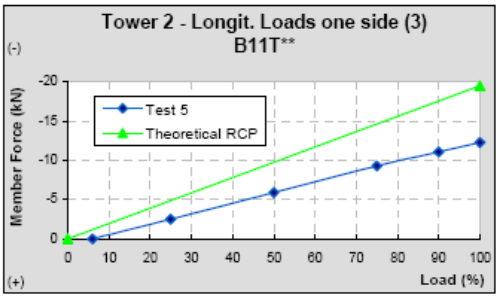

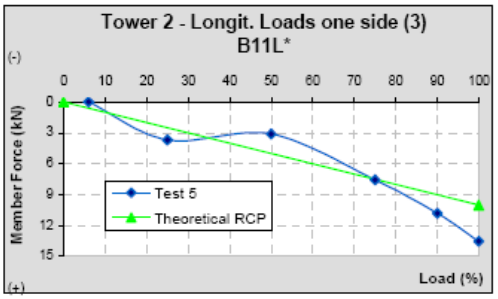

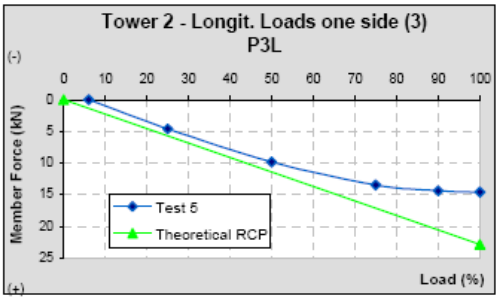

13. STRUCTURE 2 – TEST 6 (3D)

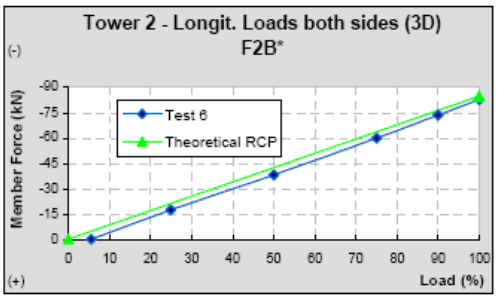

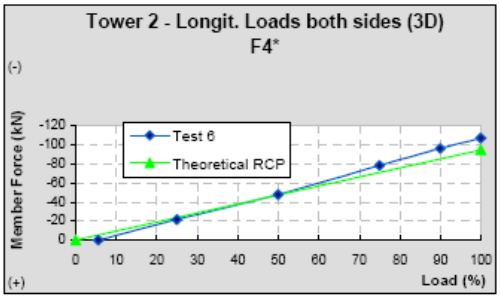

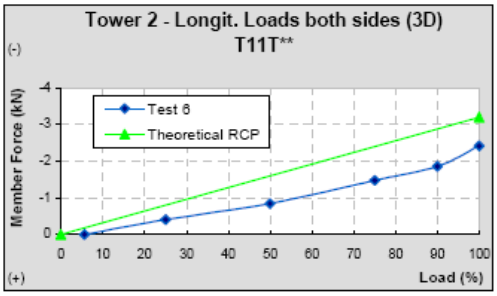

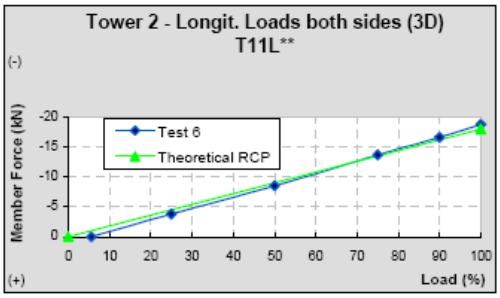

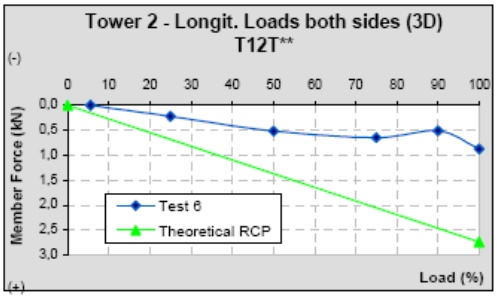

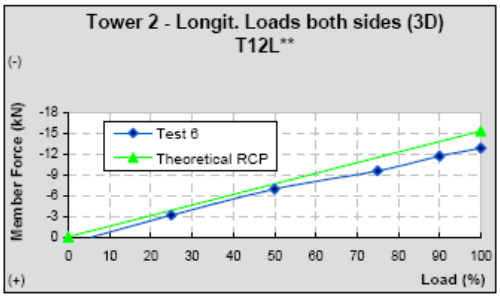

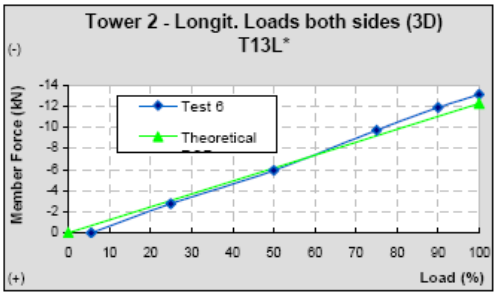

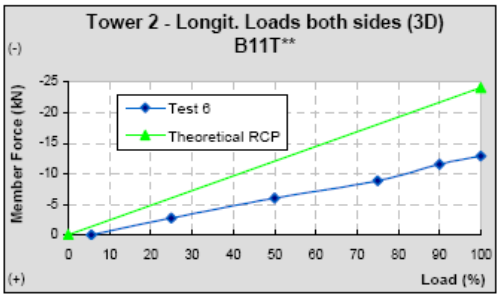

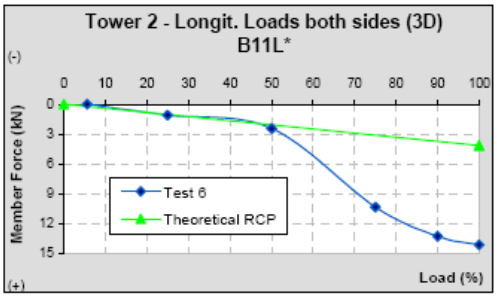

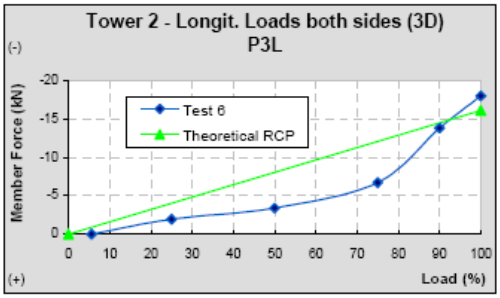

14. STRUCTURE 2 – TEST 7 (4)

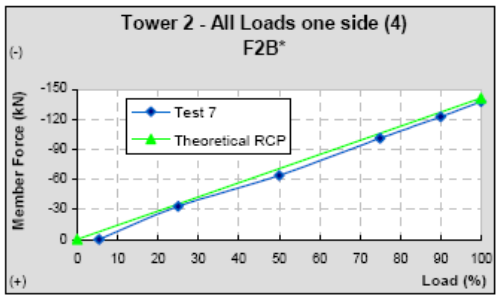

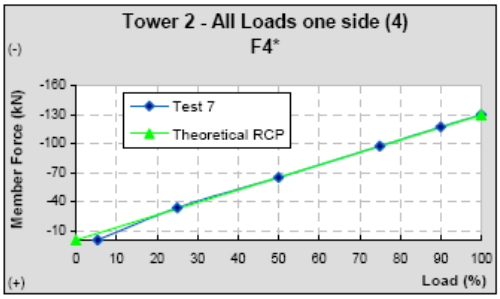

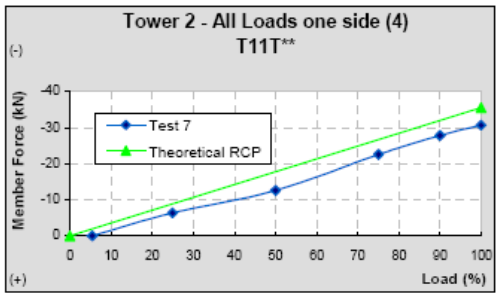

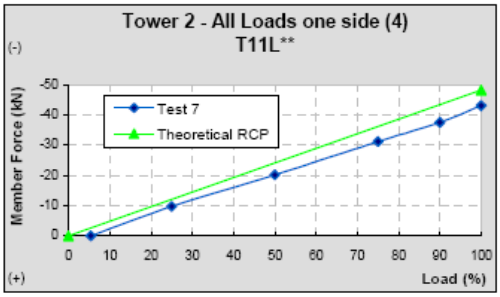

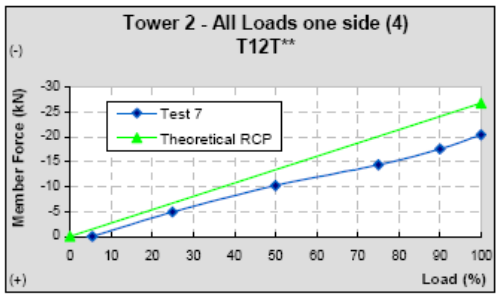

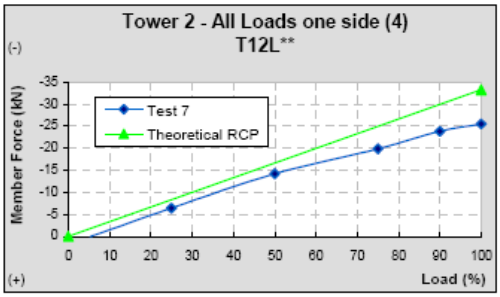

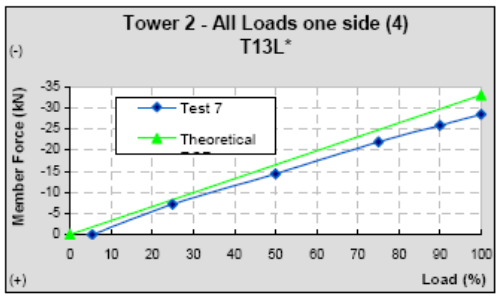

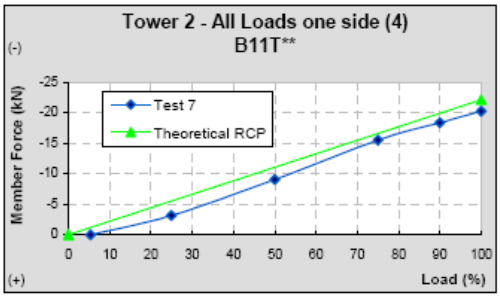

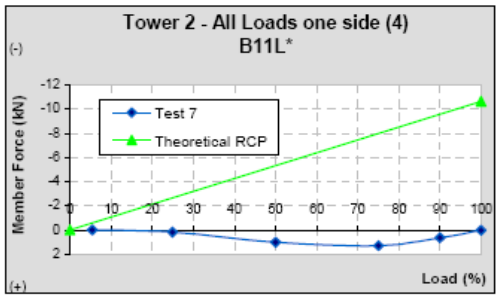

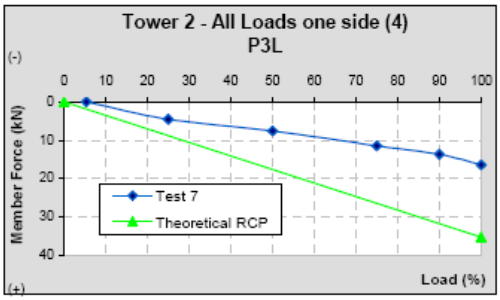

15. STRUCTURE 2 – TEST 8 (4D)

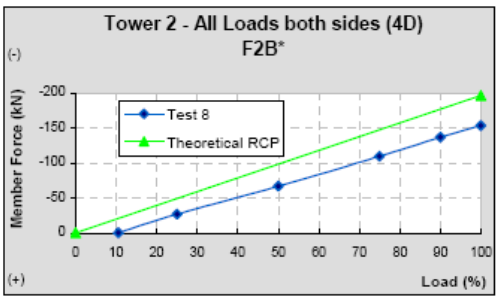

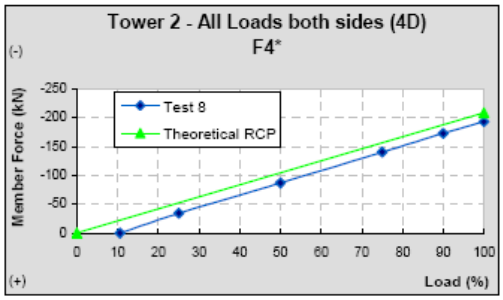

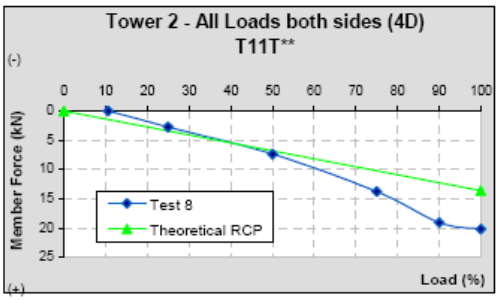

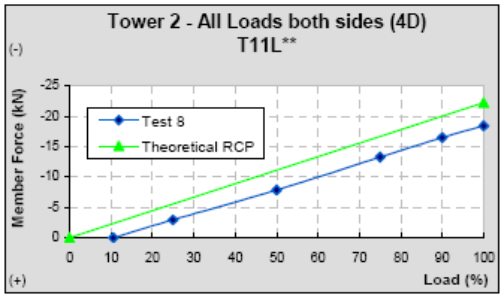

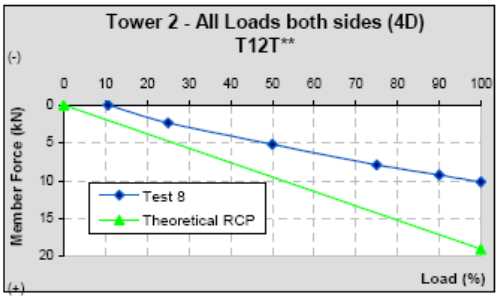

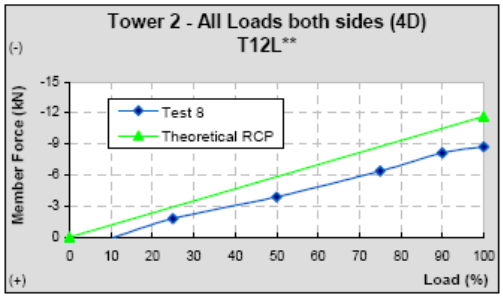

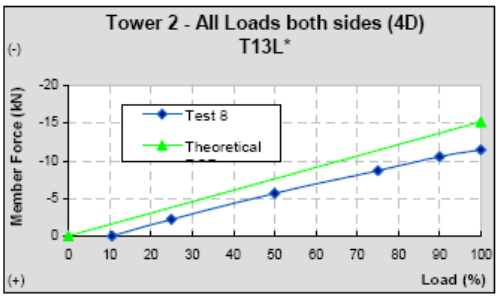

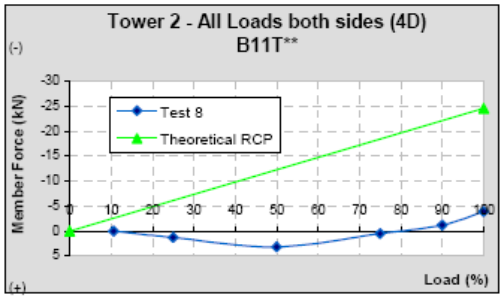

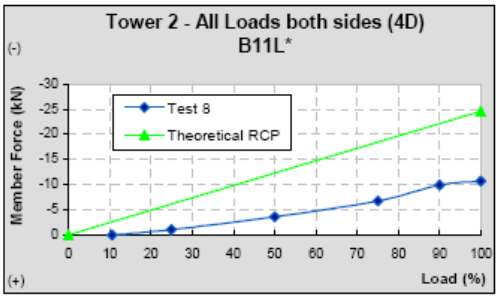

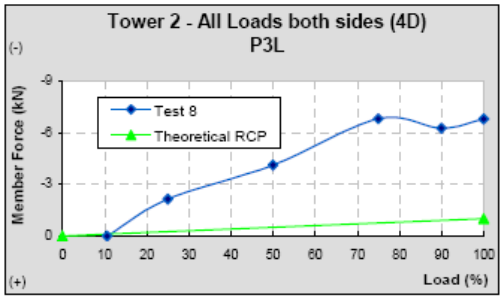

16. STRUCTURE 2A – TEST 1 (1)

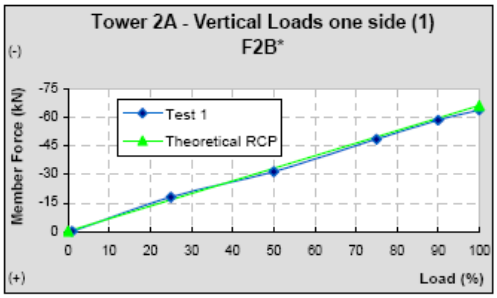

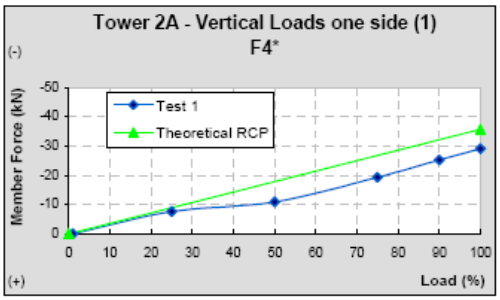

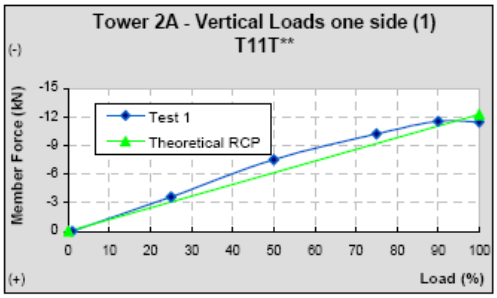

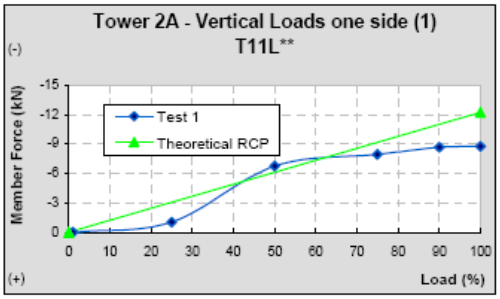

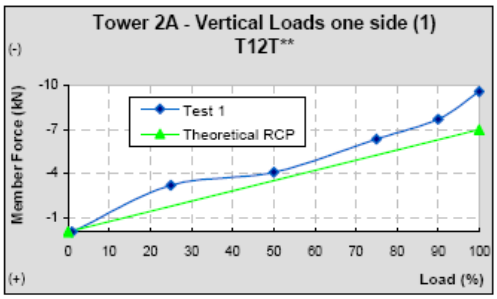

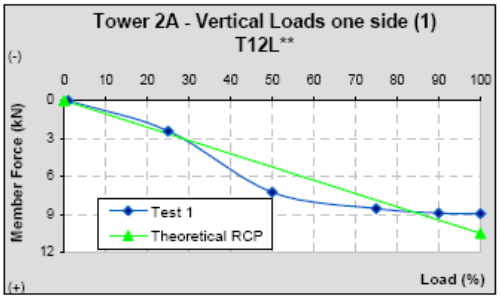

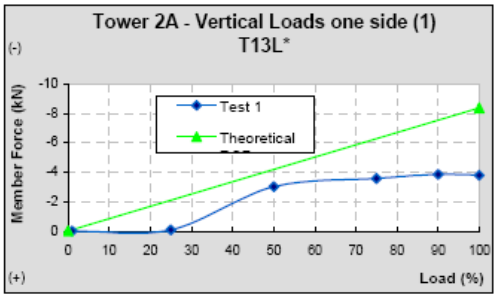

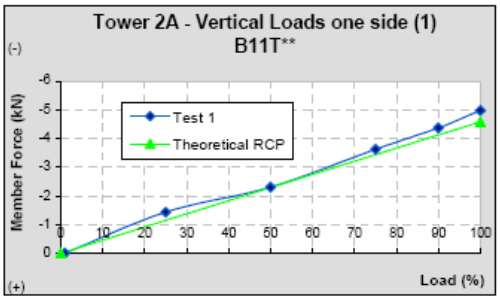

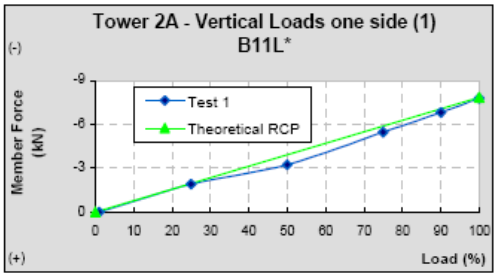

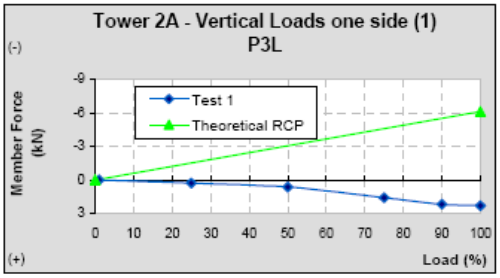

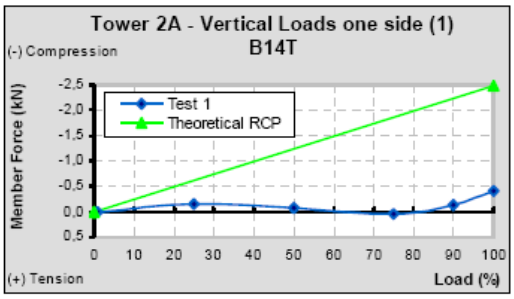
Tower 2A - Vertical Loads one side (1)
B14T
(-) Compression
Member Force (kN)
-2,5
-2,0
-1,5
-1,0
-0,5
0,0
0,5
Test 1
Theoretical RCP
0 10 20 30 40 50 60 70 80 90 100
(+) Tension
Load (%)

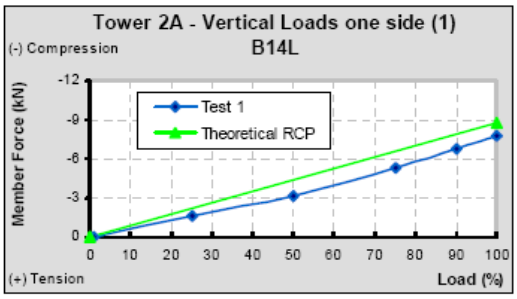
Tower 2A - Vertical Loads one side (1)
B14L
(-) Compression
Member Force (kN)
-12
-9
-6
-3
0
Test 1
Theoretical RCP
0 10 20 30 40 50 60 70 80 90 100
(+) Tension
Load (%)

17. STRUCTURE 2A – TEST 2 (1D)

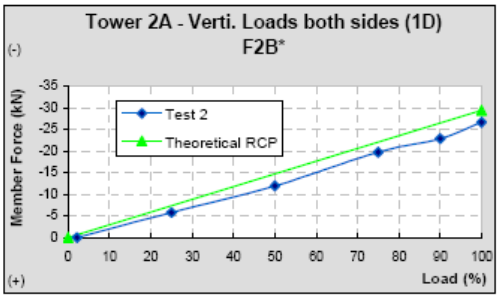

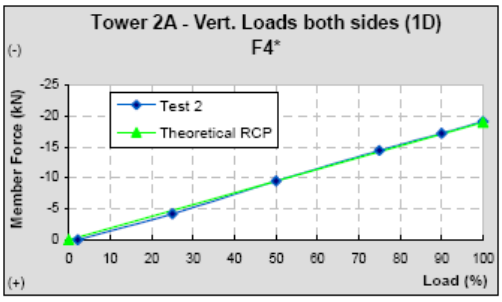

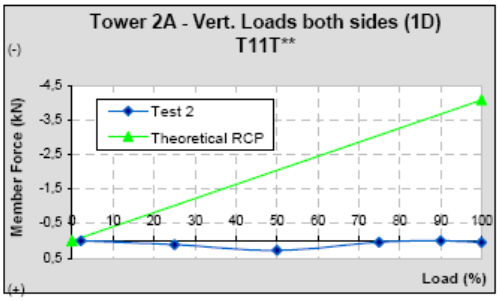

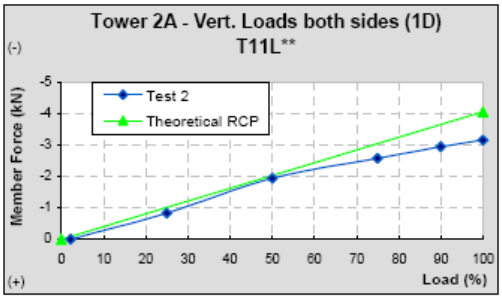

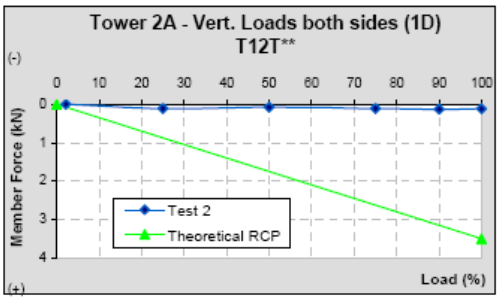

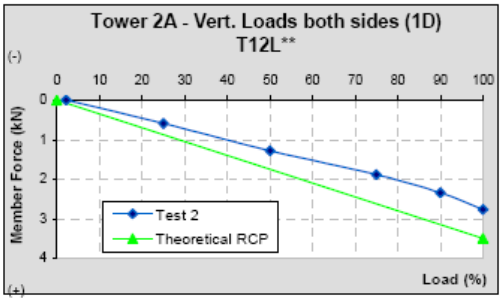

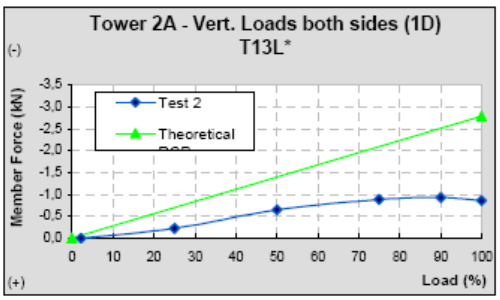

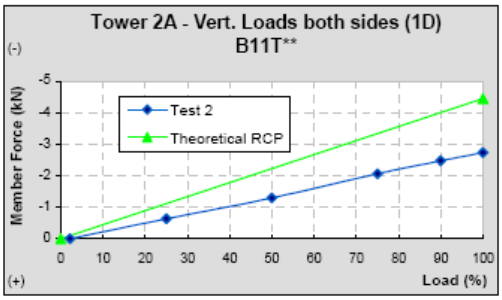

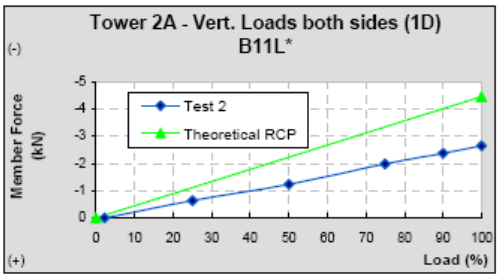

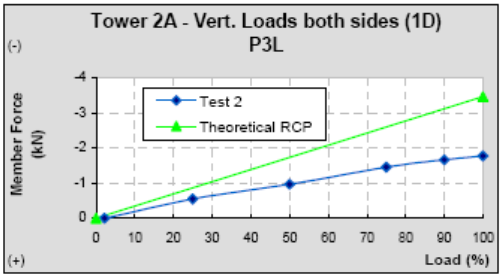

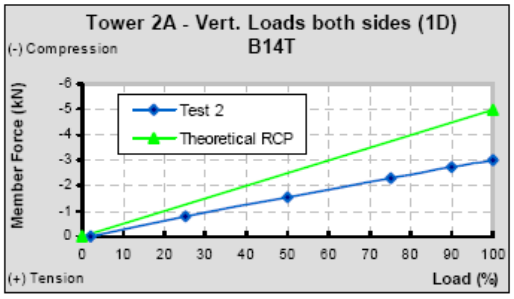
Tower 2A - Vert. Loads both sides (1D)
(-) Compression
B14T
Member Force (kN)
-6
-5
-4
-3
-2
-1
0
Test 2
Theoretical RCP
0
10
20
30
40
50
60
70
80
90
100
(+) Tension
Load (%)

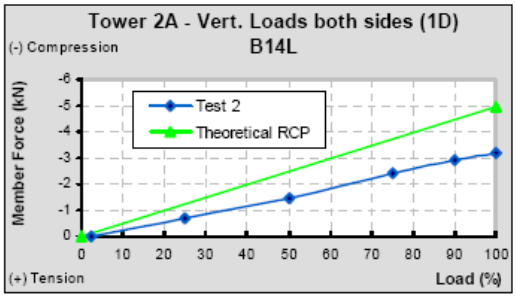
Tower 2A - Vert. Loads both sides (1D)
(-) Compression
B14L
Member Force (kN)
-6
-5
-4
-3
-2
-1
0
Test 2
Theoretical RCP
0
10
20
30
40
50
60
70
80
90
100
(+) Tension
Load (%)

18. STRUCTURE 2A – TEST 3 (2)

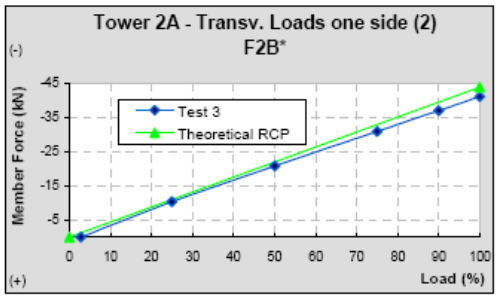

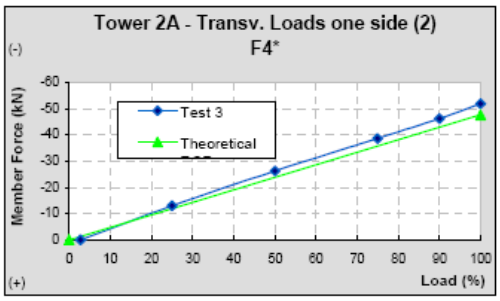

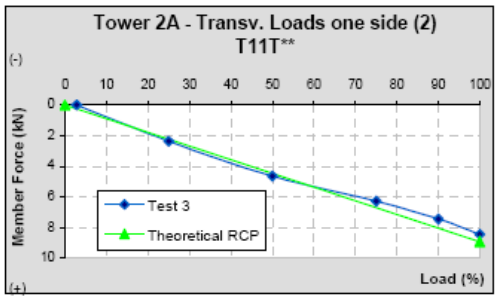

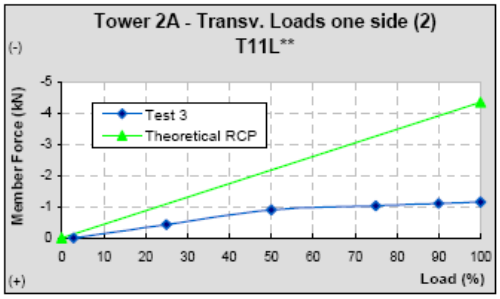

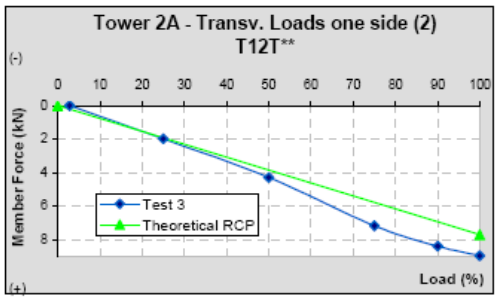

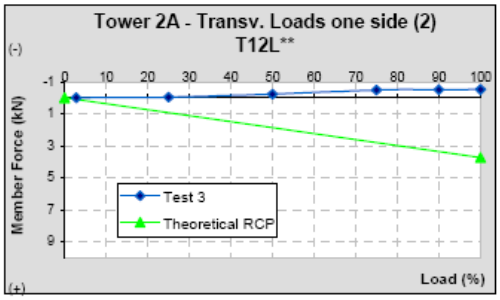

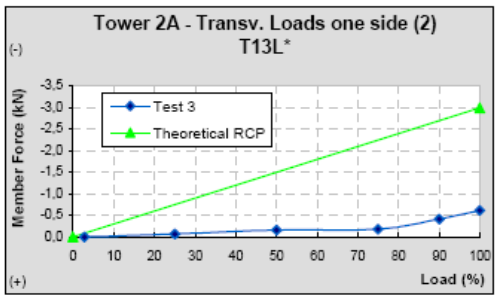

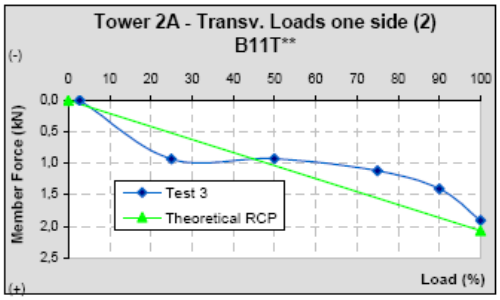

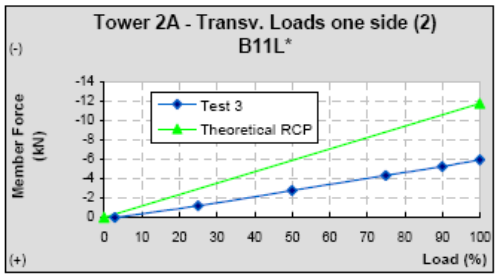

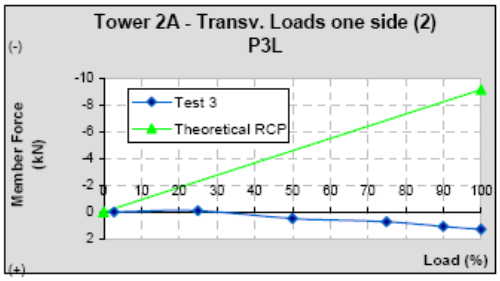

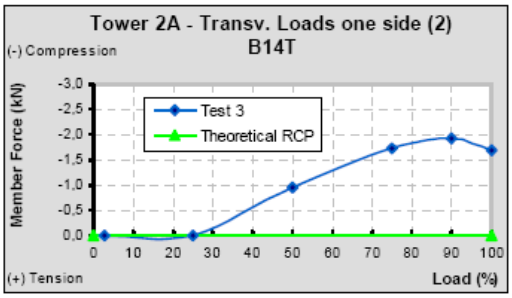
Tower 2A - Transv. Loads one side (2)
B14T
(-) Compression
Member Force (kN)
-3,0
-2,5
-2,0
-1,5
-1,0
-0,5
0,0
Test 3
Theoretical RCP
0 10 20 30 40 50 60 70 80 90 100
(+) Tension
Load (%)

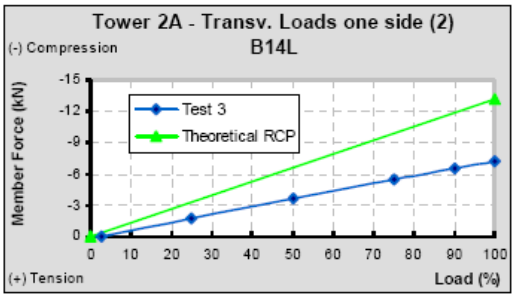
Tower 2A - Transv. Loads one side (2)
B14L
(-) Compression
Member Force (kN)
-15
-12
-9
-6
-3
0
Test 3
Theoretical RCP
0 10 20 30 40 50 60 70 80 90 100
(+) Tension
Load (%)

19. STRUCTURE 2A – TEST 4 (2D)

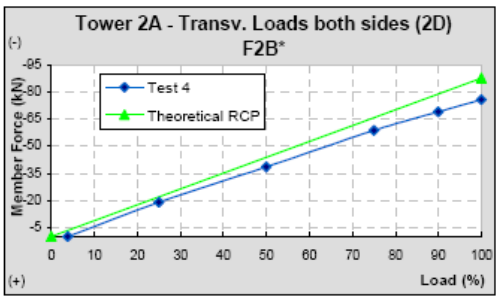

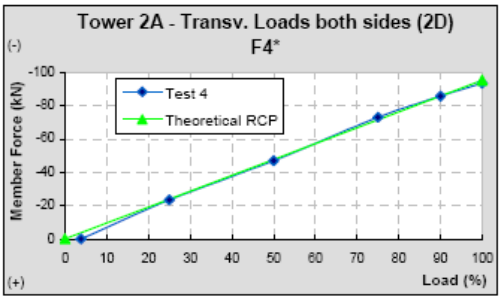

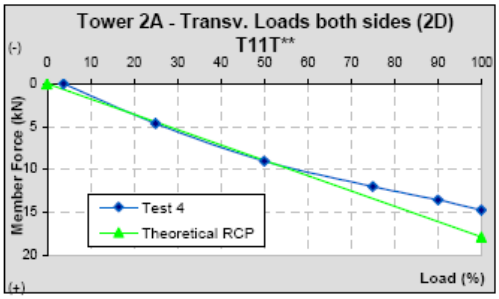

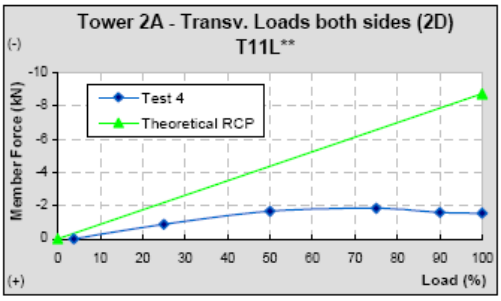

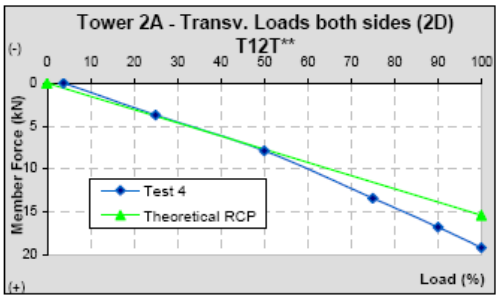

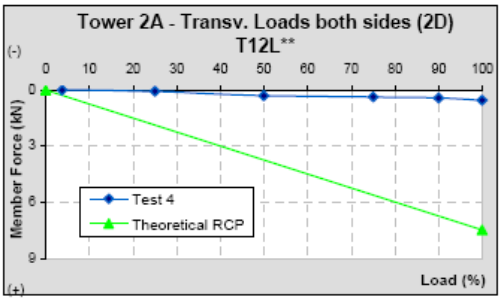

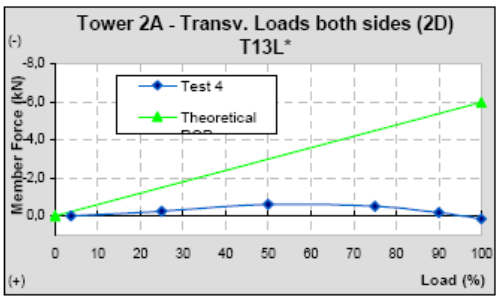

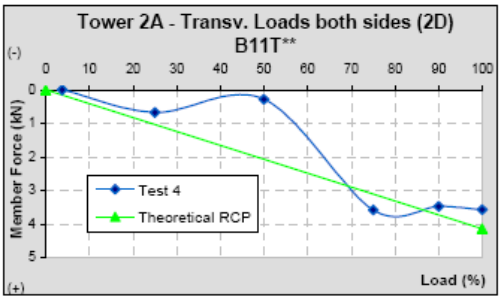

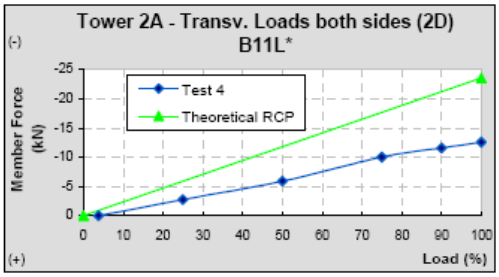

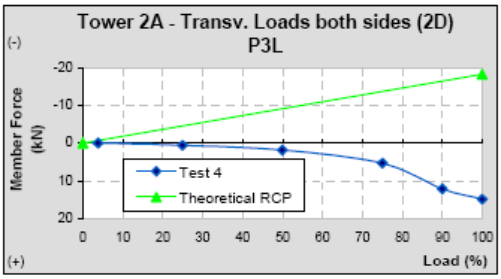

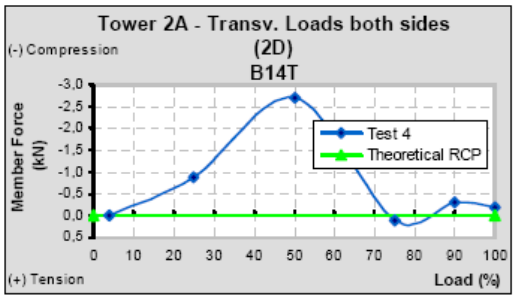
Tower 2A - Transv. Loads both sides
(2D)
B14T
(-) Compression
Member Force (kN)
-3,0
-2,5
-2,0
-1,5
-1,0
-0,5
0,0
0,5
0
10
20
30
40
50
60
70
80
90
100
Test 4
Theoretical RCP
(+) Tension
Load (%)

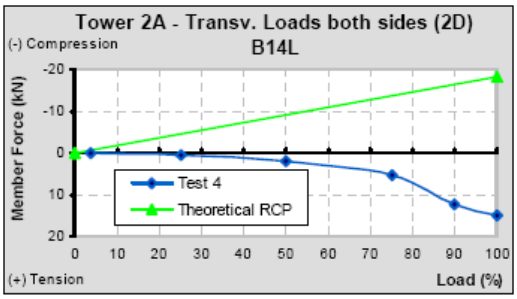
Tower 2A - Transv. Loads both sides (2D)
B14L
(-) Compression
Member Force (kN)
-20
-10
0
10
20
0
10
20
30
40
50
60
70
80
90
100
Test 4
Theoretical RCP
(+) Tension
Load (%)

20. STRUCTURE 2A – TEST 5 (3)

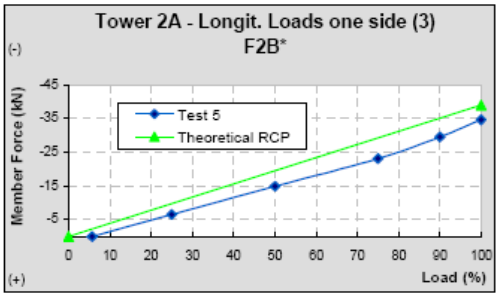

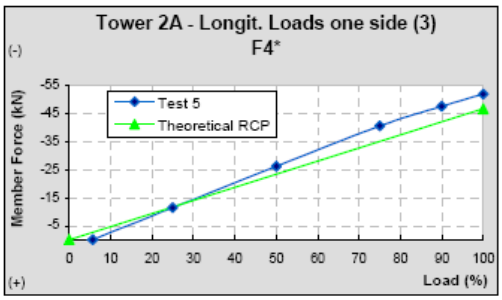

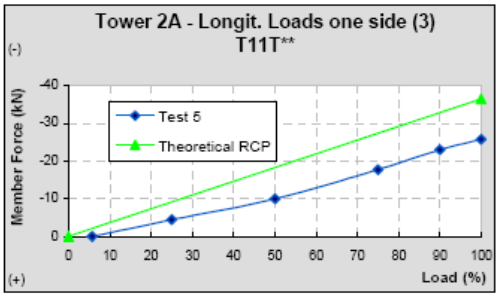

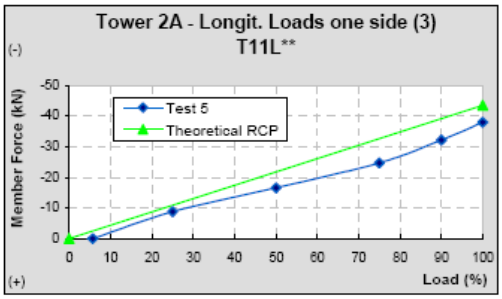

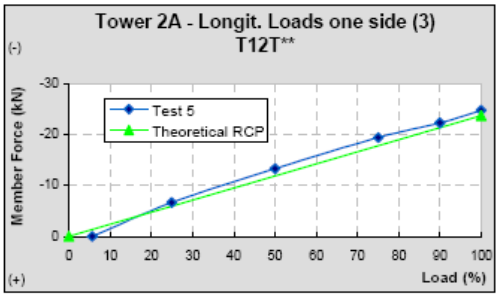

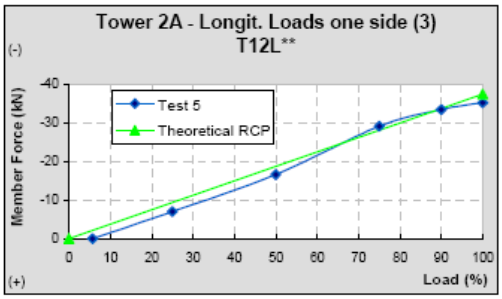

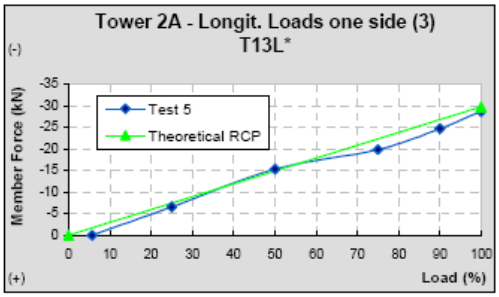

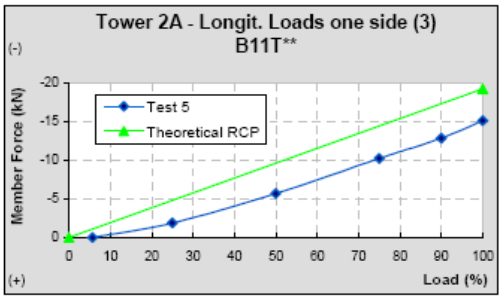

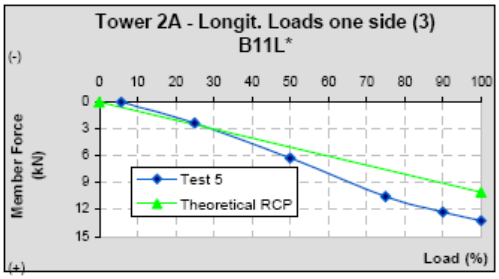

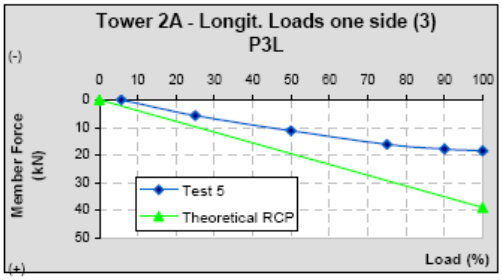

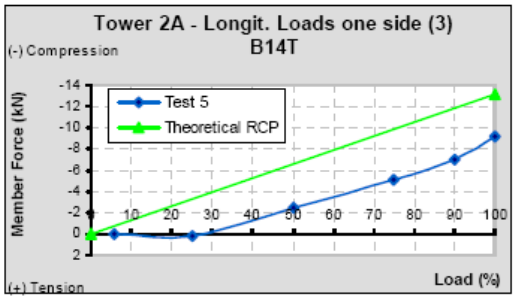
Tower 2A - Longit. Loads one side (3)
B14T
(-) Compression
Member Force (kN)
-14
-12
-10
-8
-6
-4
-2
0
2
Test 5
Theoretical RCP
10
20
30
40
50
60
70
80
90
100
(+) Tension
Load (%)

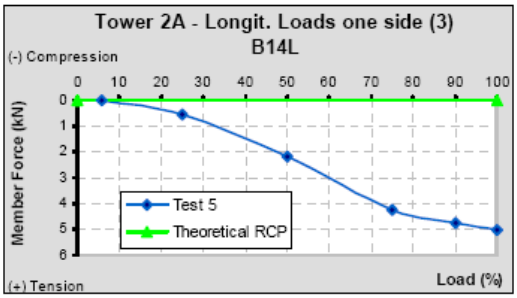
Tower 2A - Longit. Loads one side (3)
B14L
(-) Compression
Member Force (kN)
0
1
2
3
4
5
6
Test 5
Theoretical RCP
0
10
20
30
40
50
60
70
80
90
100
(+) Tension
Load (%)

21. STRUCTURE 2A – TEST 6 (3D)

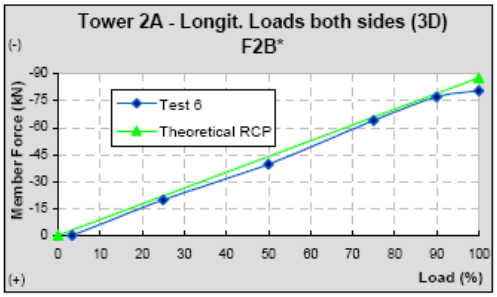

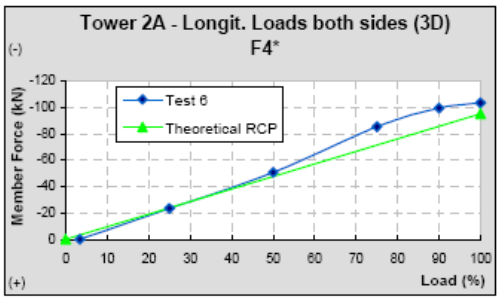

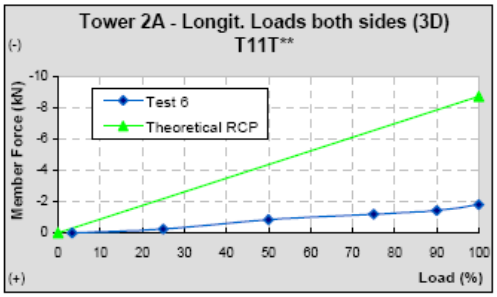

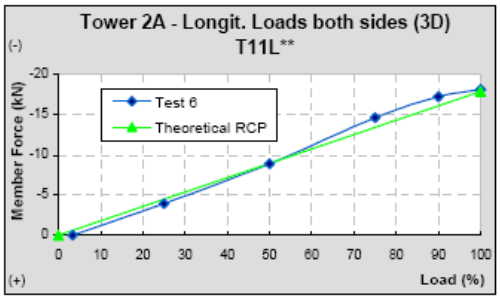

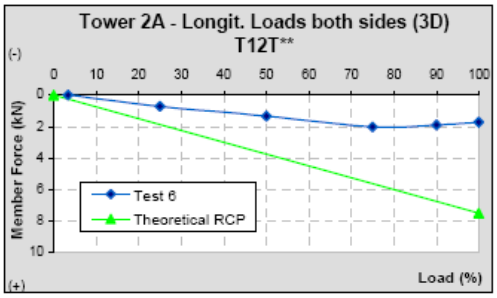

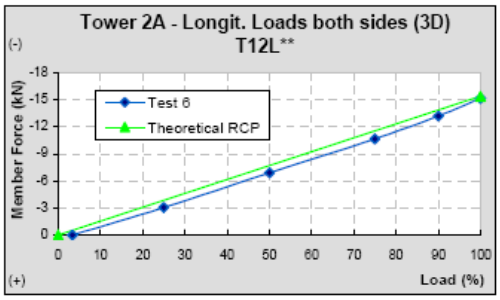

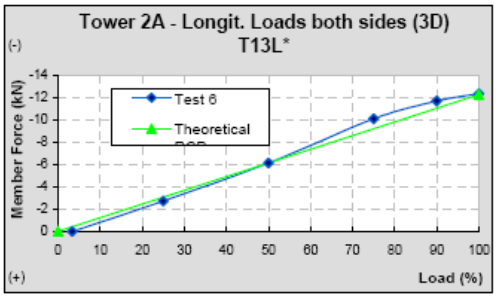

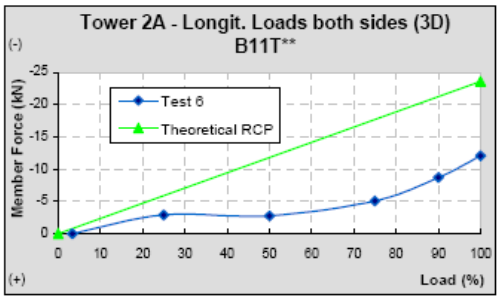

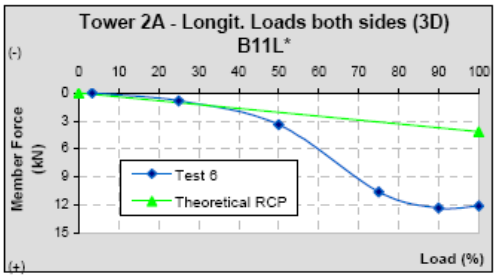

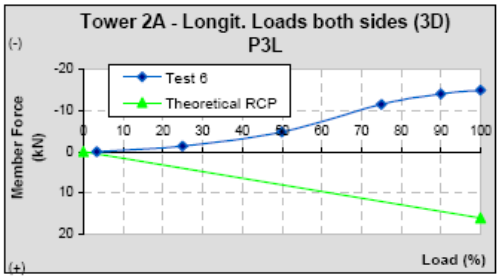

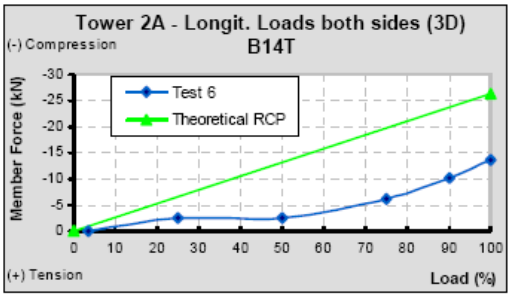
Tower 2A - Longit. Loads both sides (3D)
B14T
(-) Compression
Member Force (kN)
-30
-25
-20
-15
-10
-5
0
Test 6
Theoretical RCP
0
10
20
30
40
50
60
70
80
90
100
(+) Tension
Load (%)

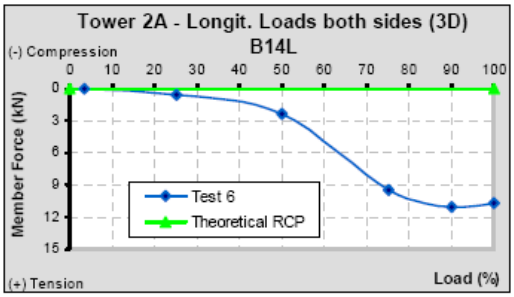
Tower 2A - Longit. Loads both sides (3D)
B14L
(-) Compression
Member Force (kN)
0
10
20
30
40
50
60
70
80
90
100
0
3
6
9
12
15
Test 6
Theoretical RCP
(+) Tension
Load (%)

22. STRUCTURE 2A – TEST 7 (4)

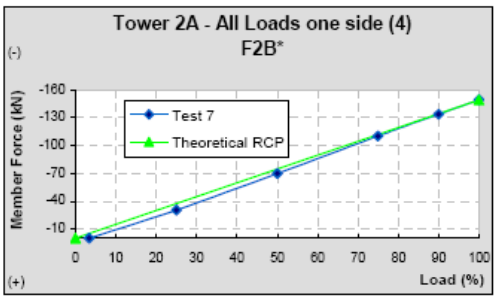

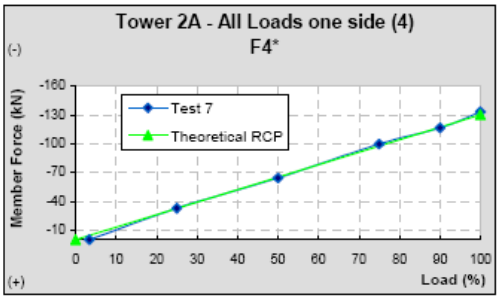

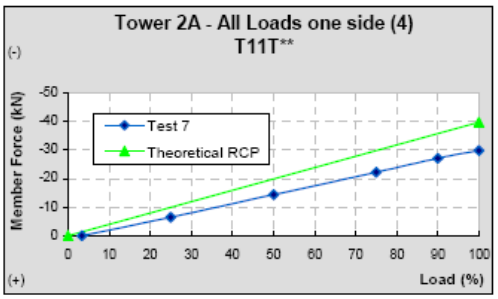

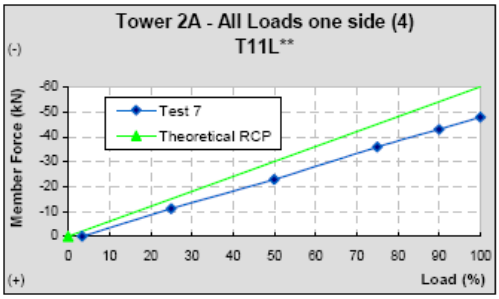

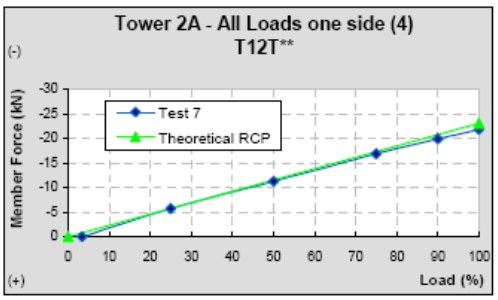

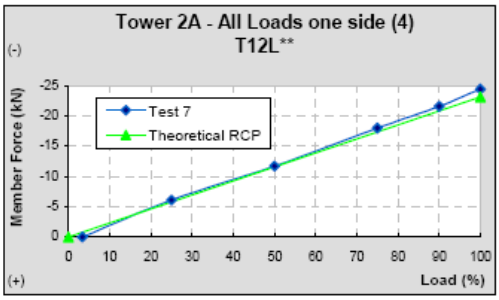

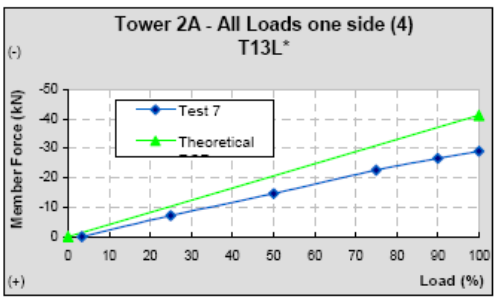

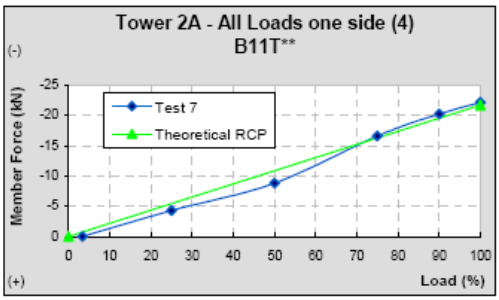

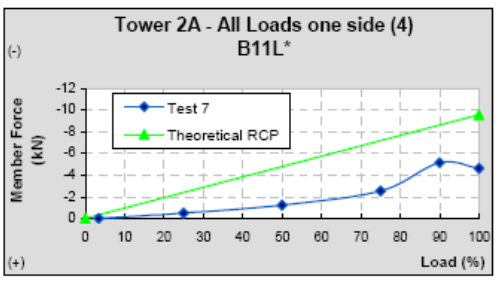

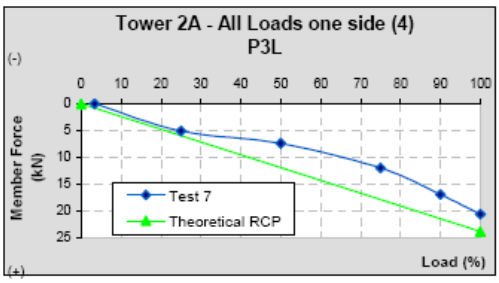

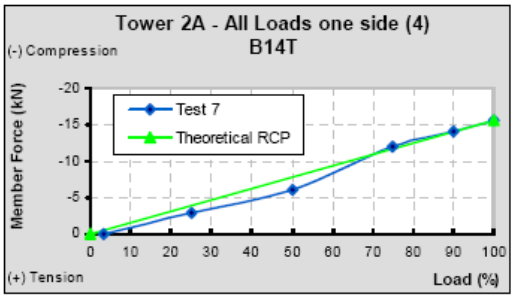
Tower 2A - All Loads one side (4)
B14T
(-) Compression
Member Force (kN)
-20
-15
-10
-5
0
Test 7
Theoretical RCP
0 10 20 30 40 50 60 70 80 90 100
(+) Tension
Load (%)

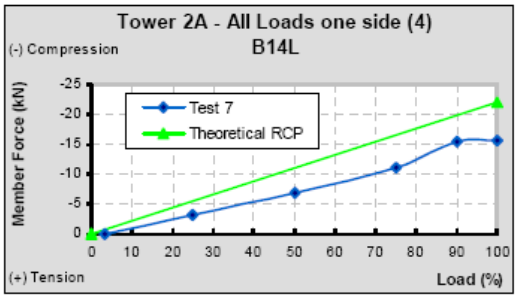
Tower 2A - All Loads one side (4)
B14L
(-) Compression
Member Force (kN)
-25
-20
-15
-10
-5
0
Test 7
Theoretical RCP
0 10 20 30 40 50 60 70 80 90 100
(+) Tension
Load (%)

23. STRUCTURE 2A – TEST 8 (4D)

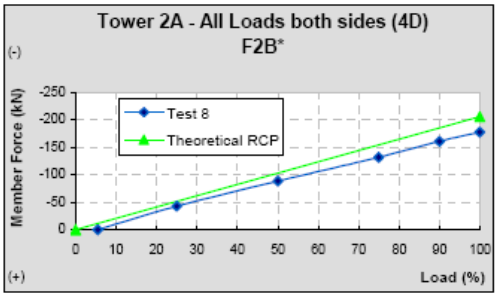

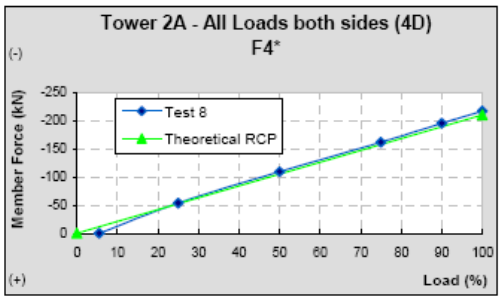

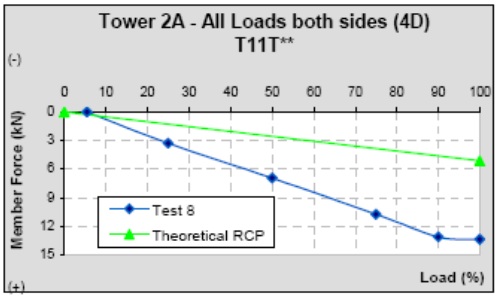

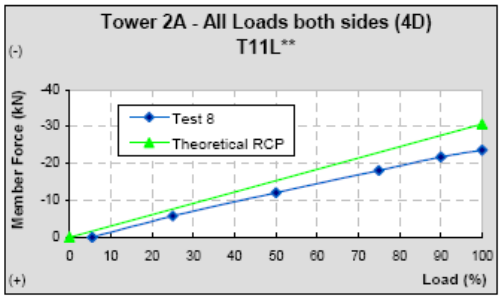

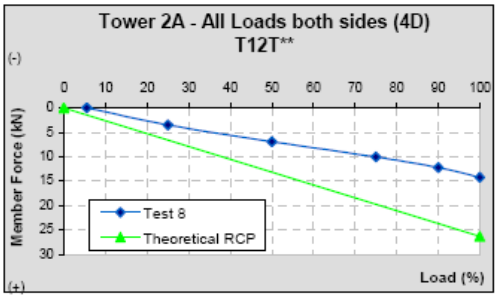

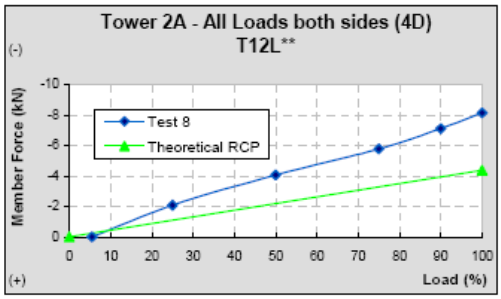

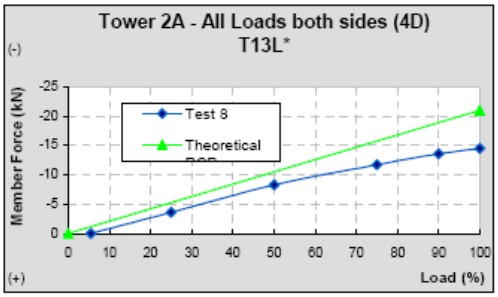

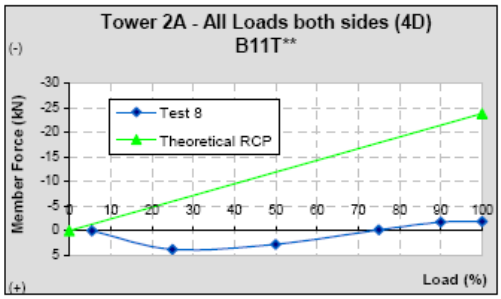

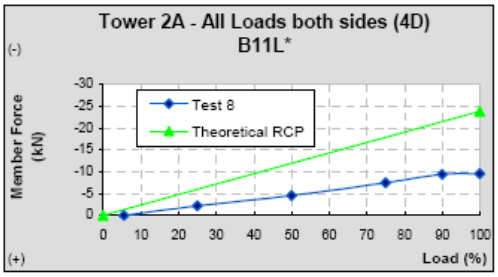

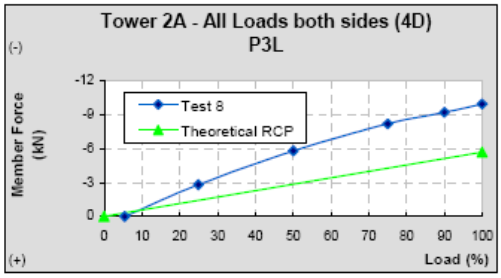

δ (mm)

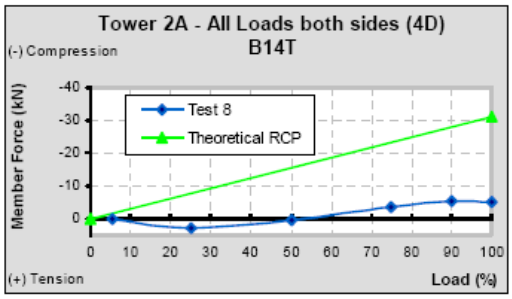
Tower 2A - All Loads both sides (4D)
B14T
(-) Compression
Member Force (kN)
-40
-30
-20
-10
0
Test 8
Theoretical RCP
0 10 20 30 40 50 60 70 80 90 100
(+) Tension
Load (%)

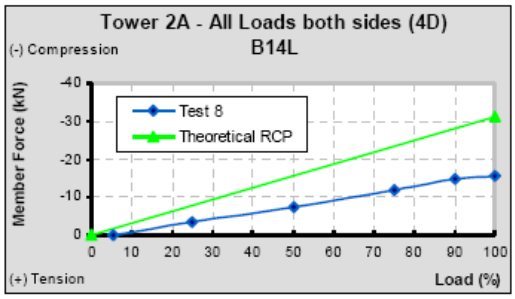
Tower 2A - All Loads both sides (4D)
B14L
(-) Compression
Member Force (kN)
-40
-30
-20
-10
0
Test 8
Theoretical RCP
0 10 20 30 40 50 60 70 80 90 100
(+) Tension
Load (%)

ISBN: 978- 2- 85873- 074-2